BUREAU OF RECLAMATION

Directed Outflow Project Technical Report 3

Directed Outflow Project, California
California-Great Basin Region

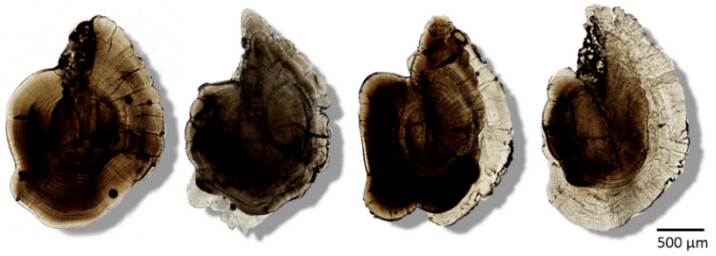

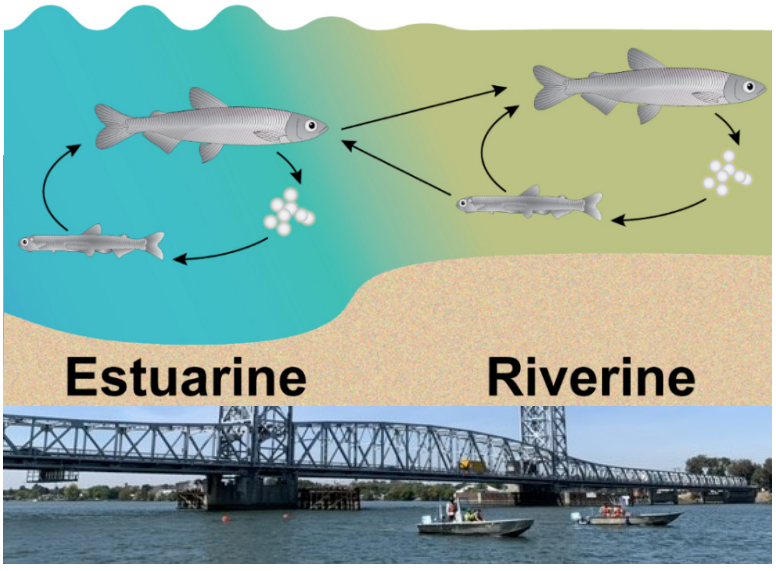

U.S. Department of the Interior

June 2022

Mission Statements

The Department of the Interior (DOI) conserves and manages the Nation's natural resources and cultural heritage for the benefit and enjoyment of the American people, provides scientific and other information about natural resources and natural hazards to address societal challenges and create opportunities for the American people, and honors the Nation's trust responsibilities or special commitments to American Indians, Alaska Natives, and affiliated island communities to help them prosper.

The mission of the Bureau of Reclamation is to manage, develop, and protect water and related resources in an environmentally and economically sound manner in the interest of the American public.

Directed Outflow Project Technical Report 3

Directed Outflow Project, California
California-Great Basin Region

prepared by

Bureau of Reclamation, Bay-Delta Office
801 I Street, Suite 140, Sacramento, CA 95814

Report Editors and Project Managers
Nick G. Bertrand, Kristin K. Arend, Ph.D., & Brian Mahardja
Science Division, U.S. Bureau of Reclamation, Bay-Delta Office

Administering Office
U.S. Bureau of Reclamation Bay-Delta Office
David Mooney, Ph.D., P.E.; Bay-Delta Office Manager
Mario Manzo, Bay-Delta Deputy Office Manager
Josh Israel, Ph.D., Bay-Delta Science Division Chief

Chapter Lead Authors*
Matthew A. Campbell
John Brandon
Bruce G. Hammock
Jonathan L. Huang
Calvin Y. Lee
Levi S. Lewis
Marie E. Stillway
*** See individual chapters for full list of coauthors**

Cover Photos: Cover Images: top: Delta Smelt Otolith images by Johnathan Huang Wildlife, Fish and Conservation Biology, University of California, Davis, Davis, California 95616.; middle: Delta Smelt Life History illustration by Adi Khen, Wildlife, Fish and Conservation Biology, University of California, Davis, Davis, California 95616, USA; bottom: EDSM Kodiak trawl sampling boats by Rob Miller, Fish and Aquatic Science Team, ICF, Sacramento California 95814, USA.

Disclaimer

This document does not represent and should not be construed to represent determination, concurrence, or policy of the U.S. Bureau of Reclamation or the U.S. Government.

Any use of trade, product, or firm names is for descriptive purposes only and does not imply endorsement by Reclamation or the U.S. Government.

PLEASE DO NOT RETURN YOUR FORM TO THE ABOVE ADDRESS.

1. REPORT DATE	**2. REPORT TYPE**	**3. DATES COVERED** *(From - To)*
June 10, 2022	Research	

4. TITLE AND SUBTITLE Directed Outflow Project: Technical Report 3	**5a. CONTRACT NUMBER** **5b. GRANT NUMBER** **5c. PROGRAM ELEMENT NUMBER**
6. AUTHOR(S) Editors: Nick G. Bertrand, Kristin K. Arend, & Brian Mahardja, Chapter Lead Authors: Matthew A. Campbell John Brandon, Bruce G. Hammock, Jonathan L. Huang, Calvin Y. Lee, Levi S. Lewis, & Marie E. Stillway	**5d. PROJECT NUMBER** **5e. TASK NUMBER** **5f. WORK UNIT NUMBER**
7. PERFORMING ORGANIZATION NAME(S) AND ADDRESS(ES) Bureau of Reclamation Bay Delta Office 801 I St., Suite 140 Sacramento CA 95814	**8. PERFORMING ORGANIZATION REPORT NUMBER**
9. SPONSORING/MONITORING AGENCY NAME(S) AND ADDRESS(ES) United States Bureau of Reclamation Bay Delta Office 801 I St., Suite 140 Sacramento CA 95814	**10. SPONSOR/MONITOR'S ACRONYM(S)** **11. SPONSOR/MONITOR'S REPORT NUMBER(S)**

12. DISTRIBUTION/AVAILABILITY STATEMENT Available from the National Technical Information Service (NTIS), Operations Division, 5285 Pt. Royal Rd, Springfield VA 22161; and
U.S. Bureau of Reclamation, Bay Delta Office Website: https://www.usbr.gov/mp/bdo/index.html

13. SUPPLEMENTARY NOTE

14. ABSTRACT The U.S. Bureau of Reclamation's Directed Outflow Program (DOP), along with collaborating agencies and non-governmental groups, are continuing efforts to evaluate the hypothesized benefits of outflow/outflow alteration to habitats and species of the Sacramento-San Joaquin Delta and connecting upper estuary (Delta). A particular focus of the DOP is to improve ecological understanding of the critically endangered Delta Smelt (*Hypomesus transpacificus*), a small short-lived osmerid fish endemic to the Delta. The DOP technical report series (https://www.usbr.gov/mp/bdo/directed-outflow.html) aims to periodically showcase ongoing DOP-related research studies. Results from DOP-related studies are anticipated to assist decision-making processes and better inform general management actions to benefit Delta habitat conditions and species such as Delta Smelt.

15. SUBJECT TERMS
Directed Outflow Project, Fall X2, Salinity, Delta Smelt, Zooplankton, Contaminants, Growth, Condition, San Francisco Bay, Delta

16. SECURITY CLASSIFICATION OF:			**17. LIMITATION OF ABSTRACT**	**18. NUMBER OF PAGES**	**19a. NAME OF RESPONSIBLE PERSON**
				284	Joshua Israel, Ph.D.
a. REPORT	**b. ABSTRACT**	**a. THIS PAGE**			**19b. TELEPHONE NUMBER** *(Include area code)*
					916-414-2405

This page intentionally left blank

Table of Contents

List of Tables

List of Figures

Suggested Citation

Entire Report

Bertrand, N.G., K.K. Arend, and B. Mahardja. Directed Outflow Project: Technical Report 3. U.S. Bureau of Reclamation, Bay-Delta Office, California-Great Basin Region, Sacramento, CA. June 10, 2022, 284 pp.

Chapter within Report

Lewis L.S., M. Willmes, L. Cavole, W. Xieu, R. A. Fichman, T.C. Hung, L. Ellison, T. Stevenson, A. A. Schultz, B. G. Hammock, S.J. Teh, and J. A. Hobbs. 2021. Experimental Assessment of Otolith-based Geochemical Reconstructions of Migratory Life History for an Imperiled Estuarine Fish Pages 11-27 in Bertrand, N.G., K.K. Arend, and B. Mahardja., editors. Directed Outflow Project: Technical Report 3. U.S. Bureau of Reclamation, Bay-Delta Office, California-Great Basin Region, Sacramento, CA. June 10, 2022, 284 pp.

Directed Outflow Project Collaborators

Alisha M. Goodbla, U.C. Davis

Amanda J. Finger U. C. Davis

Andrew Schultz, U.S. Bureau of Reclamation (Currently U.S. Fish and Wildlife Service)

April Hennessy, California Department of Fish and Wildlife*

April Smith, ICF

Andrew Kalmbach, ICF

Andrew Schultz, U.S. Fish and Wildlife Service

Brian Mahardja, U.S. Bureau of Reclamation *

Bruce Hammock, U.C. Davis*

Calvin Lee, ICF*

Catherine Johnston, U.S. Fish and Wildlife Service

Christian Denney, U.C. Davis

Christina Burdi, California Department of Fish and Wildlife*

Cody J. Chalker, U.C. Davis

Colin Brennan, ICF

Darcy Austin, State Water Contractors

Denise Barnard, U.S. Fish and Wildlife Service*

Erwin Van Nieuwenhuyse, U.S. Bureau of Reclamation

Feng Zhao, U.C. Davis

Galen Tigan, U.C. Davis

J. Ryan Cook, U.S. Fish and Wildlife Service

James Hobbs, California Department of Fish and Wildlife & U.C. Davis*

Jason Hassrick, ICF*

Jennifer Pierre, State Water Contractors

John Brandon, ICF

John Grimich, U.C. Davis

Johnathan Huang, U.C. Davis

Kristin Arend, U.S. Bureau of Reclamation*

Lauren Damon, California Department of Fish and Wildlife

Lenny Grimaldo, ICF (currently California Department of Water Resources)*

Levi Lewis, U.C. Davis*

Lori Smith, U.S. Fish and Wildlife Service

Luke Ellison, U.C. Davis

Malte Willmes, U.C. Davis*

Marie Stillway, U.C. Davis*

Matthew A. Campbell, U.C. Davis

Nann Fangue, UC Davis

Nick Bertrand, U.S. Bureau of Reclamation*

Peggy Lehman, DWR

Rachel Fichman, U.C. Davis

Ramona Zeno, ICF

Randy Baxter, California Department of Fish and Wildlife

Randy Dahlgren, U.C. Davis

Rosemary Hartman, DWR

Shawn Acuña, Metropolitan Water District of Southern California*

Shannon E.K. Joslin, U.C. Davis

Steve Slater, California Department of Fish and Wildlife*

Swee Teh, U.C. Davis*

Taylor Senegal, U.S. Fish and Wildlife Service*

Teague Corning, ICF

Tien-Chieh Hung, U.C. Davis

Tomofumi Kurobe U.C. Davis

Troy Stevenson, U.C. Davis

Wilson Ramírez-Duarte, U.C. Davis

Wilson Xieu, U.C. Davis

***denotes DOP Investigator Team**

Acknowledgments

The Directed Outflow Project is part of the Interagency Ecological Program (IEP) Annual Work Plan. Early reviews of related study plans were supported by the IEP Flow Alteration Project Work Team and the Collaborative Adaptive Management Team (special thanks to Larry Brown [U.S. Geological Survey]), and U.S. Fish and Wildlife Service (USFWS), California Department of Water Resources (DWR), California Department of Fish and Wildlife (CDFW), and U. S. Bureau of Reclamation (USBR). Permitting for this work was facilitated through CDFW (SC-4086, SC-13523, S-190810003-19127-002 and Memorandum of Understanding issued by CDFW's Delta Habitat Conservation Program and Fisheries Branch) and USWFS (TE-108507, sub-permit FWSLFWO-6.1, 1-1-96-F-1 and 1-1-98-I-1296). This study was supported by contributions from multiple IEP agency field sampling activities of fish and zooplankton (CDFW, USFWS, DOP [USBR]), as well as informed by DWR DAYFLOW. Funding and contractual support was provided by USBR (special thanks to Megan Bryant, Teresa Brown, Christina Munoz, Mouang Phan, Nandini Johnson, Brooke White, Thomas Eckert, John Ridilla, Delyssa Bloxson and Leanne Henderson), DWR, Metropolitan Water District of Southern California (special thanks to Shawn Acuña), State Water Contractors (SWC; special thanks to Jennifer Pierre, Darcy Austin and SWC staff) and State and Federal Contractors Water Agency (special thanks to Laura Valoppi). We acknowledge the support of many people from the Delta community. Further acknowledgement sections are located within each chapter of this report.

Background and Purpose

The U.S. Bureau of Reclamation's (Reclamation) Directed Outflow Program (DOP), along with collaborating agencies and non-governmental groups, are continuing efforts to evaluate the hypothesized benefits of outflow/outflow alteration and improve ecological understanding of the critically endangered Delta Smelt (*Hypomesus transpacificus*), a small short-lived osmerid fish endemic to the Sacramento-San Joaquin Delta and connecting upper estuary (Delta). The DOP technical report series (Schultz et al. 2019; https://www.usbr.gov/mp/bdo/directed-outflow.html) aims to periodically showcase ongoing DOP-related research studies. Each chapter within this report is intended for eventual submittal to a peer-reviewed scientific journal, thus formatting may vary among chapters. Comments at the top of the title page of each chapter will alert the reader of those chapters already published or submitted to a peer-reviewed journal. The following provides additional background information.

In 2008, the U.S. Fish and Wildlife Service (USFWS) issued a Biological Opinion (2008 BiOp; USFWS 2008) on Central Valley Project/State Water Project operations that concluded aspects of those operations jeopardize the continued existence of Delta Smelt and adversely modify the species' critical habitat. Action 4 (Fall X2 Action) of the 2008 BiOp required Delta outflow be maintained at an average X2 (average position of the 2 ppt isohaline from Golden Gate) no greater than 74 km for September and October following wet years and 81 km following above normal years (water-year type [wet, above normal, below normal, dry, critical] is based on measured unimpaired runoff; https://cdec.water.ca.gov/reportapp/javareports?name=WSIHIST). In 2011, Reclamation produced a fall outflow adaptive management plan based on the science underlying the Fall X2 Action and outlining how adaptive management might proceed (Reclamation 2012).

In spring 2016, USFWS requested augmentation of summer outflow from the Sacramento River to benefit the habitat and declining population of Delta Smelt, although the action never occurred. Slightly thereafter the Delta Smelt Resiliency Strategy (DSRS) was finalized in July 2016 (CNRA 2016). The DSRS articulated a suite of actions that could be implemented in the next few years to benefit Delta Smelt based on concepts detailed in Baxter et al. (2015). These actions included augmentation of Delta outflow to push the low salinity zone (0.5-6 ppt) seaward and routing of water through Yolo Bypass Toe Drain to promote food production, to benefit Delta Smelt.

In winter of 2016/2017 Reclamation formed the DOP to assist in evaluating outflow-related hypotheses and predictions (Table 1) using targeted paired biological and physical monitoring. The over-arching hypothesis is summer and fall habitat conditions are improved for juvenile Delta Smelt when X2 moves seaward (USBR 2012; Brown et al. 2014), especially when X2 overlaps the Suisun Bay-Marsh area of the Delta. Predictions are largely based on conceptual models within Baxter et al. (2015) (figures 48 and 49 in particular) and predictions in Brown et al. (2014).

In August of 2016, Reclamation and California Department of Water Resources (DWR) jointly requested a Reinitiation of Consultation on the Coordinated Long-Term Operation of the Central Valley Project (CVP) and State Water Project (SWP). The USFWS accepted the request shortly after and stated therein: "…new information is demonstrating the increasingly imperiled state of the delta smelt and its designated critical habitat, and that emerging science shows the importance of outflows to all life stages of delta smelt and to maintaining the primary constituent elements of designated critical habitat." The new Biological Opinion on operations was finalized in October of 2019 (2019

BiOp; USFWS 2019). The Delta Smelt Summer-Fall Habitat Action (SFHA) and additional measures in Table 2-1 of the 2019 BiOp outlines multiple outflow-related actions geared toward benefitting Delta Smelt habitat and ultimately its population. Such actions include the following:

> *Fall X2: Modify water operations to maintain X2 at 80 km in above normal and wet water years in September and October. Maintain low salinity habitat in Suisun Marsh and Grizzly Bay when water temperatures are suitable. Manage the low salinity zone to overlap with turbid water and available food supplies. Establish contiguous low salinity habitat from Cache Slough Complex to the Suisun Marsh.*
>
> *Suisun Marsh Salinity Control Gate: The freshening of Montezuma Slough through gate operations could provide additional low salinity habitat for Delta Smelt to forage, spawn and rear.*
>
> *Suisun Marsh and Roaring River Distribution System Food Subsidies Study: Add fish food to Suisun Marsh through coordinating managed wetland flood and drain operations in Suisun Marsh, Roaring River Distribution System food production, and reoperation of the Suisun Marsh Salinity Control Gates.*
>
> *North Delta Food Subsidies/Colusa Basin Drain Study: Augment flow in the Yolo Bypass in July and/or September by closing Knights Landing Outfall Gates and routing water from Colusa Basin into Yolo Bypass to promote fish food production.*
>
> *Sacramento River Deepwater Ship Channel Food Study: Repair or replace the West Sacramento lock system to hydraulically reconnect the ship channel with the mainstem of the Sacramento River. The ship channel has the potential to flush food production into the north Delta for Delta Smelt.*

While much has been learned regarding the impacts of environmental conditions on Delta Smelt habitat, some uncertainty remains as to how outflow-related actions, such as those listed above, may affect certain habitat factors and the species' response. We anticipate results from DOP-related studies will assist decision-making processes regarding the SFHA and better inform general management actions to benefit the wild Delta Smelt population, including augmentation of the population through supplementation using cultured fish.

Literature Cited

Baxter, R., Brown, L.R., Castillo, G., Conrad, L., Culberson, S.D., Dekar, M.P., Dekar, M., Feyrer, F., Hunt, T., Jones, K. and Kirsch, J. 2015. An updated conceptual model of Delta Smelt biology: our evolving understanding of an estuarine fish (No. 90). Interagency Ecological Program, California Department of Water Resources.

Brown, L.R., Baxter, R., Castillo, G., Conrad, L., Culberson, S., Erickson, G., Feyrer, F., Fong, S., Gehrts, K., Grimaldo, L. and Herbold, B. 2014. Synthesis of studies in the fall low-salinity zone of the San Francisco Estuary, September–December 2011. US Geological Survey Scientific Investigations Report, 5041, p.136.

California Natural Resources Agency (CNRA). 2016. Delta Smelt resiliency strategy. CNRA, Sacramento, California. Available: http://resources.ca.gov/docs/Delta-Smelt-ResiliencyStrategy-FINAL070816.pdf. (May 2019).

Schultz, A. A., editor. 2019. Directed Outflow Project: Technical Report 1. U.S. Bureau of Reclamation, Bay-Delta Office, Mid-Pacific Region, Sacramento, CA. November 2019, 318 pp.

United States Bureau of Reclamation (USBR). 2012. Adaptive management of fall outflow for delta smelt protection and water supply reliability [Internet]. Revised milestone draft dated 28 June 2012. Sacramento (CA): U.S. Bureau of Reclamation; 99 pp. Available from: https://www.waterboards.ca.gov/waterrights/water_issues/programs/bay_delta/docs/cmnt081712/dfg/cdfgusbr2012.pdf

United States Fish and Wildlife Service (USFWS). 2008. Formal Endangered Species Act consultation on the proposed coordinated operations of the Central Valley Project (CVP) and State Water Project (SWP): U.S. Fish and Wildlife Service, Sacramento, CA.

United States Fish and Wildlife Service (USFWS). 2019. Biological Opinion for the Reinitiation of Consultation on the Coordinated Operations of the Central Valley Project and State Water Project. U.S. Fish and Wildlife Service, Sacramento, CA.

Table 1. Qualitative predictions regarding the effect of X2 (location of 2 ppt salinity isohaline) in or near the Suisun Bay/Marsh area during summer and fall compared to other regions, and within this area during summer and Fall X2 Action periods.

Dynamic Abiotic Habitat Components	**X2 in/near Suisun Region During Summer or Fall Compared to Other Regions and Within Suisun Region During Summer or Fall X2 Action Periods (in parentheses)**	**Chapters within the DOP Technical Report 3 with Related Data**
Low Salinity Habitat Area	Higher (Increases)	
Habitat Complexity	Higher (Increases)	
Hydrodynamic Complexity	Higher (Increases)	
Water Temperature	Lower (Decreases)	
Turbidity	Higher (Increases)	
Contaminants*	Lower (Decreases)	6
Dynamic Biotic Habitat Components		
Delta Smelt Prey Density and Biomass	Higher (Increases)	9
Phytoplankton Density and Biomass	Higher (Increases)	
Harmful Algal Constituents/Cyanotoxins	Lower (Decreases)	
Impact of Non-Native Competitors	Lower	
Impact of Non-Native Predators	Lower	
Delta Smelt Responses		
Occupancy/Residence	Greater (Increases)	1
Health	Greater (Increases)	5,6,7
Growth	Higher (Increases)	6,7
Survival	Higher (Increases)	3
Prey Quality, Foraging Success	Better (Increases)	8
Fecundity	Higher	
Population Range/Distribution	Broader, Less Constricted	1
Life History Diversity	Greater, More Even Spread	1,2,3,4

Chapter 1: Experimental Assessment of Otolith-based Geochemical Reconstructions of Migratory Life History for an Imperiled Estuarine Fish

Authors:

Levi S. Lewis[1*], Malte Willmes[2,3], Leticia Cavole[1], Wilson Xieu[1], Rachel A. Fichman[1], Tien-Chieh Hung[4], Luke Ellison[4], Troy Stevenson[4], Andrew A. Schultz[5], Bruce G. Hammock[6], Swee Teh[6], James A. Hobbs[1,7]

[1] Wildlife, Fish and Conservation Biology, University of California Davis. 1088 Academic Surge, Davis, CA, 95616

[2]Institute of Marine Sciences, UC Santa Cruz, 115 McAllister Way, Santa Cruz, CA, 95064, USA

[3]National Marine Fisheries Service, Southwest Fisheries Science Center, 110 McAllister Way, Santa Cruz, CA, 95064, USA

[4] Fish Conservation and Culture Laboratory, Department of Biological and Agricultural Engineering, University of California Davis. 17501 Byron Hwy, Byron, CA 94514

[5] Green River Basin Fish and Wildlife Conservation Office, United States Fish and Wildlife Service, Vernal, UT, USA

[6] Cell Biology, School of Veterinary Medicine, University of California, 1089 Veterinary Medicine Drive, VetMed 3B, Davis, CA 95616, USA

[7]Bay-Delta Region, California Department of Fish and Wildlife, Stockton, CA, USA

* Corresponding Author: lewis.sci@gmail.com

Abstract

The application of otolith geochemistry to infer the migratory history of fishes first requires controlled experiments to validate methods and assess confidence in inferences gained for wild specimens. The Delta Smelt (*Hypomesus transpacificus*) is a critically endangered estuarine fish that is endemic to the upper San Francisco Estuary (SFE), California, United States, and serves as a key indicator species in the SFE. Understanding variation in habitat use and migratory behaviors of this species is critical for developing effective conservation and management actions. Although otolith-based tools have been developed and applied across multiple life stages of Delta Smelt to

reconstruct age structures, growth, phenology, and migration, several key assumptions for interpreting geochemical signatures in otoliths have yet to be validated. Here, we conducted an experiment using known-age cultured Delta Smelt and mixtures of coastal seawater and freshwaters of the upper SFE to manipulate their salinity history and examine the temporal resolution and accuracy of salinity reconstructions using otolith strontium (Sr) isotope geochemistry. Results indicated that instantaneous transitions from fresh to 3.0 ppt brackish water could be detected within ~1 week and salinity values could be reconstructed to within 0.4-1.1 ppt. These results confirm the utility of otolith geochemistry for examining the migratory behaviors of estuarine fishes in low-salinity habitats.

Keywords: salinity, age, strontium, San Francisco Estuary, Delta Smelt, otolith, isotope

Introduction

The assessment and management of fish populations require knowledge regarding their age-structure, mortality, growth, phenology, and migratory history (Maunder & Punt, 2013). Such information is particularly valuable for endangered species, where high stakes and high uncertainty can hinder the development of effective conservation policies (Meffe, 1986; Runge, 2011). The application of schlerochronology, the study of calcareous age-registering accretionary body parts such as otoliths, vertebrae, and fin spines, in fisheries science has provided several tools to help assess the status and dynamics of managed fish populations (Hunter, Laptikhovsky & Hollyman, 2018; Trofimova et al., 2020).

Otoliths (ear stones) are paired calcium carbonate structures found in the inner ears of bony fishes that are inert and accrete continuously throughout the life of a fish (Pannella, 1971; Campana, 1999). Otolith accretion often results in daily or annual ring patterns that can be used to quantify a fish's age while also providing a permanent archived chronology of its growth and environmental history (Pannella, 1971; Campana & Neilson, 1985; Campana, 1999; Campana & Thorrold, 2001; Starrs, Ebner & Fulton, 2016). Otoliths, therefore, can be used to reconstruct the life history (Hobbs et al., 2010, 2019; Gillanders et al., 2015; Rogers et al., 2019) and vital rates (Feyrer, Sommer & Hobbs, 2007; Black et al., 2011; Martino et al., 2019) of fishes, thus improving our understanding of their population dynamics and movement patterns (Campana, 1999; Starrs, Ebner & Fulton, 2016; Willmes et al., 2018a).

These data are critical for developing effective management plans for endangered species such as California's Delta Smelt (*Hypomesus transpacificus*). The Delta Smelt is an estuarine osmerid smelt that is endemic to the San Francisco Estuary, California, United States. Delta Smelt generally exhibit an annual life cycle and a complex migratory life-history (Moyle et al., 1992; Hobbs et al., 2019). Though this forage fish was historically abundant throughout the upper SFE, the population has declined since the 1980s, likely due to multiple factors including pollution, invasive species, habitat loss, hydrologic modifications, and changing environmental conditions (Feyrer, Nobriga & Sommer, 2007; Sommer et al., 2007; Moyle et al., 2016; Hobbs et al., 2017; Moyle, Hobbs & Durand, 2018). As a result, Delta Smelt are listed as threatened, endangered, and critically endangered under the federal Endangered Species Act (ESA), the California Endangered Species Act (CESA), and the International Union for Conservation of Nature (IUCN) Red List, respectively (U.S. Fish and Wildlife Service, 1993; CDFG, 2010; NatureServe, 2014).

The conservation status of Delta Smelt has resulted in several efforts to protect the species, including setting limits on freshwater exports that directly and indirectly impact the Delta Smelt population through entrainment and habitat modification (Grimaldo et al., 2009; Sommer et al., 2011; Miller et al., 2012; Moyle, Hobbs & Durand, 2018; Hammock et al., 2019; Smith, Newman & Mitchell, 2020). These restrictions on water exports have placed Delta Smelt in the crossfire between conserving species and providing a stable water supply to California's 25 million southern residents and multi-billion dollar agriculture industry (Moyle, Hobbs & Durand, 2018). As a result, studies addressing the habitat needs and responses of Delta Smelt to natural and anthropogenic perturbations have become a key priority for managers and researchers in the region (Hobbs et al., 2017). Key elements of this include quantifying the age structure, hatch dates, movement patterns, and growth rates of Delta Smelt, all of which can be obtained via otolith.

Otolith-based tools have been applied across multiple life stages of Delta Smelt to inform conservation and ecosystem management. For example, otolith increment analysis has been used to describe the daily growth response of wild Delta Smelt to environmental variation (Lewis et al., 2021), and similar analyses are currently being applied to other native fishes in the SFE. Furthermore, given the strong relationship between Sr isotope ratios and salinity in brackish waters of the SFE (Hobbs et al., 2010), geochemical analysis of Sr isotopes in Delta Smelt otoliths has allowed researchers to examine movement patterns across salinity gradients and to quantity diverse life history strategies (e.g., freshwater residents, brackish-water residents, and migrants) utilized by this migratory species (Hobbs et al., 2019).

Before otoliths can be used with confidence to inform the management of fish populations, however, otolith-based methods should first be assessed experimentally including increment periodicity (accuracy), inter-operator error (precision), and consistency in otolith-somatic size relationships (proportionality) (Campana, 2001; Campana & Thorrold, 2001). Similarly, the application of geochemical approaches also need to be experimentally validated to inform the proper interpretation of chemistry results and associated levels of confidence or uncertainty (Barnett-Johnson et al., 2005). Although otolith-based age and growth methodologies for Delta Smelt have been developed and experimentally validated across multiple life stages using known-age specimens (Hobbs et al., 2007; Xieu et al., 2021), key assumptions pertaining to the accuracy and temporal resolution of reconstructed salinity chronologies from joint otolith increment and Sr isotope profiles have yet to be assessed. Here we conducted a manipulative experiment using known-age cultured Delta Smelt and several experimental salinity treatments to examine the temporal resolution and accuracy of migratory life history reconstructions based on combined otolith growth and geochemical analyses. The approaches and results contained in this study provide a valuable step toward improving confidence in otolith-based geochemical studies of the life history of estuarine fishes, thus supporting population models, conservation efforts, and the management of estuarine ecosystems.

Methods

Laboratory-reared (F11) mature Delta Smelt were spawned, and the larvae reared in 2018-2019 at the UC Davis Fish Conservation and Culture Laboratory (FCCL) following standard methods approved by the UC Davis Institutional Animal Care and Use Committee Protocol No. 19747 (Lindberg et al., 2013). In short, fertilized eggs were incubated in columns until hatch, and all fish were held in fresh water at 16 °C. For feed, larvae (< 80 days-post-hatch, dph) received rotifers and

Artemia sp. nauplii, juveniles (80-120 dph) received *Artemia sp.* nauplii and Bio-Oregon BioVita Starter Mash (pellet food), and older juveniles and adults (> 120 dph) received Bio-Oregon BioPro2 Crum#1, each provided *ad libitum*. During culture, tanks were checked daily and fish that were either exhibiting signs of stress or collected for archival were euthanized in 500 mg MS-222 and archived in a -20 °C freezer.

All fish were reared in freshwater in larval tanks for the first 60 dph, after which all fish were transferred to an experimental system which was used to conduct the remainder of the study. The experimental system consisted of 4 tanks on each of two separate recirculating systems, thus allowing for replication within a given salinity treatment (Figure 1-1a). On the same day as the initial transfer (60 dph), System 1, containing the experimental fish, was changed to a 3-ppt mixture of freshwater and coastal seawater, and then at 132 dph it was changed again to a 6-ppt mixture of freshwater and coastal seawater. Fish were collected from each treatment at 195 dph (Figure 1-1b, Figure 1-2). Control fish remained in freshwater for the full 195 days (System 2). Water samples were collected from each system weekly for chemical analysis (Figure 1-2), and water quality (temperature and salinity) was measured daily with a YSI 2030 handheld water quality probe. Both systems were flushed weekly or bi-weekly, as needed, and salinity treatments were maintained by adding freshwater or seawater as needed based on YSI measurements.

Surviving fish were collected at the end of the 195-d experiment, euthanized in 500 mg MS-222, measured, imaged, and archived in a -20 °C freezer. For each fish, the standard length (SL), fork length (FL), and total length (TL) was measured (to the nearest 0.1 cm) using a standard ruler, and each fish was then imaged with a Canon Powershot digital camera (Canon Solutions America Inc., Melville, New York, USA), with each image including millimeter markers to facilitate image calibration. Digital measurements of SL, FL, and TL were then collected for each fish using ImageJ (version 1.8.0) (Abramoff, Magelhaes & Ram, 2006). A total of 12 fish were randomly selected from each treatment for final growth and geochemical analyses (n = 24 total).

Sagittal otoliths were dissected, mounted, and polished following established methods (Hobbs et al., 2007, 2019; Xieu et al., 2021). In short, otoliths were removed from fish using size 10 scalpel blades and ultra-fine tip forceps. Prior to sanding and polishing, whole otoliths were imaged at 40x magnification with an Amscope MU1000 10-Megapixel camera on an Olympus CH30 compound microscope. Rostrum-postrostrum and dorsal-ventral measurements were digitally measured using ImageJ (version 1.8.0). After imaging, otoliths were mounted to glass microscope slides in the sagittal plane using Crystal Bond thermoplastic glue and stored in plastic microscope slide boxes.

Mounted otoliths were wet sanded with 600, 800, and 1200 grit Buehler MicroCut silicon carbide paper and polished with 0.3-µm Buehler MicroPolish alumina on a Buehler Microcloth (Buehler, Lake Bluff, Illinois, USA). Both sides were sanded and polished to expose the core and daily increments. Polished otoliths were imaged at 400x magnification using an Amscope MU1000 10MP camera on an Olympus CH30 compound microscope and stitched together using the photo merge function in Adobe Photoshop 2020 (v. 21.1.1). Left otoliths were initially sanded; however, if the left otolith was broken, lost, or of poor quality, the right otolith was prepared in its place (Xieu et al. 2021). The quality of each otolith image was ranked from 0 to 3 (low to high, respectively), with quality 2 and 3 otoliths preferentially used in analyses.

Otolith increments were annotated, enumerated, and the widths measured from the core to the dorsal edge following established protocols (Xieu et al., 2021). Aging accuracy was quantified to

assess how well otolith-based age estimates reflected the known ages of cultured Delta Smelt. Error in accuracy of a given age estimate for a given fish, reflecting both accuracy and bias (in days), was calculated as the raw deviation from the known age of the fish. Percent error in accuracy (PEA_{fi}) of a given age estimate, an age-normalized estimate of the absolute error, was calculated as the ratio of the absolute error and the known age of the *f*th fish.

Otolith strontium isotope ($^{87}Sr/^{86}Sr$) profiles were quantified by laser-ablation multi-collector inductively coupled plasma mass spectrometry (LA-MC-ICP-MS) following established procedures for Delta Smelt (Hobbs et al., 2010, 2019). Geochemical analyses were conducted at the Interdisciplinary Center for Plasma Mass Spectrometry, University of California, Davis using a Nd:YAG 213 nm laser (New Wave Research UP213) coupled to a Nu Plasma HR MC-ICP-MS (Nu032). Otolith sections were ablated using a 40 μm spot diameter, at 5 μm s^{-1} speed rate, with the laser pulsing at 10-Hz frequency and 2.5- J/cm2 photon output. The temporal integration time in otoliths (i.e., spot size/increment size) was approximately 5-20 days.

The $^{87}Sr/^{86}Sr$ isotope ratio was normalized for instrumental mass discrimination by monitoring the $^{86}Sr/^{88}Sr$ isotope ratio ($^{86}Sr/^{88}Sr = 0.1194$), and rubidium (^{87}Rb) was corrected by monitoring the ^{85}Rb signal and assuming the same mass bias as Sr. Krypton interference (^{86}Kr) originating from the argon supply was subtracted using the on peak zero method before each analysis. Operating conditions and reproducibility of the LA-MC-ICP-MS were evaluated using in-house reference materials consisting of a modern marine otolith from a White Seabass (*Atractoscion nobilis*) collected offshore of Baja California, Mexico. Replicate analyses for the Measurement of in-house references yielded a mean $^{87}Sr/^{86}Sr$ isotope ratio of 0.70909 ± 0.00007 (n = 83, ± s.d.), with a bias of 0.000090 relative to the global average $^{87}Sr/^{86}Sr$ isotope value of modern seawater ($^{87}Sr/^{86}Sr = 0.70918$) (McArthur, Howarth & Bailey, 2001; Mokadem et al., 2015). Processing of otolith chemistry data was performed using the IsoFishR application (Willmes et al., 2018b). We applied a 5-point integration time and a 20-point moving average to the raw data. Outliers were removed based on an interquartile range (IQR) outlier criterion using a 10-point moving average window

Chemistry profiles were proportionally matched to the increment profiles for each fish following established protocols (Hobbs et al., 2019). The smooth.spline function in R, with the number of knots (nknots) and degrees of freedom (df) arguments set to the length of each chemistry profile, was used to provide a continuous model of the chemistry profile that perfectly matched the measured values. The $^{87}Sr/^{86}Sr$ values in the chemistry spline were then matched with each daily increment based on the distance from the core, thus providing merged chemistry-increment profile (Sr isotope chronologies). Major patterns in the merged Sr isotope chronologies were then characterized by applying a final smoothing spline (nknots and df each equal to 0.05*profile length). Transition timings for each fish were quantified using change point analysis conducted on the final Sr isotope chronologies using the cpt.mean function from the changepoint package in (method = AMOC method, pen.value = $3x10^{-5}$).

Each Sr isotope profile reflected the salinity history experienced by a fish throughout its lifetime. Otolith Sr isotope chronologies were converted into salinity chronologies using the established mixing model for the Sacramento-San Joaquin Delta, referenced above (Hobbs et al., 2019). Mean $^{87}Sr/^{86}Sr$ and converted salinity values were calculated using the mid 25% range of each salinity exposure period, when signals were known to be stable. Repeated measures analysis of variance (ANOVA) was used to test the effect of salinity changes on the mean otolith $^{87}Sr/^{86}Sr$ values of all experimental fish (n=12), while bias and accuracy (percent error) in otolith-based salinity values and

the timing of transitions were calculated by comparing estimated and known salinity and transition values. All ordination and modeling were conducted in the R software environment version 3.6.3 (R Core Team, 2019).

Results

Salinity treatments were successfully maintained throughout the experiment (Figure 1-2). Temperature in both treatments was maintained at 16 ± 1.6 °C during the study. Fish in the control treatment and first 60 dph of the experimental treatments experienced salinities of 0.1-0.3, whereas salinities in the experimental treatment were maintained at 3.0 ± 0.1 and 6.0 ± 0.1 from day 60-132 dph and 132-195 dph, respectively (Figure 1-2a). Geochemical signals in water Sr isotopes followed a standard mixing curve (Figure 1-2b-d), with treatments exhibiting Sr isotope ratios of 0.7073 ± 0.0002 in the 0-ppt control and experimental treatments, 0.7088 ± 0.0001 in the 3-ppt experimental treatment, and 0.7090 ± 0.0001 in the 6-ppt experimental treatment. Full-strength coastal seawater (32-ppt) exhibited Sr isotope ratio of 0.70918, matching the ocean end member (Hobbs et al. 2010, Hobbs et al. 2019).

Otolith-based age reconstructions indicated 94% aging accuracy, in alignment with previous studies of Delta Smelt (Xieu et al. 2021). Otolith Sr isotope ratios varied significantly among salinity treatments (Table 1-2, Figure 1-4). Otoliths of fish from the control system (fresh water only) began with a Sr isotope ratio of 0.7072 which declined slightly to 0.7069 later in the experiment (Figure 1-4a). Otoliths of fish from the experimental treatment also started at 0.7074 (fresh water), transitioning to 0.7088 (3 ppt) at approximately 60 dph and to 0.7090 (6 ppt) at approximately 140 dph.

Mean reconstructed salinity estimates of experimental fish varied significantly ($p < 0.001$) as a function of water chemistry (Table 1-2), with known salinities explaining 84% of the variance in otolith-based salinity estimates. Otolith-based salinities were 0.52 ± 0.3 ppt, 3.57 ± 0.77 ppt, and 6.24 ± 1.56 ppt for 0-, 3-, and 6-ppt treatments, respectively (Figure 1-4b). Thus, salinity estimates from otoliths appeared to be biased high by 0.42, 0.57, and 0.24 ppt, with an error of 0.42, 0.67, and 1.11 ppt (for 0, 3, and 6 ppt treatments, respectively) (Table 1-2, Figure 1-4b). Mean transition times for the 0-3 transition, calculated using change point analyses of individual profiles, were 56.5 ± 9.5 dph, thus indicating a bias of -3.5 days and error of 8.3 days. No change point could be calculated for the 3-6 transition from individual profiles due to a low signal to noise ratio; however, a mean increase in Sr isotope values occurred at approximately 140 dph (vs. the known transition time of 132 dph).

Discussion

Here, we conducted an experimental assessment of otolith Sr isotope-based reconstructions of salinity in Delta Smelt, a critically endangered migratory fish in the San Francisco Estuary. Although otolith Sr isotope analysis has been previously used to describe variation in the timing of downstream dispersal for Delta Smelt (Hobbs et al. 2019), the accuracy and temporal resolution of such life history reconstructions has never been quantified for this species. Results indicated that salinities could be reconstructed to within < 0.5 ppt with an absolute error of ± 0.4 to 1.1 ppt (at 0.1 and 6.0 ppt, respectively), and reconstructed 0.1-3.0 transition times were accurate to within < 1

week, though 3.0-6.0 transitions were less clear. As expected, transition times and salinity estimates became less certain with increasing salinity due to the nonlinear nature of the Sr-salinity mixing model (Hobbs et al., 2019). Nevertheless, given that migratory life histories are defined by fresh-to-brackish transitions and that the timings of such transitions can vary by > 100 days in wild fish (Hobbs et al., 2019), these results indicate relatively high levels of accuracy and temporal resolution. Thus, these results demonstrate the utility of otolith Sr isotopes for reconstructing habitat use and the timing of fresh-to-brackish transitions for migratory Delta Smelt. Such validation studies are essential to assess the confidence for all otolith-based environmental reconstructions (Campana, 1990, 2001; Barnett-Johnson et al., 2005).

The value of otolith Sr isotope salinity reconstructions is dependent upon their accuracy and temporal resolution. For example, salinity chronologies are dependent upon the joining of independent age and geochemical profiles, with errors in each influencing the overall resolution. Potential sources of uncertainty therefore include (1) increment analysis, (2) geochemical analysis, and (3) salinity conversion (mixing model). Aging error of Delta Smelt is typically low, with mean accuracy and precision typically > 95% (Xieu et al., 2021). In the present study, aging accuracy was similarly high (94%) to previous studies. Nevertheless, a small proportional error in total age could result in a considerable absolute error in temporal reconstructions for older-age fish. For example, a 5% and 10% age error on a 200 dph fish would equate to 10 and 20 days, respectively. Therefore, uncertainty in the aging process could, in part, explain some variability (bias and error) in reconstructed transition times relative to known values.

Geochemical measurements also exhibit errors that are important to quantify. By using repeated measurements of an in-house standard with known isotopic values (e.g., a marine fish otolith with an oceanic $^{87}Sr/^{86}Sr$ value of 0.70918), we are able to quantify and correct for bias and variance of isotope ratios generated by the instrument (LA-MC-ICP-MS). Based on the full record of in-house standards measured on our instrument, the accepted instrument uncertainty is 0.00005 with a bias of < 0.000001, However, the machine can yield results that are slightly high or low on a given day, thus during each run, results are checked against known standards to ensure no systematic bias.

Although instrument uncertainty is small relative to the overall range of acceptable $^{87}Sr/^{86}Sr$ values in our system (i.e., 0.7054-0.7092), instrument uncertainty becomes increasingly important at higher salinities due to the non-linear nature of the Sr isotope-salinity mixing model (Hobbs et al. 2010, Hobbs et al. 2019). For example, in freshwater, instrument uncertainty might only account for a variance in salinity of approximately 0.3 ppt. In contrast, the same instrument uncertainty can result in a variance of nearly 10 ppt as salinities approach 20 ppt. Thus, it was not surprising that the uncertainty in salinity estimates from otolith Sr isotopes increased with salinity, from ±0.42 at 0.1 ppt to 1.11 at 6 ppt. Surprisingly however, mean bias did not appear to increase with salinity. It is valuable to note that both the salinity and isotopic measurements of water samples that are used to develop the mixing model also exhibit their own levels uncertainty; however, such sources of uncertainty are relatively small compared to the other sources previously described.

Based on the methods described herein, we were able on average to reconstruct the 0.1 to 3.0 ppt transition to within < 4 days. Given that dispersal timings can vary by > 100 days in wild fish (Hobbs et al., 2019), we believe that our results reflect relatively high levels of accuracy and temporal resolution, thus providing a valuable tool for reconstructing the movements of Delta Smelt between freshwater and brackish habitats. Quantifying sources of uncertainty, lag times, and integration times in temporal components of otolith geochemical profiles is key for their proper interpretation and

effective application in fisheries management. For example, temporal integration times vary among and within individual otoliths, complicating salinity reconstructions. This is because *in situ* laser ablation analyses are dependent on a moving spot of fixed dimensions, with the chemical integration time (in days) equivalent to the spot size divided by the mean increment width.

Given that growth varies ontogenetically and in relation to environmental conditions, the temporal integration time varies significantly across an otolith, but can be difficult to account for. For example, Delta Smelt otoliths typically accrete at 2-5 μm d^{-1} (Xieu et al., 2021), thus the temporal integration time for our 40 mm spot size could range on average from 4-20 days. Given that the temporal resolution of otolith-based movements is inversely proportional to the integration time, temporal resolution should be highest for faster-growing and lowest for slower-growing individuals and life stages. This may, in part, explain way we were unable to estimate transition times for the 3.0 to 6.0 transition. For example, this transition occurred later in each fish's life, thus the ontogenetic decrease in growth rate (Xieu et al., 2021) may have increased the integration time, thus decreasing the temporal resolution and our ability to consistent detect a clear changepoint.

Controlled experiments, like the one used in the present study, are needed in order to interpret geochemical signatures in fish otoliths. Our results, based on an experimental approach using known-age cultured specimens and experimental manipulations of salinity, demonstrated that otoliths can provide valuable reconstructions of the early life history of Delta Smelt in freshwater and low-salinity estuarine habitats. Future studies, including controlled *in situ* mesocosm studies, as well as studies using wild-caught fish, could shed additional light on the interpretation of otolith geochemical signatures in wild Delta Smelt. Such experimental approaches can greatly improve the interpretation of otolith-derived metrics that are commonly used to inform and improve the management and conservation of estuarine species.

Acknowledgements

We thank our colleagues at the UC Davis Fish Conservation and Culture Laboratory for their expertise and efforts in rearing and archiving known-age Delta Smelt. Furthermore, the UC Davis Department of Wildlife, Fish, and Conservation Biology; Veterinary Medicine; and Center for Aquatic Biology and Aquaculture for laboratory and logistical support. Constructive reviews from the anonymous reviewers greatly improved the manuscript. This study was funded in part by grants from the California Department of Fish and Wildlife (P1896028) to L. Lewis and J. Hobbs and the U.S. Bureau of Reclamation Directed Outflow Project (R17AC00129) to L. Lewis, J. Hobbs, and S. Teh. The views expressed are those of the authors and do not represent the official opinion of any employer, institution, or government agency.

References

Abramoff Md, Magelhaes Pj, Ram Sj. 2006. Image Processing With Imagej. In: *Optical Imaging Techniques In Cell Biology*. Crc Press, 249–258. Doi: 10.1201/9781420005615.Ax4.

Barnett-Johnson R, Ramos Fc, Grimes Cb, Macfarlane Rb. 2005. Validation Of Sr Isotopes In Otoliths By Laser Ablation Multicollector Inductively Coupled Plasma Mass Spectrometry (La-Mc-Icpms): Opening Avenues In Fisheries Science Applications. 62:6.

Black Ba, Allman Rj, Schroeder Id, Schirripa Mj. 2011. Multidecadal Otolith Growth Histories For Red And Gray Snapper (Lutjanus Spp.) In The Northern Gulf Of Mexico, Usa: Multidecadal Otolith Growth Histories For Red And Gray Snapper. *Fisheries Oceanography* 20:347–356. Doi: 10.1111/J.1365-2419.2011.00588.X.

Campana Se. 1990. How Reliable Are Growth Back-Calculations Based On Otoliths? *Canadian Journal Of Fisheries And Aquatic Sciences* 47:2219–2227. Doi: 10.1139/F90-246.

Campana Se. 1999. Chemistry And Composition Of Fish Otoliths: Pathways, Mechanisms And Applications. *Marine Ecological Progress Series* 188:263–297.

Campana Se. 2001. Accuracy, Precision And Quality Control In Age Determination, Including A Review Of The Use And Abuse Of Age Validation Methods. *Journal Of Fish Biology* 59:197–242. Doi: 10.1006/Jfbi.2001.1668.

Campana Se, Casselman Jm. 1993. Stock Discrimination Using Otolith Shape Analysis. *Canadian Journal Of Fisheries And Aquatic Sciences* 50:1062–1083. Doi: 10.1139/F93-123.

Campana Se, Neilson Jd. 1985. Microstructure Of Fish Otoliths. *Canadian Journal Of Fisheries And Aquatic Sciences* 42:1014–1032. Doi: 10.1139/F85-127.

Campana Se, Thorrold Sr. 2001. Otoliths, Increments, And Elements: Keys To A Comprehensive Understanding Of Fish Populations? *Canadian Journal Of Fisheries And Aquatic Sciences* 58. Doi: Https://Doi.Org/10.1139/F00-177.

Cdfg. 2010. State & Federally Listed Endangered & Threatened Animals Of California. California Department Of Fish & Game,State Of California, The Natural Resources Agency, California. *The Natural Rsources Agency, California*.

Feyrer F, Nobriga Ml, Sommer Tr. 2007. Multidecadal Trends For Three Declining Fish Species: Habitat Patterns And Mechanisms In The San Francisco Estuary, California, Usa. *Canadian Journal Of Fisheries And Aquatic Sciences* 64:723–734. Doi: 10.1139/F07-048.

Feyrer F, Sommer T, Hobbs J. 2007. Living In A Dynamic Environment: Variability In Life History Traits Of Age-0 Splittail In Tributaries Of San Francisco Bay. *Transactions Of The American Fisheries Society* 136:1393–1405. Doi: 10.1577/T06-253.1.

Gillanders Bm, Izzo C, Doubleday Za, Ye Q. 2015. Partial Migration: Growth Varies Between Resident And Migratory Fish. *Biology Letters* 11:20140850. Doi: 10.1098/Rsbl.2014.0850.

Grimaldo Lf, Sommer T, Van Ark N, Jones G, Holland E, Moyle Pb, Herbold B, Smith P. 2009. Factors Affecting Fish Entrainment Into Massive Water Diversions In A Tidal Freshwater Estuary: Can Fish Losses Be Managed? *North American Journal Of Fisheries Management* 29:1253–1270. Doi: 10.1577/M08-062.1.

Hammock Bg, Moose Sp, Solis Ss, Goharian E, Teh Sj. 2019. Hydrodynamic Modeling Coupled With Long-Term Field Data Provide Evidence For Suppression Of Phytoplankton By Invasive Clams And Freshwater Exports In The San Francisco Estuary. *Environmental Management* 63:703–717. Doi: 10.1007/S00267-019-01159-6.

Hobbs Ja, Bennett Wa, Burton Je, Baskerville-Bridges B. 2007. Modification Of The Biological Intercept Model To Account For Ontogenetic Effects In Laboratory-Reared Delta Smelt (Hypomesus Transpacificus). *Fishery Bulletin* 105:30–38.

Hobbs Ja, Lewis Ls, Ikemiyagi N, Sommer T, Baxter Rd. 2010. The Use Of Otolith Strontium Isotopes (Sr-87/Sr-86) To Identify Nursery Habitat For A Threatened Estuarine Fish. *Environmental Biology Of Fishes* 89:557–569. Doi: 10.1007/S10641-010-9672-3.

Hobbs Ja, Lewis Ls, Willmes M, Denney C, Bush E. 2019. Complex Life Histories Discovered In A Critically Endangered Fish. *Scientific Reports* 9:1–12. Doi: 10.1038/S41598-019-52273-8.

Hobbs Ja, Moyle Pb, Fangue N, Connon Re. 2017. Is Extinction Inevitable For Delta Smelt And Longfin Smelt? An Opinion And Recommendations For Recovery. *San Francisco Estuary And Watershed Science* 15:1–19. Doi: 10.15447/Sfews.2017v15iss2art2.

Hunter E, Laptikhovsky V, Hollyman P. 2018. Innovative Use Of Sclerochronology In Marine Resource Management. *Marine Ecology Progress Series* 598:155–158. Doi: 10.3354/Meps12664.

Lewis Ls, Denney C, Willmes M, Xieu W, Fichman Ra, Zhao F, Hammock Bg, Schultz Aa, Fangue N, Hobbs Ja. 2021. Otolith-Based Approaches Indicate Strong Effects Of Environmental Variation On Growth Of A Critically Endangered Estuarine Fish. *Marine Ecology Progress Series* 676:37–56.

Martino Jc, Fowler Aj, Doubleday Za, Grammer Gl, Gillanders Bm. 2019. Using Otolith Chronologies To Understand Long - Term Trends And Extrinsic Drivers Of Growth In Fisheries. *Ecosphere* 10. Doi: 10.1002/Ecs2.2553.

Maunder Mn, Punt Ae. 2013. A Review Of Integrated Analysis In Fisheries Stock Assessment. *Fisheries Research* 142:61–74. Doi: 10.1016/J.Fishres.2012.07.025.

Mcarthur Jm, Howarth Rj, Bailey Tr. 2001. Strontium Isotope Stratigraphy: Lowess Version 3: Best Fit To The Marine Sr - Isotope Curve For 0–509 Ma And Accompanying Look - Up Table For Deriving Numerical Age. *The Journal Of Geology* 109:155–170. Doi: 10.1086/319243.

Meffe Gk. 1986. Conservation Genetics And The Management Of Endangered Fishes. :11.

Miller Wj, Manly Bfj, Murphy Dd, Fullerton D, Ramey Rr. 2012. An Investigation Of Factors Affecting The Decline Of Delta Smelt (Hypomesus Transpacificus) In The Sacramento-San Joaquin Estuary. *Reviews In Fisheries Science* 20:1–19. Doi: 10.1080/10641262.2011.634930.

Mokadem F, Parkinson Ij, Hathorne Ec, Anand P, Allen Jt, Burton Kw. 2015. High-Precision Radiogenic Strontium Isotope Measurements Of The Modern And Glacial Ocean: Limits On Glacial–Interglacial Variations In Continental Weathering. *Earth And Planetary Science Letters* 415:111–120. Doi: 10.1016/J.Epsl.2015.01.036.

Moyle Pb, Brown Lr, Durand Jr, Hobbs Ja. 2016. Delta Smelt: Life History And Decline Of A Once Abundant Species In The San Francisco Estuary. *San Francisco Estuary And Watershed Science* 14:1–30. Doi: 10.15447/Sfews.2016v14iss2art6.

Moyle Pb, Herbold B, Stevens De, Miller Lw. 1992. Life History And Status Of Delta Smelt In The Sacramento-San Joaquin Estuary, California. *Transactions Of The American Fisheries Society* 121:67–77. Doi: 10.1577/1548-8659(1992)121<0067:Lhasod>2.3.Co;2.

Moyle Pb, Hobbs Ja, Durand Jr. 2018. Delta Smelt And Water Politics In California. *Fisheries* 43:42–51. Doi: 10.1002/Fsh.10014.

Natureserve. 2014. *Hypomesus Transpacificus. The Iucn Red List Of Threatened Species* 2014. Doi: Https://Dx.Doi.Org/10.2305/Iucn.Uk.2014-3.Rlts.T10722a174778740.En.

Otterlei E. 2002. Temperature Dependent Otolith Growth Of Larval And Early Juvenile Atlantic Cod (Gadus Morhua). *Ices Journal Of Marine Science* 59:851–860. Doi: 10.1006/Jmsc.2001.1300.

Pannella G. 1971. Fish Otoliths: Daily Growth Layers And Periodical Patterns. *Science* 173:1124. Doi: 10.1126/Science.173.4002.1124.

R Core Team. 2019. R: A Language And Environment For Statistical Computing.

Rogers Ta, Fowler Aj, Steer Ma, Gillanders Bm. 2019. Resolving The Early Life History Of King George Whiting (Sillaginodes Punctatus: Perciformes) Using Otolith Microstructure And Trace Element Chemistry. *Marine And Freshwater Research* 70:1659. Doi: 10.1071/Mf18280.

Runge Mc. 2011. An Introduction To Adaptive Management For Threatened And Endangered Species. *Journal Of Fish And Wildlife Management* 2:220–233. Doi: 10.3996/082011-Jfwm-045.

Smith We, Newman Kb, Mitchell L. 2020. A Bayesian Hierarchical Model Of Postlarval Delta Smelt Entrainment: Integrating Transport, Length Composition, And Sampling Efficiency In Estimates Of Loss. *Canadian Journal Of Fisheries And Aquatic Sciences* 77:789–813. Doi: 10.1139/Cjfas-2019-0148.

Sommer T, Armor C, Baxter R, Breuer R, Brown L, Chotkowski M, Culberson S, Feyrer F, Gingras M, Herbold B, Kimmerer W, Mueller-Solger A, Nobriga M, Souza K. 2007. The Collapse Of Pelagic Fishes In The Upper San Francisco Estuary. *Fisheries* 32:270–277. Doi: 10.1577/1548-8446(2007)32[270:Tcopfi]2.0.Co;2.

Sommer T, Mejia F, Nobriga Ml, Feyrer F, Grimaldo Lf. 2011. The Spawning Migration Of Delta Smelt In The Upper San Francisco Estuary. *San Francisco Estuary And Watershed Science* 9:1–16.

Starrs D, Ebner Bc, Fulton Cj. 2016. All In The Ears: Unlocking The Early Life History Biology And Spatial Ecology Of Fishes. *Biological Reviews* 91:86–105. Doi: 10.1111/Brv.12162.

Trofimova T, Alexandroff Sj, Mette Mj, Tray E, Butler Pg, Campana Se, Harper Em, Johnson Ala, Morrongiello Jr, Peharda M, Schöne Br, Andersson C, Andrus Cft, Black Ba, Burchell M, Carroll Ml, Delong Kl, Gillanders Bm, Grønkjær P, Killam D, Prendergast Al, Reynolds Dj, Scourse Jd, Shirai K, Thébault J, Trueman C, De Winter N. 2020. Fundamental Questions And Applications Of Sclerochronology: Community-Defined Research Priorities. *Estuarine, Coastal And Shelf Science* 245:106977. Doi: 10.1016/J.Ecss.2020.106977.

U.S. Fish And Wildlife Service. 1993. Determination Of Threatened Status For The Delta Smelt. *Federal Register* 58:12854–12864. Doi: Http://Ecos.Fws.Gov/Docs/Federal_Register/Fr2751.Pdf.

Vignon M, Morat F. 2010. Environmental And Genetic Determinant Of Otolith Shape Revealed By A Non-Indigenous Tropical Fish. *Marine Ecology Progress Series* 411:231–241.

Willmes M, Hobbs Ja, Sturrock Am, Bess Z, Lewis Ls, Glessner Jjg, Johnson Rc, Kurth R, Kindopp J. 2018a. Fishery Collapse, Recovery, And The Cryptic Decline Of Wild Salmon On A Major California River. *Canadian Journal Of Fisheries And Aquatic Sciences* 75:1836–1848. Doi: 10.1139/Cjfas-2017-0273.

Willmes M, Ransom Km, Lewis Ls, Denney Ct, Glessner Jjg, Hobbs Ja. 2018b. Isofishr: An Application For Reproducible Data Reduction And Analysis Of Strontium Isotope Ratios (87sr/86sr) Obtained Via Laser-Ablation Mc-Icp-Ms. *Plos One* 13:E0204519. Doi: 10.1371/Journal.Pone.0204519.

Xieu W, Lewis Ls, Zhao F, Fichman Ra, Willmes M, Hung T-C, Ellison L, Stevenson T, Tigan G, Schultz Aa, Hobbs Ja. 2021. Experimental Validation Of Otolith-Based Age And Growth Reconstructions Across Multiple Life Stages Of A Critically Endangered Estuarine Fish. *Peerj* 9:E12280. Doi: 10.7717/Peerj.12280.

452

453 # Tables

454 Table 1-1. Samples included in age and geochemical analyses.

Treatment	Tank	Collection Date	Age	N
Control	6	12/12/2019	195	5
	7	12/12/2019	195	3
	8	12/12/2019	195	4
Experimental	1	12/12/2019	195	3
	2	12/12/2019	195	3
	3	12/12/2019	195	3
	4	12/12/2019	195	3
Total				**24**

455

456

457 Table 1-2. Treatment effects on otolith chemistry and salinity estimates.

458 Results of repeated measures ANOVA examining differences in mean otolith $^{86}Sr/^{88}Sr$ values for each salinity exposure
459 while accounting for the repeated measurements on each fish otolith (Figure 1-4a,b). Bias and mean absolute error of
460 otolith-based salinity estimates are also provided for each salinity exposure and for the 0-3 salinity transition.
461 Transition timings could not be estimated for the 3-6 transition due to low signal:noise values.

Result	Term	Df	SS	MSE	F	P	R^2
Repeated Measures ANOVA	Salinity Period	2	196.70	98.37	90.94	<0.001	0.84
	Error(fishid)	11	10.22	0.93			
	Residuals	22	23.80	1.08			

462

Bias and Error	Salinity	Bias	Error (abs)	Units
Salinity Estimates	0.1 ppt	0.42	0.42	ppt
	3.0 ppt	0.57	0.67	ppt
	6.0 ppt	0.24	1.11	ppt
Transition Timing	0-3 Transition	-3.50	8.30	days
	3-6 Transition	na	na	days

463

464

Figures

Figure 1-1. Experimental design showing (a) arrangement of experimental tanks at the FCCL and (b) transport of coastal seawater for generating salinity treatments.

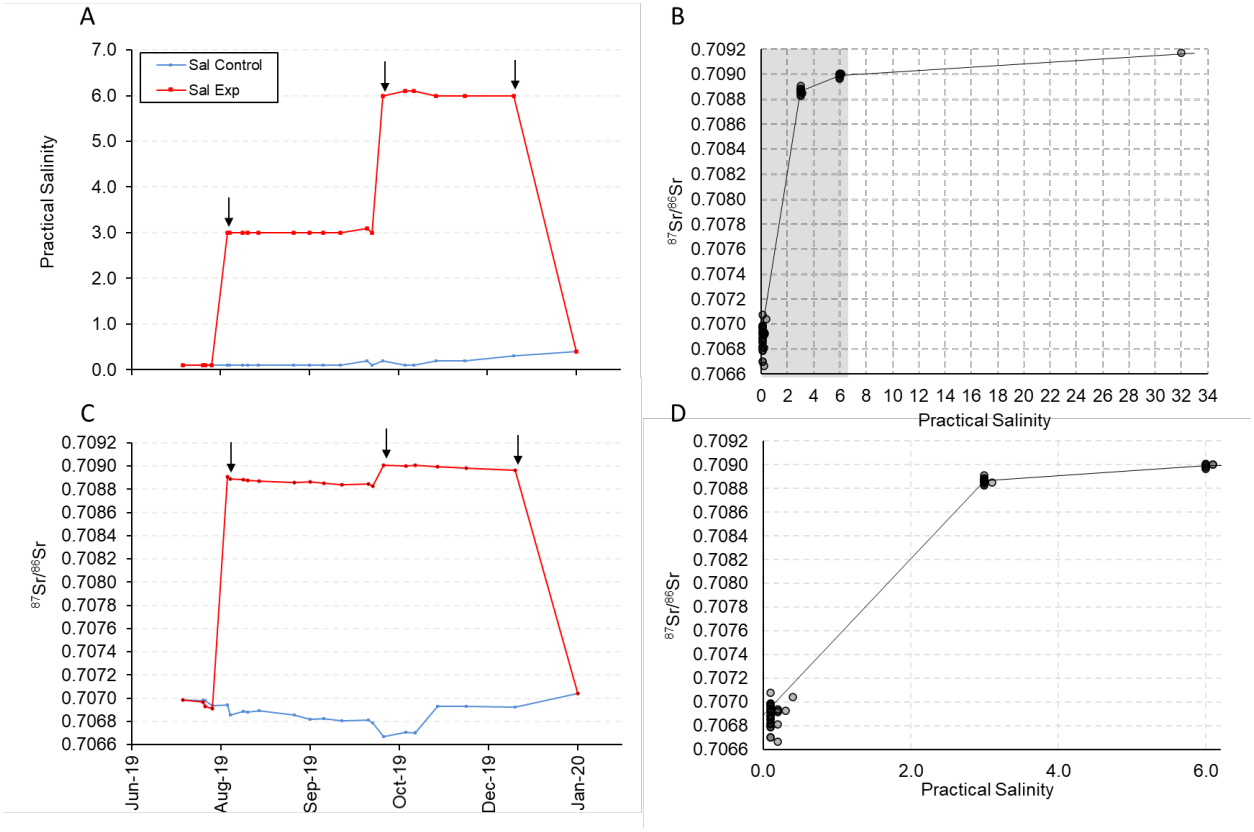

Figure 1-2. Experimental treatments showing the timing of salinity transitions (a), associated changes in water chemistry (c), and relationships between salinity and Sr isotope ratios (b,d).

Shading in (b) represents the zoomed area plotted in (d).

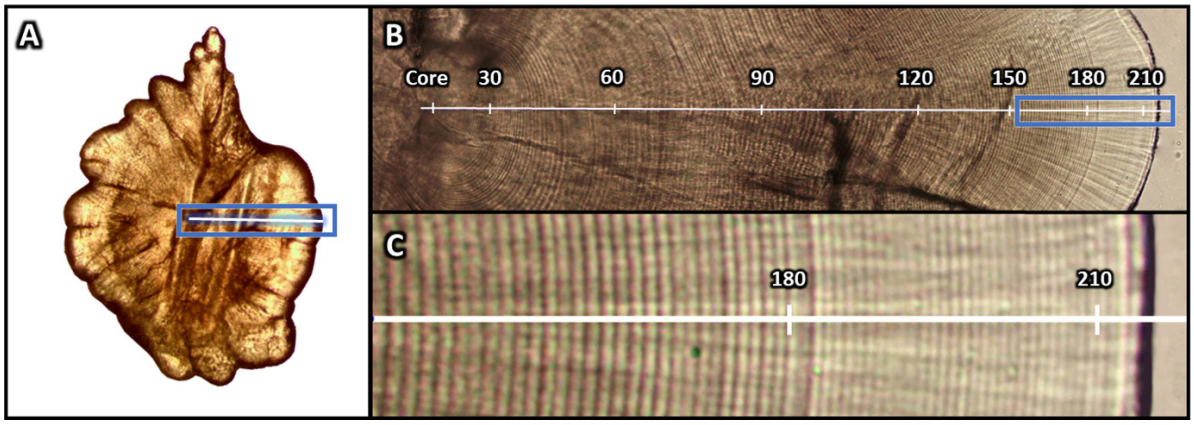

Figure 1-3. Example of a Delta Smelt otolith (a) and increment profiles from core to edge.

Laser ablation chemistry was conducted along the same trajectory as the aging trajectory (white line). Figure from Xieu et al. (2021).

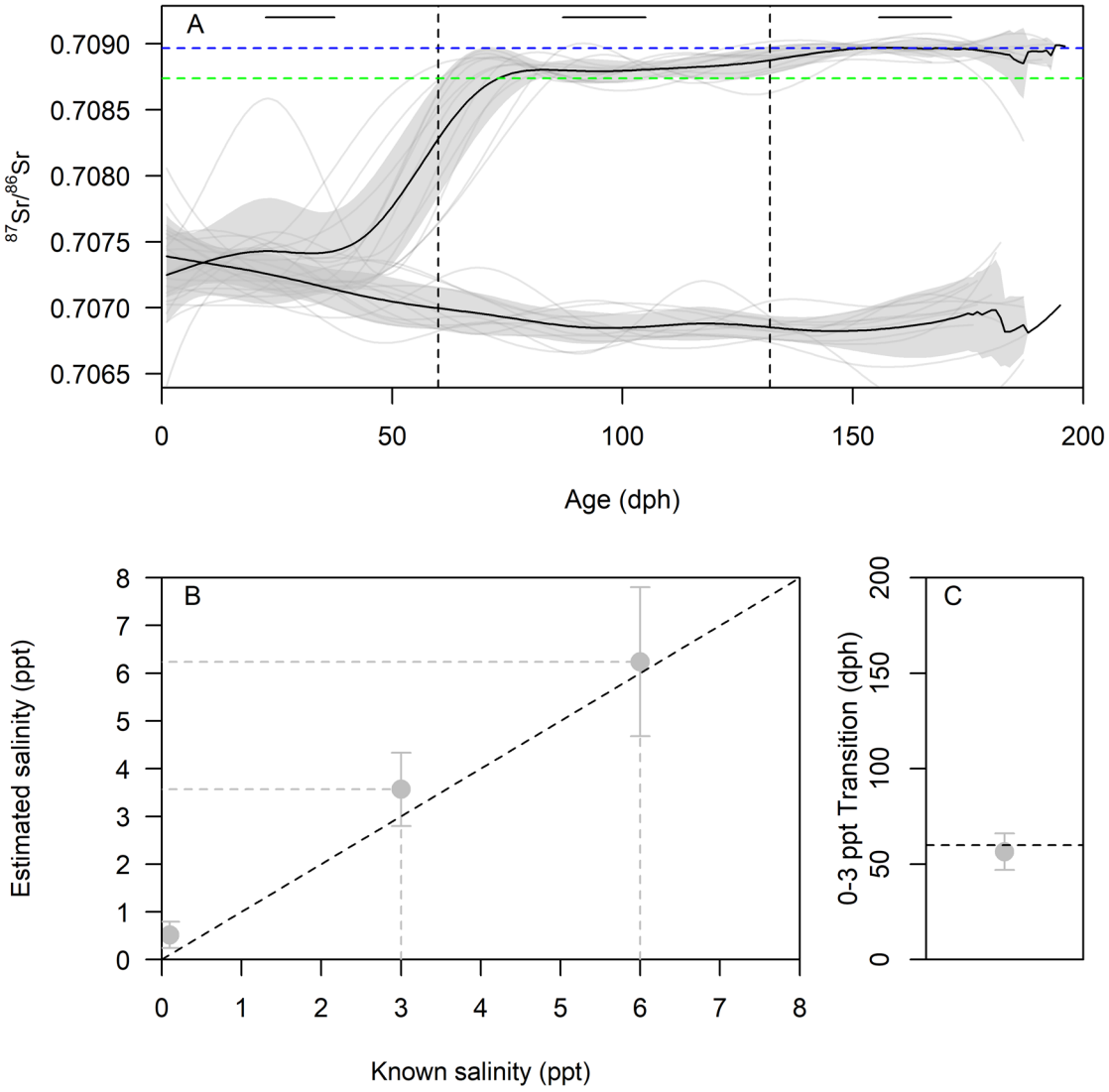

Figure 1-4. Results of otolith geochemical reconstructions of salinity history.

(a) Otolith-based strontium isotope profiles for fish from each of the experimental treatments (n = 24). Black smooth line and grey shading represent the mean and 1 s.d. for each treatment. Vertical dashed lines represent known transition points for experimental fish. Horizontal dashed blue and green lines represent 3- and 6-ppt salinity values based on the established Sr-salinity mixing model. Horizontal bars represent the ranges over which mean values were calculated. (b) Reconstructed salinities for each known salinity treatment for the experimental treatment (n = 12). Black dashed line represents 1:1 and grey dashed lines represent the known and mean estimated salinities. (c) Transition timing for the 0-3 ppt transition experienced by fish in the experimental treatment (n = 12). Horizontal line represents the known 0-3 ppt transition timing. Points and error bars in (b) and (c) reflect the mean ± 1 s.d.

494

495 This page intentionally left blank

496

Chapter 2: Polygenic Discrimination of Migratory Phenotypes in an Estuarine Forage Fish

Authors:

Matthew A. Campbell[1], Shannon E.K. Joslin[1], Alisha M. Goodbla[1], Malte Willmes[2,3], James A. Hobbs[4,5] , Levi S. Lewis[5] and Amanda J. Finger[1*]

Affiliations:

[1]Genomic Variation Laboratory, Department of Animal Science,
University of California, Davis One Shields Avenue Davis, CA 95616, USA
Airport Rd, Stockton, CA 95206, USA

[2]Institute of Marine Sciences, UC Santa Cruz, 115 McAllister Way, Santa Cruz, CA, 95064, USA

[3]National Marine Fisheries Service, Southwest Fisheries Science Center, 110 McAllister

[4] Bay-Delta Region, California Department of Fish and Wildlife, Stockton, 2109 Arch

[5]Otolith Geochemistry and Fish Ecology Lab, Department of Wildlife, Fish and Conservation Biology, University of California, Davis, 1 Shields Ave, Davis, CA 95616
Way, Santa Cruz, CA, 95064, USA

[*]Corresponding Author

Genomic Variation Laboratory, 2403 Meyer Hall, Department of Animal Science
University of California Davis, One Shields Avenue
Davis, CA 95616
ajfinger@ucdavis.edu

Abstract

Migration is a complex phenotypic trait with some species containing migratory and non-migratory individuals. Such life history variation may be attributed in part to plasticity, epigenetics, or genetics. Although considered semi-anadromous, recent studies using otolith geochemistry have revealed life history variation within the critically endangered Delta Smelt. Broadly categorizable as migratory or freshwater residents, we examined RADseq data to test for a relationship between genetic variation and migratory behaviors. As previously shown, we do not find neutral population genetic structure within Delta Smelt; however, we found significant evidence for associations between genetic variants and life history categories. Furthermore, Discriminant Analysis of Principal Components, hierarchical clustering, and machine learning resulted in accurate assignment of fish into freshwater resident or migratory classes based on their genotypes. These results suggest the presence of

adaptive genetic variants relating to life history variation within a panmictic population. Hypotheses supporting this observation are genotype dependent habitat choice and spatially variable selection that both could operate each generation and are not exclusive. Given that cultured Delta Smelt are being used a reserve population, supply for population augmentation, and represent the majority of all individuals in the species, we recommend that the hatchery management strategy consider the frequencies of life history-associated alleles and how to maintain this important aspect of Delta Smelt biological variation while under captive propagation.

Keywords: Adaptive Genetic Variation; Delta Smelt; Migration; Osmeridae; Resident Ecotype; Semi-Anadromy

1. Introduction

The causes of migration may be viewed as both ultimate and proximate (Tinbergen 1963). Ultimate questions are concerned with the broader evolutionary causes, origins, and consequences of migration. The scale of these questions allows comparison across taxa and unifying themes to be proposed such as the increasing food availability hypothesis and diadromy in fishes (Gross et al. 1988). Proximate questions are focused on individuals and the expression of migratory behavior and associated traits in response to environmental cues, genetic background and non-genetic parental affects e.g. (Ferguson et al. 2019). These proximate questions are much more limited in the applicability of results across taxonomic levels. In particular, genetic contributions to the control of migration have been widely documented across the literature e.g. (Liedvogel et al. 2011); however, the identification of a shared genomic region associated with migratory timing in two divergent species of Pacific salmon (*Oncorhynchus*) is atypical (Prince et al. 2017).

Studying the causes of migration relies on the characterization of migratory syndromes – a compendium of movement patterns, behavioral, morphological, and physical traits – of individuals within a population (Sih et al. 2004; Dingle 2006). In the most extreme cases, such as partial migration, within the same population some individuals (migrants) exhibit migratory behaviors, making movements across habitats, whereas others are non-migrating (residents) that complete their life cycle within a single habitat type (Chapman et al. 2012; Kendall et al. 2014; Hobbs et al. 2019). Individuals of a species exhibiting different migratory syndromes are subject to different selection pressures in the form of suites of predators, physical environmental conditions, trophic resources, growth rates, and anthropogenic disturbances (Gross 1987; Moyle and Cech 2004). The complexity of alternative migratory syndromes may be reflected by a complex genetic background with hundreds of loci co-varying between distinct ecotypes e.g. (Pavey et al. 2015). Life history variation and ecotypic differentiation may also be influenced by multiple genes (e.g., over 1,000) that are consolidated into supergenes (Thorneycroft 1975; Lowry and Willis 2010; Pearse et al. 2014; Tuttle et al. 2016; Pearse et al. 2019), with the possibility of multiple (two to several) supergene complexes present within a single species (Huang et al. 2020; Campbell et al. 2021). Despite this potential complexity, large differences in behavioral phenotypes result from minor differences in the genome. For example, major differences in migration timing (e.g., spring-run versus fall-run Chinook Salmon) are associated with a simple Mendelian polymorphism (Thompson et al. 2020). Epigenetic control of migration in Rainbow Trout (*Oncorhynchus mykiss*) has been demonstrated (Baerwald et al. 2016), indicating that heritable non-genetic variation can be considered. In contrast, it is also possible that life history and ecotypic diversity may simply represent phenotypic plasticity without a heritable foundation (Gotthard and Nylin 1995).

Although California's critically endangered Delta Smelt (*Hypomesus transpacificus*) has been broadly described as semi-anadromous (Moyle et al. 1992; Sommer et al. 2011), recent results based on otolith geochemical analyses have identified complex migratory histories in this species (Hobbs et al. 2019). As originally described, the Delta Smelt population is dominated in most years by a semi-anadromous migratory (MIG) phenotype that spawns in freshwater and rears in brackish waters of the San Francisco Estuary. However, Hobbs et al. (2019) also identified a significant fraction of the population as freshwater residents (FWR) as well as a rarer phenotype that hatches and rears in low-salinity brackish habitats (BWR). Although Delta Smelt can be found in different regions of the estuary, no geographic population structuring has been identified for this species, thus it is managed as a single panmictic population (Fisch et al. 2011).

Given that the Delta Smelt population is now < 1% of its former levels (Moyle et al. 2016; Hobbs et al. 2017), the survival of the species now rests largely on hatchery production, which serves as both a genetic-reserve population and a source of fish for supplementation of the wild population. Although culture practices have attempted to follow sound genetic management guidelines, recently this has been hampered by limited introductions of genetic diversity coming from the few wild-caught broodstock in each year that are now no longer possible due to the decline of the naturally reproducing Delta Smelt. No natural origin Delta Smelt contributed to hatchery broodstock in 2020 and 2021. Furthermore, strong hatchery domestication pressures exist on the reserve population (Finger et al. 2018). Any potential genetic diversity associated with life history variation has yet to be considered in the genetic management of the species, thus leaving captive propagation and planned genetic monitoring following the release of cultured individuals into the wild uninformed with respect to life history diversity.

Here, we conduct an interdisciplinary study, combining the results of otolith geochemistry and Restriction site Associated DNA sequencing (RADseq), to investigate several important questions regarding the potential genetic underpinning for the migratory behaviors of Delta Smelt and related implications for species management and conservation. Specifically, we examine whether there is evidence for a genetic basis of life-history variation within Delta Smelt, how any such genetic basis might be characterized, and how well the migratory phenotype of an individual can be predicted from its genotype. Results of this work illuminate the control of migratory behaviors in Delta Smelt and how such phenotypic diversity might be incorporated into culture and supplementation strategies.

2. Materials and Methods

2.1 Samples and Phenotypic Classification

The Delta Smelt otoliths used in this study are part of a long-term dataset and the methods are detailed in Lewis et al. (2021). In short, Delta Smelt were collected by the California Department of Wildlife during the Spring Kodiak Trawl survey between January and March 2013. Otoliths were extracted and prepared for geochemical analysis following the same methods as Hobbs et al. (2019). Otoliths are calcium carbonate structures in the inner ear of most bony fishes that form continuously throughout the life of a fish (Campana 1999). The geochemical analysis of the otoliths can be used to reconstruct movement between different habitats, along rivers and within the different salinities of estuarine environments. Otoliths in this study were analyzed in-situ at the UC Davis Interdisciplinary Center for Plasma Mass Spectrometry using a multi-collector inductively coupled plasma mass spectrometer (*Nu Plasma HR* from Nu Instrument Inc.) interfaced with a

Nd:YAG 213 nm laser (New Wave Research UP213) (LA-MC-ICP-MS). Strontium isotope ratios ($^{87}Sr/^{86}Sr$) were obtained from the core to the ventral edge of the otolith, representing the entire lifespan of the fish. Individuals expressing a freshwater resident (FWR) phenotype exhibit $^{87}Sr/^{86}Sr$ profiles with values remaining below 0.7075 across the entire profile (entire life span), corresponding with practical salinities < 0.5 (i.e., "freshwater"). In contrast, individuals expressing a semi-anadromous migratory (MIG) phenotype exhibit $^{87}Sr/^{86}Sr$ profiles that begin at values < 0.7075 for at least the first 30 days post-hatch, followed by a transition into brackish-water habitats, identified by $^{87}Sr/^{86}Sr$ values between 0.7075 and 0.7092.

2.2 Genetic Analysis

Total genomic DNA was extracted from tissues using a Qiagen DNEasy extraction kit following the manufacturer's protocols. Restriction Site Associated DNA sequencing (RADseq) libraries were generated with the SbfI enzyme with the Best Rad protocol (Ali et al. 2016). Libraries were sequenced with 150 base pair paired-end sequencing on an Illumina HiSeq 4000 (with version x chemistry) at the UC Davis Genome Center.

Sequence data files were aligned to the Delta Smelt reference genome (GCA_021917145.1) with the Burrows-Wheeler Aligner (BWA) using the MEM algorithm (Li and Durbin 2009). Resulting alignments were sorted, PCR duplicates removed and coverage in terms of the number of aligned reads were calculated with SAMtools (Li et al. 2009). We removed individuals from the analysis that constituted the bottom 25% of coverage in terms of aligned reads and lacked complete phenotype classification and sex metadata. For all analyses, we analyzed assembled contigs of the Delta Smelt genome greater than 500 kbp.

We examined signal for neutral genetic structure of sampled Delta Smelt with PCAngsd through Principal Component (PC) analysis (Meisner and Albrechtsen 2018). PCAngsd required a genotype likelihood file that we generated through ANGSD using a SAMtools likelihood model (-GL 1) in the Beagle format (-doGlf 2) (Korneliussen et al. 2014). For quality control thresholds, we required a site to be present in 90% of individuals (-minInd 108), a significance value of 1e-6 (SNP_pval), a minimum mapping quality of 20 (-minMapQ), and a minimum base quality of 20 (-minQ). The resulting genotype likelihoods were analyzed with the default settings of PCAngsd, which includes a minimum minor allele frequency (MAF) of 0.05.

Genetic variants associated with life history variation were identified through a Genome-Wide Association Study (GWAS) implemented in ANGSD. We used a generalized linear framework (-doAsso 2) and provided sex as a covariate (-cov). We applied the following options to the program to provide quality control –minMapQ 20, -minQ 20, -SNP_pval 1e6 and -minInd 91. We specified a SAMtools genotyping model (-GL 1) and -minCount 2. To determine a significance threshold, we do not use a Bonferroni correction as sites in the genome are not independent. We include in our expectations that we expect a false positive concomitant with the discontinuous genome coverage of the Sbf1 RADseq data utilized in the study. Our significance level is then based on a ratio of prior odds and posterior odds with an expected 25 genetic variants that may contribute to life-history variation. Our prior probability *P(T)* is then 25 / number of variants examined, and the prior odds is *P(T)*/1-*P(T)*. Posterior odds may be calculated based on 95% certainty of observing a significant effect that is real: 0.95/(1-0.95). The significance level can be calculated with an upper bound of power (1), such that α = Prior Odds * 1 / Posterior Odds.

We examined the strength of the signal in the genetic data to separate Delta Smelt in FWR and MIG categories with Discriminant Analysis of Principal Components (DAPC), hierarchical clustering and machine learning approaches. With these approaches we used called genotypes generated by ANGSD (-doGeno 2) producing a data set of 0, 1, 2 coded variation. We applied the same quality control thresholds as used previously, with the following changes: a MAF specified (-minMaf 0.05); posterior cutoff specified (-postCutoff 0.9) and a 90% missing individual threshold (-minInd 109). The genotypes were uploaded into R for further analysis (R Development Core Team 2020).

Discriminant Analysis of Principal Components identifies the largest axis of variation between pre-defined groups. We conducted DAPC using the *adegenet* package in R (Jombart 2008) with migratory phenotype supplied as an *a priori* grouping variable. We visualized the ability of DAPC to classify the fish into phenotype classes by visualizing the first discriminant function and generating histograms of the posterior probability of assignment to prior classes. We also examined the contributions (loadings) of each site to the separation of phenotypic classes, and whether genotype calls accurately categorize phenotypes (predictive power). We examined the top 200 associated variants identified by GWAS with ANGSD for respective genotype calls and then generated a heatmap with the *heatmap.2* function of the gplots package. Clustering of samples and loci was done with Ward's distance, and missing data was not treated. The same set of 200 most-associated SNPs was then analyzed with a *k*-nearest neighbor (knn) approach for classification after treating missing data with the *na.roughfix* function of the randomForest package. We divided our dataset into a training data set of 30 randomly selected FWR and 30 randomly selected MIG fish. With the training data set, we identified a best *k* with a repeated *k*-fold cross validation using the *trainControl* and *train* functions of the caret library. A best *k* was identified as being most accurate after 100 sampling events and 10 folds for odd values of *k* from one to 29. The selected best *k* was then applied to all samples for the top associated variants and a cross table of accuracy computed with the *CrossTable* function of the gmodels library.

3. Results

After filtering for coverage and complete metadata, our dataset contained 60 FWR and 61 MIG individuals closely split between sexes (Table 2-1). Sample metadata is reported in Supplemental Document S1. The FWR resident individuals were largely restricted to the northern region of the Sacramento-San Joaquin Delta while MIG individuals were more-widely distributed (Figure 2-1A). Principal Component analysis of 18,765 SNPs did not suggest that phenotype classification and genetic structuring were closely related overall (Figure 2-1B). We identified five significantly associated variants from 13,376 sites examined by GWAS located on four linkage groups (Figure 2-2, Table 2-2). Two of the most-associated variants were found in close proximity, only 153 bp apart, on lg02. The complete association test results are provided as Supplemental Document S2.

Calling genotypes produced 9,068 variants (provided as a R data binary as Supplemental File S1). Within DAPC, we specified 110 PCs (n.pca=110) and a single axis for discriminant analysis (n.da=1). The samples largely were separated into two groups with high posterior probability of assignment (Figure 2-3). Freshwater resident individuals had a mean posterior assignment probability of 0.999 to the FWR class and 6.77×10^{-4} to the MIG class. The mean posterior assignment for the MIG to MIG class was 0.983, with 1.70×10^{-2} of MIG fish to the FWR class. A single MIG individual had a FWR posterior assignment of 1.00, causing a large overall reduction in

MIG posterior assignment probability. The sites contributing more than 0.0005 to the loadings are provided in Supplemental Document S3.

Hierarchical clustering with the 200 genotypes having the strongest phenotypic association creates two major groupings each representing a majority FWR or a majority MIG (Supplemental Figure 2-S1). Most, 88% (53/60), of FWR compose a cluster and most 95% (58/61) of MIG individuals compose the other cluster. The same 200 genotypes exhibited the highest accuracy with knn with k = 13 neighbors (94%, Figure 2-4A). Subsequently, we were able to successfully assign 88% of FWR individuals and 98% of the MIG individuals for an overall accuracy of 94% (Figure 2-4B).

4. Discussion

Summary of results/conclusions

Most spawning of Delta Smelt occurs in freshwaters of the Sacramento-San Joaquin Delta (Hobbs et al. 2019). The majority of offspring express a migratory syndrome and disperse downstream to rear in estuarine habitats within the SFE (semi-anadromous migrants, MIG); however, a significant fraction of the population can remain in freshwater spawning habitats year-round (freshwater residents, FWR). The presence of any genetic foundations for this observed variation in migratory behaviors and adaptive genetic variation relevant to these alternative selective regimes is an important gap in our understanding of the molecular mechanisms underlying life history diversity in this species. Here, we combined otolith Sr isotope geochemistry and genetic sequencing to explore genotype-phenotype associations with respect to the migratory life history of Delta Smelt. Results indicated a significant association between phenotypic and genotypic variation, suggesting that life history complexity in Delta Smelt exhibits a heritable genetic foundation, indicative of evolutionary processes that select for diverse traits. Though more work is needed, translation of this adaptive genetic variation into management-relevant tools remains an under-explored and likely valuable option for improving conservation and recovery efforts for this imperiled endemic species.

Evolutionary Origin of Delta Smelt & Delta Smelt Life History Diversity

The evolutionary origins of Delta Smelt point to a mid-Pliocene to early Pleistocene divergence from Surf Smelt (*H. pretiosus*), a widely-distributed marine species (Ilves and Taylor 2007). A likely scenario is that Delta Smelt diverged through glacial isolation in a freshwater basin in western California, such as in the Pleistocene lakes of the southern San Joaquin Valley (Norris and Webb 1990). Post-glaciation, Delta Smelt were reconnected with the estuary and likely thrived in both freshwater and estuarine habitats. The currently observed diversity in life history is likely a result of pre-existing adaptation to a wide variety of habitats historically available in the Sacramento-San Joaquin Delta (Hobbs et al. 2019). Freshwater inputs that provided large amounts of habitat for FWR Delta Smelt more widely across the Sacramento-San Joaquin Delta have largely now been removed as a result of water diversion and habitat destruction (San Francisco Estuary Institute-Aquatic Science Center (SFEI-ASC) 2014; Hutton et al. 2017). As a result, FWR Delta Smelt were identified largely from the Sacramento Deep Water Ship Channel in the northern region of the Sacramento-San Joaquin Delta. Life history variation within Delta Smelt is likely of ancient origin and constitutes an important aspect of the species' biology.

Genetic Association vs Causative Polymorphisms

Species may react to heterogeneous environments through local adaptation or phenotypic plasticity. The evidence for population genetic structure and associated neutral genetic divergence indicating

local adaptation is lacking in Delta Smelt (Figure 2-1B). The alternative view, that the phenotypic plasticity is underlying life history variation in Delta Smelt is undercut by our results indicating that there is a genetic association with migratory phenotypes in Delta Smelt that is polygenic (Figure 2-2). Two non-exclusive hypothesis may be proposed to explain the observed patterns in Delta Smelt: Genotype-dependent habitat choice and intra-generational spatially varying selection resulting in ecotypic differentiation but not large genetic differentiation e.g. (Pavey et al. 2015). These two hypotheses would recreate generationally the observed patterns within Delta Smelt in terms of phenotype and genotype and have been observed in other organisms e.g. (Bourret et al. 2014; Soria-Carrasco Víctor et al. 2014; Pavey et al. 2015).

The reduced representation sequence data used in this study is unlikely to sample the causative polymorphisms, but should be able to sample regions that are in linkage disequilibrium with a causative genome region. As a result, the variants identified are likely not causative polymorphisms, but may exhibit some linkage to causative polymorphisms. Evaluation of the functional differences reflected by observed genotypic differences rests on further evaluation with more complete genome coverage and understanding of the Delta Smelt's genome. Very strong associations and extremely high assignment accuracy are not expected given the data type; however, we did identify statistically significant associations with life history variation and had high classification success. Overall, we did not identify a clear single region of association; rather at least four separate chromosomal regions were implicated by GWAS. The strongest association identified on lg02 (site 11230464) also contributed the greatest to the separation of FWR and MIG fish through DAPC (Supplemental Document S3). As a whole, the genetic signatures of FWR and MIG fish permitted classification with >90% accuracy into phenotypic class with simple algorithms (Ward's distance clustering, knn).

Management Implications

The Sacramento-San Joaquin Delta is now unable to sustain large numbers of Delta Smelt, with captive Delta Smelt comprising nearly all Delta Smelt in existence. As our results indicate a FWR genetic background and a MIG genetic background, the preservation of life history-associated variants during captive propagation is warranted to maintain the full portfolio of Delta Smelt life histories for reintroduction into suitable habitats. Many diadromous species have evolved diverse portfolios of migratory behaviors that allow them to persist within stochastic environments. Partial migration (co-occurring migratory and resident phenotypes), for example, can enhance the stability and resilience of populations to natural and anthropogenic disturbances (Lundberg 1988; Greene et al. 2010) by serving as a bet-hedging strategy that spreads risk and enhances resilience to environmental stochasticity (Roff 1993, Rochet 2000, Schindler et al. 2010, Moore et al. 2014, Hodge et al. 2016, Brennan et al. 2019). Once quantified, this intraspecific phenotypic variation in migratory behaviors can be translated into management-relevant tools that are key to effective management and conservation (Schindler et al. 2010). Management practices should account for and incorporate such variation, as focusing on a single life history phenotype may not maximize population stability in the long-term (Hilborn et al. 2003; Greene et al. 2010; Schindler et al. 2010; Brennan et al. 2019).

In addition to monitoring life history associated variants in the hatchery population, continued monitoring of highly-associated variants through the course of the reintroduction effort is also advisable. Although the genetic variants identified in this paper are useful for these purposes, there are limitations in genome coverage and the Delta Smelt in this study are all from a single brood year (2012). Monitoring of Delta Smelt life history adaptive genetic variation would be best served

through the identification of genetic or structural variants more closely linked to life history variation through whole-genome sequencing and corroboration across more brood years of Delta Smelt.

Future Research

Though informative, here we only examined a single cohort of Delta Smelt. The importance and prevalence of these associations through time are unknown and genome coverage was not complete. Furthermore, patterns in the relative abundance of each phenotype are likely to covary with changes in environmental conditions that may exert phenotype-specific effects on survival and behavior. For example, variation in freshwater outflow is known to affect dispersal, habitat suitability, and population dynamics of several species (Jassby et al. 1995; Kimmerer 2002). Laboratory studies (Swanson et al. 2000, Feyrer et al. 2007, Nobriga et al. 2008, Komoroske et al. 2014, 2015, Jeffries et al. 2016) and observations of the wild population of Delta Smelt (Lewis et al. 2021; Hammock et al. 2022) indicate strong sensitivity to variation in temperature. In addition to longitudinal studies of life history traits, studies examining the degree to which genotypic and phenotypic variation corresponds with variation in the sensitivity of Delta Smelt to environmental variation remains an unexplored direction of inquiry.

Data Availability

Scripts for analysis and generation of figures in this manuscript are available at https://github.com/MacCampbell/delta-smelt. Demultiplexed sequence data has been deposited with NCBI into the Sequence Read Archive under BioProject XXXXX.

Acknowledgements

We are grateful to our collaborators at the California Department of Fish and Wildlife and U.S. Fish and Wildlife Service for providing Delta Smelt specimens from field collections for use in this study, and the Teh Lab at UC Davis who helped obtain, dissect, and archive specimens. We also thank the many past and present students and staff in the Otolith Geochemistry and Fish Ecology Laboratory at UC Davis who contributed to fish dissections, otolith preparation, and analysis. Otolith archives were maintained in accordance with an approved California Department of Fish and Wildlife Service Section 2081a Memorandum of Understanding to L. Lewis, M. Willmes, and J. Hobbs. Funding for this project was provided in part by grants from the California Department of Fish and Wildlife (CDFW) contracts E1183004, D1583004 and P1696005, and the U.S. Bureau of Reclamation (USBR) contracts R13AP20022 and R17AC00129 to J. Hobbs, S. Teh, and L. Lewis. Additional support was provided by the Delta Stewardship Council (DSC) via postdoctoral fellowships to M. Willmes (Grant No. 1167) and L. Lewis (Grant Nos. 2279, 5298). The content of this material and views described herein do not necessarily reflect the views and policies of the CDFW, USBR, DSC, or UC Davis; nor does mention of trade names or commercial products constitute endorsement or recommendation for use.

References

Ali OA, O'Rourke SM, Amish SJ, Meek MH, Luikart G, Jeffres C, Miller MR. 2016. RAD Capture (Rapture): Flexible and efficient sequence-based genotyping. Genetics. 202(2):389–400. doi:10.1534/genetics.115.183665.

Baerwald MR, Meek MH, Stephens MR, Nagarajan RP, Goodbla AM, Tomalty KMH, Thorgaard GH, May B, Nichols KM. 2016. Migration-related phenotypic divergence is associated with epigenetic modifications in rainbow trout. Molecular Ecology. 25(8):1785–1800. doi:10.1111/mec.13231.

Bourret V, Dionne M, Bernatchez L. 2014. Detecting genotypic changes associated with selective mortality at sea in Atlantic salmon: polygenic multilocus analysis surpasses genome scan. Mol Ecol. 23(18):4444–4457. doi:10.1111/mec.12798.

Brennan SR, Schindler DE, Cline TJ, Walsworth TE, Buck G, Fernandez DP. 2019. Shifting habitat mosaics and fish production across river basins. Science. 364(6442):783–786. doi:10.1126/science.aav4313.

Campana SE. 1999. Chemistry and composition of fish otoliths: pathways, mechanisms and applications. Mar Ecol Prog Ser. 188:263–297.

Campbell MA, Anderson EC, Garza JC, Pearse DE. 2021. Polygenic basis and the role of genome duplication in adaptation to similar selective environments. J Hered.(esab049). doi:10.1093/jhered/esab049. [accessed 2021 Nov 23]. https://doi.org/10.1093/jhered/esab049.

Chapman BB, Skov C, Hulthén K, Brodersen J, Nilsson PA, Hansson L-A, Brönmark C. 2012. Partial migration in fishes: definitions, methodologies and taxonomic distribution. Journal of Fish Biology. 81(2):479–499. doi:10.1111/j.1095-8649.2012.03349.x.

Dingle H. 2006. Animal migration: is there a common migratory syndrome? J Ornith. 147(2):212–220. doi:10.1007/s10336-005-0052-2.

Ferguson A, Reed TE, Cross TF, McGinnity P, Prodöhl PA. 2019. Anadromy, potamodromy and residency in brown trout *Salmo trutta*: the role of genes and the environment. J Fish Biol. 95(3):692–718. doi:10.1111/jfb.14005.

Feyrer F, Nobriga ML, Sommer TR. 2007. Multidecadal trends for three declining fish species: Habitat patterns and mechanisms in the San Francisco Estuary, California, USA. Canadian Journal of Fisheries and Aquatic Sciences. 64(4):723–734. doi:10.1139/F07-048.

Finger AJ, Mahardja B, Fisch KM, Benjamin A, Lindberg J, Ellison L, Ghebremariam T, Hung T-C, May B. 2018. A Conservation Hatchery Population of Delta Smelt Shows Evidence of Genetic Adaptation to Captivity After 9 Generations. Journal of Heredity. 109(6):689–699. doi:10.1093/jhered/esy035.

Fisch KM, Henderson JM, Burton RS, May B. 2011. Population genetics and conservation implications for the endangered delta smelt in the San Francisco Bay-Delta. Conserv Genet. 12(6):1421–1434. doi:10.1007/s10592-011-0240-y.

Gotthard K, Nylin S. 1995. Adaptive plasticity and plasticity as an adaptation: A Selective review of plasticity in animal morphology and life history. Oikos. 74(1):3–17. doi:10.2307/3545669.

Greene CM, Hall JE, Guilbault KR, Quinn TP. 2010. Improved viability of populations with diverse life-history portfolios. Biol Lett. 6(3):382–386. doi:10.1098/rsbl.2009.0780. [accessed 2021 Oct 3]. https://royalsocietypublishing.org/doi/10.1098/rsbl.2009.0780.

Gross MR, editor. 1987. Evolution of diadromy in fishes. (American fisheries society symposium).

368 Gross MR, Coleman RM, McDowall RM. 1988. Aquatic productivity and the evolution of
369 diadromous fish migration. Science. 239(4845):1291–1293.
370 doi:10.1126/science.239.4845.1291.
371 Hammock BG, Hartman R, Dahlgren RA, Johnston C, Kurobe T, Lehman PW, Lewis LS, Van
372 Nieuwenhuyse E, Ramírez-Duarte WF, Schultz AA, et al. 2022. Patterns and predictors of
373 condition indices in a critically endangered fish. Hydrobiologia. 849(3):675–695.
374 doi:10.1007/s10750-021-04738-z.
375 Hilborn R, Quinn TP, Schindler DE, Rogers DE. 2003. Biocomplexity and fisheries sustainability.
376 Proc Natl Acad Sci USA. 100(11):6564. doi:10.1073/pnas.1037274100.
377 Hobbs JA, Lewis LS, Willmes M, Denney C, Bush E. 2019. Complex life histories discovered in a
378 critically endangered fish. Sci Rep. 9(1):16772. doi:10.1038/s41598-019-52273-8.
379 Hobbs JA, Moyle PB, Fangue N, Connon RE. 2017. Is extinction inevitable for Delta Smelt and
380 Longfin Smelt? An opinion and recommendations for recovery. San Franc Estuary
381 Watershed Sci. 15(2). doi:10.15447/sfews.2017v15iss2art2.
382 Hodge BW, Wilzbach MA, Duffy WG, Quiñones RM, Hobbs JA. 2016. Life history diversity in
383 Klamath River steelhead. Transactions of the American Fisheries Society. 145(2):227–238.
384 Huang K, Andrew RL, Owens GL, Ostevik KL, Rieseberg LH. 2020. Multiple chromosomal
385 inversions contribute to adaptive divergence of a dune sunflower ecotype. Molecular
386 Ecology. 29(14):2535–2549. doi:10.1111/mec.15428.
387 Hutton PH, Rath JS, Roy SB. 2017. Freshwater flow to the San Francisco Bay-Delta estuary over
388 nine decades (Part 2): Change attribution. Hydrological Processes. 31(4):2516–2529.
389 Ilves KL, Taylor EB. 2007. Evolutionary and biogeographical patterns within the smelt genus
390 *Hypomesus* in the North Pacific Ocean. J Biogeogr. 35(1):48–64. doi:10.1111/j.1365-
391 2699.2007.01782.x.
392 Jassby AD, Kimmerer WJ, Monismith SG, Armor C, Cloern JE, Powell TM, Schubel JR, Vendlinski
393 TJ. 1995. Isohaline position as a habitat indicator for estuarine populations. Ecological
394 Applications. 5(1):272–289. doi:10.2307/1942069.
395 Jeffries KM, Connon RE, Davis BE, Komoroske LM, Britton MT, Sommer T, Todgham AE,
396 Fangue NA. 2016. Effects of high temperatures on threatened estuarine fishes during
397 periods of extreme drought. Journal of Experimental Biology. doi:10.1242/jeb.134528.
398 Jombart T. 2008. adegenet: a R package for the multivariate analysis of genetic markers.
399 Bioinformatics. 24(11):1403–1405. doi:10.1093/bioinformatics/btn129.
400 Kendall NW, McMillan JR, Sloat MR, Buehrens TW, Quinn TP, Pess GR, Kuzishchin KV, McClure
401 MM, Zabel RW. 2014. Anadromy and residency in steelhead and rainbow trout (*Oncorhynchus*
402 *mykiss*): a review of the processes and patterns. Can J Fish Aquat Sci. 72(3):319–342.
403 doi:10.1139/cjfas-2014-0192.
404 Kimmerer WJ. 2002. Effects of freshwater flow on abundance of estuarine organisms: physical
405 effects or trophic linkages? Marine Ecology Progress Series. 243:39–55.
406 doi:10.3354/meps243039.
407 Komoroske LM, Connon RE, Jeffries KM, Fangue NA. 2015. Linking transcriptional responses to
408 organismal tolerance reveals mechanisms of thermal sensitivity in a mesothermal endangered
409 fish. Molecular Ecology. doi:10.1111/mec.13373.
410 Komoroske LM, Connon RE, Lindberg J, Cheng BS, Castillo G, Hasenbein M, Fangue NA. 2014.
411 Ontogeny influences sensitivity to climate change stressors in an endangered fish.
412 Conservation Physiology. 2(1):cou008–cou008. doi:10.1093/conphys/cou008.
413 Korneliussen TS, Albrechtsen A, Nielsen R. 2014. ANGSD: Analysis of Next Generation
414 Sequencing Data. BMC Bioinform. 15:356. doi:10.1186/s12859-014-0356-4.

Lewis LS, Denney C, Wilmes M, Xieu W, Fichman RA, Zhao F, Hammock BG, Schultz A, Fangue N, Hobbs JA. 2021. Otolith-based approaches indicate strong effects of environmental variation on growth of a Critically Endangered estuarine fish. Mar Ecol Prog Ser. 676:37–56.

Li H, Durbin R. 2009. Fast and accurate short read alignment with Burrows–Wheeler transform. Bioinformatics. 25(14):1754–1760. doi:10.1093/bioinformatics/btp324.

Li H, Handsaker B, Wysoker A, Fennell T, Ruan J, Homer N, Marth G, Abecasis G, Durbin R, 1000 Genome Project Data Processing Subgroup. 2009. The sequence alignment/map format and SAMtools. Bioinformatics. 25(16):2078–2079. doi:10.1093/bioinformatics/btp352.

Liedvogel M, Åkesson S, Bensch S. 2011. The genetics of migration on the move. Trends Ecol Evol. 26(11):561–569. doi:10.1016/j.tree.2011.07.009.

Lowry DB, Willis JH. 2010. A widespread chromosomal inversion polymorphism contributes to a major life-history transition, local adaptation, and reproductive isolation. PLoS Biol. 8(9). doi:10.1371/journal.pbio.1000500.

Lundberg P. 1988. The evolution of partial migration in Birds. Trends in Ecology & Evolution. 3(7):172–175. doi:10.1016/0169-5347(88)90035-3. [accessed 2021 Sep 8]. https://linkinghub.elsevier.com/retrieve/pii/0169534788900353.

McDowall RM. 1997. The evolution of diadromy in fishes (revisited) and its place in phylogenetic analysis. Rev Fish Biol Fish. 7(4):443–462. doi:10.1023/A:1018404331601.

Meisner J, Albrechtsen A. 2018. Inferring population structure and admixture proportions in low-depth NGS data. Genetics. 210(2):719. doi:10.1534/genetics.118.301336.

Moore JW, Yeakel JD, Peard D, Lough J, Beere M. 2014. Life-history diversity and its importance to population stability and persistence of a migratory fish: steelhead in two large North American watersheds. Journal of Animal Ecology. 83(5):1035–1046. doi:10.1111/1365-2656.12212.

Moyle PB, Brown LR, Durand JR, Hobbs, J. A. 2016. Delta Smelt: Life history and decline of a once-abundant species in the San Francisco Estuary. San Franc Estuary Watershed Sci. 14(2).

Moyle PB, Cech JJ. 2004. An introduction to ichthyology. NJ: Prentice-Hall.

Moyle PB, Herbold B, Stevens DE, Miller LW. 1992. Life History and Status of Delta Smelt in the Sacramento-San Joaquin Estuary, California. Trans Am Fish Soc. 121(1):67–77. doi:10.1577/1548-8659(1992)121<0067:LHASOD>2.3.CO;2.

Nobriga ML, Sommer TR, Feyrer F, Fleming K. 2008. Long-term trends in summertime habitat suitability for delta smelt. San Francisco Estuary and Watershed Science. doi:10.15447/sfews.2008v6iss1art1.

Norris RM, Webb RW. 1990. Geology of California. 2nd ed. Toronto: John Wiley & Sons.

Pavey SA, Gaudin J, Normandeau E, Dionne M, Castonguay M, Audet C, Bernatchez L. 2015. RAD sequencing highlights polygenic discrimination of habitat ecotypes in the panmictic American eel. Curr Biol. 25(12):1666–1671. doi:10.1016/j.cub.2015.04.062.

Pearse DE, Barson NJ, Nome T, Gao G, Campbell MA, Abadía-Cardoso A, Anderson EC, Rundio DE, Williams TH, Naish KA, et al. 2019. Sex-dependent dominance maintains migration supergene in rainbow trout. Nat Ecol Evol. doi:10.1038/s41559-019-1044-6. https://doi.org/10.1038/s41559-019-1044-6.

Pearse DE, Miller MR, Abadía-Cardoso A, Garza JC. 2014. Rapid parallel evolution of standing variation in a single, complex, genomic region is associated with life history in steelhead/rainbow trout. Pro R Soc B. 281(1783). doi:10.1098/rspb.2014.0012.

Prince DJ, O'Rourke SM, Thompson TQ, Ali OA, Lyman HS, Saglam IK, Hotaling TJ, Spidle AP, Miller MR. 2017. The evolutionary basis of premature migration in Pacific salmon highlights the utility of genomics for informing conservation. Sci Adv. 3(8):e1603198. doi:10.1126/sciadv.1603198.

R Development Core Team. 2020. R: A language and environment for statistical computing. Vienna, Austria: R Foundation for Statistical Computing. http://www.R-project.org/.

Rochet M-J. 2000. May life history traits be used as indices of population viability? Journal of Sea Research. 44(1):145–157. doi:10.1016/S1385-1101(00)00041-1.

Roff D. 1993. Evolution Of Life Histories: Theory and Analysis. Springer Science & Business Media. [accessed 2021 Aug 3]. https://books.google.com/books?hl=en&lr=&id=_pv37gw8CIoC&oi=fnd&pg=PP13&dq=Roff+population+life+history+diversity&ots=-pFdTErkGg&sig=daZ18A9yYTtYVwjgGlvOC9EeQyA#v=onepage&q=Roff%20population%20life%20history%20diversity&f=false.

San Francisco Estuary Institute-Aquatic Science Center (SFEI-ASC). 2014. A Delta Transformed: Ecological Functions, Spatial Metrics, and Landscape Change in the Sacramento-San Joaquin Delta. Prepared for the California Department of Fish and Wildlife and Ecosystem Restoration Program. Richmond, CA: San Francisco Estuary Institute-Aquatic Science Center Report No.: 729.

Schindler DE, Hilborn R, Chasco B, Boatright CP, Quinn TP, Rogers LA, Webster MS. 2010. Population diversity and the portfolio effect in an exploited species. Nature. 465(7298):609–612. doi:10.1038/nature09060.

Sih A, Bell A, Johnson JC. 2004. Behavioral syndromes: an ecological and evolutionary overview. Trends in Ecology & Evolution. 19(7):372–378. doi:10.1016/j.tree.2004.04.009.

Sommer T, Mejia FH, Nobriga M, Feyrer F, Grimaldo L. 2011. The spawning migration of delta smelt in the Upper San Francisco Estuary. San Franc Estuary Watershed Sci. 9(2):2. doi:10.15447/sfews.2014v9iss2art2.

Soria-Carrasco Víctor, Gompert Zachariah, Comeault Aaron A., Farkas Timothy E., Parchman Thomas L., Johnston J. Spencer, Buerkle C. Alex, Feder Jeffrey L., Bast Jens, Schwander Tanja, et al. 2014. Stick insect genomes reveal natural selection's role in parallel speciation. Science. 344(6185):738–742. doi:10.1126/science.1252136.

Swanson C, Reid T, Young PS, Cech Jr JJ. 2000. Comparative environmental tolerances of threatened delta smelt (Hypomesus transpacificus) and introduced wakasagi (H. nipponensis) in an altered California estuary. Oecologia. 123(3):384–390. doi:10.1007/s004420051025.

Thompson NF, Anderson EC, Clemento AJ, Campbell MA, Pearse DE, Hearsey JW, Kinziger AP, Garza JG. 2020. A complex phenotype in salmon controlled by a simple change in migratory timing. Science. 370(6516):609. doi:10.1126/science.aba9059.

Thorneycroft HB. 1975. A CYTOGENETIC STUDY OF THE WHITE-THROATED SPARROW, ZONOTRICHIA ALBICOLLIS (GMELIN). Evolution. 29(4):611–621. doi:10.1111/j.1558-5646.1975.tb00855.x.

Tinbergen N. 1963. On aims and methods of ethology. Zeitschrift für Tierpsychologie. 20:410–433.

Tuttle EM, Bergland AO, Korody ML, Brewer MS, Newhouse DJ, Minx P, Stager M, Betuel A, Cheviron ZA, Warren WC, et al. 2016. Divergence and functional degradation of a sex chromosome-like supergene. Curr Biol. 26(3):344–350. doi:10.1016/j.cub.2015.11.069.

Tables

Table 2-1. Summary of delta smelt examined in this study reported by phenotype and sex.

Phenotype	Sex	Average Aligned Reads	Sample Size	Total N for Phenotype
FWR	Male	1,080,559	34	60
FWR	Female	1,022,383	26	
MIG	Male	892,302	32	61
MIG	Female	1,091,578	29	

Table 2-2. Most highly-associated genetic variants from association testing.

For each site the chromosome, position, major allele, minor allele, minor allele frequency and *p* – values are reported.

Chromosome	Position	Major	Minor	Frequency	*p* - value
lg01	2467271	G	A	0.09	2.8×10^{-5}
lg02	11230311	A	C	0.31	3.1×10^{-5}
lg02	11230464	T	G	0.30	1.0×10^{-5}
lg15	2268817	C	T	0.24	3.6×10^{-5}
lg23	7996307	G	A	0.15	3.9×10^{-5}

Figures

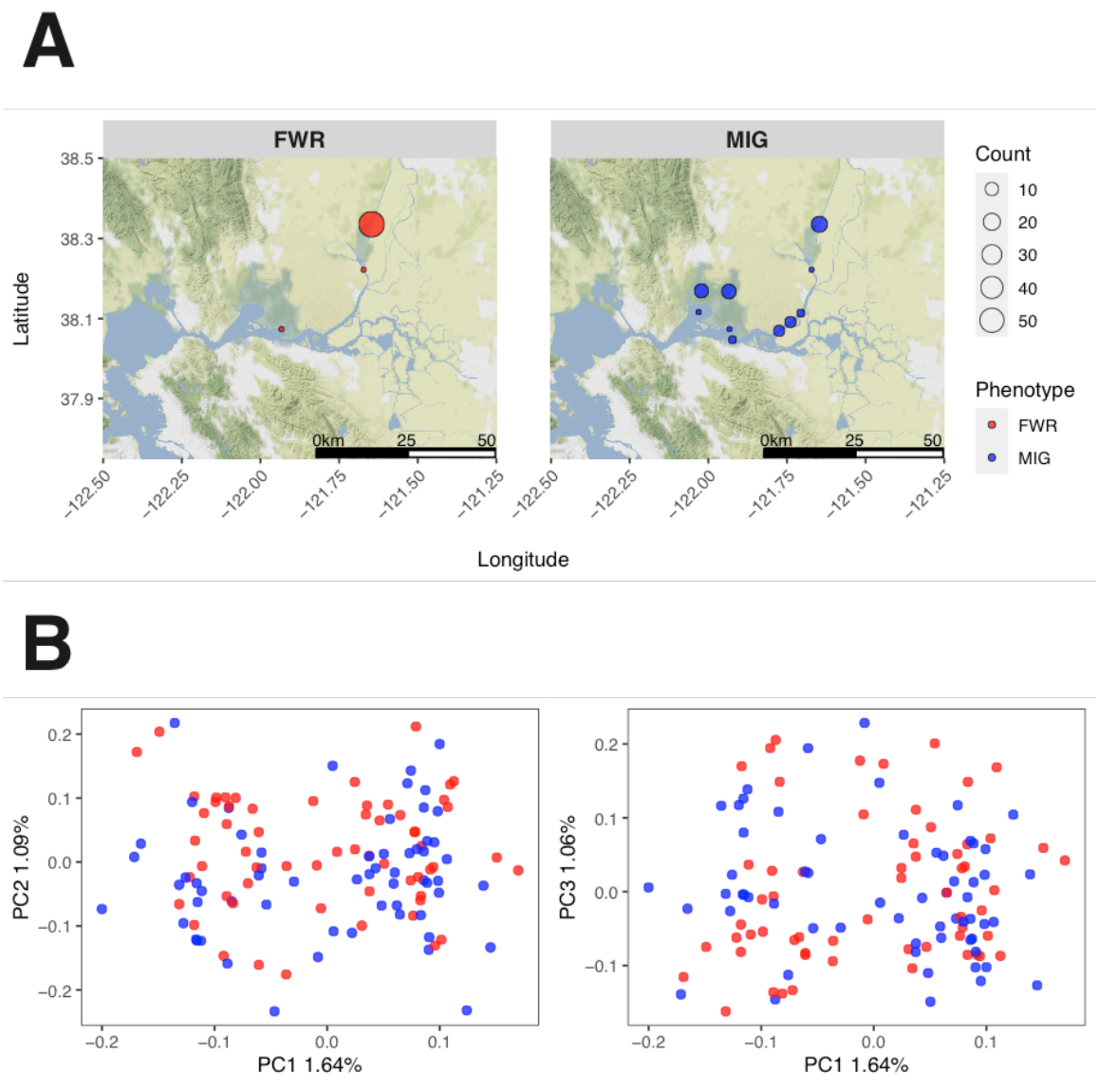

Figure 2-1. Panel A shows the geographic distribution of delta smelt samples examined in this study, facets are split between freshwater resident (FWR) and migratory (MIG) individuals.

Panel B shows a Principal Component (PC) analysis of individuals examined in this study. The facets are split between a plot of PC1 vs PC2 and PC1 vs PC3. In both panels, freshwater residents are indicated by red and migratory by blue.

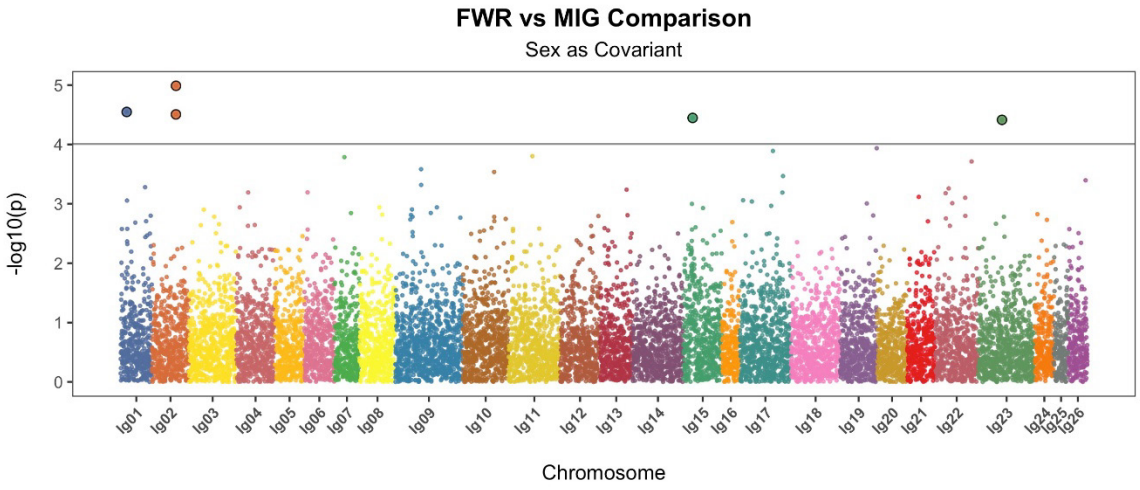

Figure 2-2. Manhattan plot of genome-wide association testing contrasting freshwater resident (FWR) and migratory (MIG) delta smelt individuals.

Sex was provided as a covariant and the linkage groups of the delta smelt genome assembly are shown. Sites exceeding the significance threshold are indicated with larger filled circles and the significance level (p = 9.9e-05, -log10(p) = 4.00).

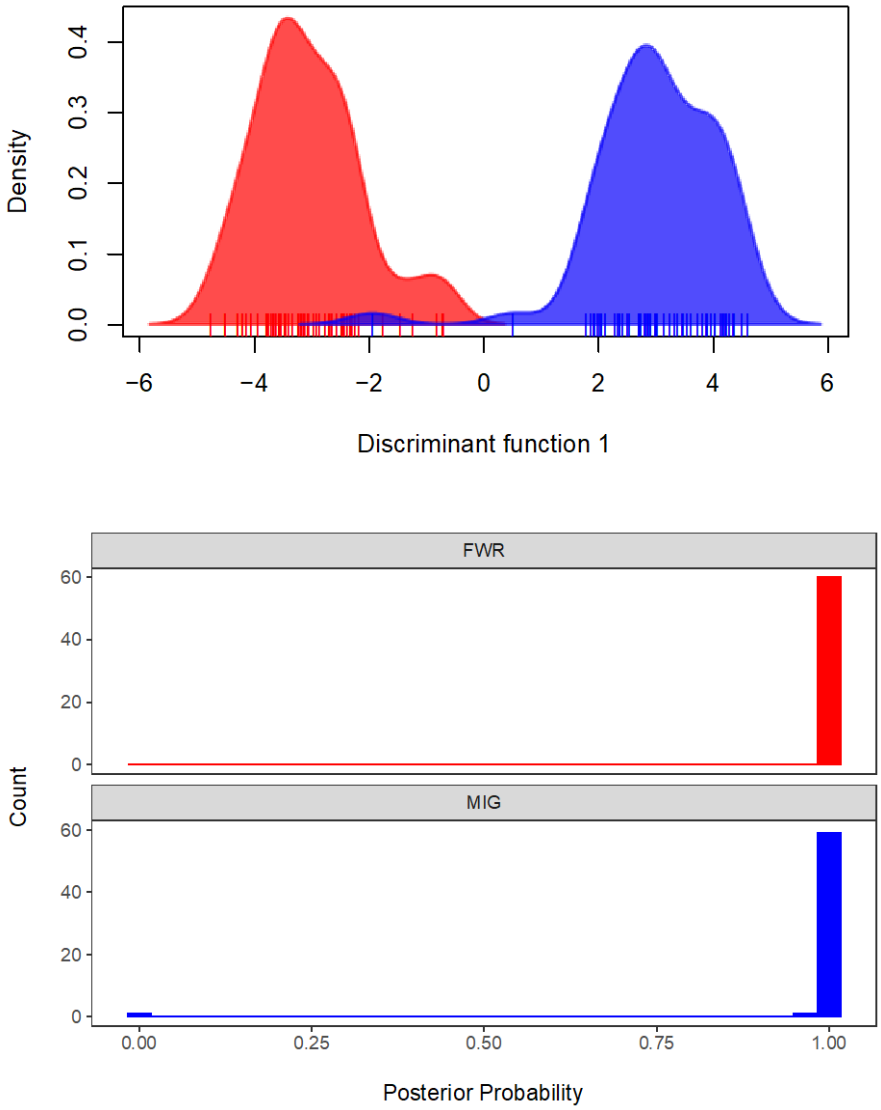

Figure 2-3. Panel A shows density of delta smelt individuals along the discriminant function generated by Discriminant Analysis of Principal Components (DAPC).

Red indicates freshwater resident (FWR) and blue migratory (MIG). Individuals are indicated by with a carpet plot. Panel B plots the posterior probability of fish being assigned to the phenotypic class of origin. FWR individuals are plotted in a facet in red and MIG are plotted in a second facet in blue.

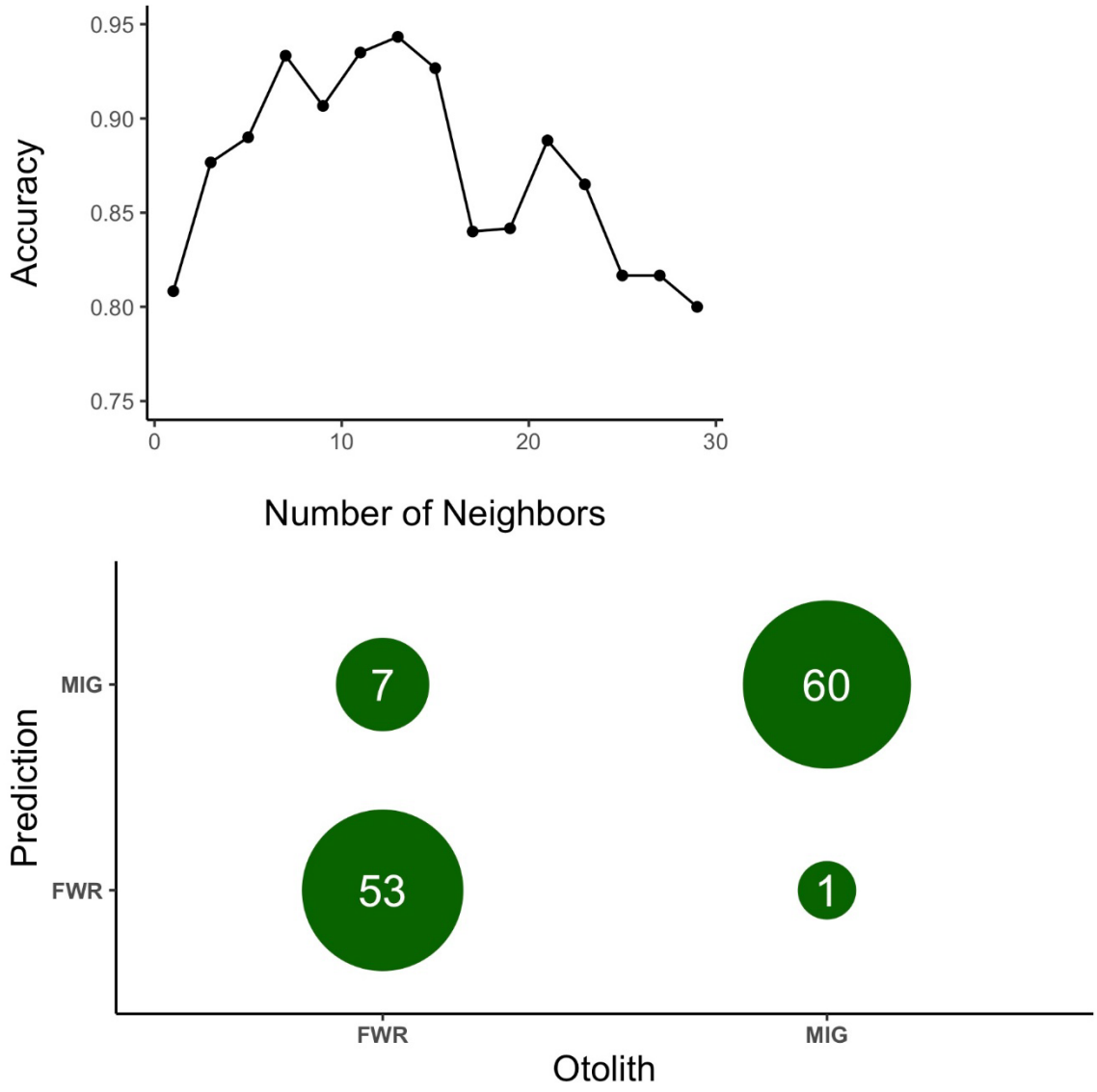

Figure 2-4. Results of *k*-nearest neighbor classification of life history phenotypes.

Panel A shows overall accuracy from cross-validation identifying an optimal number of neighbors with half the data set as a training set (0.94, k = 13). Panel B shows the success in assigning the dataset to categories based on the training data set as a cross table.

544

545 This page intentionally left blank

546

Chapter 3: Climate Variability Alters the Migratory Life History of California's Critically Endangered Delta Smelt

Authors:

Levi Lewis[1], Christian Denney[1], Malte Willmes[2,3], Leticia Cavole[1], Wilson Xieu[1], Eva Bush[1], Nann Fangue[1], Justin J. Glessner[4], Bruce Hammock[5], Swee Teh[5], Andrew A. Schultz[6], James A. Hobbs[1,7]

[1] Wildlife, Fish and Conservation Biology, University of CA, Davis, Davis, CA, USA

[2]Institute of Marine Sciences, UC Santa Cruz, 115 McAllister Way, Santa Cruz, CA, 95064, USA

[3]National Marine Fisheries Service, Southwest Fisheries Science Center, 110 McAllister Way, Santa Cruz, CA, 95064, USA

[4] Interdisciplinary Center for Plasma Mass Spectrometry, University of CA, Davis CA, USA

[5] Department of Anatomy, Physiology, and Cell Biology, University of CA, Davis, CA, USA

[6] Green River Basin Fish and Wildlife Conservation Office, United States Fish and Wildlife Service, Vernal, UT, USA

[7] Bay-Delta Region, California Department of Fish and Wildlife, Stockton, CA, USA

Abstract

Estuarine fishes have evolved diverse life history portfolios that can enhance population stability and resilience to stochastic variation in climate. The Delta Smelt, a critically endangered annual fish that is endemic to the upper San Francisco Estuary, expresses several distinct migratory and resident phenotypes; however, temporal variation in the relative importance of these life-history phenotypes remains unknown. Using an archive of > 2000 Delta Smelt collected from 2003-2019, we measured otolith Strontium isotope ($^{87}Sr/^{86}Sr$) ratios of each fish to determine its life history phenotype. We then examined interannual variation in the phenotypic composition of each annual cohort's life history and asked how each life history responded to variation in regional climate. The migratory phenotype was dominant in all years examined; however, a resident freshwater phenotype was also present in most years and occasionally abundant, while a resident brackish-origin phenotype was also observed, but never abundant. The relative abundance of each phenotype changed in response to variation in climate, with cooler-drier years favoring more freshwater residents, and warmer-wetter years favoring migrants and brackish-origin fish. These results suggest that, historically, during cooler climate conditions and prior to widespread degradation of freshwater habitats, the Delta Smelt population might have largely been comprised of the freshwater resident phenotype. If true, climate change could, in part, explain the contemporary dominance of the migratory phenotype,

with continued warming of the estuary further reducing the diversity and resilience of the remaining Delta Smelt population.

Keywords: partial migration, otolith, Strontium isotopes, San Francisco Estuary, freshwater outflow, climate change, temperature

Introduction

Climate change is rapidly altering the abiotic conditions of aquatic environments globally, impacting the population dynamics, distributions, and movements of aquatic organisms (Pershing et al. 2015, Morley et al. 2018, Avaria-Llautureo et al. 2021). In estuaries, abiotic environments are naturally variable, with climate change likely driving even greater variability (Swain et al. 2018). Although estuarine fishes have adopted many strategies to survive within naturally stressful and unpredictable environments (Moyle et al. 2010, Potter et al. 2013), climate change is likely to create additional challenges for even these highly plastic species. In the San Francisco Estuary (SFE), USA, for example, reduced freshwater outflows, elevated salinities, intensified droughts and floods, and warming waters (Cloern et al. 2011, Swain et al. 2018) are expected to compound with naturally variable conditions (Gasith & Resh 1999, Moyle et al. 2010) and multiple anthropogenic disturbances (Nichols et al. 1986) to possibly drive several migratory species to extinction (Moyle et al. 2011, Brown et al. 2016, Hobbs et al. 2017).

Some estuarine species have evolved diverse portfolios of migratory behaviors in order to persist within their dynamic environments. For example, partial migration (the presence of both migratory and resident phenotypes in a population) can enhance the stability and resilience of populations to natural and anthropogenic disturbances (Lundberg 1988, Greene et al. 2010). Such phenotypic diversity can serve as a bet-hedging strategy, whereby a diverse portfolio of behaviors within a population spreads risk and enhances resilience to environmental stochasticity (Roff 1993, Rochet 2000, Schindler et al. 2010, Moore et al. 2014, Hodge et al. 2016, Brennan et al. 2019). Descriptions of intraspecific phenotypic variation in migratory behaviors, and translation of this life history diversity into management-relevant tools, remains key to developing effective fisheries management and conservation policies (Schindler et al. 2010). For example, stocks or contingents that express different migratory behaviors often occupy distinct habitats throughout their lives and are exposed to different suites of natural and anthropogenic stressors. Focusing management actions only on a specific life history phenotype, therefore, may not maximize population stability in the long-term (Schindler et al. 2010, Greene et al. 2010, Brennan et al. 2019).

Fish otolith ("ear stone") geochemistry can be used to reconstruct individual fish movements and can quantify variation in fish life history strategies are valuable for informing fisheries management and conservation efforts (Rochet 2000, Schindler et al. 2010, Moore et al. 2014).. This approach relies on otoliths recording the geochemical and environmental conditions previously experienced by each individual fish (Campana 1999). In rivers, for example, Strontium isotopes ($^{87}Sr/^{86}Sr$) vary predictably with the geology of their surrounding watersheds (Barnett-Johnson et al. 2008, Bataille & Bowen 2012, Willmes et al. 2021). In estuaries, Strontium isotopes mix conservatively between freshwater and seawater end members to provide predictable patterns that correlate strongly with salinity (Ingram & DePaolo 1993, Hobbs et al. 2010, 2019, Phillis et al. 2011). Since $^{87}Sr/^{86}Sr$ is conservatively incorporated into the calcified structures of fishes with little or no fractionation (Walther & Limburg 2012), measurements from otoliths can be used to reconstruct the origins and

movements of fishes among different habitats in freshwater systems (Barnett-Johnson et al. 2008, Willmes et al. 2021) and among salinity zones in estuarine habitats (Hobbs et al. 2010, 2019). For example, this tool allows for the quantification of different migratory phenotypes expressed by diadromous species (Brennan et al. 2015a, Sturrock et al. 2015, Hodge et al. 2016, Hobbs et al. 2019), allowing researchers to reconstruct the life history and movement of fishes.

Although life history diversity has been broadly examined for several abundant, large-bodied species that support valuable recreational and commercial fisheries (Brennan et al. 2015, Sturrock et al. 2020), much less is known about life history diversity in "less charismatic" forage fishes such as endangered Delta Smelt (*Hypomesus transpacificus*). The Delta Smelt is an annual pelagic fish in the family Osmeridae that is endemic to fresh and low-salinity (< 10 psu) waters of the upper San Francisco Estuary. Though historically abundant, the population has declined dramatically since the 1980s to < 1% of its historic abundance (Mac Nally et al. 2010, Thomson et al. 2010, Moyle et al. 2016). Several likely interacting mechanisms for this decline have been proposed including water exports (Smith et al. 2020), habitat loss (Feyrer et al. 2007, Nobriga et al. 2008), introduction of non-native species (Kimmerer et al. 1994, Nobriga et al. 2013), pollution (Fong et al. 2016), and climate change (Knowles & Cayan 2002, Cloern et al. 2011, Brown et al. 2016). The species is now listed as threatened, endangered, and critically endangered according federal, state, and international conservation assessments, respectively (U.S. Fish and Wildlife Service 1993, CDFG 2010, NatureServe 2014) and is believed to be at immediate risk of extinction (Hobbs et al. 2017). Policies for conserving Delta Smelt have occasionally limited freshwater exports that support California's multi-billion-dollar agriculture industry and 29 million southern residents, thus placing this endangered species in the crossfire between stakeholders focused on species and habitat conservation and those focused on water supply and agriculture (Moyle et al. 2018, Reis et al. 2019, Scoville 2019).

The Delta Smelt was initially described as an annual semi-anadromous migratory species, characterized by spring spawning and hatching in freshwater habitats upstream, followed by downstream dispersal to low-salinity brackish habitats (e.g., 0.5-6 psu) in the summer, and upstream migration to freshwater spawning habitats again in winter (Moyle et al. 1992, Dege & Brown 2004, Sommer et al. 2011). This migratory behavior is believed to maximize fitness by enhancing feeding (Hammock et al. 2017, 2019); however, field observations have suggested that some Delta Smelt may remain in certain habitats year-round (Nobriga et al. 2008, Merz et al. 2011, Murphy & Hamilton 2013, Polansky et al. 2019). Reconstruction of individual migration histories using otolith $^{87}Sr/^{86}Sr$ geochemistry identified multiple life history phenotypes in the 2011 Delta Smelt cohort (Hobbs et al. 2019) (Figure 3-1). This study reconciled both views, by reconstructing the individual migratory histories and the identification of multiple life history phenotypes in the 2011 Delta Smelt cohort (Hobbs et al. 2019) (Figure 3-1). For example, though the bulk of the population exhibited semi-anadromous migrations (migratory phenotype—MIG), a substantial fraction of individuals hatched and reared in freshwater habitats year-round (freshwater resident phenotype—FWR), while a few others hatched and reared directly in low-salinity brackish-water habitats (brackish-water resident phenotype—BWR) (Figure 3-1D). Thus, Delta Smelt exhibited both resident and migratory phenotypes, similar to 'partial migration' observed in other migratory species such as rainbow trout (Hendry 2004, Moore et al. 2014, Gillanders et al. 2015, Hodge et al. 2016).

Since Hobbs et al. (2019) only examined a single cohort of Delta Smelt the importance and prevalence of each migratory phenotype through time remained unknown. Furthermore, the relative abundance of each phenotype was likely to be influenced by interannual variation in environmental

conditions that may exert phenotype-specific effects on survival and behavior. For example, interannual variation in freshwater outflow can influence downstream dispersal, the suitability of habitats, and the population dynamics of estuarine species (Jassby et al. 1995, Kimmerer 2002b). Similarly, water temperatures during the warmest summer months are associated with low abundance and physiological stress for Delta Smelt, and can vary considerably among years and habitats (Swanson et al. 2000, Feyrer et al. 2007, Nobriga et al. 2008, Komoroske et al. 2014, 2015, Jeffries et al. 2016). Thus, environmental conditions may favor one life history strategy or another from year to year, predictably altering their relative abundances.

We used otolith $^{87}Sr/^{86}Sr$ to identify the life histories of > 2000 adult Delta Smelt collected during winter-spring of 2003-2019. We then examined how the relative contributions of each phenotype to the adult spawning population likely varied among years, regions of the estuary, and between males and females. Last, we explored how the phenotypic composition of each cohort varied in relation to regional patterns in climate (i.e., freshwater outflow and water temperature). Given that Delta Smelt are sensitive to thermal stress (Komoroske et al. 2014b, 2015, Lewis et al. 2021), we predicted that cooler-wetter years, when there is more suitable freshwater habitat, would support a relatively larger population of freshwater resident phenotypes, and that warmer-dryer years (i.e., drought) would correspond with more migratory and brackish-origin fish. Results of this work are key for informing dynamic population models, guiding conservation hatchery and supplementation programs, and for developing new management actions to sustain this critically endangered endemic species.

Methods

Study Site

The San Francisco Estuary is the largest semi-enclosed estuary along the West Coast of North and South America (area of ~ 11913 km^2). Most freshwater enters the estuary through the Sacramento-San Joaquin River Delta. The freshwater that is not exported flows into Suisun Bay, where it mixes with higher salinity bay waters, creating a broad gradient in salinity (Nichols et al. 1986). Freshwater flows into the Delta vary seasonally and interannually, reflecting a Mediterranean climate with cool-wet winters, dry-hot summers, and high interannual variability in total precipitation, commonly categorized as "dry" (drought) and "wet" years (Dettinger & Cayan 2003, Cloern et al. 2011), the effects of which are exacerbated by water diversions and exports, particularly in drought years, especially in the late summer and fall (Reis et al. 2019).

California, like other "hydraulic societies" (Scoville 2019), is characterized by a large and intricately engineered water storage and transport system comprised of thousands of dams, reservoirs, levees, and diversions that profoundly impact the hydrology of the SFE. Freshwater flows into the SFE are highly regulated by several major dams and reservoirs which can capture approximately half the total annual runoff in average years. Approximately 60% of the available freshwater flow is diverted annually out of the system, primarily by agriculture upstream or by the California State Water Project (SWP) and the federal Central Valley Project (CVP) water export facilities, which each divert flows southward to support agricultural and municipal demands (Cloern & Jassby 2012a, Reis et al. 2019, Hammock et al. 2019b). This hydrologic alteration compounds with many other anthropogenic stressors including invasive species, pollution, and climate change; jeopardizing the existence of native species and ecosystem services (Nichols et al. 1986, Moyle et al. 2011, Gilby et al. 2021).

Sample Collection

Adult Delta Smelt were collected throughout their range during the spawning season (January-May) by the California Department of Fish and Wildlife's Spring Kodiak Trawl (SKT) Survey (Damon & Chorazyczewski 2021) from 2003 to 2019. Given that Delta Smelt is mostly an annual species, the cohort year (or year-class) is defined as the survey year minus 1 (resulting in cohort years of 2002 to 2018. The SKT survey uses a 7.6-m wide by 1.8-m depth Kodiak trawl towed between two boats at the surface for 10-minutes per tow among 40 fixed sampling stations located from the Napa River in the west to the San Joaquin River in the south and the Sacramento River Deep Water Ship Channel to the north, encompassing the known distribution of adult Delta Smelt (Figure 3-2). At each station, up to 30 individuals were given unique serial codes, and fork-length was measured to the nearest 1 mm) before being frozen in liquid nitrogen and subsequently stored at -80 ºC (Teh et al. 2016). Otoliths of approximately 30-200 fish were dissected and analyzed in each year, except for 2008 (when no samples were preserved for otolith analysis) and in 2017-2018 when abundances and catches reached historic lows. Where possible, samples were stratified among regions in approximate proportion to the total SKT catch for that year (Table 3-1, Supplement 1).

A total of 2,162 Delta Smelt were included in the study, with 1,053 from the North Delta (including the upper Sacramento River, Shipping Channel, and associated sloughs), 17 from the South Delta (including the upper San Joaquin River, Shipping Channel, and associated sloughs), 486 from the Central Delta (including the Lower Sacramento River, Lower San Joaquin River and their Confluence), and 606 from the West Delta (including Suisun Bay-Marsh, Lower Napa River, and Carquinez Straight) (Figure 3-2B, Table 3-1). Samples were largely representative across years and regions, averaging overall 21% of the entire catch during the study period (Table 3-1, Supplement 1). Many years exceeded this value (e.g., 67%, 71%, 91%, and 100% of the catch in years 2013, 2014, 2017, and 2018, respectively), typically when overall catches were relatively low (e.g., only 7 fish captured in 2018). Samples from years with higher abundances typically reflected lower proportional coverage (e.g., 3%, 10%, and 11% in 2003, 2004, and 2002, respectively), when catches often exceeded 1000 fish. Similarly, regions were well sampled with 22%, 9%, 26%, and 18% of the total 2013-2019 SKT Survey catch included from the North Delta, South Delta, Central Delta, and West Delta, respectively (Table 3-1). The South Delta exhibited the lowest representation (17 total fish, 9% of the catch) due the rarity of catches and limited archival samples in this region. Despite this robust coverage across years and regions, some individual region-year combinations were over- or under-represented, particularly in 2002-2004, 2010, and 2016 (Supplement 1).

Otolith Preparation and Analysis

Sagittal otoliths were prepared and analyzed according to Hobbs et al. (2019). In short, otoliths were dissected from fish and soaked in 95% ethanol for a minimum of 24 hours. All adherent tissue was removed, and otoliths were dried and mounted onto microscope glass slides with Crystal Bond® thermoplastic resin in the sagittal plane. Otoliths were then sanded with Buehler 800-1200 grit wet-dry sandpaper and polished with 0.3-micron alumina on a polishing wheel. Otoliths were then rinsed in Milli-Q water and mounted on petrographic slides for Sr-isotope analysis at the UC Davis Interdisciplinary Center for Plasma Mass Spectrometry (http://icpms.ucdavis.edu).

Each otolith was analyzed continuously from the core (hatch) to the dorsal edge (capture), thus encompassing the full life history of each fish (Figure 3-1). In-situ analysis of otolith Strontium isotopes was conducted using a multi-collector inductively coupled plasma mass spectrometer (*Nu Plasma HR* from Nu Instrument Inc.) interfaced with a Nd:YAG 213 nm laser (New Wave Research

UP213) (LA-MC-ICP-MS). Laser settings included a 40-μm spot diameter, scan speed of 10 μm/s, frequency of 10-Hz, and photon output of 5-10 J/cm^2. Helium was used as the carrier gas and was mixed with Argon between the laser sample cell and the plasma source. Gas blank and background signals were monitored until ^{84}Kr and ^{86}Kr stabilized after the sample change. Background values were measured for 30 seconds before each sample was analyzed. Ratios of ^{87}Sr/^{86}Sr were internally normalized by comparing the measured ^{86}Sr/^{88}Sr ratios to the expected ratio of 0.1194, thus correcting for mass discrimination. The signal on mass 85 was monitored to account for any ^{87}Rb interference on ^{87}Sr.

During each daily analysis, aragonite from a marine fish otolith (white seabass, *Atractoscion nobilis)* and a marine coral (unknown sp.) were analyzed as internal standards using the same laser parameters at the beginning and end of each day, with at least three replicate laser transects per standard. The analytical accuracy was evaluated by comparing the results of replicate analyses of the otolith and coral reference materials at the beginning and end of analytical sessions to the modern seawater ^{87}Sr:^{86}Sr value of 0.70918 (McArthur et al. 2001). Based on the recent 10-year record of coral reference data at UC Davis, the LA-MC-ICPMS instrument yielded a mean uncertainty of ± 0.0001 (2σ) relative to the known value, confirming the accuracy of the isotopic measurements. Strontium isotope ratios were converted into practical salinity (psu) following a standard mixing curve using the mean Strontium isotope ratio and salinity of outflowing Delta freshwater (0.7071 and 0.4 ppt, respectively) and the global ocean (0.70918 and 32 ppt, respectively) as end members (Hobbs et al. 2019) (Figure 3-1C).

Life-history Assignments

Each fish was assigned to a migratory life history phenotype based on its full ^{87}Sr/^{86}Sr profile. As previously described (Hobbs et al. 2019), three primary phenotypes could readily be distinguished based on the "larval" (< 30 days-post-hatch; dph) and "adult" (140-170 dph) isotope values relative to the "freshwater" upper salinity threshold of 0.5 psu (or ^{87}Sr/^{86}Sr = 0.7075) (Figure 3-1D). Fish classified to the migratory (MIG) phenotype were born in freshwater habitats and subsequently demonstrated a migration to low-salinity brackish habitats. In contrast, fish classified to the freshwater resident (FWR) phenotype were born in freshwater and remained there for most of their lives, and similarly, fish classified to the brackish-water resident (BWR) phenotype were born and remained primarily within low-salinity (0.5-10 psu) brackish habitats. The 0.5 psu salinity threshold is supported by previous work indicating that habitats above and below this value exhibit unique characteristics that can affect the distribution and condition of Delta Smelt in time and space (Feyrer et al. 2007b, Hammock et al. 2017, 2019a, Lewis et al. 2021).

The relative proportion of each life history phenotype in each annual sample was assumed to be representative of the corresponding cohort. We believed this to be a reasonable assumption given that (a) sampling effort in each year was consistent and spatially stratified throughout the full range of the species (Figure 3-2A-B), (b) subsamples typically reflected significant proportions of the total catch (Table 3-1), and (c) subsamples were selected in relation to spatial and temporal patterns in the overall catch for each year (Table 3-1, Figure 3-2A-B). To explore patterns in the overall abundances of each phenotype, proportions from each sample were directly scaled to previously published abundance estimates for Delta Smelt based on catches in the SKT survey (Polansky et al., 2019). The relative abundance of each phenotype for each cohort was then further explored in relation to cohort year, region, sex and in relation to environmental conditions. Finally, patterns in the overall abundance among years and variance across years were examined for each phenotype (see Statistical Analyses).

Interannual variation in environmental conditions

We predicted that the life history portfolio of Delta Smelt would vary with interannual changes in regional climate. For example, thermal stress in freshwater habitats during warm summers (Nobriga et al. 2008a, Komoroske et al. 2015) is likely to cause differential mortality and encourage Delta Smelt to migrate to cooler coastal conditions downstream, and interannual variation in freshwater outflow is known to significantly alters the distribution of fishes throughout the estuary (Jassby et al. 1995, Kimmerer 2002b, Grimaldo et al. 2020). To explore these hypotheses, we first quantified the mean daily summer (June-August) temperature and freshwater outflow for each annual cohort (2002-2018) included in this study. The summer period corresponds with the juvenile-subadult rearing period when downstream dispersal is most likely to be influenced by variation in environmental conditions. Mean daily water temperatures (ºC) were derived from 15-min continuous measurements collected by the California Department of Water Resources (DWR)-maintained sondes at four stations distributed upstream to downstream, respectively, across the Delta: Antioch (ANH), Rio Vista (RIV), Mallard Slough (MAL) and Martinez (MTZ) (http://cdec.water.ca.gov/) (Figure 3-2A-C, Figure 3-S2.2). Similarly, mean daily freshwater outflows ("outflow," in thousands of acre-feet, TAF d^{-1}) were derived from DWR Dayflow hydrologic model for the Delta (https://data.cnra.ca.gov/dataset/dayflow) (Figure 3-2D, Figure 3-S1.1). Outflow values reflect the net, tidally-averaged quantity of freshwater that flows out of the Delta, westward of Chipps Island (38°03'19"N 121°54'43"W). Both environmental indices were then contrasted with annual patterns in the relative abundance of each life history phenotype to quantify responses of the Delta Smelt life history portfolio to interannual variation in climate.

Statistical Analyses

Variation in Delta Smelt life-histories among years, regions, and sexes

To quantify the potential regional, temporal, and sex-based variation in the relative abundances of each life history phenotype, we constructed contingency tables examining the differences in the proportions of each phenotype in relation to the cohort year (2002-2018), region of capture (North Delta, Central Delta, West Delta, South Delta), and sex (male or female). We then used the Pearson goodness-of-fit test statistic (χ^2, equation 1) to evaluate the null hypothesis that each year, region, or sex represent the same distribution, respectively, as defined by the expected proportions given the data. The test statistic is calculated using

$$\chi^2 = \sum \frac{(O_i - E_i)^2}{E_i} \quad (1)$$

where O_i = the observed proportion in the ith cell and E_i is the expected proportion in the ith cell of the 2-factor contingency table.

Climate effects on Delta Smelt life histories

To examine empirical relationships between regional climate and Delta Smelt life history, we constructed a series of multinomial logistic regression models (MLRMs) which quantified the probabilities of fish from a given cohort belonging to each life history phenotype given the independent, additive, and interactive effects of interannual variation in temperature and freshwater outflow (Table 3-2, Equations 2,3). MLRMs are a direct extension of binomial logistic regression models (BLRMs), but can be used to predict the probability of membership to three or more nominal response categories based on a set of independent predictors (Douma & Weedon 2019). For k=3 categorical responses levels (FWR, BWR, MIG), k-1 independent linearized binary models

can be constructed to predict the log-odds of the first and second levels (relative to the selected 'reference' level, here MIG). Probabilities of each level can be solved by exponentiating both sides of each equation and solving for $P(Y_i)$, with the probability of the reference level equal to 1-*P(FWR)-P(BWR)*. For example, the additive temperature and outflow (T+O) $MLRM_{MIG}$ consisted of

$$ln\left(\frac{P(FWR)}{P(MIG)}\right) = \beta_{1,0} + \beta_{1,1}T + \beta_{1,2}O \quad (2)$$

and

$$ln\left(\frac{P(BWR)}{P(MIG)}\right) = \beta_{2,0} + \beta_{2,1}T + \beta_{2,2}O \quad (3)$$

where $ln\left(\frac{P(Y_i)}{P(Y_k)}\right)$ = log odds for each non-reference level, T = mean daily summer temperature, O = log_{10}-transformed mean daily summer outflow, and β_{ki} = unknown parameters that are jointly estimated using maximum likelihood.

MLRMs, unlike BLRMs, have the advantage of simultaneously examining the effects of environmental predictor variables (e.g., freshwater outflow and temperature) on the probability of membership to all three life history categories, while accounting for the joint dependency of each proportion which must all sum to 1. This advantage, however, comes at the cost of increased model complexity and difficulty in evaluation relative to BLRMs. For this reason, we also constructed independent BLRMs (following Table 3-2) that separately examined the probability of membership to each of the three life history phenotypes as functions of temperature and outflow. For example, the additive T+O BLRM for the probability of FWR consists of

$$ln\left(\frac{P(FWR)}{1-P(FWR)}\right) = \beta_0 + \beta_1 T + \beta_2 O. \quad (4)$$

Results of the individual BLRMs were contrasted with those from the MLRMs to further evaluate the stability and performance of the MLRMs. All analyses were conducted in R (version 4.1.2). BLRMs were fit using the *glm* function (family = "binomial") and MLRMs were fit using the *multinom* function in the *nnet* package. The "aggregated" response variable was a matrix of the proportion of fish assigned solely to the FWR phenotype (BLRMs) or to each of the three phenotypes (MLRM), with the total number of fish in each sample provided as 'weights' for each annual cohort. As described above, proportions (using log-odds-ratios) were modeled as the independent, additive, and interactive effects of the mean daily summer temperature and mean daily log_{10}-transformed summer freshwater outflow of each respective cohort year (year = replicate). Temperature and outflow values were not significantly correlated among years ($t = 0.261$, $df = 14$, $p = 0.798$, and $R^2 = 0.01$) and, thus, could be examined jointly.

Models examining the individual, additive, and interactive effects of temperature and outflow were first contrasted within BLRM and MLRM model sets, with the preferred model in each set identified as having the lowest Akaike information criterion (AIC) value. Using the preferred model, separate BLRMs were then fit for each of the three migratory phenotypes ($BLRM_{FWR}$, $BLRM_{MIG}$, $BLRM_{BWR}$) as well as the $MLRM_{MIG}$ which predicted the joint probability of all three life histories using MIG as the reference group (Table 3-3). McFadden's Pseudo R^2 (MFPR) was examined for each model as a measure of model fit; however, Pseudo R^2 values cannot be interpreted the same as the coefficient of

329 determination (R^2) based on ordinary least squares (OLS) and can only be compare within model
330 sets. For binomial logistic regression models, MFPR values from 0.2 to 0.4 represent 'good' model
331 fits (Louviere et al. 2000).

332 Evaluation and interpretation of model fits for aggregated MLRMs is less clear. Given that MLRMs
333 are extensions of the associated BLRMs, we followed the standard practice of contrasting MLRM
334 results with those from their component BLRMs. Additionally, we compared the expected values
335 (the predicted proportions of each migratory phenotype) from the $MLRM_{MIG}$ to the observed values
336 for each year. Differences between observed and predicted (OP) values were compared using a
337 correlational value relative to the unity line (Theil 1961, Smith & Rose 1995). This correlational
338 measure is approximately similar to a traditional R^2, except examines how well the OP relationship
339 matches the 1:1 expectation. This measure, which we have called OPR (in contrast to the MFPR), is
340 calculated as:
341

342 $$OPR = 1 - \frac{\Sigma(y_i - y_p)^2}{\Sigma(y_i - \hat{y}_i)^2} \quad (5)$$

343 where y_i is the observed value, y_p is the model predict value and $\hat{y}_i$ is the mean of the observed
344 values. The OPR was calculated separately for each life history examined in the MLM and
345 contrasted with MFPR values from the BLRM to further assess the fit of the MLRM.

346 # Results

347 ## Interannual variation in climate: temperature and freshwater outflow

348 Mean daily summer temperatures varied from 19.5 to 23°C, with values in the North Delta (station
349 RIV) consistently 1-2 °C warmer than in the West Delta (station MRZ) (Figure 3-2B). The mean
350 summer temperature Delta-wide was characterized by relatively high (> 21°C) values from 2000 to
351 2008, a brief period of low values (< 21°C) from 2009 to 2012 and high values again from 2013 to
352 2018. The RIV and ANH stations exhibited the highest mean daily temperatures, with values often
353 exceeding 22°C. Mean daily summer freshwater outflow varied among years by up to 10-fold, with
354 the highest outflow values observed in 2006 (35.2 TAF), 2011(44.9 TAF), and 2017 (31.5 TAF) and
355 lowest values observed in 2008 (3.9 TAF), 2014 (8.5 TAF) and 2015 (9.3 TAF) (Figure 2D). These
356 interannual patterns in temperature and outflow were used to examine the effects of climate on
357 Delta Smelt life histories.

358 ## Variation in the life history portfolio of Delta Smelt: time, region, sex, and
359 abundance

360 Of the 2,162 individual Delta Smelt examined from 16 year-classes, 69.1% were identified as the
361 migratory phenotype (MIG), 24.3% as freshwater residents (FWR), and 6.6% as brackish residents
362 (BWR) (Figure 3-3A). Though these primary life history categories could readily be applied to most
363 individuals, we also observed evidence for sub-categories within each primary life-history category.
364 For example, several fish identified as FWR exhibited increases in Strontium isotope values, similar
365 to MIG, but only briefly crossed the 0.5 psu freshwater threshold (Figure 3-3B). Similarly, several
366 fish identified as MIG started life at or near the 0.5 psu threshold or migrated from fresh water to
367 values only slightly above this threshold (Figure 3-3C). Furthermore, many of the individuals
368 classified as BWR exhibited excursions below the 0.5 psu threshold, though originating and
369 remaining in brackish-water habitats for the majority of their life history Figure 3-3D). These

variations further highlight the complexity of life history patterns exhibited by Delta Smelt. For this study, we chose to focus on the three primary patterns described by Hobbs et al. (2019) to emphasize previously unexplored broad spatial and temporal patterns in Delta Smelt life histories and how they vary in relation to regional climate.

MIG was the dominant life history of Delta Smelt across all sexes, regions, and years (except 2010 where FWR = 52%) (Figure 3-4). Life history composition did not vary significantly between sexes (Figure 3-4A) but differed significantly among regions (Figure 3-4B) and cohort years (Figure 3-4C) (Table 3-2). FWR were most abundant in the North Delta where flows from the Sacramento River maintain freshwater habitats year-round. BWR were most abundant in the West Delta, where oceanic waters mix with Delta waters to maintain brackish-water habitats. Though spatial patterns in life histories matched expectations based on known spatial patterns in habitats, observations of a few BWR in the ND and a few FWR in the WD suggested that fish could make short-term movements that are difficult to identify using otolith geochemistry.

Although the MIG phenotype was generally dominant, interannual variation in the phenotypic composition of Delta Smelt was pronounced (Figure 3-4D). For example, FWR comprised 30-50% of all samples examined in 2002, 2007, 2010, and 2012, but less than 3% in 2006 and 2018 (Figure 3-4C). BWR were generally rare (< 10% and often absent), but contributed to > 20% of the sample in the 2003 and 2006 cohorts. The estimated abundance of Delta Smelt also varied greatly during this time period, ranging from 1.2 million fish in 2011 to < 30,000 fish in 2018 (Figure 3-4D). The relative abundance of each phenotype did not appear to correspond with variation in overall abundance, with high and low proportions of FWR and MIG present in years of relatively high and low abundance. As for total abundance, the scaled abundance of each phenotype also varied greatly among years (Figure 3-4D). For example, 2006 exhibited the lowest abundance of FWR fish (4,519), whereas a 10-fold greater abundance of FWR fish (490,130) was estimated in 2002. In 2015, 15,978 total MIG fish were estimated to be present in the Delta, whereas a 50-fold greater number of MIG fish (782,998) was estimated in 2011. Zero BWR were observed in 2002, 2015, and 2016; however, an abundance of 185,120 BWR was estimated in 2003.

Effects of regional climate on Delta Smelt life history

For both the binomial and multinomial model sets, the additive model exhibited the lowest AIC and was therefore selected for further comparisons (Supplement 3). Separate binomial models were fit for each of the three migratory phenotypes in addition to the multinomial model which predicted the join probability of all three life histories using the MIG fish as the reference group. All models were significantly different than the intercept-only model (Table 3-3), and additive models were significantly better than single factor models based on likelihood ratio tests. Pseudo R^2 (MFPR) values indicated good to excellent model fit for all binomial models (Louviere et al. 2000). FWR and BWR fish exhibited the strongest responses to environmental conditions (MFPR = 0.394 and 0.386 respectively), with MIG fish exhibiting a relatively weaker response (MFPR = 0.156). The additive multinomial model exhibited the lowest AIC and highest MFPR (Supplement 3), however the MFPR value (0.06) was low relative to the binomial models. We did not view this as concerning given that MFPR does not reflect the fraction of variance explained (e.g., vs the OLS R^2) and interpretations of various pseudo-R^2 formulations for multinomial models remains unclear, and possible even ore so for aggregated models (here, aggregated to cohort year). However, comparison of observed verses expected values for the multinomial model with the MFPR values from the associated binomial models indicated that the multinomial model performed similarly to the individual binomial models (Figure 3-5A-C). The OPR based on the multinomial model showed a

similar pattern to the MFPR values from the binomial models, with FWR and BWR fish exhibiting the highest correlations between expected and observed (0.467 and 0.299, respectively) while the MIG correlation was more moderate (0.21).

The functional responses of Delta Smelt life histories to variation in climate were visualized as 3D surfaces reflecting the MLRM-based predicted proportion of each migratory phenotype in a given year in relation to its corresponding mean daily summer temperature and outflow (Figure 3-5D-F). FWR fish were most prevalent in years with lower summer temperatures and outflow, decreasing rapidly from 50% to 0% in the warmest-wettest years (Figure 3-5D). In contrast, the MIG life history increased from 40% to 80% with increasing outflow and temperature values; however, declined slightly at the highest ranges of each metric (Figure 3-5E). This decline coincided with a rapid increase in the prevalence of BWR fish from 0-20% at the highest temperature-outflow conditions (Figure 3-5F).

Discussion

Context

Our study showed Delta Smelt employ diverse migratory life history strategies to survive within the dynamic and unpredictable habitats of the upper San Francisco Estuary. Furthermore, the relative abundances of different migratory phenotypes are not static, but instead vary temporally in relation to interannual patterns in climate. In dynamic ecosystems, such diverse life-history portfolios can serve as biological buffers against environmental stochasticity (Greene et al. 2010, Brennan et al. 2019), thus conferring long-term stability and resilience in populations of organisms (Lundberg 1988, Schindler et al. 2010, Blüthgen et al. 2016). In fishes, life history diversity includes intraspecific variation in age and size of first reproduction (Huntsman et al. 2021), emigration phenology (Sturrock et al. 2020), residence time in fresh and marine waters (Erkinaro et al. 2019), age structure (Moore et al. 2014), and migratory behavior (Courter et al. 2013, Morita et al. 2014). Most studies of migratory behaviors in estuarine species, however, have focused on species with high economic and social value, such as salmonids, while focusing less on smaller, rare species such as Delta Smelt. Diversity in nature can confer higher stability and resilience to climatic extremes. Managing the SFE to conserve the phenotypic diversity of Delta Smelt and take advantage of this resiliency may be a new and critical tool for staying it's extinction.

Delta Smelt express three primary migratory phenotypes in the SFE, with most of the population migrating from downstream estuarine waters to upstream fresh waters. We observed opposing relationships with environmental factors for the FWR phenotype compared to MIG & BWR. The FWR phenotype was most abundant during cool and dry conditions (e.g., 2002 and 2010) whereas the MIG and BWR phenotypes were most common during warm and wet years (e.g., 2006). These trends suggest that abiotic (e.g., hydrology-driven) and biotic (e.g., physiologically-driven) mechanisms may influence the dominant life history expressed by the Delta Smelt. In years of high summer outflow, sufficient fresh water can disperse larvae and early life stages downstream, leading to a greater contribution of MIG and BWR fish, while in years with low summer water temperatures and outflow, FWR fish that remain in the upper estuary, were favored. This may explain why warm, dry periods are associated with large declines in Delta Smelt abundance. Low outflow conditions favor FWR fish, but the habitats those FWR would need to occupy may become to warm.

Sex & Region

Though life-histories did not vary between sexes, life history compositions did vary significantly among Delta Smelt collected in different regions of the SFE and from different annual cohorts. As we expected, the FWR phenotype was most prevalent in the ND, where flows form the Sacramento River maintain freshwater habitats year-round. Similarly, the BWR phenotype was most prevalent in the WD, where ocean influence maintains low-salinity brackish-water habitat year-round. Also, as expected, the MIG phenotype was prevalent in all habitats. The capture of a few fish in the WD that were classified as FWR, and a few fish in the ND that were classified as BWR (Figure 3-4B), however, suggests that some rapid movements between habitats are possible and may not be detectible in otolith Strontium isotope profiles due to a time lag for elements from the surrounding water to be incorporated into the otoliths. In agreement with this, previous studies observed that changes in water chemistry can take up to 2 weeks to stabilize in the otolith composition of Chinook Salmon (*Oncorhynchus tshawytscha*) (Miller 2011), and up to 21 days to stabilize in the otoliths of Black Bream (*Acanthopagrus butcheri*) (Elsdon & Gillanders 2005) and the estuarine Large-mouth Bass (*Micropterus salmoides*) (Lowe et al. 2009).

Climate (general)

Delta Smelt life histories also varied significantly among years and in relation to patterns in regional climate, suggesting that Delta Smelt migratory behaviors were influenced by past climate conditions and are likely to be strongly affected by future climate change. For example, though our study confirmed that the contemporary population is dominated by the MIG phenotype, the increased prevalence of the FWR phenotype in cooler conditions also suggest that the historic Delta Smelt population, prior to anthropogenic alteration and warming (Li et al. 2000) of freshwater habitats, may have included a much larger, persistent FWR contingent throughout the Sacramento-San Joaquin River Delta (Moyle et al. 1992). If true, climate-induced warming, up to 2°C by 2050 and 4-8°C by 2100 (Dettinger et al. 2016), could lead to further reductions in life history diversity and increased vulnerability to extinction for this species, as warm, dry conditions are projected to become more prevalent. The identification and incorporation of such life-history diversity may significantly enhance long-term effectiveness of conservation efforts, as observed elsewhere in highly productive fisheries (Greene et al. 2010) and in relatively pristine watersheds (Moore et al. 2014, Brennan et al. 2019).

Temperature

The observed responses of Delta Smelt life histories to variation in summer temperature matched our predictions based on both phylogeny and prior studies examining physiological responses to temperature. Delta Smelt reside near the southern-most (thermal) limit of the Osmeridae family, a group of stenothermal fishes commonly found in coastal temperate-subarctic waters of the northern Pacific and Atlantic Oceans (Moyle 2002, Garwood 2017). Enhanced feeding in downstream habitats has been described as a likely mechanism supporting a migratory life history (Hammock et al. 2017, 2019a) but thermal refuge from stressful summer temperatures in freshwater habitats is as an equally likely mechanism. Furthermore, high summer water temperatures are negatively correlated with Delta Smelt subadult abundance in the fall (Mac Nally et al. 2010), suggesting that thermal stress may result in high mortality.

Empirical support for this hypothesis comes from several laboratory experiments using cultured specimens (Komoroske et al. 2014a, 2015, Jeffries et al. 2016, Frank et al. 2017) and observations in wild fish (Lewis et al. 2021, Hammock et al. 2021) which, together, have documented multiple

negative physiological responses to water temperatures > 20-23 °C (e.g., cellular stress, reduced body condition, reduced growth rate, and increased disease susceptibility). Such warm conditions are commonly experienced during summer in freshwater portions of the Delta (Figure 3-S2.2) and are likely to intensify in frequency and magnitude as the regional climate warms as climate change progresses (Nobriga et al. 2008b, Dettinger et al. 2016, Brown et al. 2016). This will likely increase the physiological selective pressure for fish to migrate from warmer freshwater habitats upstream to cooler low-salinity brackish habitats downstream (Figure 3-3C), thus increasingly favoring MIG and BWR phenotypes over FWR. Such prior selection may have also contributed to the dominance of the MIG phenotype in contemporary cohorts of Delta Smelt.

Outflow

The observed responses of Delta Smelt life histories to variation in freshwater outflow did not match our predictions. We predicted that years with higher summer outflows ('wet' years) would result in a greater quantity and quality of freshwater habitats, thus favoring the FWR phenotype. Instead, we observed the opposite pattern, with relatively fewer FWR, and more MIG and BWR, occurring in years with higher outflow (Figure 3-5D-F). Thus, fewer fish remained or survived in freshwater habitats through the summer in years with higher outflow, and the quantity and distribution of freshwater habitats did not appear to asymmetrically benefit the FWR population. We hypothesize that his was due to enhanced downstream advection in wetter years. For example, the geographic distribution of physical gradients in water quality and aquatic species are strongly affected by variation in freshwater outflow (Jassby et al. 1995, Monismith et al. 2002, Kimmerer 2002a). Though counter-intuitive, increased freshwater outflows may physically reduce the number of FWR that remain in upstream habitats due to increased physical downstream transport, while decreased outflow would favor residence in upstream habitats. To anecdotally support this hypothesis, we note observations of adult Delta Smelt that were collected in brackish habitats far westward of their normal range in the West Delta (e.g., the Petaluma River) in years of extreme outflow (J. Hobbs, unpublished data), as well as concentrations of Delta Smelt in the Lower Sacramento River during periods of drought (Herbold 1994). If true, this physical mechanism of dispersal would explain the negative relationship between the FWR phenotype and freshwater outflow.

This observed effect of outflow on Delta Smelt life-histories contrasts with the lack of a clear outflow-abundance relationship for this species. For example, the overall abundance of Delta Smelt is highly variable among years of similarly high freshwater flow (IEP-MAST 2015). In 2006, for example, high summer outflow (> 30,000 TAF d^{-1} or 37 million m^3 d^{-1}) did not increase the abundance of Delta Smelt, and the proportion of FWR fish was < 3%. In contrast, 2011 experienced similarly high summer flows (> 40,000 TAF d^{-1} or 49 million m^3 d^{-1}), with a positive response in both total abundance and the proportion of FWR fish (~ 20%). A key difference between these two high-outflow years is that they each experienced different thermal conditions, with 2006 being relatively warm and 2011 being relatively cool (Figure 3-2C). Given these patterns, temperature appears to be a stronger predictor of the prevalence of FWR than freshwater outflow (Table 3-S.31).

Multiple Stressors

In this study, we focused on temperature and freshwater outflow as two major indicators of interannual variation in climate that could affect Delta Smelt life histories. However, many other stressors could interact with these predictors to generate the patterns described herein. For example, high summer temperatures in the SFE are often accompanied by increased pathogen outbreaks,

contaminant loads (e.g., metals, pesticides, ammonia), harmful algal blooms (HAB) (e.g., *Microcystis aeruginosa*), increased mortality due to predation, and elevated metabolic demand. For example, sublethal contaminant exposure may impact physiological condition (Hammock et al. 2015) or impair essential biological functions (Connon et al. 2011a b) in Delta Smelts. In wetland habitats, high precipitation and storm water runoff may increase the bioavailability of toxins such as Pb that can impact fish health (McGourty et al. 2009) and temperature may increase sensitivity to such toxins (Brooks et al. 2012). High temperatures could also affect prey abundance or foraging success in certain habitats, as survival is correlated with summer zooplankton abundance (Kimmerer 2008, Hammock et al. 2017, 2019a, 2021). Last, increased temperatures may also increase susceptibility to predation by increasing foraging by predators or decreasing avoidance abilities of prey (Davis et al. 2019, Nobriga et al. 2021). Regardless of the ultimate drivers of these patterns, the proximal responses of each migratory phenotype to environmental variation suggest that the Delta Smelt life-history portfolio is sensitive to and likely to change with future climate change.

Limitations/Caveats/Strengths

Although Delta Smelt populations have been surveyed since the 1960s otolith data for adults only became available in the last 20 years (Moyle et al. 1992, Hobbs et al. 2010), precluding our ability to test for adaptation processes and phenotypic variation between multiple wet and dry years common to the California weather. Still, the underlying processes observed in the three high outflow years in this study (e.g., 2006, 2011 and 2017) are likely to be representative and have only occurred 9 times since monitoring began in the SFE (1967, 1969, 1983, 1995, 1996, 1998, 2011, 2017, and 2019). We also recognize that the number of life history strategies identified based on otolith $^{87}Sr/^{86}Sr$ patterns is somewhat arbitrary and simplified, and that fish can have rapid transitions between brackish and freshwater habitats (Figure 3-3, Figure 3-S4.1). In addition, the position of the low-salinity zone (LSZ) can change dramatically, such that a stationary fish can experience high salinity gradients and be misidentified as a migratory. We believe that by including thousands of samples distributed throughout the estuary (Supplement 1) and by observing clear profile trends with defined thresholds (supplementary table S4.1), these limitations did not impact our main results.

Delta Smelt is an annual species for which the short lifespan can accelerate the expression of distinct life history strategies phenotypes, potentially at faster rates than in other well-studied families (e.g., salmonids). By analyzing the isotopic compositions of thousands of fish otoliths in the last 2 decades collected across the SFE, striking differences in hydrological conditions were still observed (daily summer outflow varied 10-fold, and temperature often exceeded thermal limits), resulting in intra annual phenotypic plasticity for this species. However, Delta Smelt abundance in recent years are extremely low, leading to the potential underestimation of the contribution of alternative life history tactics, such as the FWR and BWR groups. This fact, aligned with the difficulty of obtaining archeological samples (i.e., paucity of fossils and extremely small otoliths), suggest that modeling studies may be one of the few suitable options to estimate past and future climate influences on Delta smelt populations (Cloern et al. 2011, Brown et al. 2013).

Present and future climate of the SFE

The Mediterranean-type climate of the SFE likely exacerbates the effects of climate change impacts on the system. For instance, the SFE has high seasonal water temperature variation (up to ~ 20°C) (Baxter et al. 2015) and great interannual hydrological variation in the form of droughts and wet periods, such that freshwater outflow can vary among years by more than 10-fold (Feyrer et al. 2007b). With climate change, the system is becoming warmer, with more frequent wet and drought

extremes and altered flow patterns (Cloern & Jassby 2012b, Swain et al. 2018). It is predicted (Knowles & Cayan 2002) that the projected 2.1°C temperature increase by 2090 will result in the loss of approximately half of the average April snowpack storage in the upper San Francisco Estuary watershed. This will, in turn, reduce the spring-summer outflow by ~ 20% of its historical annual levels, increasing the water salinity within the estuary. Other estimates suggest perhaps even more rapid warming of to 4-8 °C by the end of this century (Dettinger et al. 2016, Pierce et al. 2018).

Conclusions

Previous cooling periods were essential to generate the diversity of species in the genus *Hypomesus* through habitat compression and reduced dispersal success (Ilves & Taylor 2008). Delta Smelt, *Hypomesus transpacificus,* potentially originated during the Pleistocene glacial period (~ 2.5 – 0.7 mya), when ancestral marine populations were isolated in inland lakes of the southern San Joaquin Valley (Norris & Webb 1990). Since then, it has experienced marked climatic variation. However, the last four decades are the warmest since 1850 (IPCC 2021), challenging the ability of this species to adapt and persist in the near future.

Here we demonstrate that Delta Smelt exhibit a diverse migratory life history portfolio that has persisted over the last 2 decades and is sensitive to variation in regional climate. As for other fishes, this diversity of life histories likely has increased population stability and resilience in the face of environmental stochasticity. However, the Delta Smelt population has plummeted to < 1% of its historic abundance and remains highly vulnerable to extinction. Its annual life history, low fecundity, and endemism within a small geographic each contribute to this vulnerability. Furthermore, Delta Smelt feeding and growth appear highly sensitive to predicted increases in water temperature and clarity (Brown et al. 2016, Hestir et al. 2016, Lewis et al. 2021). We show that the life history of Delta Smelt is also sensitive to variation in climate, with those remaining in freshwater habits likely to experience the greatest proportional losses with future warming. The presence of a strong FWR contingent may have historically been an important feature of the population prior to significant warming and degradation of these habitats. Thus, year-round management of freshwater habitats, including population supplementation, habitat restoration, and establishment of thermal refuges, to maintain life history diversity may be a valuable strategy for preventing the extinction of this sentinel species.

Acknowledgments

We are grateful to our collaborators at the California Department of Fish and Wildlife and U.S. Fish and Wildlife Service for providing Delta Smelt specimens from field collections for use in this study, and the Teh Lab at UC Davis who helped obtain, dissect, and archive specimens. We also thank the many past and present students and staff in the Otolith Geochemistry and Fish Ecology Laboratory at UC Davis who contributed to fish dissections, otolith preparation, and analysis. Otolith archives were maintained in accordance with an approved California Department of Fish and Wildlife Service Section 2081a Memorandum of Understanding to L. Lewis, M. Willmes, and J. Hobbs. Funding for this project was provided in part by grants from the California Department of Fish and Wildlife (CDFW) contracts E1183004, D1583004 and P1696005, and the U.S. Bureau of Reclamation (USBR) contracts R13AP20022 and R17AC00129 to J. Hobbs, S. Teh, and L. Lewis. Additional support was provided by the Delta Stewardship Council (DSC) via postdoctoral fellowships to M. Willmes (Grant No. 1167) and L. Lewis (Grant Nos. 2279, 5298). The content of this material and views described herein do not necessarily reflect the views and policies of the CDFW, USBR, DSC,

632 or UC Davis; nor does mention of trade names or commercial products constitute endorsement or
633 recommendation for use.

634 References

635 Avaria-Llautureo J, Venditti C, Rivadeneira MM, Inostroza-Michael O, Rivera RJ, Hernández CE,
636 Canales-Aguirre CB (2021) Historical warming consistently decreased size, dispersal and
637 speciation rate of fish. Nature Climate Change 11:787–793.
638 Barnett-Johnson R, Pearson TE, Ramos FC, Grimes CB, MacFarlane RB (2008) Tracking natal
639 origins of salmon using isotopes, otoliths, and landscape geology. Limnology and
640 Oceanography 53:1633–1642.
641 Bataille CP, Bowen GJ (2012) Mapping 87Sr/86Sr variations in bedrock and water for large scale
642 provenance studies. Chemical Geology 304:39–52.
643 Baxter R (no date)An updated conceptual model of Delta Smelt biology: Our evolving
644 understanding of an estuarine fish. https://pubs.er.usgs.gov/publication/70141018
645 (accessed October 12, 2021)
646 Blüthgen N, Simons NK, Jung K, Prati D, Renner SC, Boch S, Fischer M, Hölzel N, Klaus VH,
647 Kleinebecker T, Tschapka M, Weisser WW, Gossner MM (2016) Land use imperils plant
648 and animal community stability through changes in asynchrony rather than diversity. Nat
649 Commun 7:10697.
650 Brennan SR, Schindler DE, Cline TJ, Walsworth TE, Buck G, Fernandez DP (2019) Shifting habitat
651 mosaics and fish production across river basins. Science 364:783–786.
652 Brennan SR, Zimmerman CE, Fernandez DP, Cerling TE, McPhee MV, Wooller MJ (2015a)
653 Strontium isotopes delineate fine-scale natal origins and migration histories of Pacific
654 salmon. Science advances 1:e1400124.
655 Brennan SR, Zimmerman CE, Fernandez DP, Cerling TE, McPhee MV, Wooller MJ (2015b)
656 Strontium isotopes delineate fine-scale natal origins and migration histories of Pacific
657 salmon. Sci Adv 1:e1400124.
658 Brooks ML, Fleishman E, Brown LR, Lehman PW, Werner I, Scholz N, Mitchelmore C, Lovvorn
659 JR, Johnson ML, Schlenk D, van Drunick S, Drever JI, Stoms DM, Parker AE, Dugdale R
660 (2012) Life Histories, Salinity Zones, and Sublethal Contributions of Contaminants to
661 Pelagic Fish Declines Illustrated with a Case Study of San Francisco Estuary, California,
662 USA. Estuaries and Coasts 35:603–621.
663 Brown LR, Bennett WA, Wagner RW, Morgan-King T, Knowles N, Feyrer F, Schoellhamer DH,
664 Stacey MT, Dettinger M (2013) Implications for Future Survival of Delta Smelt from Four
665 Climate Change Scenarios for the Sacramento–San Joaquin Delta, California. Estuaries and
666 Coasts 36:754–774.
667 Brown LR, Komoroske LM, Wagner RW, Morgan-King T, May JT, Connon RE, Fangue NA (2016)
668 Coupled Downscaled Climate Models and Ecophysiological Metrics Forecast Habitat
669 Compression for an Endangered Estuarine Fish. PLOS ONE 11:e0146724.
670 Campana SE (1999) Chemistry and composition of fish otoliths: pathways, mechanisms and
671 applications. Marine Ecological Progress Series 188:263–297.
672 CDFG (2010) State & federally listed endangered & threatened animals of California. California
673 Department of Fish & Game,State of California, The Natural Resources Agency, California.
674 The Natural Rsources Agency, California.
675 Cloern JE, Jassby AD (2012a) Drivers of change in estuarine-coastal ecosystems: Discoveries from
676 four decades of study in San Francisco Bay. Reviews of Geophysics 50.

677 Cloern JE, Jassby AD (2012b) Drivers of change in estuarine-coastal ecosystems: Discoveries from
678 four decades of study in San Francisco Bay. Rev Geophys 50:RG4001.
679 Cloern JE, Knowles N, Brown LR, Cayan D, Dettinger MD, Morgan TL, Schoellhamer DH, Stacey
680 MT, van der Wegen M, Wagner RW, Jassby AD (2011) Projected Evolution of California's
681 San Francisco Bay-Delta-River System in a Century of Climate Change. PLOS ONE
682 6:e24465.
683 Connon RE, Beggel S, D'Abronzo LS, Geist JP, Pfeiff J, Loguinov AV, Vulpe CD, Werner I (2011a)
684 Linking molecular biomarkers with higher level condition indicators to identify effects of
685 copper exposures on the endangered delta smelt (Hypomesus transpacificus). Environmental
686 Toxicology and Chemistry 30:290–300.
687 Connon RE, Deanovic LA, Fritsch EB, D'Abronzo LS, Werner I (2011b) Sublethal responses to
688 ammonia exposure in the endangered delta smelt; Hypomesus transpacificus (Fam.
689 Osmeridae). Aquatic Toxicology 105:369–377.
690 Courter II, Child DB, Hobbs JA, Garrison TM, Glessner JJG, Duery S (2013) Resident rainbow
691 trout produce anadromous offspring in a large interior watershed. Can J Fish Aquat Sci
692 70:701–710.
693 Damon L, Chorazyczewski A (2021) Interagency Ecological Program San Francisco Estuary 20mm
694 Survey 1995-2021.
695 Davis BE, Hansen MJ, Cocherell DE, Nguyen TX, Sommer T, Baxter RD, Fangue NA, Todgham
696 AE (2019) Consequences of temperature and temperature variability on swimming activity,
697 group structure, and predation of endangered delta smelt. Freshw Biol 64:2156–2175.
698 Dege M, Brown LR (2004) Effect of outflow on spring and summertime distribution and abundance
699 of larval and juvenile fishes in the upper San Francisco Estuary. In: *Early Life History of Fishes*
700 *in the San Francisco Estuary and Watershed*. Feyrer F, Brown LR, Brown RL, Orsi JJ (eds) p 49–
701 65
702 Dettinger M, Anderson J, Anderson M, Brown LR, Cayan D, Maurer E (2016) Climate Change and
703 the Delta. 14:27.
704 Dettinger M, Cayan D (2003) Interseasonal covariability of Sierra Nevada streamflow and San
705 Francisco Bay salinity. JOURNAL OF HYDROLOGY 277:164–181.
706 Douma JC, Weedon JT (2019) Analysing continuous proportions in ecology and evolution: A
707 practical introduction to beta and Dirichlet regression. Methods in Ecology and Evolution
708 10:1412–1430.
709 Elsdon T, Gillanders B (2005) Strontium incorporation into calcified structures: separating the
710 effects of ambient water concentration and exposure time. Mar Ecol Prog Ser 285:233–243.
711 Erkinaro J, Czorlich Y, Orell P, Kuusela J, Falkegård M, Länsman M, Pulkkinen H, Primmer CR,
712 Niemelä E (2019) Life history variation across four decades in a diverse population complex
713 of Atlantic salmon in a large subarctic river. Can J Fish Aquat Sci 76:42–55.
714 Feyrer F, Nobriga ML, Sommer TR (2007a) Multidecadal trends for three declining fish species:
715 habitat patterns and mechanisms in the San Francisco Estuary, California, USA. Can J Fish
716 Aquat Sci 64:723–734.
717 Feyrer F, Nobriga ML, Sommer TR (2007b) Multidecadal trends for three declining fish species:
718 Habitat patterns and mechanisms in the San Francisco Estuary, California, USA. Canadian
719 Journal of Fisheries and Aquatic Sciences 64:723–734.
720 Fong S, Louie S, Werner I, Davis J, Connon RE (2016) Contaminant effects on California bay-delta
721 species and human health. San Francisco Estuary and Watershed Science 14.
722 Frank DF, Hasenbein M, Eder K, Jeffries KM, Geist J, Fangue NA, Connon RE (2017)
723 Transcriptomic screening of the innate immune response in delta smelt during an
724 Ichthyophthirius multifiliis infection. AQUACULTURE 473:80–88.

Garwood RS (2017) Historic and contemporary distribution of Longfin Smelt (Spirinchus thaleichthys) along the California coast. CALIFORNIA FISH AND GAME 103:23.

Gasith A, Resh VH (1999) Streams in Mediterranean Climate Regions: Abiotic Influences and Biotic Responses to Predictable Seasonal Events. Annual Review of Ecology and Systematics 30:51–81.

Gilby BL, Weinstein MP, Baker R, Cebrian J, Alford SB, Chelsky A, Colombano D, Connolly RM, Currin CA, Feller IC, Frank A, Goeke JA, Goodridge Gaines LA, Hardcastle FE, Henderson CJ, Martin CW, McDonald AE, Morrison BH, Olds AD, Rehage JS, Waltham NJ, Ziegler SL (2021) Human Actions Alter Tidal Marsh Seascapes and the Provision of Ecosystem Services. Estuaries and Coasts 44:1628–1636.

Gillanders BM, Izzo C, Doubleday ZA, Ye Q (2015) Partial migration: growth varies between resident and migratory fish. Biol Lett 11:20140850.

Greene CM, Hall JE, Guilbault KR, Quinn TP (2010) Improved viability of populations with diverse life-history portfolios. Biol Lett 6:382–386.

Grimaldo L, Burns J, Miller RE, Kalmbach A, Smith A, Hassrick J, Brennan C (2020) Forage Fish Larvae Distribution and Habitat Use During Contrasting Years of Low and High Freshwater Flow in the San Francisco Estuary. SFEWS 18.

Hammock BG, Hartman R, Dahlgren RA, Johnston C, Kurobe T, Lehman PW, Lewis LS, Van Nieuwenhuyse E, Ramírez-Duarte WF, Schultz AA, Teh SJ (2021) Patterns and predictors of condition indices in a critically endangered fish. Hydrobiologia.

Hammock BG, Hartman R, Slater SB, Hennessy A, Teh SJ (2019a) Tidal Wetlands Associated with Foraging Success of Delta Smelt. Estuaries and Coasts 42:857–867.

Hammock BG, Hobbs JA, Slater SB, Acuña S, Teh SJ (2015) Contaminant and food limitation stress in an endangered estuarine fish. Science of The Total Environment 532:316–326.

Hammock BG, Moose SP, Solis SS, Goharian E, Teh SJ (2019b) Hydrodynamic Modeling Coupled with Long-term Field Data Provide Evidence for Suppression of Phytoplankton by Invasive Clams and Freshwater Exports in the San Francisco Estuary. Environmental Management 63:703–717.

Hammock BG, Slater SB, Baxter RD, Fangue NA, Cocherell D, Hennessy A, Kurobe T, Tai CY, Teh SJ (2017) Foraging and metabolic consequences of semi-anadromy for an endangered estuarine fish. PLOS ONE 12:e0173497.

Hendry A (2004) To sea or not to sea? Anadromy versus non-anadromy in salmonids. Evolution Illuminated : Salmon and Their Relatives.

Hestir EL, Schoellhamer DH, Greenberg J, Morgan-King T, Ustin SL (2016) The Effect of Submerged Aquatic Vegetation Expansion on a Declining Turbidity Trend in the Sacramento-San Joaquin River Delta. Estuaries and Coasts 39:1100–1112.

Hobbs JA, Lewis LS, Ikemiyagi N, Sommer T, Baxter RD (2010) The use of otolith strontium isotopes (87 Sr/86 Sr) to identify nursery habitat for a threatened estuarine fish. Environmental biology of fishes 89:557–569.

Hobbs JA, Lewis LS, Willmes M, Denney C, Bush E (2019) Complex life histories discovered in a critically endangered fish. Scientific Reports 9:16772.

Hobbs JA, Moyle PB, Fangue N, Connon RE (2017) Is Extinction Inevitable for Delta Smelt and Longfin Smelt? An Opinion and Recommendations for Recovery. SFEWS 15:1–19.

Hodge BW, Wilzbach MA, Duffy WG, Quiñones RM, Hobbs JA (2016) Life history diversity in Klamath River steelhead. Transactions of the American Fisheries Society 145:227–238.

Huntsman BM, Lynch AJ, Caldwell CA, Abadi F (2021) Intrinsic and extrinsic drivers of life-history variability for a south-western cutthroat trout. Ecol Freshw Fish 30:100–114.

772 Ilves KL, Taylor EB (2008) Evolutionary and Biogeographical Patterns within the Smelt Genus
773 Hypomesus in the North Pacific Ocean. Journal of Biogeography 35:48–64.
774 Ingram BL, DePaolo DJ (1993) A 4300 year strontium isotope record of estuarine paleosalinity in
775 San Francisco Bay, California. Earth and Planetary Science Letters 119:103–119.
776 Jassby AD, Kimmerer WJ, Monismith SG, Armor C, Cloern JE, Powell TM, Schubel JR, Vendlinski
777 TJ (1995) Isohaline position as a habitat indicator for estuarine populations. Ecological
778 Applications 5:272–289.
779 Jeffries KM, Connon RE, Davis BE, Komoroske LM, Britton MT, Sommer T, Todgham AE,
780 Fangue NA (2016) Effects of high temperatures on threatened estuarine fishes during
781 periods of extreme drought. Journal of Experimental Biology.
782 Kimmerer W (2008) Losses of Sacramento River Chinook Salmon and Delta Smelt to Entrainment
783 in Water Diversions in the Sacramento-San Joaquin. SFEWS 6.
784 Kimmerer W (2002a) Physical, biological, and management responses to variable freshwater flow
785 into the San Francisco estuary. Estuaries 25:1275–1290.
786 Kimmerer WJ (2002b) Effects of freshwater flow on abundance of estuarine organisms: physical
787 effects or trophic linkages? Marine Ecology Progress Series 243:39–55.
788 Kimmerer WJ, Gartside E, Orsi JJ (1994) Predation by an introduced clam as the likely cause of
789 substantial declines in zooplankton of San Francisco Bay. Marine Ecology Progress Series
790 113:81–93.
791 Knowles N, Cayan D (2002) Potential effects of global warming on the Sacramento/San Joaquin
792 watershed and the San Francisco estuary. Geophysical Research Letters 29.
793 Komoroske L, Connon R, Lindberg J, Cheng B, Castillo G, Hasenbein M, Fangue N (2014a)
794 Ontogeny influences sensitivity to climate change in an endangered fish. Conservation
795 Physiology 2:cou008.
796 Komoroske LM, Connon RE, Jeffries KM, Fangue NA (2015) Linking transcriptional responses to
797 organismal tolerance reveals mechanisms of thermal sensitivity in a mesothermal endangered
798 fish. Molecular Ecology.
799 Komoroske LM, Connon RE, Lindberg J, Cheng BS, Castillo G, Hasenbein M, Fangue NA (2014b)
800 Ontogeny influences sensitivity to climate change stressors in an endangered fish.
801 Conservation Physiology 2:cou008–cou008.
802 Lewis LS, Denney C, Willmes M, Xieu W, Fichman RA, Zhao F, Hammock BG, Schultz AA,
803 Fangue N, Hobbs JA (2021) Otolith-based approaches indicate strong effects of
804 environmental variation on growth of a Critically Endangered estuarine fish. Mar Ecol Prog
805 Ser 676:37–56.
806 Li H-C, Bischoff JL, Ku T-L, Lund SP, Stott LD (2000) Climate Variability in East-Central
807 California during the Past 1000 Years Reflected by High-Resolution Geochemical and
808 Isotopic Records from Owens Lake Sediments. Quat res 54:189–197.
809 Louviere J, Hensher D, Swait J (2000) Stated choice methods: analysis and application.
810 Lowe MR, DeVries DR, Wright RA, Ludsin SA, Fryer BJ (2009) Coastal largemouth bass
811 (Micropterus salmoides) movement in response to changing salinity. Can J Fish Aquat Sci
812 66:2174–2188.
813 Lundberg P (1988) The evolution of partial migration in Birds. Trends in Ecology & Evolution
814 3:172–175.
815 Mac Nally R, Thomson JR, Kimmerer WJ, Feyrer F, Newman KB, Sih A, Bennett WA, Brown L,
816 Fleishman E, Culberson SD, Castillo G (2010a) Analysis of pelagic species decline in the
817 upper San Francisco Estuary using multivariate autoregressive modeling (MAR). Ecological
818 Applications 20:1417–1430.

819 Mac Nally R, Thomson JR, Kimmerer WJ, Feyrer F, Newman KB, Sih A, Bennett WA, Brown L,
820 Fleishman E, Culberson SD, Castillo G (2010b) Analysis of pelagic species decline in the
821 upper San Francisco Estuary using multivariate autoregressive modeling (MAR). Ecological
822 Applications 20:1417–1430.
823 McArthur JM, Howarth R, Bailey T (2001) Strontium isotope stratigraphy: LOWESS version 3: best
824 fit to the marine Sr-isotope curve for 0–509 Ma and accompanying look-up table for
825 deriving numerical age. The Journal of Geology 109:155–170.
826 McGourty CR, Hobbs JA, Bennett WA, Green PG, Hwang H-M, Ikemiyagi N, Lewis L, Cope JM
827 (2009) Likely Population-Level Effects of Contaminants on a Resident Estuarine Fish
828 Species: Comparing Gillichthys mirabilis Population Static Measurements and Vital Rates in
829 San Francisco and Tomales Bays. Estuaries and Coasts 32:1111–1120.
830 Merz JE, Hamilton S, Bergman PS, Cavallo B (2011) Spatial perspective for delta smelt: a summary
831 of contemporary survey data. CALIFORNIA FISH AND GAME 97:164–189.
832 Miller JA (2011) Effects of water temperature and barium concentration on otolith composition
833 along a salinity gradient: Implications for migratory reconstructions. Journal of Experimental
834 Marine Biology and Ecology 405:42–52.
835 Monismith S, Kimmerer W, Burau J, Stacey M (2002) Structure and flow-induced variability of the
836 subtidal salinity field in northern San Francisco Bay. Journal of Physical Oceanography
837 32:3003–3019.
838 Moore JW, Yeakel JD, Peard D, Lough J, Beere M (2014a) Life-history diversity and its importance
839 to population stability and persistence of a migratory fish: steelhead in two large North
840 American watersheds. Journal of Animal Ecology 83:1035–1046.
841 Moore JW, Yeakel JD, Peard D, Lough J, Beere M (2014b) Life-history diversity and its importance
842 to population stability and persistence of a migratory fish: steelhead in two large North
843 American watersheds. J Anim Ecol 83:1035–1046.
844 Morita K, Tamate T, Kuroki M, Nagasawa T (2014) Temperature-dependent variation in alternative
845 migratory tactics and its implications for fitness and population dynamics in a salmonid fish.
846 J Anim Ecol 83:1268–1278.
847 Morley JW, Selden RL, Latour RJ, Frölicher TL, Seagraves RJ, Pinsky ML (2018) Projecting shifts in
848 thermal habitat for 686 species on the North American continental shelf. PLOS ONE
849 13:e0196127.
850 Moyle PB (2002) Inland Fishes of California: Revised and Expanded. University of California Press.
851 Moyle PB, Bennett WA, Fleenor WE, Lund JR (2010) Habitat Variability and Complexity in the
852 Upper San Francisco Estuary. SFEWS 8.
853 Moyle PB, Brown LR, Durand JR, Hobbs JA (2016) Delta smelt: Life history and decline of a once
854 abundant species in the San Francisco Estuary. San Francisco Estuary and Watershed
855 Science 14:1–30.
856 Moyle PB, Herbold B, Stevens DE, Miller LW (1992) Life History and Status of Delta Smelt in the
857 Sacramento-San Joaquin Estuary, California. Transactions of the American Fisheries Society
858 121:67–77.
859 Moyle PB, Hobbs JA, Durand JR (2018) Delta Smelt and Water Politics in California. Fisheries
860 43:42–50.
861 Moyle PB, Katz JVE, Quiñones RM (2011) Rapid decline of California's native inland fishes: A
862 status assessment. Biological Conservation 144:2414–2423.
863 Murphy DD, Hamilton SA (2013) Eastward Migration or Marshward Dispersal: Exercising Survey
864 Data to Elicit an Understanding of Seasonal Movement of Delta Smelt. San Francisco
865 Estuary and Watershed Science 11.
866 NatureServe (2014) *Hypomesus transpacificus*. The IUCN Red List of Threatened Species 2014.

867 Nichols FH, Cloern JE, Luoma SN, Peterson DH (1986) The Modification of an Estuary. Science
868 231:567–573.
869 Nobriga ML, Loboschefsky E, Feyrer F (2013) Common Predator, Rare Prey: Exploring Juvenile
870 Striped Bass Predation on Delta Smelt in California's San Francisco Estuary.
871 TRANSACTIONS OF THE AMERICAN FISHERIES SOCIETY 142:1563–1575.
872 Nobriga ML, Michel CJ, Johnson RC, Wikert JD (2021) Coldwater fish in a warm water world:
873 Implications for predation of salmon smolts during estuary transit. Ecology and Evolution
874 11:10381–10395.
875 Nobriga ML, Sommer TR, Feyrer F, Fleming K (2008a) Long-term trends in summertime habitat
876 suitability for delta smelt. San Francisco Estuary and Watershed Science.
877 Nobriga ML, Sommer TR, Feyrer F, Fleming K (2008b) Long-Term Trends in Summertime Habitat
878 Suitability for Delta Smelt, Hypomesus transpacificus. San Francisco Estuary and Watershed
879 Science 6:1–13.
880 Norris RM, Webb RW (1990) Geology of California. Second Edition.
881 Pershing AJ, Alexander MA, Hernandez CM, Kerr LA, Le Bris A, Mills KE, Nye JA, Record NR,
882 Scannell HA, Scott JD, Sherwood GD, Thomas AC (2015) Slow adaptation in the face of
883 rapid warming leads to collapse of the Gulf of Maine cod fishery. Science 350:809–812.
884 Phillis CC, Ostrach DJ, Ingram BL, Weber PK (2011) Evaluating otolith Sr/Ca as a tool for
885 reconstructing estuarine habitat use. Canadian Journal of Fisheries and Aquatic Sciences
886 68:360–373.
887 Pierce DW, Kalansky JF, Cayan DR (2018) Climate, drought, and sea level rise scenarios for
888 California's fourth climate change assessment. California Energy Commission and California
889 Natural Resources Agency.
890 Polansky L, Mitchell L, Newman KB (2019) Using Multistage Design-Based Methods to Construct
891 Abundance Indices and Uncertainty Measures for Delta Smelt - Polansky - 2019 -
892 Transactions of the American Fisheries Society - Wiley Online Library. American Fisheries
893 Society 148:710–724.
894 Potter IC, Tweedley JR, Elliott M, Whitfield AK (2013) The ways in which fish use estuaries: a
895 refinement and expansion of the guild approach. Fish Fish 16:230–239.
896 Reis G, Howard J, Rosenfield J (2019) Clarifying Effects of Environmental Protections on
897 Freshwater Flows to—and Water Exports from—the San Francisco Bay Estuary. San
898 Francisco Estuary and Watershed Science 17:1–22.
899 Rochet M-J (2000) May life history traits be used as indices of population viability? Journal of Sea
900 Research 44:145–157.
901 Roff D (1993) Evolution Of Life Histories: Theory and Analysis. Springer Science & Business
902 Media.
903 Schindler DE, Hilborn R, Chasco B, Boatright CP, Quinn TP, Rogers LA, Webster MS (2010)
904 Population diversity and the portfolio effect in an exploited species. Nature 465:609–612.
905 Scoville C (2019) Hydraulic society and a "stupid little fish": toward a historical ontology of
906 endangerment. Theory and Society 48:1–37.
907 Smith EP, Rose KA (1995) Model goodness-of-fit analysis using regression and related techniques.
908 Ecological Modelling 77:49–64.
909 Smith WE, Newman KB, Mitchell L (2020) A Bayesian hierarchical model of postlarval delta smelt
910 entrainment: integrating transport, length composition, and sampling efficiency in estimates
911 of loss. Can J Fish Aquat Sci 77:789–813.

912 Sommer T, Mejia F, Nobriga ML, Feyrer F, Grimaldo LF (2011) The Spawning Migration of Delta
913 Smelt in the Upper San Francisco Estuary. San Francisco Estuary and Watershed Science
914 9:1–16.
915 Sturrock AM, Carlson SM, Wikert JD, Heyne T, Nusslé S, Merz JE, Sturrock HJW, Johnson RC
916 (2020) Unnatural selection of salmon life histories in a modified riverscape. Global Change
917 Biology 26:1235–1247.
918 Sturrock AM, Wikert JD, Heyne T, Mesick C, Hubbard AE, Hinkelman TM, Weber PK, Whitman
919 GE, Glessner JJ, Johnson RC (2015) Reconstructing the migratory behavior and long-term
920 survivorship of juvenile Chinook salmon under contrasting hydrologic regimes. PloS one
921 10:e0122380.
922 Swain DL, Langenbrunner B, Neelin JD, Hall A (2018) Increasing precipitation volatility in twenty-
923 first-century California. Nature Clim Change 8:427–433.
924 Swanson C, Reid T, Young PS, Cech Jr JJ (2000) Comparative environmental tolerances of
925 threatened delta smelt (Hypomesus transpacificus) and introduced wakasagi (H.
926 nipponensis) in an altered California estuary. Oecologia 123:384–390.
927 Teh SJ, Baxa DV, Hammock BG, Gandhi SA, Kurobe T (2016) A novel and versatile flash-freezing
928 approach for evaluating the health of Delta Smelt. Aquatic Toxicology 170:152–161.
929 Theil H (1961) Economic forecasts and policy. North Holland, Amsterdam.
930 Thomson JR, Kimmerer WJ, Brown LR, Newman KB, Mac Nally R, Bennett WA, Feyrer F,
931 Fleishman E (2010) Bayesian change point analysis of abundance trends for pelagic fishes in
932 the upper San Francisco Estuary. Ecological Applications 20:1431–1448.
933 U.S. Fish and Wildlife Service (1993) Determination of Threatened Status for the Delta Smelt.
934 Federal Register 58:12854–12864.
935 Walther BD, Limburg KE (2012) The use of otolith chemistry to characterize diadromous
936 migrations. Journal of Fish Biology 81:796–825.
937 Willmes M, Jacinto EE, Lewis LS, Fichman RA, Bess Z, Singer G, Steel A, Moyle P, Rypel AL,
938 Fangue N, Glessner JJG, Hobbs JA, Chapman ED (2021) Geochemical Tools Identify the
939 Origins of Chinook Salmon Returning to a Restored Creek. Fisheries 46:22–32.
940
941

Tables

Table 3-1. Sample sizes of Delta Smelt analyzed in this study by cohort year and region.

Values in parentheses show sample sizes as the proportion of the total catch in the respective region and year. No samples were archived in 2008 (not shown). Regions as in Figure 3-2: North Delta (ND), South Delta (SD), Central Delta (CD) and West Delta (WD). Cells containing "0 (0.00)" indicate that there was catch but no samples were collected for otolith analyses, as opposed to "No catch" cells in which no Delta Smelt were caught by the survey in that year/region.

Cohort Year	ND	SD	CD	WD	Total
2002	149 (0.14)	0 (0.00)	1 (0.01)	12 (0.06)	162 (0.11)
2003	25 (0.07)	0 (0.00)	22 (0.05)	19 (0.01)	66 (0.03)
2004	64 (0.08)	5 (0.71)	17 (0.20)	64 (0.12)	150 (0.10)
2005	94 (0.24)	4 (0.40)	9 (0.69)	76 (0.46)	183 (0.32)
2006	93 (0.22)	No catch	25 (0.28)	48 (0.24)	166 (0.24)
2007	96 (0.46)	0 (0.00)	51 (0.49)	17 (0.77)	164 (0.49)
2009	53 (0.26)	No catch	114 (0.42)	46 (0.42)	213 (0.36)
2010	137 (0.52)	7 (1.00)	32 (0.89)	22 (0.16)	198 (0.44)
2011	92 (0.15)	0 (0.00)	34 (0.19)	73 (0.18)	199 (0.17)
2012	110 (0.65)	0 (0.00)	30 (0.48)	75 (0.69)	215 (0.63)
2013	85 (0.66)	0 (0.00)	55 (0.81)	97 (0.62)	237 (0.67)
2014	14 (0.64)	1 (0.50)	66 (0.66)	33 (0.89)	114 (0.71)
2015	22 (0.49)	No catch	6 (0.86)	6 (0.67)	34 (0.56)
2016	18 (0.78)	0 (0.00)	6 (0.03)	10 (0.59)	34 (0.13)
2017	1 (0.50)	No catch	13 (0.93)	6 (1.00)	20 (0.91)
2018	No catch	No catch	5 (1.00)	2 (1.00)	7 (1.00)
Total	1053 (0.22)	17 (0.09)	486 (0.26)	606 (0.18)	2162 (0.21)

Table 3-2. Results of separate Pearson χ^2 goodness of fit tests examining variation in the frequencies of each life history type among years, regions, and sexes.

Model	χ^2	DF	P
Year	389.5	30	<0.001
Region	538.5	6	<0.001
Sex	5.1	2	0.079

955 Table 3-3. Results of logistic regression models examining the additive effects of climate
956 on the Delta Smelt life-history portfolio.

957 Separate BLRMs were fit for each of the three migratory phenotypes (subscripts) and contrasted with an MLRM which
958 predicted the joint probability of all three life histories using MIG as the reference group. All models examined
959 interannual patterns in the relative abundance of the respective phenotypes as functions of the additive effects of
960 mean daily summer temperature (°C) and outflow (log_{10}, TAF^{-d}). Subscripts for models indicate the selected reference
961 level. Coefficients for each term are provided, along with the overall p-value and MFPR value each model (relative to
962 the respective intercept-only model).

Model	Term	Coefficient	p-value	MFPR
$BLRM_{FWR}$	Intercept (β_0)	29.071	<0.001	0.394
	Temperature (β_1)	-1.331		
	Outflow (β_2)	-1.977		
$BLRM_{MIG}$	Intercept (β_0)	-13.603	<0.001	0.156
	Temperature (β_1)	0.666		
	Outflow (β_2)	0.382		
$BLRM_{BWR}$	Intercept (β_0)	-27.345	<0.001	0.386
	Temperature (β_1)	1.006		
	Outflow (β_2)	2.772		
$MLRM_{MIG}$	$Intercept_{FWR}$ ($\beta_{1,0}$)	49.069	<0.001	0.06
	$Temperature_{FWR}$ ($\beta_{1,1}$)	-2.028		
	$Outflow_{FWR}$ ($\beta_{1,2}$)	-4.221		
	$Intercept_{BWR}$ ($\beta_{2,0}$)	21.569		
	$Temperature_{BWR}$ ($\beta_{2,1}$)	-0.763		
	$Outflow_{BWR}$ ($\beta_{2,2}$)	-2.466		

963

964

Figures

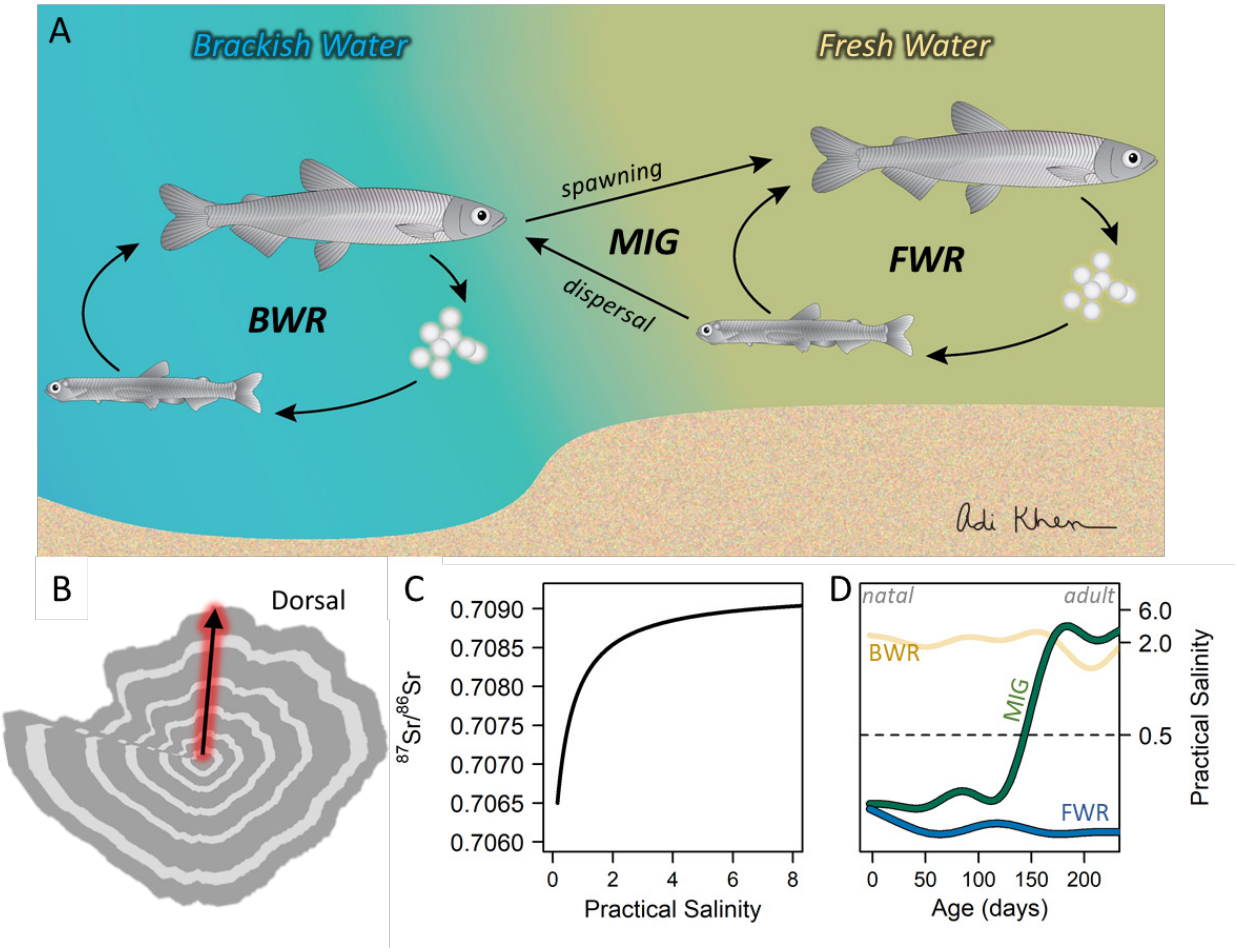

Figure 3-1. The complex life history of Delta Smelt.

(A) Most individuals are semi-anadromous migrants (MIG) that move upstream into tidal freshwater habitats in winter and spring to spawn, with juveniles dispersing downstream into brackish habitats where they feed and grow in the summer. Some individuals can hatch and remain in freshwater habitats (freshwater residents, FWR) or in brackish-water habitats (brackish-water residents, BWR) year-round (after Hobbs et al 2019). (B) Life history profiles were reconstructed by analyzing Strontium isotopes along the dorsal lobe of the sagittal otolith of each fish (rings are conceptual only), with (C) Strontium isotope values converted into salinity values using a standard mixing model. (D) Salinity profiles were then merged with daily growth increment profiles to provide salinity chronologies for each fish. The three life-history phenotypes could be distinguished by examining the natal (e.g., < 30 days-post-hatch, dph) and juvenile-subadult (e.g., 140-170 dph) habitat for each fish.

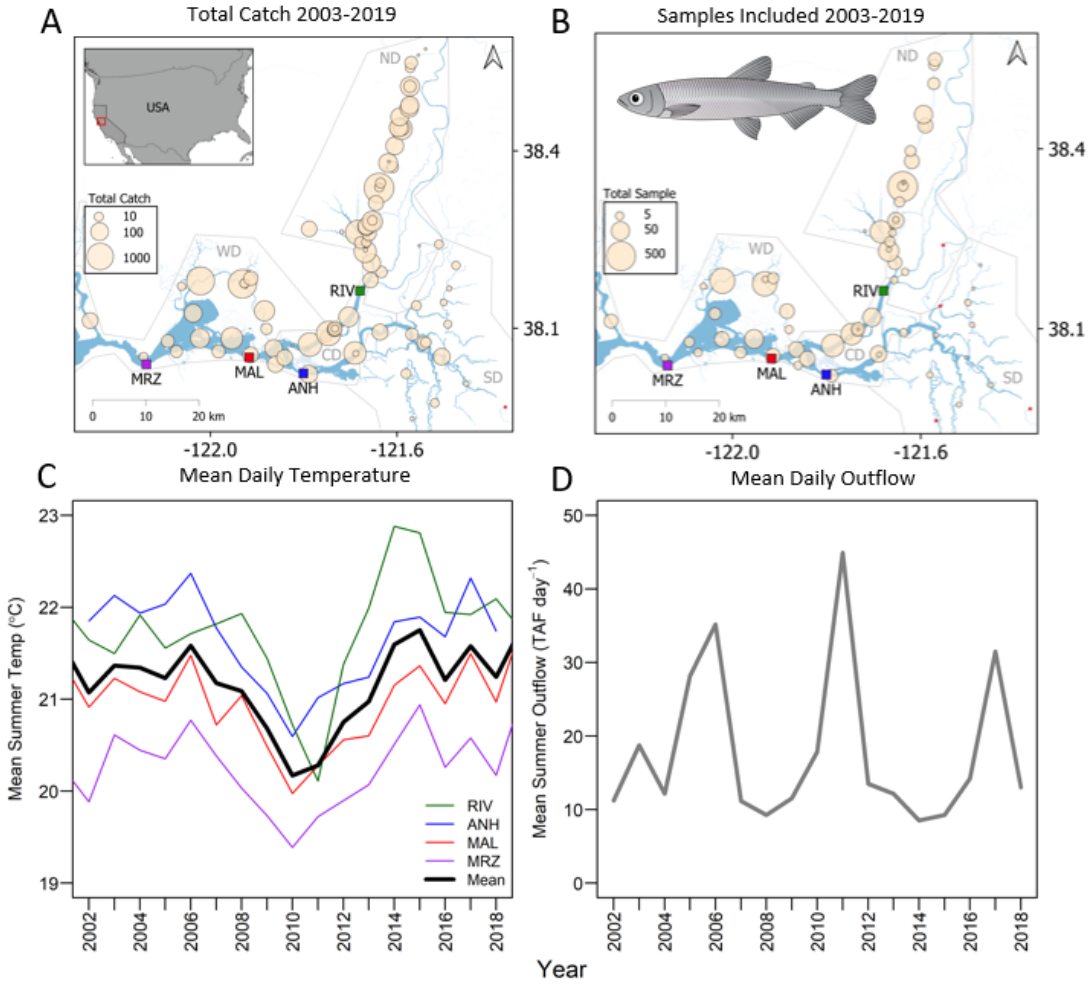

978

979 Figure 3-2. Delta Smelt collections and interannual variation in environmental conditions
980 in the SFE.

981 Total catch of juveniles through adults (A) and the subset of samples included in this study (B) of Delta Smelt from
982 each sampling station throughout the species' range. Circle sizes are proportional to the total catch and sample sizes,
983 respectively; rectangles represent sonde locations that provided water temperatures in. (C) Interannual variation in
984 mean daily summer water temperatures (June-July) at 4 long-term monitoring stations. (D) Interannual variation in
985 mean daily summer outflow based on the CA Department of Water Resource's "Dayflow" model
986 (http://www.water.ca.gov/dayflow/). Sonde locations are Rio Vista (RIV), Antioch (ANH), Mallard (MAL), and Martinez
987 (MRZ). Regions are North Delta (ND), South Delta (SD), Central Delta (CD), and West Delta (WD), as defined in Hobbs
988 et al. (2019).

989

990

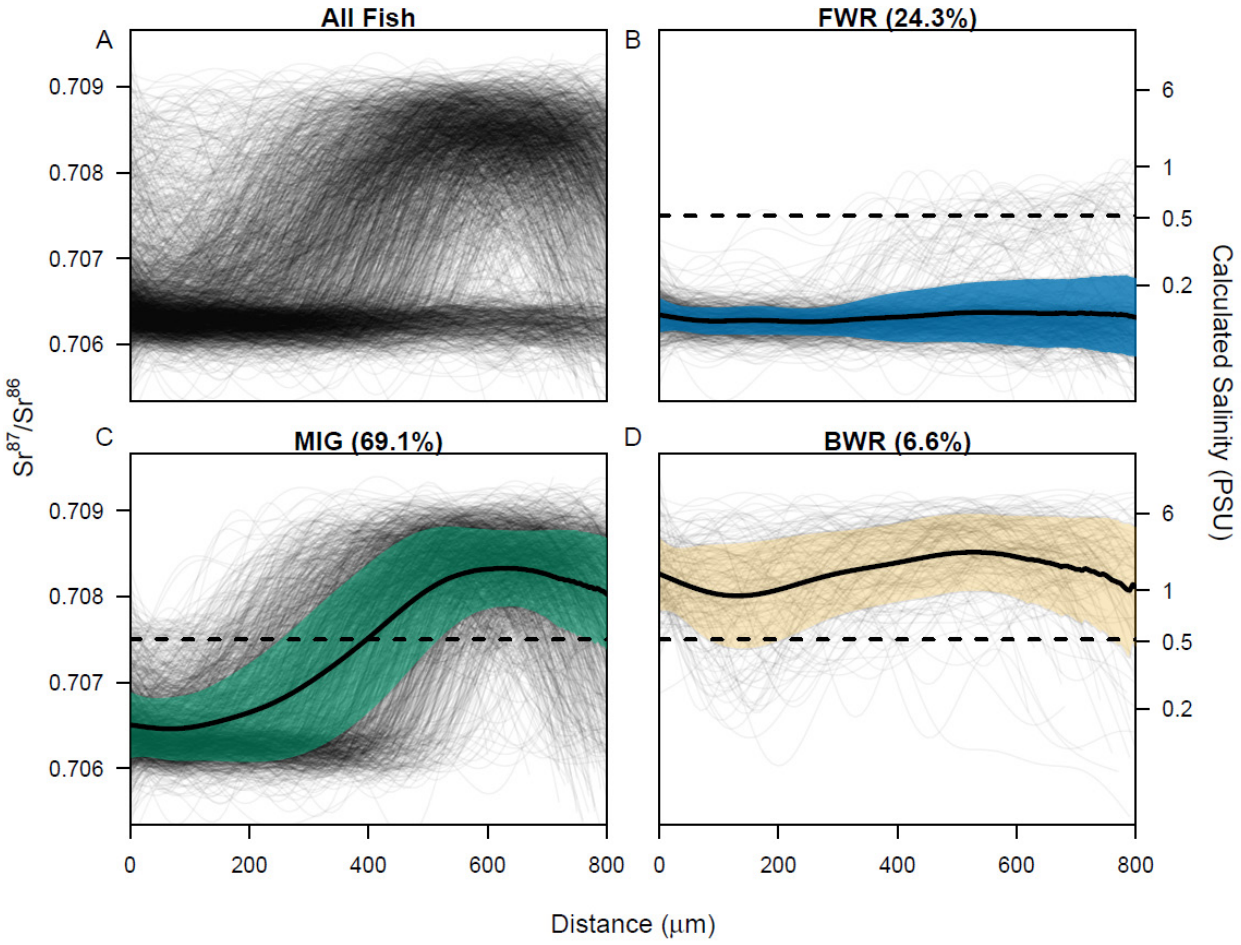

Figure 3-3. Strontium isotope profiles of all Delta Smelt (n = 2162) examined in the study.

All profiles (A) were categorized into each of the 3 migratory phenotypes: FWR (B), MIG (C), BWR (D). Bold lines and shading represent the mean and standard deviation for each group. Dashed lines represent the upper salinity threshold for freshwater habitats in the Delta (salinity = 0.5, $^{87}Sr/^{86}Sr$ = 0.7075).

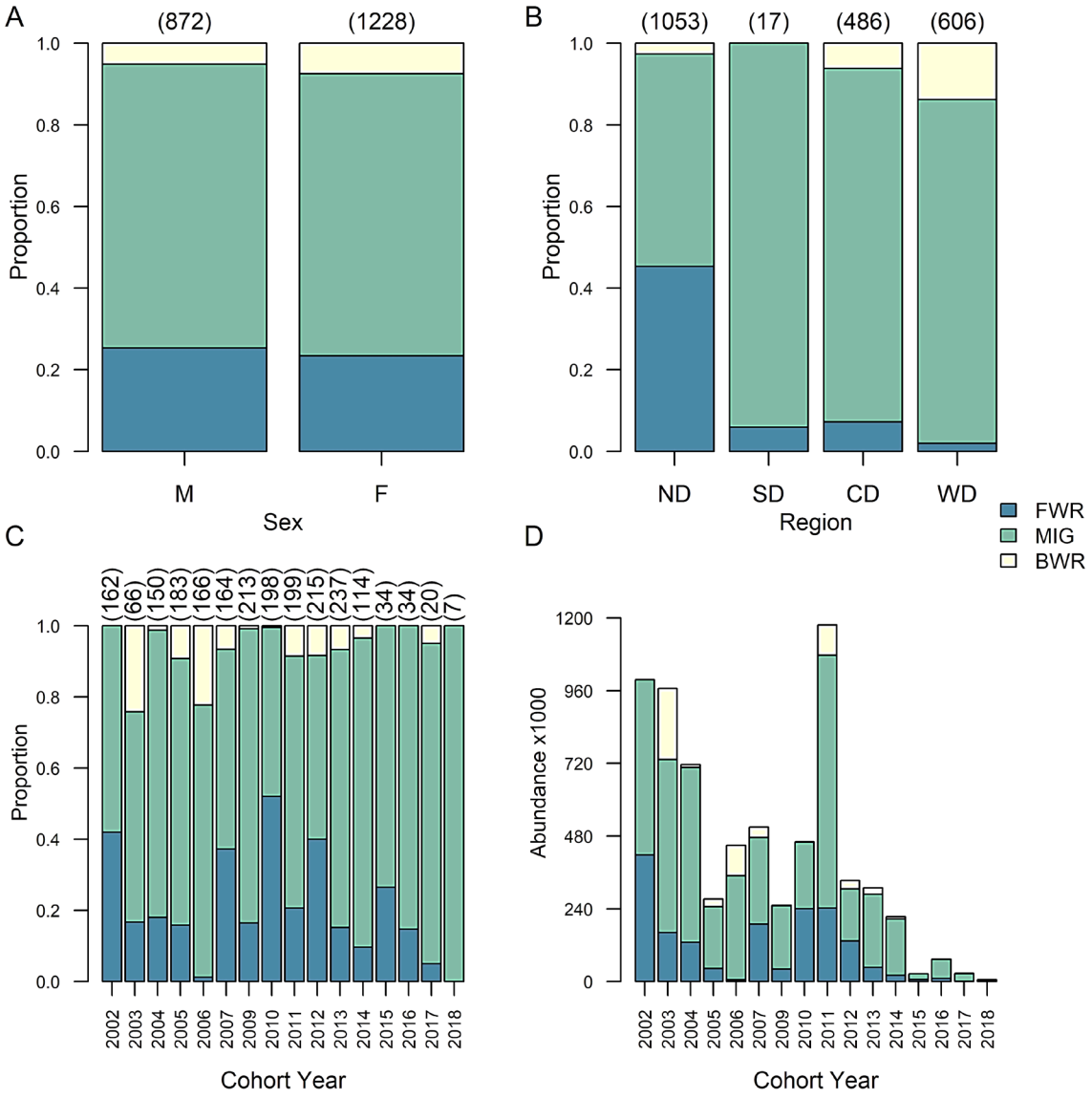

Figure 3-4. Variation in the migratory life history portfolio of Delta Smelt.

The relative abundance of each migratory phenotype was examined as a function of (A) sex (M-male, F-female), (B) region of capture, and (C) year-class (cohort year). Abundances of each phenotype (D) were examined by rescaling proportions in each sample to the corresponding annual population size based on Polansky et al. (2019). Numbers in parentheses reflect respective sample sizes (no samples were examined in 2008; not shown). Regions as in Figure 3-2 (ND: North Delta; SD: South Delta; CD: Central Delta and WD: West Delta).

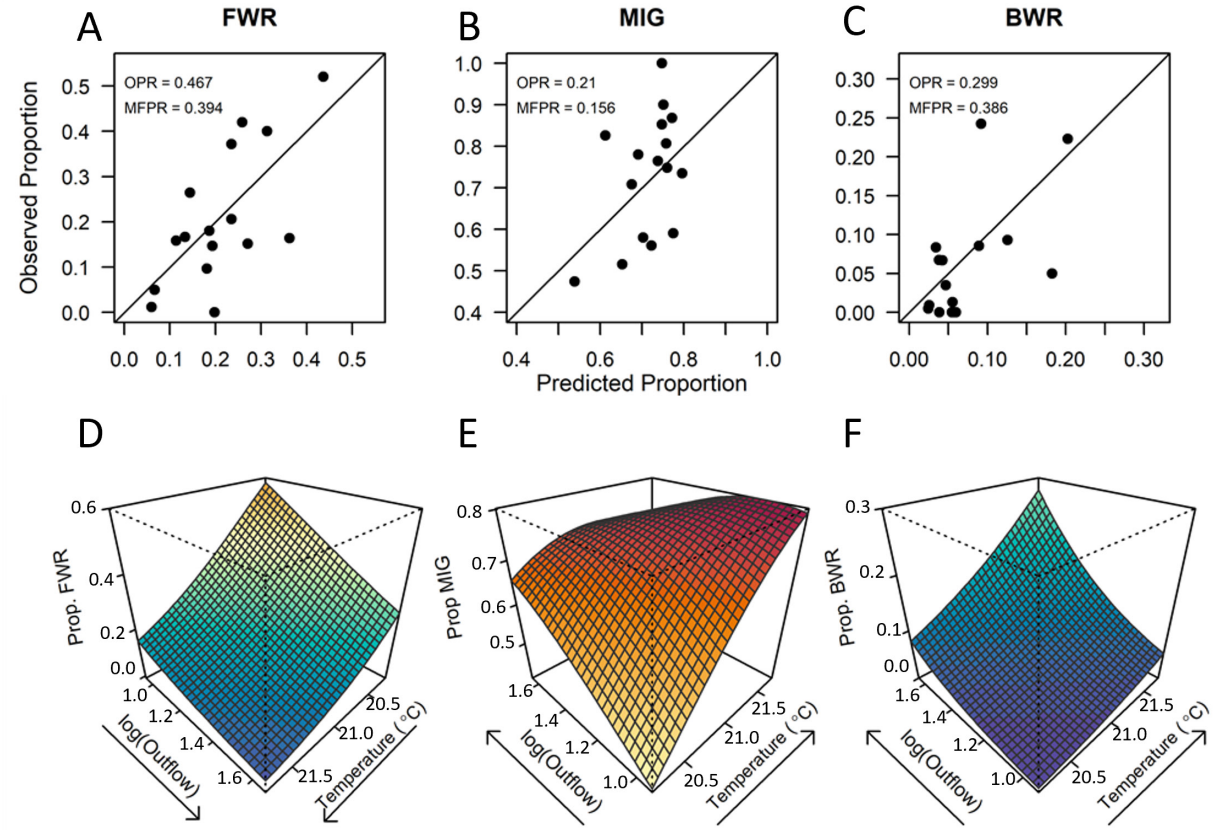

Figure 3-5. Results of the selected multinomial logistic regression model (T+O) examining the responses of each Delta Smelt life history phenotype to climate variability.

Observed versus predicted proportions for each year in the $MLRM_{MIG}$ were compared for (A) FWR, (B) MIG, and (C) BWR migratory phenotypes. Respective perspective plots (surfaces in D-F) represent the joint responses of each phenotype to the additive effects of interannual variation in summer water temperature and outflow. For A-C, diagonal lines represent 1:1 (perfect match), OPR reflects the respective fit for each phenotype based on MLRM predictions, and MFPR reflects the respective fit for each phenotype based on the individual BLRM predictions (Table 2). Note: temperature and outflow axes are reversed in D relative to E-F, y-axis ranges vary in A-C, and z-axis ranges vary among D-F with colors denoting the respective proportions along the full z-axis scale (blue = 0, red = 1).

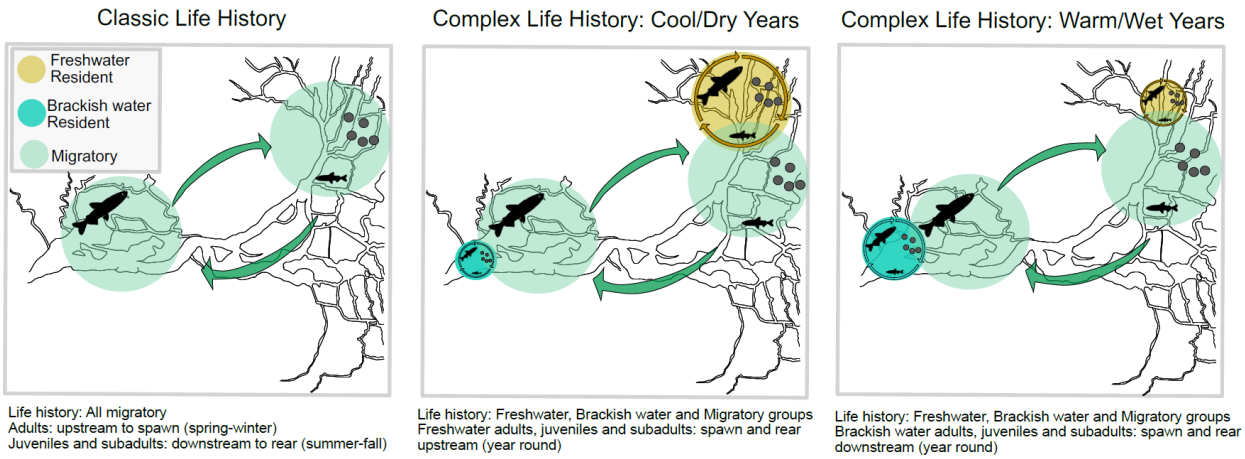

Figure 3-6. Conceptual models showing the MIG life history of Delta Smelt (A) and results of the present study showing the effects of climate on the more complex life-history portfolio, emphasizing (B) an increase in the proportion of FWR in cool-dry years and (C) an increase in BWR in the warmest, wettest years.

Chapter 4: Phenological Changes in Delta Smelt in Relation to Variation in Climate

Authors:

Levi S. Lewis[1], Leticia Cavole[1], Christian Denney[1], Wilson Xieu[1], Feng Zhao[1], Rachel A. Fichman[1], Malte Willmes[2,3], Bruce G. Hammock[4], Swee Teh[4], Andrew A. Schultz[5], James A. Hobbs[1,6]

[1] Wildlife, Fish and Conservation Biology, University of CA, Davis, Davis, CA, USA

[2]Institute of Marine Sciences, UC Santa Cruz, 115 McAllister Way, Santa Cruz, CA, 95064, USA

[3]National Marine Fisheries Service, Southwest Fisheries Science Center, 110 McAllister Way, Santa Cruz, CA, 95064, USA

[4] Department of Anatomy, Physiology, and Cell Biology, University of CA, Davis, CA, USA

[5] Green River Basin Fish and Wildlife Conservation Office, United States Fish and Wildlife Service, Vernal, UT, USA

[6] Bay-Delta Region, California Department of Fish and Wildlife, Stockton, CA, USA

Abstract

The seasonal timings of events (i.e., phenology) in plant and animal populations are strongly influenced by environmental conditions, and thus are sensitive to changes in climate. Such changes are particularly challenging for sensitive species such as Delta Smelt, *Hypomesus transpacificus*, that are confined to small geographic ranges. The Delta Smelt is a critically endangered pelagic forage fish that is endemic to the San Francisco Estuary (SFE), California, USA. Several field and laboratory studies suggest that Delta Smelt are physiologically sensitive to variation in water temperature, with growth, reproduction, and fitness likely to be impacted by climate change. However, no studies have examined empirically whether the phenology of wild Delta Smelt is sensitive to interannual variation in climate. Here, we used otolith-based tools to reconstruct the ages and hatch dates of >2,600 wild Delta Smelt that were collected from throughout their geographic range over a 20-year period. Interannual variation in hatch dates was assessed and modeled as the individual, additive, and interactive effects of interannual variation in water temperature and freshwater outflow. Results indicated that hatch dates vary significantly among years, by up to 60 days, with warmer years exhibiting significantly earlier hatch dates than cooler years. Winter temperatures alone explained 21% of the interannual variation in median hatch dates, with hatching occurring 8.8 days earlier per 1 °C increase in mean winter temperature. Results of this work provide the first empirical test of the thermal threshold model for Delta Smelt reproduction, thus providing a stronger understanding of this species' thermal sensitivity and the likely phenological impacts of future warming due to global climate change.

Introduction

All living organisms have biological clocks and endogenous rhythms that interact with their surrounding environment to facilitate growth, survival, and reproduction. The phenology of plant and animal populations is defined by the timing of seasonal processes such as recruitment, migration, and reproduction, each of which can be driven by a variety of biological and physical mechanisms (Walther et al., 2002; Visser & Both, 2005; Liang, 2019). Originally, the term was coined by terrestrial ecologists observing the appearance of plants in spring and the arrival and departure date records on birds and butterflies from temperate ecosystems, mainly across the northern hemisphere (Menzel et al., 2006; Parmesan, 2007). For example, in flowering plants, the timing of phenological events (e.g., leafing, flowering, and fruiting) is significantly correlated with air temperatures, often occurring earlier as climates warm (Menzel et al., 2006), and altering ecological relationships (Liu et al., 2011). As in terrestrial habitats, some phenological patterns in aquatic systems are observable using remote sensing (Platt et al., 2009; Ustin et al., 2015); however, those of mobile aquatic species, like small fishes, are much more challenging to quantify (Genner et al., 2010; Asch, 2015; Woods et al., 2021).

The phenology of aquatic organisms appears to be particularly sensitive to changing environmental conditions and global climate change. For example, the magnitude of phenological shifts in aquatic ecosystems can be greater, occur more rapidly, and be more complex than those observed in terrestrial habitats (Edwards & Richardson, 2004; Burrows et al., 2011). Phenological patterns in estuaries, coastal lagoons, and bays, are of particular interest as climate variability can be rapid and drastic in these systems, exposing aquatic organisms to anomalous abiotic environmental conditions that can disrupt otherwise fine-tuned biological clocks. Subtle changes in environmental conditions and seasonal patterns can induce metabolic and physiological responses that ultimately translate into phenological shifts that impair population dynamics. For example, phenological shifts could result biological decoupling such as asynchrony in consumer-prey interactions that can significantly impact recruitment dynamics, also known as "match-mismatch" hypothesis, (Cushing, 1969, 1990).

In many systems, climate-induced warming can result in the early arrival of spring, the lengthening of the summer (i.e., growing season), and the delayed onset of fall, thus altering the reproductive phenology of terrestrial and aquatic organisms (Visser et al., 2004, 2006; Parmesan, 2007; Pankhurst & Munday, 2011; Hovel et al., 2017). For example, long-term shifts were observed for *Gymnocypris selincuoensis*, an endemic fish from the Tibetan Plateau, with its reproductive phenology advancing by nearly 3 d decade^{-1} from the 1920-200 (Tao et al., 2018). In the California Current Ecosystem, approximately 40% of all fish species have experienced phenological shifts in peak larval abundance, also with a mean rate of change of 3-4 days earlier per decade (Asch, 2015). To date, however, most research on the reproductive phenology of fishes has focused on habitats at higher latitudes or species that are associated with valuable fisheries such as cold-water salmonids (Keefer et al., 2008; Myers et al., 2017; Sparks et al., 2019), gadids (Hutchings & Myers, 1994; Morgan et al., 2013; Rogers & Dougherty, 2019), and abundant pelagic forage fishes (Hernández-Santoro et al., 2019; Polte et al., 2021). Much less is known about the phenological responses of rare species, thus limiting our understanding of their sensitivity to climate change.

In California, remarkable variation in climatic conditions has occurred over the past 2,000 years (Stine, 1994), requiring that its native animal and plant communities evolve and adapt to extreme interannual variation in weather and hydrological conditions. In addition to interannual variability

regional climate, the hydroclimate of local environments, such as the San Francisco Estuary (SFE), are rapidly warming through time, forcing fish to adapt to new and changing conditions (Brown et al., 2016; Cloern et al., 2011; Dettinger et al., 2016). For example, the climate for watersheds of the SFE is predicted to warm by ~ 4°C by the end of this century, which will substantially reduce snowpack, advance the timing of snowmelt, increase air and water summer temperatures, and extend the summer season (Dettinger et al., 2016), likely disrupting the natural phenology of endemic species, making them even more susceptible to other anthropogenic impacts. For example, the SFE is a highly invaded system, with many non-native predators and competitors that can impact native species (Callaway & Josselyn, 1992; Moyle, 1995), and may be more resistant or resilient to climate change (Turner et al., 2010).

Climate variability, habitat alteration (through water outflow controls), and species invasions can alter the phenology of aquatic species in the SFE system through abiotic (e.g., temperature, outflow, precipitation, riparian shading, elevation, photoperiod) and biotic (i.e., competition, predation) mechanisms. To date, however, few studies have attempted to understand the phenology of fishes in this system, restricting analysis to anadromous species that depend on oceanic plankton blooms during the upwelling season, such as the hatchery-origin fall run Chinook Salmon *Oncorhynchus tshawytscha* (Satterthwaite et al., 2014) and non-native species whose migratory behavior is delayed with high outflow and cool water conditions, such as the Striped Bass *Morone saxatilis* (Goertler et al., 2021). Unraveling the relationships between abiotic environmental conditions and fish phenology is key to predicting how climate change will alter the timing of relevant ecological events, especially for species that have reached historic lows in abundance and have limited geographic ranges, such as the SFE's endemic Delta Smelt.

Delta Smelt (*Hypomesus transpacificus*) is a small, annual pelagic forage fish that was once one of the most abundant species in the system, and likely served an important ecological role in the SFE. However, the population has declined to < 1% of historic (pre-1980s) levels, and the species is now protected under the U.S. Federal ("threatened") and California State ("endangered") Endangered Species Acts. Delta Smelt exhibit a complex life history, with most individuals being semi-anadromous, and a variable fraction of the population remaining resident in fresh or brackish waters throughout the year (Hobbs et al., 2019). In the laboratory, Delta Smelt exhibit plasticity in spawning behavior; they can lay their eggs in different types of substrate and spawn at various nighttime hours under laboratory-controlled conditions (Tsai et al., 2021). Although annual, individuals in the laboratory also appear to be able to reproduce multiple times if spawning conditions remain favorable (Damon et al., 2016; Kurobe et al., 2016). Little is known, however, about the wild population, for which precise spawning locations and behaviors remain unknown, and eggs have never been observed (Moyle et al., 1992; Bennett, 2005; Moyle et al., 2016).

Delta Smelt is a temperate species for which the timing of maturation, spawning, fertilization, and hatching (i.e., phenology) are strongly correlated with temperatures during winter and spring (Bennett, 2005; Brown et al., 2013). When water temperature decreases to < 20 °C in the fall, Delta Smelt begin to allocate most of their energetic reserves into gonad development until temperatures rise again to > 12-15 °C in the spring. This period is known as the "temperature-dependent maturation window." When temperature starts to increase above 12°C in the spring Delta Smelt begin to spawn, with spawning continuing until temperatures rise above 20 °C in the summer. This period is known as the "temperature-dependent spawning window" (Bennett, 2005; Brown et al., 2013) (Figure 4-1B). Given the temperature dependency of maturation and spawning, changes in water temperature (e.g., due to climate change) are likely to affect the timing of Delta Smelt

reproduction and recruitment. For example, warmer waters may compress and shift the maturation and spawning windows to earlier times in the year (Figure 4-1C).

Although laboratory studies using cultured fish and observations of fish catch data support this "thermal threshold" model for Delta Smelt reproduction, the predictions of this model have yet to be contrasted with empirical observations of patterns in the phenology of the wild Delta Smelt population and associated variation in regional climate. Here, we used otolith-based tools to reconstruct the ages and hatch dates of >2,600 wild-caught Delta Smelt that were archived from throughout their geographic range over a 20-year period. We quantified interannual variation in hatch date distributions and modeled these in relation to interannual variation in water temperatures and freshwater outflow. By examining the phenology of the wild Delta Smelt population, our results provide the first empirical test of the thermal threshold reproduction model, thus providing a stronger understanding of this species' thermal sensitivity and the likely phenological impacts of future warming due to global climate change.

Methods

Study Site

The San Francisco Estuary (SFE) is the largest estuary on the west coast of the United States, encompassing an area of approximately 11,913 km^2, with an average depth of 6 meters and average annual air temperature of 14°C (Engle et al., 2007). This system is formed by the confluence of the Sacramento and San Joaquin Rivers (Delta) and marine waters originating from the Pacific Ocean, west of the Golden gate (by the city of San Francisco, California). The harbor and ecosystems in the San Francisco Estuary-Bay supports the 5th largest economy on the planet, delivers water to more than 25 million people, and provides nursery, breeding and rearing sites for over 1,000 species of animals, including ~160 species of fish that uses its estuarine waters for at least one stage during their life cycles. However, the hydroclimatic and salinity conditions inside the estuary are heavily influenced by water diversions from the Sacramento and San Joaquin Rivers for urban and agricultural uses (Nichols et al., 1986; Brown et al., 2013). The SFE was designated a Wetland of International Importance and currently comprises 77% of the remaining wetlands in California (BCDC, 2021; https://bcdc.ca.gov/bay_estuary.html), a state where wetlands were 95% of wetland habitats have been lost or severely degraded. The above exemplifies the unique value of the SFE to its human and non-human components, including species found nowhere else on earth, such as its endemic and critically endangered Delta Smelt.

Sample Collection

The SFE is one of the most heavily monitored and studied ecosystems in the world with considerable research efforts focused on native fishes. Since Delta Smelt are critically endangered and wild specimens are extremely rare, Delta Smelt specimens were collected and provided by several state and federal monitoring programs: 20-mm Survey (20-mm), Covered cod-end (CCE), Central Valley Project (CVP), Enhanced Delta Smelt Monitoring Program (EDSM), Fall Midwater Trawl Survey (FMTW), Gear Evaluation Survey (GES), San Francisco Bay Study (SFBS), Summer Townet Survey (TNS), and Yolo Bypass Survey (YB) (Table 4-1). The final collection comprised 20 years of data, from 1999 to 2019 (no samples were available in 2003). Most samples were collected in Suisun Bay and the Sacramento River Deep Water Ship Channel (SDWSC) (Figure 4-1A). Each individual was given a serial number upon capture, its fork length recorded, and it was preserved in liquid nitrogen or 95% ethanol.

Otolith Preparation and Aging

Sagittal otoliths were analyzed following established protocols (Hobbs et al., 2019; Xieu et al., 2021). Sagittal otoliths were extracted and stored either dry or in 95% ethanol. In preparation for mounting, the membrane surrounding the otoliths was removed by soaking in 95% ethanol for a minimum of 24 hours. Otoliths were mounted on glass slides with Crystal Bond® thermoplastic resin in the sagittal plane. Once mounted, the otoliths were sanded sulcus side up until the most recent, edge rings were visible, and then turned and sanded with wet-dry sandpaper (Buehler 800 and 1200 grit) until the core rings could be distinguished; and finally, the otoliths were polished with a polishing cloth and 0.3-micron polishing alumina. The prepared slides were digitized with a 12 Megapixel AM Scope digital camera attached to an Olympus CH30 compound microscope at a magnification of 20X. Otolith increments were counted, and the ring widths recorded (in μm) from the core to dorsal edge of each otolith using Image-J *(http://imagej.nih.gov/ij/)*. Each otolith was aged by a minimum of two analysts. Agreement between the analysts was checked using an average coefficient of variation (ACV) of <10% for quality assurance. If two age readings were greater than 10% ACV, the otolith was read by a third analyst and reassessed. If agreement could not be reached with additional reads, the otoliths with ACV > 10% were removed from analysis. Hatch date for each fish was calculated by subtracting the mean otolith-based age estimate from the known capture date (Figure 4-2).

Environmental metrics

To examine environmental influences on the reproductive phenology of Delta Smelt, we quantified interannual variation in climate and hydrology of the upper SFE. First, interannual variation in water temperature was quantified using a "Winter Temperature Index" (WTI). The WTI was calculated as the mean Delta water temperature during winter (Jan-Mar), averaging across 4 stations: Sacramento River at Hood (SRH), Antioch (ANH), Mallard Slough (MAL) and Martinez (MTZ). Stations were selected to span the full spatial (Delta) and temporal (1999-2017) scope of the study, while minimizing data gaps. Measurements were recorded at 15-min intervals at these stations by sondes maintained by the California Department of Water Resources (DWR): (http://cdec.water.ca.gov/) (Figure 4-1A). Minor gaps in temperature data were imputed using the mice package in R, and checked visually for congruence.

As for the WTI, mean daily freshwater outflow was quantified for each year using the DWR Dayflow hydrologic model for the Delta (https://data.cnra.ca.gov/dataset/dayflow). Outflow is defined by the net quantity of freshwater that flows out of the Delta, westward of Chipps Island (38°03'19"N 121°54'43"W). Mean daily outflow (in $m^3 s^{-1}$ or 1000x acre-feet per day TAF d^{-1}) was averaged for each year from January to June. These months include the main hydrologic cycle in the Delta, including winter precipitation and summer snowmelt. This period also encompasses the full spawning window of Delta Smelt (i.e., oocytes are mature in February through April; Kurobe et al. 2016). Both environmental indices were then contrasted with annual patterns of hatch dates to quantify responses of Delta Smelt spawning activities to interannual variation in hydroclimatic conditions in the SFE for the past 20 years.

Statistical Analyses

We used linear models to investigate interannual variation in hatch dates and the effects of water temperature and freshwater outflow on hatch timing for each year from 1999 through 2019 (except for 2003). Interannual variation in hatch date distributions was first assessed by ANOVA. Next, a series of nested linear models examining the independent, additive, and interactive effects of mean

Delta water temperatures and outflows on median hatch dates were constructed. The median was chosen as a robust estimate of the central tendency of the hatch distributions, being less influenced by skewness and outliers. Models including the additive and interactive effects of temperature and outflow were included given that these variables were not correlated (p=0.14, R^2=0.07). The subset of single-factor (temperature or outflow) and multi-factor (temperature + outflow, temperature * outflow) were compared using the corrected Akaike Information Criterion (AIC_c) (Table 4-2). To assess stability and confidence in the coefficients (i.e., slope) of the robust model, a full version of this model, including all individual fish as replicates, was also examined and contrasted with the robust model. Analyses were conducted using the R statistical software package (R Core Team, 2019).

Results

Interannual variation in climate

Water temperatures in the Delta varied among regions, seasons, and years (Figure 4- 3A). In general, the cooler fall season started at around day 300 (November 1st) and lasted until day 90 (31st March). In certain years, such as 1999, 2011 and 2017, the transition to the onset of warmer days took longer to establish (Figure 4- 3A), and winters were colder than normal (Figure 4- 3B). The timing of the spawning window for Delta Smelt, as defined by water temperatures between 12-20°C (solid vertical lines in Figure 4- 3A). From 1999 to around 2006, the Antioch (ANH) station, located close to the mouth of the San Joaquin River (Figure 4- 1A), exhibited the highest water temperatures among stations (Figure 4- 3A). This trend started to change in 2007, and between 2013-2015, Sacramento River Hood (SRH) station recorded the highest water temperatures on record (~ 24-25°C), often exceeding thermal thresholds for Delta Smelt's early life development (Komoroske et al., 2014).

Similar to WTI, monthly averages of freshwater outflow (TAF) showed high interannual variability (Figure 4- 3C) in the first half of the year, although the two time series were not significantly correlated (p=0.14, R^2=0.07). The years of 2006, 2011 and 2017 were the wettest years in our record (Figure 4- 3C). The month of February was particularly wet in 2017, with mean outflows approximately 10-fold greater than baseline levels (i.e., 7,500 m^3s^{-1}) (Figure 4- 3C).

Interannual variation in Delta Smelt phenology

Using otoliths, we were able to estimate the age and hatch dates for 2,698 Delta Smelt from 20 cohorts between 1999 and 2019. Delta Smelt started to hatch as early as February, peaked in April, and decreased considerably by the end of May (Figure 4- 4A). This trend characterized the protracted spawning season for this species, with some years showing bimodal hatch date distributions (e.g., 2000, 2007, 2011, 2017). Years marked by high freshwater outflow (2006, 2011, 2017 and 2019) appeared to exhibit the latest theoretical onset of the spawning window based on thermal threshold model (Figure 4- 4A).

Median hatch dates of wild Delta Smelt varied among annual cohorts by up to 60 days (ANOVA, $F_{19, 2676}$ = 70.58, p<0.001, R^2 = 0.329, Figure 4- 4B). Cohorts from 2014-2016 and 2019 exhibited the earliest hatch dates, whereas those from 1999, 2001-2005, and 2011 exhibited the latest hatch dates (Figure 4- 4B-C). Median hatch dates were best described by the temperature-only ("T") model, which exhibited the highest R^2 and lowest AIC_c values of all models examined (Table 4-2). Thus, median hatch dates were significantly correlated with winter water temperatures ($F_{1,18}$ =6.09, p=0.024, R^2=0.211, Table 4-2), but did not appear to vary with the independent, additive, or

interactive effects of freshwater outflow (Table 4-2). Temperature appeared to have a relatively strong effect on phenology, with median hatch dates occurring 8.78 (± 3.56 se) days earlier for each 1°C increase in the WTI (Figure 4- 4C). In contrast to the robust (median) model, the full model indicated even greater thermal sensitivity with mean hatch dates shifting by 10.41 (± 0.49 se) days earlier for each 1°C increase in the WTI ($p < 0.001$, $R^2=0.14$, Table 4-3). Thus, results of the full model corroborated the robust model, while indicating a steeper, more precise, and highly significant slope estimate.

Discussion

Freshwater, estuarine, and marine fish species across the globe often exhibit life cycles that are closely synchronized with seasonal changes in water temperature. In spring-spawning species, such as Delta Smelt, increasing water temperatures often cue the late stages of reproductive development, thus establishing a species phenology, including the timing of spawning, hatching, metamorphosis, and migration (Pankhurst & Munday, 2011). Such temperature-dependent phenological patterns can be highly sensitive to variation in climate. For example, epipelagic and mesopelagic fishes in the California Current Ecosystem have experienced phenological changes of 3-4 d decade^{-1} in response to warming ocean temperatures (Asch, 2015). Similarly, Pacific Herring (*Clupea pallasii*) in British Columbia spawn ~10 days earlier when mean winter temperatures are 1-1.5 °C warmer (Ware & Tanasichuk, 1989) and spawning of Walleye Pollock (*Gadus chalcogrammus*) occurs 21 days earlier in the year due to warming water temperatures in the Gulf of Alaska (Rogers & Dougherty, 2019). Similarly, spawning by Delta Smelt in the SFE is predicted to shift by up to 5 d decade^{-1} earlier under the most extreme climate scenarios (Brown et al., 2016). These changes in the timing of major events in each species' life cycle can disrupt key processes (e.g., match-mismatch with food production), ultimately leading to recruitment failure and population collapse.

To empirically evaluate the sensitivity of Delta Smelt reproductive phenology to environmental change, we used otolith-based tools to back-calculate the hatch dates of approximately 2,700 wild specimens that were collected and archived over a 20-year period in the San Francisco Estuary. We identified significant interannual variation in Delta Smelt phenology, with hatch dates varying among annual cohorts by > 60 days. Hatch dates and winter temperatures were strongly correlated, with hatching occurring approximately 9 days earlier per 1 °C increase in the winter temperature index (WTI). Hatch dates did not appear to be affected by variation in freshwater outflow. Results of our empirical study of wild fish corroborate previous laboratory studies and models indicating that the reproductive phenology of Delta Smelt is sensitive to variation in regional climate.

The Delta Smelt is a small annual species with relatively low fecundity and an extremely limited geographic range (Moyle et al., 1992, 2016). These life history attributes, together with its high sensitivity to environmental variability, greatly increase its vulnerability to environmental change. Thus, unlike fishes that live in large marine ecosystems, like the California Current, Delta Smelt are unable to adjust their geographic distributions in response to local and global warming. Given their inability to migrate to more suitable latitudes, the temperature-dependent phenological changes observed here suggests that future warming is likely to strongly affect the timing of spawning and recruitment of Delta Smelt in the SFE (Brown et al., 2013, 2016; Cloern et al., 2011; Dettinger et al., 2016). Based on these results, future studies that forecast changes in winter temperatures can now assess, with greater confidence, how Delta Smelt spawning phenology is likely to change in response

to various climate scenarios (Brown et al., 2016). Such an approach can be applied to many species across ecosystems.

Our empirical results of the thermal sensitivity of Delta Smelt reproduction support the conclusions of previous theoretical estimates based on coupled climate-ecophysiological models of Delta Smelt reproduction (Brown et al., 2016). Based on various climate forecasts, the authors conclude that Delta Smelt spawning phenology could shift to earlier times in the year at a rate of 1-5 d decade^{-1}. Based on our results, this would correspond with an increase in the WTI of 0.1-0.5 °C decade^{-1}. Therefore, given that Delta water temperatures are predicted to rise at a rate of up to 0.4 °C decade^{-1} (Cloern et al., 2011), there appears to be strong agreement between the predicted (theoretical) and observed (empirical) sensitivity of Delta Smelt reproduction to climate-induced warming of the Delta.

In addition to modeling overall changes in Delta Smelt phenology, Brown et al. (2016) quantified spatial heterogeneity in forecasts of environmental conditions and associated changes in the spawning window. For example, temperature and phenological changes at sites in the North Delta and San Joaquin River appeared to be the most sensitive to climate change. Given that Delta Smelt express several different life histories and may be able to spawn in different parts of the Delta (Hobbs et al., 2019), such spatial variation could be informative. However, spatial patterns in the water temperature data in our timeseries was somewhat complex. For example, of the four sonde stations selected for our 20-year time-series, the Antioch Station (ANH) exhibited the highest water temperatures in most years, except during the 2013-2015 drought, when the Sacramento River Station (SRH) switched from being one of the coolest sites to being the warmest site in the study (Figure 4- 3A). This suggests that modeling of spatial patterns may be complex. Nevertheless, spatially explicit scenarios could provide a more refined estimate of the likely impacts of climate change on Delta Smelt reproduction.

Here, we used 12 °C as the lower thermal threshold that determines the beginning of the spawning window. Our value is lower than the temperature (15 °C) typically used in thermal threshold models of Delta Smelt reproduction (Bennett, 2005; Brown et al., 2016); however, this higher value is based largely on laboratory studies using cultured specimens. For example, when fish are strip-spawned in the laboratory, hatching success and larval survival appear to be optimized at 15-17 °C (Baskerville-Bridges et al., 2005). The spawning behaviors of wild Delta Smelt, however, may deviate from those in culture conditions. For example, field collections suggest that Delta Smelt may spawn in the wild at temperatures as cool as 7-15°C (Wang, 1986), and Delta Smelt are known begin to spawning naturally, on their own, in the laboratory at temperatures as low as 12°C (Baskerville-Bridges et al., 2005). Thus, our lower threshold of 12 °C is likely more representative of natural spawning conditions *in situ*. We used the standard value of 20 °C for the upper thermal threshold. This value is supported by laboratory studies (Baskerville-Bridges et al., 2005) and by field surveys (Bennett, 2005; Nobriga et al., 2008) indicating that larval survival and abundance decline at temperatures > 20 °C. Similarly, wild-caught "maturing" subadult Delta Smelt also exhibit both reduced body condition (Hammock et al., 2022) and reduced growth (Lewis et al., 2021) as water temperatures approach and exceed 20°C.

Schlosser (1987) postulated that the reproductive phenology might affect recruitment more severely in warm water streams with temporally variable outflows, low habitat heterogeneity, and low refugia availability from non-optimal conditions . Due to channelization and regulation of flows, these characteristics are now often observed for several regions of the SFE. In the SFE, spawning peaks

337 often occur during or shortly after high outflow events for several fish species, including Striped
338 Bass *Morone saxatilis* (Sommer et al., 2007; Goertler et al., 2021), Longfin Smelt *Spirinchus thaleichthys*
339 (Nobriga & Rosenfield, 2016), and Splittail *Pogonichthys macrolepidotus* (Feyrer et al., 2006). However,
340 our analysis did not detect significant changes of spawning/hatching dates with hydrological
341 variations (i.e., freshwater outflow) (Table 4-1). Interestingly, in other river systems, summer-
342 spawning fishes have a stronger relationship between timing of spawning and outflow than spring-
343 spawners, such as Delta Smelt, demonstrating the diversity of phenological responses depending on
344 the life cycle of each species (Krabbenhoft et al., 2014). Interestingly, years with high outflow (>100
345 TAF day $^{-1}$) and moderate winter temperatures (<12°C), such as 2011 and 2017, appeared to have
346 protracted spawning seasons for Delta Smelt (Figure 4- 4A), suggesting that high outflow regimes
347 are likely important for supporting multiple bouts of successful spawning within a season (Damon et
348 al., 2016).

349 The empirical results described herein using ~ 2,700 wild Delta Smelt were generated using validated
350 otolith-based approaches (Xieu et al., 2021) and are supported by expectations based on theoretical
351 models of Delta Smelt reproduction (Bennett, 2005; Brown et al., 2016). Nevertheless, several key
352 uncertainties regarding interannual patterns in hatch dates should be considered. First, catches of
353 this endangered species are often sparse in the wild, thus, samples are often unbalanced in time,
354 space, and in relation to environmental variation. For example, although the average sample size per
355 cohort was 135 specimens, some years had as few as 16 individuals whereas other years had > 300
356 individuals (Table 4-1). Furthermore, specimens were collected throughout their range by different
357 monitoring programs that sampled using a variety of different gear types that are deployed in
358 different regions, at different times, and exhibit different size-selectivity (Table 4-1). For example,
359 the inclusion of gear types that sample different life stages in different seasons could result in
360 different degrees of selection that could modify hatch date frequencies of cohorts. Similarly, it is also
361 possible that patterns in observed hatch dates better reflect patterns in larval survival rather than
362 interannual variation in spawning. Last, although the Delta Smelt population does not exhibit spatial
363 genetic structure (Fisch et al., 2011), it is possible that fish collected in different regions might
364 exhibit region-specific differences in life history (Hobbs et al., 2019), including hatch dates. Despite
365 these caveats, the observed patterns in hatch dates largely matched predictions based on the
366 thermal-threshold model of Delta Smelt reproduction, thus providing the first empirical test of this
367 important model using wild Delta Smelt.

368 Estuaries are among the most productive ecosystems worldwide, functioning as major migratory,
369 spawning, nursery, and rearing grounds for a variety of aquatic organisms (Beck et al., 2001; Canuel
370 & Hardison, 2016; Lotze et al., 2006). Changes in the reproductive phenology and recruitment
371 dynamics of a species may intersect with other phenological patterns in an estuary, such as food
372 production, a phenomenon known as the "match-mismatch" hypothesis (Cushing, 1969, 1990).
373 Examples of the match-mismatch hypothesis in estuaries, however, remain relatively scarce in the
374 literature (Fortier & Gagné, 1990; Philippart et al., 2003; Peer & Miller, 2014; Chevillot et al., 2017).
375 Delta Smelt larvae and juveniles feed mainly on the calanoid copepods *Eurytemora affinis* and
376 *Pseudodiaptomus forbesi* during spring through fall (Slater & Baxter, 2014). *E. affinis* appears to be most
377 abundant in the Delta in March, whereas *P. forbesi* is more abundant in the Delta during June- July
378 (Bollens et al., 2014). How such trophic variation intersects with variation in Delta Smelt recruitment
379 dynamics remains an important topic of interest. This is especially true in the SFE, where primary
380 and secondary production have decreased over the past 3 decades due to non-native clams and
381 hydrologic alterations (Hammock et al., 2019; Winder & Jassby, 2011), and seasonal patterns in peak

production appear to shifting, like the hatch dates of Delta Smelt, to earlier times of the year (Merz et al., 2016).

The Delta Smelt is an important indicator of ecosystem health in the SFE, serving as sentinel or bioindicator of ecological change (Moyle et al., 2018). Using a 20-year archive of specimens, we demonstrate empirically that the reproductive phenology of wild Delta Smelt is sensitive to variation in climate. Thus, these results confirm lab-based estimates of thermal sensitivity and subsequent extrapolations of the likely impacts of future warming on Delta Smelt reproduction. When combined with recent results indicating a strong negative effect of warmer temperatures on the growth and body condition of wild Delta Smelt (Hammock et al., 2022; Lewis et al., 2021), all evidence suggests that the Delta ecosystem is likely to become increasingly inhospitable to Delta Smelt and other native species over the next several decades. These results confirm that, in addition to changes in growth and condition, conservation efforts will also need to consider and mitigate the effects of future climate change on the reproductive phenology of this critically endangered species.

Acknowledgments

We are grateful to our collaborators at the California Department of Fish and Wildlife and U.S. Fish and Wildlife Service for providing Delta Smelt specimens from field collections for use in this study, and members of the Teh Lab at UC Davis who helped obtain, dissect, and archive specimens. We also thank the many past and present students and staff in the Otolith Geochemistry and Fish Ecology Laboratory at UC Davis who contributed to fish dissections, otolith preparation, and analysis. Otolith archives were maintained in accordance with an approved California Department of Fish and Wildlife Service Section 2081a Memorandum of Understanding to L. Lewis, M. Willmes, and J. Hobbs. Funding for this project was provided in part by grants from the California Department of Fish and Wildlife (CDFW) contracts E1183004, D1583004 and P1696005, and the U.S. Bureau of Reclamation (USBR) contracts R13AP20022 and R17AC00129 to J. Hobbs, S. Teh, and L. Lewis. Additional support was provided by the Delta Stewardship Council (DSC) via postdoctoral fellowships to M. Willmes (Grant No. 1167) and L. Lewis (Grant Nos. 2279, 5298). The content of this material and views described herein do not necessarily reflect the views and policies of the CDFW, USBR, DSC, or UC Davis; nor does mention of trade names or commercial products constitute endorsement or recommendation for use.

References

Asch, R. G. (2015). Climate change and decadal shifts in the phenology of larval fishes in the California Current ecosystem. *Proceedings of the National Academy of Sciences*, *112*(30), E4065–E4074. https://doi.org/10.1073/pnas.1421946112

Baskerville-Bridges, B., Lindberg, J. C., Van Eenennaam, J. P., & Doroshov, S. I. (2005). *Delta Smelt Culture and Research Program Final Report: 2003-2005* (CALFED Bay-Delta Program, p. 22). University of California, Davis.

Beck, M. W., Heck, K. L., Able, K. W., Childers, D. L., Eggleston, D. B., Gillanders, B. M., Halpern, B., Hays, C. G., Hoshino, K., Minello, T. J., Orth, R. J., Sheridan, P. F., & Weinstein, M. P. (2001). The Identification, Conservation, and Management of Estuarine and Marine Nurseries for Fish and Invertebrates. *BioScience*, *51*(8), 633. https://doi.org/10.1641/0006-3568(2001)051[0633:TICAMO]2.0.CO;2

Bennett, W. A. (2005). Critical Assessment of the Delta Smelt Population in the San Francisco Estuary, California. *San Francisco Estuary and Watershed Science*, *3*(2). https://doi.org/10.15447/sfews.2005v3iss2art1

Bollens, S., Breckenridge, J., Cordell, J., Simenstad, C., & Kalata, O. (2014). Zooplankton of tidal marsh channels in relation to environmental variables in the upper San Francisco Estuary. *Aquatic Biology*, *21*(3), 205–219. https://doi.org/10.3354/ab00589

Brown, L. R., Bennett, W. A., Wagner, R. W., Morgan-King, T., Knowles, N., Feyrer, F., Schoellhamer, D. H., Stacey, M. T., & Dettinger, M. (2013). Implications for Future Survival of Delta Smelt from Four Climate Change Scenarios for the Sacramento–San Joaquin Delta, California. *Estuaries and Coasts*, *36*(4), 754–774. https://doi.org/10.1007/s12237-013-9585-4

Brown, L. R., Komoroske, L. M., Wagner, R. W., Morgan-King, T., May, J. T., Connon, R. E., & Fangue, N. A. (2016). Coupled Downscaled Climate Models and Ecophysiological Metrics Forecast Habitat Compression for an Endangered Estuarine Fish. *PLOS ONE*, *11*(1), e0146724. https://doi.org/10.1371/journal.pone.0146724

Burrows, M. T., Schoeman, D. S., Buckley, L. B., Moore, P., Poloczanska, E. S., Brander, K. M., Brown, C., Bruno, J. F., Duarte, C. M., Halpern, B. S., Holding, J., Kappel, C. V., Kiessling, W., O'Connor, M. I., Pandolfi, J. M., Parmesan, C., Schwing, F. B., Sydeman, W. J., & Richardson, A. J. (2011). The Pace of Shifting Climate in Marine and Terrestrial Ecosystems. *Science*, *334*(6056), 652–655. https://doi.org/10.1126/science.1210288

Callaway, J. C., & Josselyn, M. N. (1992). The Introduction and Spread of Smooth Cordgrass (Spartina alterniflora) in South San Francisco Bay. *Estuaries*, *15*(2), 218. https://doi.org/10.2307/1352695

Canuel, E. A., & Hardison, A. K. (2016). Sources, Ages, and Alteration of Organic Matter in Estuaries. In Carlson, CA and Giovannoni, SJ (Ed.), *ANNUAL REVIEW OF MARINE SCIENCE, VOL 8* (Vol. 8, pp. 409–434). https://doi.org/10.1146/annurev-marine-122414-034058

Chevillot, X., Drouineau, H., Lambert, P., Carassou, L., Sautour, B., & Lobry, J. (2017). Toward a phenological mismatch in estuarine pelagic food web? *PLOS ONE*, *12*(3), e0173752. https://doi.org/10.1371/journal.pone.0173752

Cloern, J. E., Knowles, N., Brown, L. R., Cayan, D., Dettinger, M. D., Morgan, T. L., Schoellhamer, D. H., Stacey, M. T., van der Wegen, M., Wagner, R. W., & Jassby, A. D. (2011). Projected Evolution of California's San Francisco Bay-Delta-River System in a Century of Climate Change. *PLoS ONE*, *6*(9), e24465. https://doi.org/10.1371/journal.pone.0024465

Cushing, D. H. (1969). The Regularity of the Spawning Season of Some Fishes. *ICES Journal of Marine Science*, *33*(1), 81–92. https://doi.org/10.1093/icesjms/33.1.81

Cushing, D. H. (1990). Plankton Production and Year-class Strength in Fish Populations: An Update of the Match/Mismatch Hypothesis. In *Advances in Marine Biology* (Vol. 26, pp. 249–293). Elsevier. https://doi.org/10.1016/S0065-2881(08)60202-3

Damon, L. J., Slater, S. B., & Baxter, R. D. (2016). Fecundity and reproductive potential of wild female Delta Smelt in the upper San Francisco Estuary, California. *California Fish and Game*, *102*(4), 188–210.

Dettinger, M., Anderson, J., Anderson, M., Brown, L. R., Cayan, D., & Maurer, E. (2016). *Climate Change and the Delta*. *14*(3), 27.

Edwards, M., & Richardson, A. J. (2004). Impact of climate change on marine pelagic phenology and trophic mismatch. *Nature*, *430*(7002), 881–884. https://doi.org/10.1038/nature02808

Engle, V. D., Kurtz, J. C., Smith, L. M., Chancy, C., & Bourgeois, P. (2007). A Classification of U.S. Estuaries Based on Physical and Hydrologic Attributes. *Environmental Monitoring and Assessment*, *129*(1–3), 397–412. https://doi.org/10.1007/s10661-006-9372-9

Feyrer, F., Sommer, T., & Harrell, W. (2006). Managing floodplain inundation for native fish: Production dynamics of age-0 splittail (Pogonichthys macrolepidotus) in California's Yolo Bypass. *Hydrobiologia*, *573*(1), 213–226. https://doi.org/10.1007/s10750-006-0273-2

Fisch, K. M., Henderson, J. M., Burton, R. S., & May, B. (2011). Population genetics and conservation implications for the endangered delta smelt in the San Francisco Bay-Delta. *Conservation Genetics*, *12*(6), 1421–1434. https://doi.org/10.1007/s10592-011-0240-y

Fortier, L., & Gagné, J. A. (1990). Larval Herring (*Clupea harengus*) Dispersion, Growth, and Survival in the St, Lawrence Estuary: Match/Mismatch or Membership/Vagrancy? *Canadian Journal of Fisheries and Aquatic Sciences*, *47*(10), 1898–1912. https://doi.org/10.1139/f90-214

Genner, M. J., Halliday, N. C., Simpson, S. D., Southward, A. J., Hawkins, S. J., & Sims, D. W. (2010). Temperature-driven phenological changes within a marine larval fish assemblage. *Journal of Plankton Research*, *32*(5), 699–708. https://doi.org/10.1093/plankt/fbp082

Goertler, P., Mahardja, B., & Sommer, T. (2021). Striped bass (Morone saxatilis) migration timing driven by estuary outflow and sea surface temperature in the San Francisco Bay-Delta, California. *Scientific Reports*, *11*(1), 1510. https://doi.org/10.1038/s41598-020-80517-5

Hammock, B. G., Hartman, R., Dahlgren, R. A., Johnston, C., Kurobe, T., Lehman, P. W., Lewis, L. S., Van Nieuwenhuyse, E., Ramírez-Duarte, W. F., Schultz, A. A., & Teh, S. J. (2022). Patterns and predictors of condition indices in a critically endangered fish. *Hydrobiologia*, *849*(3), 675–695. https://doi.org/10.1007/s10750-021-04738-z

Hammock, B. G., Moose, S. P., Solis, S. S., Goharian, E., & Teh, S. J. (2019). Hydrodynamic Modeling Coupled with Long-term Field Data Provide Evidence for Suppression of Phytoplankton by Invasive Clams and Freshwater Exports in the San Francisco Estuary. *Environmental Management*, *63*(6), 703–717. https://doi.org/10.1007/s00267-019-01159-6

Hernández-Santoro, C., Contreras-Reyes, J. E., & Landaeta, M. F. (2019). Intra-seasonal variability of sea surface temperature influences phenological decoupling in anchovy (Engraulis ringens). *Journal of Sea Research*, *152*, 101765. https://doi.org/10.1016/j.seares.2019.101765

Hobbs, J. A., Lewis, L. S., Willmes, M., Denney, C., & Bush, E. (2019). Complex life histories discovered in a critically endangered fish. *Scientific Reports*, *9*(1), 16772. https://doi.org/10.1038/s41598-019-52273-8

Hovel, R. A., Carlson, S. M., & Quinn, T. P. (2017). Climate change alters the reproductive phenology and investment of a lacustrine fish, the three-spine stickleback. *Global Change Biology*, *23*(6), 2308–2320. https://doi.org/10.1111/gcb.13531

Hutchings, J., & Myers, R. (1994). Timing of cod reproduction: Interannual variability and the influence of temperature. *Marine Ecology Progress Series*, *108*, 21–31. https://doi.org/10.3354/meps108021

Keefer, M. L., Peery, C. A., & Caudill, C. C. (2008). Migration Timing of Columbia River Spring Chinook Salmon: Effects of Temperature, River Discharge, and Ocean Environment. *Transactions of the American Fisheries Society*, *137*(4), 1120–1133. https://doi.org/10.1577/T07-008.1

Komoroske, L. M., Connon, R. E., Lindberg, J., Cheng, B. S., Castillo, G., Hasenbein, M., & Fangue, N. A. (2014). Ontogeny influences sensitivity to climate change stressors in an endangered fish. *Conservation Physiology*, *2*(1), cou008–cou008. https://doi.org/10.1093/conphys/cou008

Krabbenhoft, T. J., Platania, S. P., & Turner, T. F. (2014). Interannual variation in reproductive phenology in a riverine fish assemblage: Implications for predicting the effects of climate change and altered flow regimes. *Freshwater Biology*, *59*(8), 1744–1754. https://doi.org/10.1111/fwb.12379

Kurobe, T., Park, M. O., Javidmehr, A., Teh, F.-C., Acuña, S. C., Corbin, C. J., Conley, A. J., Bennett, W. A., & Teh, S. J. (2016). Assessing oocyte development and maturation in the threatened Delta Smelt, Hypomesus transpacificus. *Environmental Biology of Fishes*, *99*(4), 423–432. https://doi.org/10.1007/s10641-016-0483-z

Lewis, L., Denney, C., Willmes, M., Xieu, W., Fichman, R., Zhao, F., Hammock, B., Schultz, A., Fangue, N., & Hobbs, J. (2021). Otolith-based approaches indicate strong effects of environmental variation on growth of a Critically Endangered estuarine fish. *Marine Ecology Progress Series*, *676*, 37–56. https://doi.org/10.3354/meps13848

Liang, L. (2019). Phenology. In *Reference Module in Earth Systems and Environmental Sciences*. Elsevier. https://doi.org/10.1016/B978-0-12-409548-9.11739-7

Liu, Y., Reich, P. B., Li, G., & Sun, S. (2011). Shifting phenology and abundance under experimental warming alters trophic relationships and plant reproductive capacity. *Ecology*, *92*(6), 1201–1207. https://doi.org/10.1890/10-2060.1

Lotze, H. K., Lenihan, H., Bourque, B. J., Bradbury, R. H., Cooke, R. G., Kay, M. C., Kidwell, S. M., Kirby, M. X., Peterson, C. H., & Jackson, J. B. C. (2006). Depletion, degradation, and recovery potential of estuaries and coastal seas. *Science*, *312*(5781), 1806–1809. https://doi.org/10.1126/science.1128035

Menzel, A., Sparks, T. H., Estrella, N., Koch, E., Aasa, A., Ahas, R., Alm-Kübler, K., Bissolli, P., Braslavská, O., Briede, A., Chmielewski, F. M., Crepinsek, Z., Curnel, Y., Dahl, Å., Defila, C., Donnelly, A., Filella, Y., Jatczak, K., Måge, F., … Zust, A. (2006). European phenological response to climate change matches the warming pattern. *Global Change Biology*, *12*(10), 1969–1976. https://doi.org/10.1111/j.1365-2486.2006.01193.x

Merz, J. E., Bergman, P. S., Simonis, J. L., Delaney, D., Pierson, J., & Anders, P. (2016). Long-Term Seasonal Trends in the Prey Community of Delta Smelt (Hypomesus transpacificus) Within the Sacramento-San Joaquin Delta, California. *Estuaries and Coasts*, *39*(5), 1526–1536. https://doi.org/10.1007/s12237-016-0097-x

Morgan, M. J., Wright, P. J., & Rideout, R. M. (2013). Effect of age and temperature on spawning time in two gadoid species. *Fisheries Research*, *138*, 42–51. https://doi.org/10.1016/j.fishres.2012.02.019

Moyle, P. B. (1995). *Fish: An Enthusiast's Guide*. University of California Press.

Moyle, P. B., Brown, L. R., Durand, J. R., & Hobbs, J. A. (2016). Delta Smelt: Life History and Decline of a Once-Abundant Species in the San Francisco Estuary. *San Francisco Estuary and Watershed Science*, *14*(2). https://doi.org/10.15447/sfews.2016v14iss2art6

Moyle, P. B., Herbold, B., Stevens, D. E., & Miller, W. (1992). Life History and Status of Delta Smelt in the Sacramento-San Joaquin Estuary, California. *Transactions of the American Fisheries Society*, *121*(1), 67–77.

Moyle, P. B., Hobbs, J. A., & Durand, J. R. (2018). Delta Smelt and Water Politics in California. *Fisheries*, *43*(1), 42–50. https://doi.org/10.1002/fsh.10014

Myers, B. J. E., Lynch, A. J., Bunnell, D. B., Chu, C., Falke, J. A., Kovach, R. P., Krabbenhoft, T. J., Kwak, T. J., & Paukert, C. P. (2017). Global synthesis of the documented and projected effects of climate change on inland fishes. *Reviews in Fish Biology and Fisheries*, *27*(2), 339–361. https://doi.org/10.1007/s11160-017-9476-z

Nichols, F. H., Cloern, J. E., Luoma, S. N., & Peterson, D. H. (1986). The Modification of an Estuary. *Science*, *231*(4738), 567–573. https://doi.org/10.1126/science.231.4738.567

Nobriga, M. L., Sommer, T. R., Feyrer, F., & Fleming, K. (2008). Long-Term Trends in Summertime Habitat Suitability for Delta Smelt, Hypomesus transpacificus. *San Francisco Estuary and Watershed Science*, *6*(1). https://doi.org/10.15447/sfews.2008v6iss1art1

564 Pankhurst, N. W., & Munday, P. L. (2011). Effects of climate change on fish reproduction and early
565 life history stages. *Marine and Freshwater Research*, *62*(9), 1015.
566 https://doi.org/10.1071/MF10269
567 Parmesan, C. (2007). Influences of species, latitudes and methodologies on estimates of phenological
568 response to global warming. *Global Change Biology*, *13*(9), 1860–1872.
569 https://doi.org/10.1111/j.1365-2486.2007.01404.x
570 Peer, A. C., & Miller, T. J. (2014). Climate Change, Migration Phenology, and Fisheries Management
571 Interact with Unanticipated Consequences. *North American Journal of Fisheries Management*,
572 *34*(1), 94–110. https://doi.org/10.1080/02755947.2013.847877
573 Philippart, C. J. M., van Aken, H. M., Beukema, J. J., Bos, O. G., Cadée, G. C., & Dekker, R. (2003).
574 Climate-related changes in recruitment of the bivalve Macoma balthica. *Limnology and*
575 *Oceanography*, *48*(6), 2171–2185. https://doi.org/10.4319/lo.2003.48.6.2171
576 Platt, T., White, G. N., Zhai, L., Sathyendranath, S., & Roy, S. (2009). The phenology of
577 phytoplankton blooms: Ecosystem indicators from remote sensing. *Ecological Modelling*,
578 *220*(21), 3057–3069. https://doi.org/10.1016/j.ecolmodel.2008.11.022
579 Polte, P., Gröhsler, T., Kotterba, P., von Nordheim, L., Moll, D., Santos, J., Rodriguez-Tress, P.,
580 Zablotski, Y., & Zimmermann, C. (2021). Reduced Reproductive Success of Western Baltic
581 Herring (Clupea harengus) as a Response to Warming Winters. *Frontiers in Marine Science*, *8*,
582 589242. https://doi.org/10.3389/fmars.2021.589242
583 Rogers, L. A., & Dougherty, A. B. (2019). Effects of climate and demography on reproductive
584 phenology of a harvested marine fish population. *Global Change Biology*, *25*(2), 708–720.
585 https://doi.org/10.1111/gcb.14483
586 Satterthwaite, W., Carlson, S., Allen-Moran, S., Vincenzi, S., Bograd, S., & Wells, B. (2014). Match-
587 mismatch dynamics and the relationship between ocean-entry timing and relative ocean
588 recoveries of Central Valley fall run Chinook salmon. *Marine Ecology Progress Series*, *511*, 237–
589 248. https://doi.org/10.3354/meps10934
590 Slater, S. B., & Baxter, R. D. (2014). Diet, Prey Selection, and Body Condition of Age-0 Delta Smelt,
591 Hypomesus transpacificus, in the Upper San Francisco Estuary. *San Francisco Estuary and*
592 *Watershed Science*, *12*(3). https://doi.org/10.15447/sfews.2014v12iss3art1
593 Sparks, M. M., Falke, J. A., Quinn, T. P., Adkison, M. D., Schindler, D. E., Bartz, K., Young, D., &
594 Westley, P. A. H. (2019). Influences of spawning timing, water temperature, and climatic
595 warming on early life history phenology in western Alaska sockeye salmon. *Canadian Journal*
596 *of Fisheries and Aquatic Sciences*, *76*(1), 123–135. https://doi.org/10.1139/cjfas-2017-0468
597 Stine, S. (1994). Extreme and persistent drought in California and Patagonia during mediaeval time.
598 *Nature*, *369*(6481), 546–549. https://doi.org/10.1038/369546a0
599 Tao, J., He, D., Kennard, M. J., Ding, C., Bunn, S. E., Liu, C., Jia, Y., Che, R., & Chen, Y. (2018).
600 Strong evidence for changing fish reproductive phenology under climate warming on the
601 Tibetan Plateau. *Global Change Biology*, *24*(5), 2093–2104. https://doi.org/10.1111/gcb.14050
602 Tsai, Y.-J. J., Chase, S. N., Carson, E. W., Zweig, L., & Hung, T.-C. (2021). Delta Smelt (Hypomesus
603 transpacificus) Exhibit Wide Variation in Spawning Behavior: An Investigation of Substrate
604 Type, Diel Timing, and Participants. *Estuaries and Coasts*. https://doi.org/10.1007/s12237-
605 021-01030-0
606 Turner, T. F., Krabbenhoft, T. J., & Burdett, A. S. (2010). Reproductive Phenology and Fish
607 Community Structure in an Arid-Land River System. *American Fisheries Society Symposium*, *73*,
608 427–446.
609 Ustin, S. L., Santos, M. J., Hestir, E. L., Khanna, S., Casas, A., & Greenberg, J. (2015). Developing
610 the capacity to monitor climate change impacts in Mediterranean estuaries. *Evolutionary*
611 *Ecology Research*, *16*, 529–550.

612 Visser, M. E., & Both, C. (2005). Shifts in phenology due to global climate change: The need for a
613 yardstick. *Proceedings of the Royal Society B: Biological Sciences*, *272*(1581), 2561–2569.
614 https://doi.org/10.1098/rspb.2005.3356
615 Visser, M. E., Both, C., & Lambrechts, M. M. (2004). Global Climate Change Leads to Mistimed
616 Avian Reproduction. In *Advances in Ecological Research* (Vol. 35, pp. 89–110). Elsevier.
617 https://doi.org/10.1016/S0065-2504(04)35005-1
618 Visser, M. E., Holleman, L. J. M., & Gienapp, P. (2006). Shifts in caterpillar biomass phenology due
619 to climate change and its impact on the breeding biology of an insectivorous bird. *Oecologia*,
620 *147*(1), 164–172. https://doi.org/10.1007/s00442-005-0299-6
621 Walther, G.-R., Post, E., Convey, P., Menzel, A., Parmesan, C., Beebee, T. J. C., Fromentin, J.-M.,
622 Hoegh-Guldberg, O., & Bairlein, F. (2002). Ecological responses to recent climate change.
623 *Nature*, *416*(6879), 389–395. https://doi.org/10.1038/416389a
624 Wang, J. C. S. (1986). *Fishes of the Sacramento-San Joaquin estuary and adjacent waters, California: A guide to*
625 *the early life histories.* (No. 9; p. 690). IEP Technical Report.
626 Ware, D. M., & Tanasichuk, R. W. (1989). Biological Basis of Maturation and Spawning Waves in
627 Pacific Herring (*Clupea harengus pallasi*). *Canadian Journal of Fisheries and Aquatic Sciences*,
628 *46*(10), 1776–1784. https://doi.org/10.1139/f89-225
629 Winder, M., & Jassby, A. D. (2011). Shifts in Zooplankton Community Structure: Implications for
630 Food Web Processes in the Upper San Francisco Estuary. *Estuaries and Coasts*, *34*(4), 675–
631 690. https://doi.org/10.1007/s12237-010-9342-x
632 Woods, T., Kaz, A., & Giam, X. (2021). Phenology in freshwaters: A review and recommendations
633 for future research. *Ecography*, *n/a*(n/a). https://doi.org/10.1111/ecog.05564
634 Xieu, W., Lewis, L. S., Zhao, F., Fichman, R. A., Willmes, M., Hung, T.-C., Ellison, L., Stevenson,
635 T., Tigan, G., Schultz, A. A., & Hobbs, J. A. (2021). Experimental validation of otolith-based
636 age and growth reconstructions across multiple life stages of a critically endangered estuarine
637 fish. *PeerJ*, *9*, e12280. https://doi.org/10.7717/peerj.12280
638

639

Tables

Table 4-1. Number of fish used in the hatch date analysis by year and survey.

Year	20mm	CCE	CVP	EDSM	FMWT	GES	GES-TNS	SFBS	TNS	YB	Total
1999	80	0	0	0	64	0	0	0	119	0	263
2000	0	0	57	0	7	0	0	0	0	0	64
2001	0	0	26	0	59	0	0	0	165	0	250
2002	0	0	0	0	0	0	0	0	139	0	139
2004	63	0	0	0	0	0	0	0	0	0	63
2005	0	0	0	0	30	0	0	0	66	0	96
2006	0	0	0	0	28	0	0	0	62	0	90
2007	0	0	0	0	10	0	0	0	48	0	58
2008	0	0	0	0	0	0	0	0	28	0	28
2009	0	0	0	0	4	0	0	11	4	0	19
2010	0	0	0	0	5	0	0	0	46	2	53
2011	0	0	0	0	95	0	0	2	172	0	269
2012	0	0	0	0	34	97	0	0	89	6	226
2013	0	0	0	0	9	176	0	0	109	15	309
2014	0	147	0	0	6	0	41	12	70	3	279
2015	0	0	0	0	5	0	0	46	15	31	97
2016	0	0	0	0	6	0	0	1	0	6	13
2017	0	0	0	95	2	0	0	0	27	0	124
2018	0	0	0	138	0	0	0	0	2	0	140
2019	0	0	0	118	0	0	0	0	0	0	118
Total	**143**	**147**	**83**	**351**	**364**	**273**	**41**	**72**	**1161**	**63**	**2698**

Surveys are described in the Supplementary Materials.

Table 4-2. Comparison of nested linear models examining Delta Smelt phenology (median hatch dates) as the fixed continuous effects of water temperature (T) and freshwater outflow (O).

Model	DF	Residual DF	F	P	Adj. R^2	AICc
T	**1**	**18**	**6.09**	**0.024**	**0.211**	**159.9**
O	1	18	0.818	0.378	-0.010	164.9
T+O	2	17	2.901	0.082	0.167	163.1
T*O	3	16	1.822	0.184	0.115	166.7

The temperature-only model ("T", bold) was selected given its higher coefficient of determination (R^2) and lower Akaike information criterion value (AIC_c).

655 Table 4-3. Results of the selected model ("T") examining variation among cohorts in
656 median hatch dates as a function of interannual variation in the winter temperature
657 index (WTI).

Model	Term	Coefficients	SE	t	p	R^2	p_2
Median	Intercept	202.64	39.95	5.072	<0.001	0.211	0.024
	WTI	-8.78	3.56	-2.468	0.024		
Full	Intercept	222.36	5.48	40.58	<0.001	0.140	<0.001
	WTI	-10.41	0.49	-21.08	<0.001		

658 Coefficients based on both the robust ("median") and full versions of the model are provided.

Figures

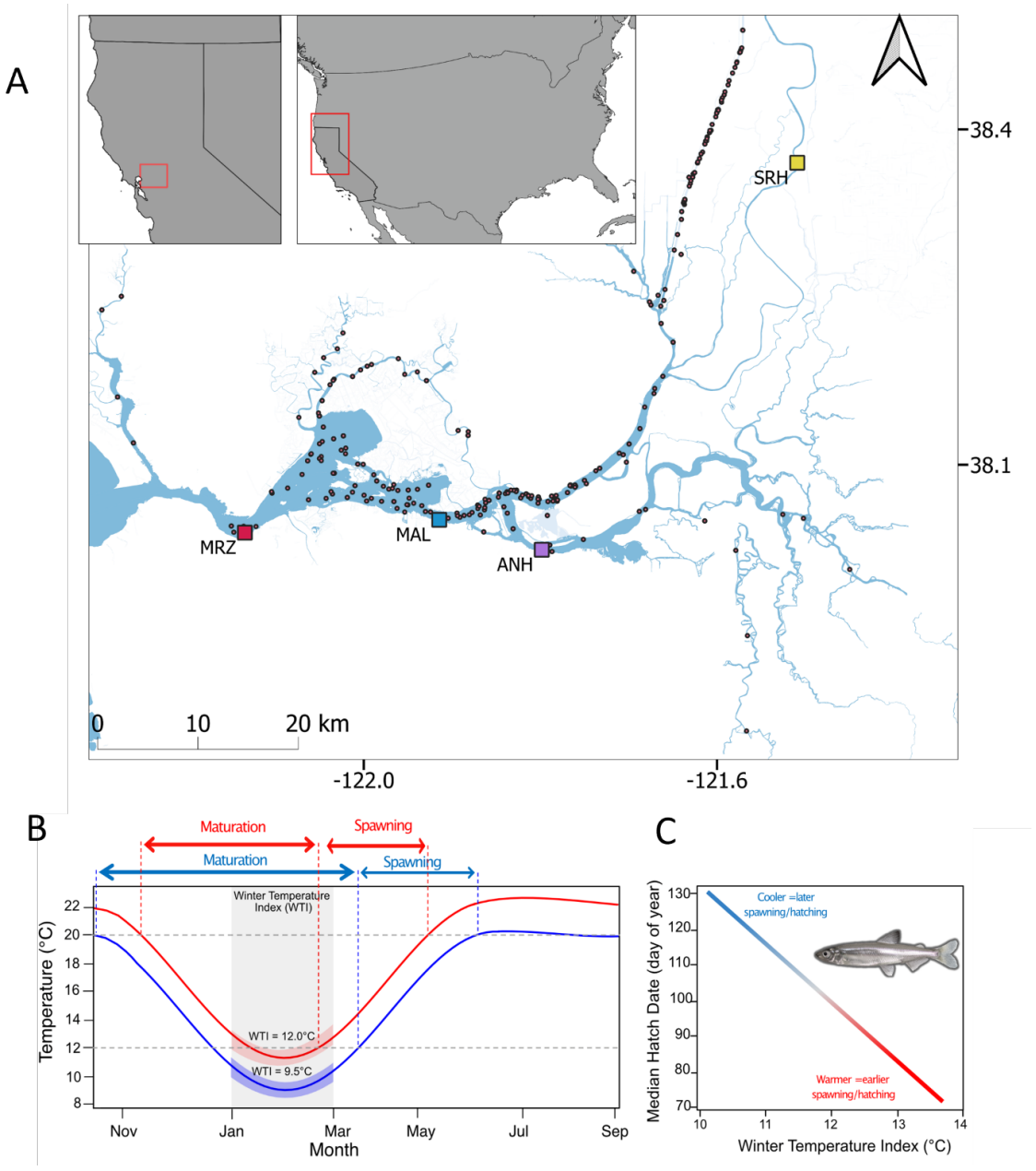

Figure 4-1. Study site and conceptual model of Delta Smelt reproduction, showing the sampling locations and conceptual diagrams of the thermal threshold model for Delta Smelt reproduction.

(A) Map of the study site showing the geographic range of Delta Smelt. Points represent the stations from which Delta Smelt specimens were collected and squares represent locations at which sondes collected continuous water temperature data. Sonde locations include: Sacramento River Hood (SRH), Antioch (ANH), Mallard (MAL), and Martinez (MRZ). (B) The thermal threshold model for Delta Smelt reproduction, showing the temperature dependency of the maturation and spawning windows and (C) the resultant hypothesized effects of variation in the winter temperatures.

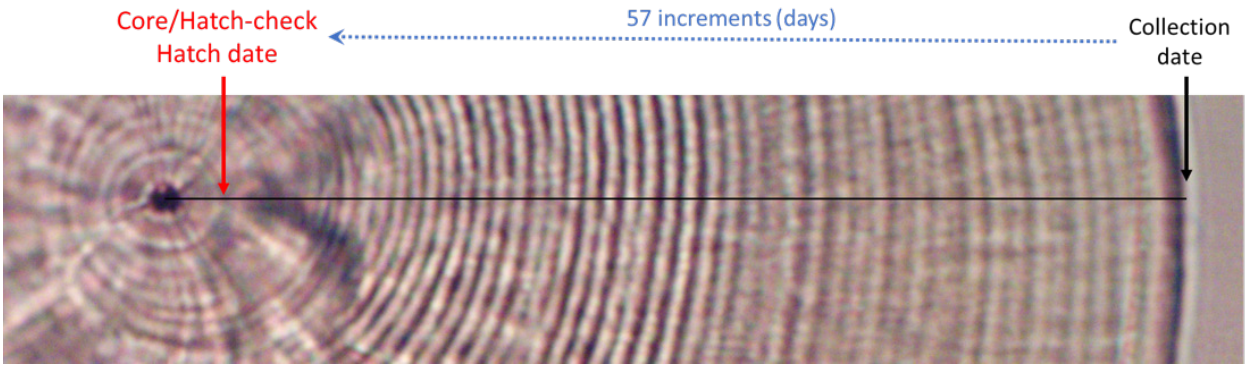

Figure 4-2. Otolith-based methods to back calculate age and hatch dates from the known collection date.

Daily rings are counted from the core to edge, representing the dates that fish hatched and were collected, respectively. Hatch dates can be estimated by subtracting the total number of daily rings (days) from the known collection date.

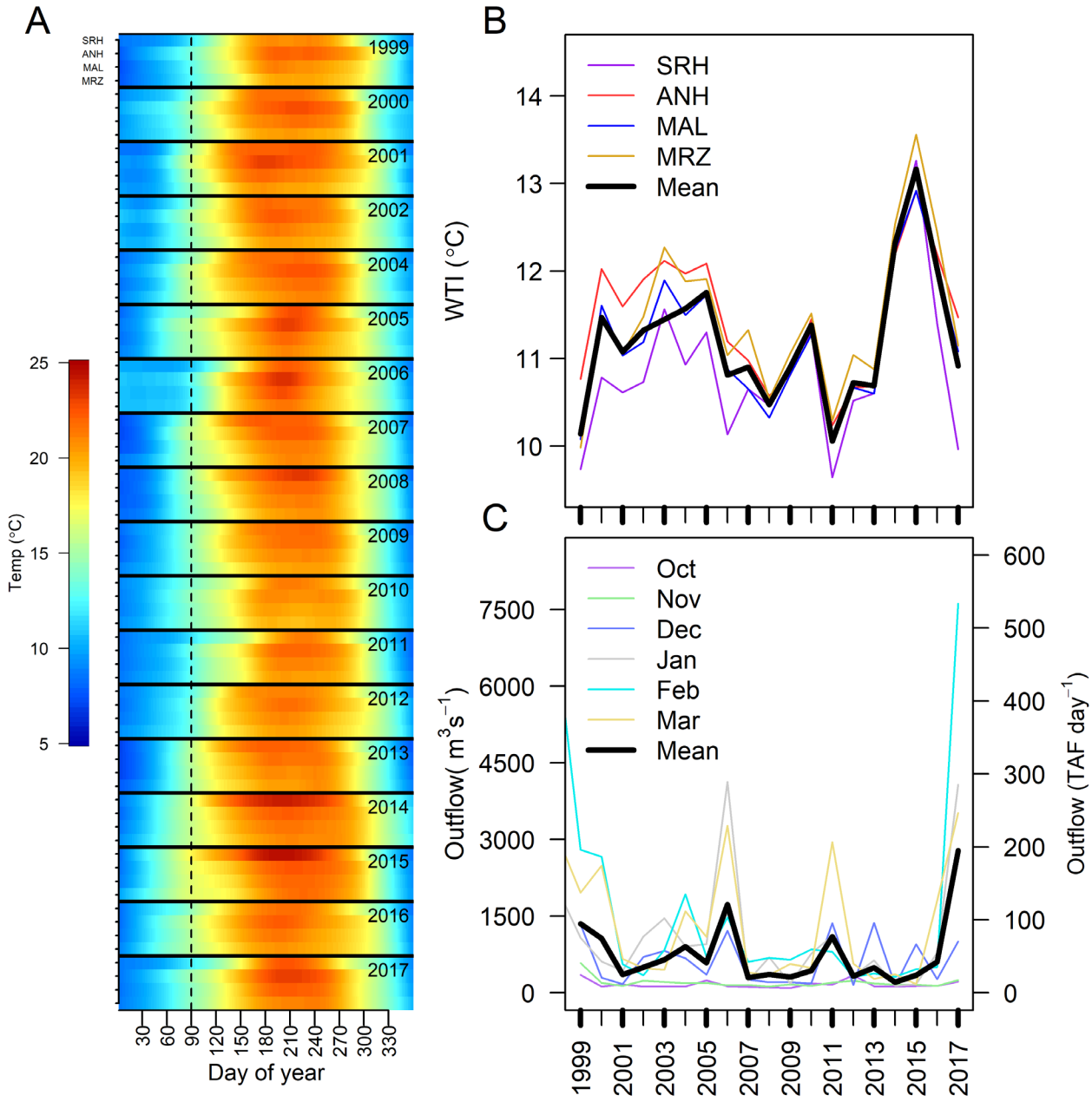

Figure 4-3. Interannual variation in environmental conditions in the upper San Francisco Estuary.

(A) Heatmap of seasonal and interannual patterns in water temperature based on the long-term time series from 4 sonde stations maintained by the California Department of Water Resources: Sacramento River Hood (SRH), Antioch (ANH), Mallard (MAL) and Martinez (MRZ) (Figure 4-1) (https://cdec.water.ca.gov/). The dashed vertical line marks the end of the January-March window for the Winter Temperature Index (WTI). (B) Interannual variation in mean daily water temperature from January- March (WTI) at long-term monitoring stations. (C) Interannual variation in mean daily outflow (January to June) from the "Dayflow" model (https://data.ca.gov/dataset/dayflow).

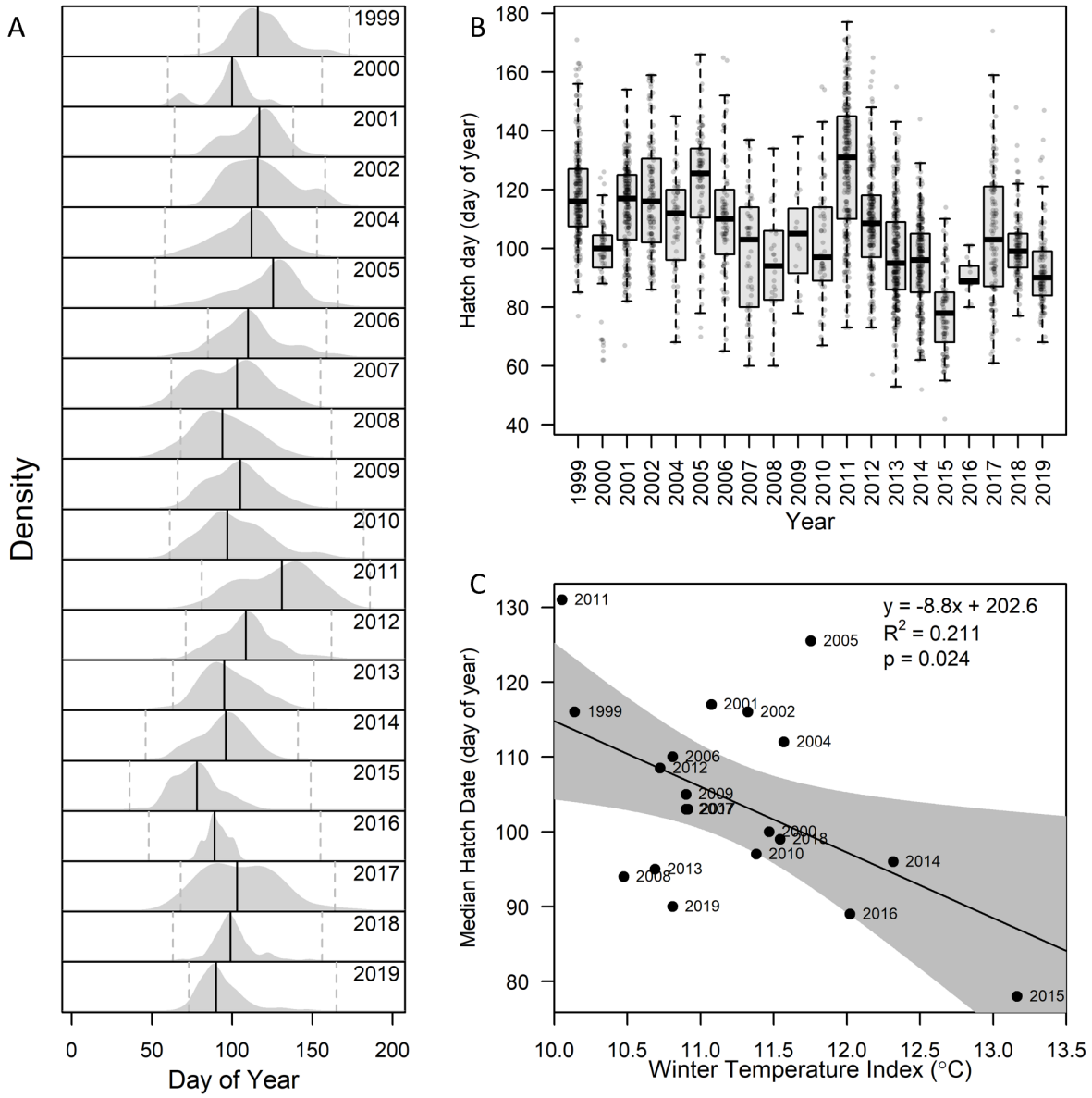

686

687 Figure 4-4. Hatching trends among fish cohorts and winter water temperatures.

688 (A) Hatch distributions from otolith-based age estimates. The dashed vertical line shows the 12-20°C spawning
689 window, and solid vertical line indicates the estimated median hatch date for each respective cohort. (B) Boxplots
690 showing the hatch dates of all fishes collected and aged in each year (1999-2019, minus 2003). (C) Linear relationship
691 between median hatch dates and the winter temperature index (WTI). Gray shading in (C) represents the 95%
692 confidence interval for the best-fit line (black) (see Table 4-3 for detail).

693

Chapter 5: Quantifying Morphological and Crystalline Anomalies in Otoliths of Wild and Cultured Delta Smelt

Author:

Huang, Jonathan L.[1], Malte Willmes[1,2], Rachel A. Fichman[1], Tien-Chieh Hung[3], Luke T. Ellison[3], Troy A. Stevenson[3], Nann Fangue[4], Swee Teh[5], Andrew Schultz[6], John Grimsich[7], Cody J. Chalker[8], Bruce G. Hammock[9], James A. Hobbs[1,10] Levi S. Lewis[1*]

[1]Otolith Geochemistry and Fish Ecology Laboratory, Department of Wildlife, Fish, and Conservation Biology, UC Davis

[2]Institute for Marine Sciences, UC Santa Cruz

[3]Fish Culture and Conservation Laboratory, Department of Engineering, UC Davis

[4]Conservation Physiology Laboratory, Department of Wildlife, Fish, and Conservation Biology, UC Davis

[5]Aquatic Toxicology Laboratory, Department of Veterinary Medicine, UC Davis

[6] Green River Basin Fish and Wildlife Conservation Office, United States Fish and Wildlife Service, Vernal, UT, USA

[7] Earth and Planetary Science, UC Berkeley

[8] Department of Chemistry, UC Davis

[9] Aquatic Health program, Department of Veterinary Medicine, UC Davis

[10]California Department of Fish and Wildlife

*corresponding author (lewis.sci@gmail.com)

Abstract

Developmental abnormalities in otoliths can impact growth and survival in teleost fishes. Here, we quantified the frequency and severity of developmental anomalies in Delta Smelt otoliths (*Hypomesus transpacificus*), a critically endangered estuarine fish that is endemic to the San Francisco Estuary. Otolith anomalies, including left-right asymmetry and anomalous crystalline polymorphs (i.e., vaterite), were compared between wild and cultured populations using digital image analysis. Visual estimates of vaterite were validated using X-ray diffraction, Raman spectroscopy, and laser ablation ICPMS. Results indicated that otoliths of cultured Delta Smelt were 50 times more likely to contain vaterite and 20 times more likely to contain relatively large (≥15%) amounts of vaterite. Similarly,

cultured fish exhibited three times greater asymmetry than wild fish. Larger, faster-growing, cultured fish were more likely to exhibit vateritic otoliths, though growth did not affect asymmetry. These results indicate that cultured Delta Smelt exhibit a significantly higher frequency of vestibular abnormalities which are known to reduce fitness and survival. Such hatchery effects on otolith development could have important implications for captive culture practices and the supplementation of the wild Delta Smelt population with cultured individuals.

Keywords: Vaterite, otolith, Delta Smelt, San Francisco, hatchery, development, asymmetry

Introduction

Otoliths, or "ear stones", are calcified structures in teleost fishes that perform critical sensory functions including hearing, balance, and linear acceleration. Three pairs of otoliths (sagittal, lapillus, and asteriscus) are present within the fish's cranium and are metabolically inert. These structures are composed primarily of calcium carbonate ($CaCO_3$) and grow continuously, in proportion to fish size, through the symmetrical production of daily growth increments. The biomineralization of $CaCO_3$ also incorporates a variety of elements from the ambient water, thus providing a record of a fish's environmental history. Therefore, otoliths serve as permanent records of the age, growth rate, and life history of fishes (Campana 1999).

The sagittal otolith is often the largest in many fishes and is typically comprised of the aragonitic $CaCO_3$ polymorph. However, growth anomalies including asymmetry (Panfili et al., 2005), irregular size (Sweeting et al. 2004), and the vateritic $CaCO_3$ polymorph can occur (Gauldie, 1986). In particular, the replacement of aragonite by vaterite in teleost fishes causes otoliths to be less dense, less stable, and more transparent (Kamhi, 1963; Tomás, 2003). Vateritic otoliths have been observed in many fish species including Lake Trout (*Salvelinus namaycush*; Melancon et al. 2005), Atlantic herring (*Clupea harengus*; Tomás and Geffen 2003), Lake Sturgeon (*Acipenser fulvescens*; Pracheil et al. 2017), Atlantic Salmon (*Salmo salar*; Reimer et al. 2016), and Chinook salmon (*Oncorhynchus tshawytscha*; Gauldie 1986). Abnormal otoliths are most prominent in hatchery-reared populations, with up to 50% of otoliths in hatchery fish containing vaterite (versus 8% in wild fish) and with vateritic compositions of up to 91% (Reimer et al., 2016; Tomás, 2003).

The effects of anomalies in fish otoliths remain poorly understood. However, anomalies in otoliths have been associated with acute and chronic stress (Campana 2005; Kern et al. 2017) and are known to result in impaired function, thus potentially negatively impacting fitness through foraging, navigation, and predator avoidance (Kondrachuk, 2003; Lychakov and Rebane, 2005; Oxman et al., 2007; Reimer et al., 2016; Vignon and Aymes, 2020). Moreover, the formation of vaterite is associated with loss of otolith microstructures and alteration of relative elemental concentrations, including enrichment in Mn/Ca and Mg/Ca, and depletion in Sr/Ca, Ba/Ca, and Na/Ca (Melancon et al. 2005; Tzeng et al. 2007; Macdonald et al. 2012), thus complicating age, growth, and life-history reconstructions based on otolith analyses (Budnik et al., 2020).

The Delta Smelt *(Hypomesus transpacificus*) is an estuarine forage fish that is endemic to the San Francisco Estuary (SFE). This migratory zooplanktivore is adapted to cool, turbid, low-salinity habitats (Lewis et al., 2021; Moyle et al., 2016) and exhibits a complex life history that allows it to exist within the dynamic low-salinity habitats of the SFE (Hobbs et al. 2019). Although historically abundant, its population has declined to <1% of 1980s levels, leading to its listing as threatened and

endangered under the federal (US Fish and Wildlife, 1993) and state (California Department of Fish and Wildlife, 2021) endangered species act, respectively. This population decline is likely due to multiple human impacts including hydrological modifications resulting from dams and exports, direct entrainment in water diversions, pollution, invasive species, trophic collapse, and climate change (Kimmerer et al., 1994; Moyle et al., 2018, 2016; Sommer et al., 2007; Winder and Jassby, 2011). Municipal and agricultural demands for freshwater have made conservation of this imperiled fish a difficult and controversial issue in California politics and resource management (Moyle et al. 2018).

To conserve Delta Smelt, a hatchery program has been developed that produces Delta Smelt each year to support experiments, serve as a reserve population, and provide cultured fish to be outplanted to supplement the remaining wild population (Lessard et al., 2018; Lindberg et al., 2013). However, the effects of hatchery conditions on the fitness of cultured Delta Smelt due to domestication and the effectiveness of releasing cultured fish into the wild remains poorly understood (Hobbs et al., 2017). For example, little is known about the comparative health, fitness, and survival of cultured versus wild individuals.

Comparing rates of developmental abnormalities provides a valuable approach to examining differences in health and fitness among fish populations, such as those observed in otoliths. However, otoliths anomalies have never been quantified for wild or cultured Delta Smelt. Here, we used an interdisciplinary approach to quantify and contrast developmental abnormalities in Delta Smelt, including asymmetry and the presence of irregular $CaCO_3$ crystalline structure (e.g., vaterite) in sagittal otoliths. Specifically, we quantified and compared otolith developmental anomalies (crystalline structure, asymmetry, and chemistry) between wild and cultured fish and examined the potential influence of rearing conditions (e.g., food availability and temperature). The chemical elements chosen here are elements commonly found in aragonitic otolith, but are known to become enriched or depleted relative to calcium in the presence of vaterite (Tomás and Geffen, 2003; Tzeng et al., 2007). By quantifying developmental abnormalities in cultured and wild Delta Smelt populations, we can better understand their relative health, the likely survival of cultured fish in natural environments, and the potential effectiveness of hatchery production and supplementation as a conservation and management tool.

Methods

Sample Collection

This study took advantage of an experiment examining the effects of temperature and food availability on otolith growth and chemistry in Delta Smelt conducted in 2019. Cultured (F11) Delta Smelt were hatched and reared at the UC Davis Fish Conservation and Culture Laboratory (FCCL) in 2019 following established protocols (Hammock et al., 2020; Lindberg et al., 2013). In short, fish were spawned and reared in freshwater (0.1 ppt) at 16°C for 120 days (50 – 60 mm length), then individually tagged using a Visible Implant Alphanumeric (VIA) tag and distributed between four tanks (80/tank) with varying temperatures (14°C or 18°C) and varying feed (ad libitum or no feed) resulting in four distinct treatments: 14°C fed, 14°C unfed, 18°C fed, 18°C unfed. Fish were subsequently monitored and fed daily for 60 days. After the treatment period, fish were euthanized using 500 mg/L MS-222 and frozen at -20°C. Otoliths were then dissected from the fish heads and stored in 95% ethanol. Upon dissection, significant vaterite was observed, thus providing an opportunity to examine the prevalence of vaterite in cultured Delta Smelt. Results for cultured fish

were compared to those of wild Delta Smelt that were also collected in 2019 by the US Fish and Wildlife Service's Enhanced Delta Smelt Monitoring (EDSM) 20mm Kodiak trawl survey (USFWS et al., 2020) (Table 5-1.). Similarly, wild Delta Smelt otoliths were dissected from the fish head and stored in 95% ethanol.

Otolith Preparation

Sagittal otoliths from adult Delta Smelt were dissected using size 10 scalpel blades. Whole otolith images were then taken sulcus side down with Amscope MU1000 10MP camera on a Leica SteroZoom7 dissecting scope at 20x or 30x magnification with millimeter markers. After imaging, otoliths were mounted to glass microscope slides with thermoplastic glue and stored in plastic microscope slide boxes. A subset of otoliths (n = 20) representing all vaterite categories (I-IV) was selected to quantify whole otolith polymorph composition using X-ray powder diffraction (XRD). Otoliths selected for XRD were removed from crystal bond with 99.5% acetone to prevent contamination. Otoliths were then sonicated in MiliQ water, dried, and stored in glass vials prior to analysis. An additional subset (n = 5; Figure 5-2) of samples, representing all vaterite categories (I-IV), was selected and prepared for analysis by Raman spectroscopy and laser ablation. These samples were sanded on the sulcus side with 600, 800, and 1200 grit sandpaper and polished with polishing cloth and 0.3-µm alumina.

Visual Analysis

A total of 478 otoliths from both wild and hatchery-reared fish were analyzed (Figure 5-1), with any broken or partially missing otoliths excluded (n = 16). Otoliths were digitally measured for dorsal-ventral radius, otolith area, and percent vaterite area using ImageJ (Version 2.0; Abràmoff et al. 2004). Differences between left and right otolith dimensions were used to estimate otolith asymmetry for each fish following equation 1, where *dv*L and *dv*R are the dorsal-ventral measurements for the left and right otolith, respectively.

$$\text{Asymmetry (\%)} = \left|\frac{(dvL - dvR)}{dvR}\right| * 100\% \quad (1)$$

Total otolith surface area (Oto_{SA}) was measured automatically from digital images using the 'Analyze Particle' operation in image J (Igathinathane et al., 2008). Vaterite was identified by its transparent coloration and delineated from aragonite using the 'Freehand' operation in ImageJ. The surface area of vaterite Vat_{SA} in each otolith was calculated by subtracting the area of aragonite from Oto_{SA}. Oto_{SA} and Vat_{SA} were then used to calculate vaterite prevalence according to Equation 2. Each otolith was then designated into one of four categories defined by the abundance of vaterite: I (<1%), II (1-15%), III (15-30%), IV (>30%) (Figure 5-1.).

$$\text{Vaterite Prevalence} = \frac{VatSA}{OtoSA} * 100\% \quad (2)$$

Raman Spectroscopy

Raman spectroscopy was used to confirm visual observations of vaterite and aragonite. Raman spectroscopy is a non-destructive technique using excitation by a laser light source and the unique spectral shifts due to bond vibration and rotation to identify different crystalline polymorphs (Gauldie et al. 1997; Melancon et al. 2005). Analyses were performed at the Keck Spectral Imaging Facility, UC Davis, using a Renishaw Confocal Raman Microscope equipped with a diode laser with an excitation wavelength of 785 nm at 0.37 mm working distance, a 50x objective, and a grating of 1800 grating/mm, calibrated to wavelength of 520 cm^{-1} on a silicone standard. Spectra were

collected with an integration time of 10 seconds and a wavelength range of 130–1200 cm^{-1}. Five otoliths were selected for Raman spectroscopy, spanning the full range of vaterite categories (I-IV). Multiple spots were analyzed along a transect from the otolith core to the ventral edge: (1) aragonite, (2) aragonite edge, (3) vaterite edge, (4) vaterite, with additional transects conducted in the most vateritic (category IV) otolith (Figure 5-2.). Peaks were automatically detected in each spectrum using the "findpeaks" function in the *pracma* package (Borchers, 2021) in R (v. 2.6.3) and confirmed graphically.

X-ray Diffraction

Validation of the percent composition ("prevalence") of vaterite in otoliths was conducted using x-ray diffraction (XRD). XRD is a destructive technique that examines the X-ray scattering pattern of a crushed (powdered) crystalline sample to identify the relative abundances of different crystalline polymorphs (Carlström, 1963; Gauldie, 1993). A total of 20 otoliths from cultured Delta Smelt were selected for analysis, spanning the range of vaterite categories (I-IV). Each otolith was then crushed to a fine powder and scanned for 80 minutes on a PANalytical X'Pert Pro diffractometer equipped with a PW3064 sample spinner and Co x-ray tube X'Celerator detector using a scan range of 20°-70° 2θ with a step size of 0.0017° 2θ. All XRD analyses were performed at the X-Ray Diffraction Lab, UC Berkeley, CA.

LA-ICPMS

Elemental concentrations in otoliths (relative to Ca) were measured using a Photon Machines 193nm ArF Excimer laser with a HelEx dual-volume LA cell coupled to a Thermo Element XR HR-ICPMS in the Yin Lab at the Department of Earth and Planetary Sciences at UC Davis. The repetition rate of the laser was set at 10 Hz and fluence was ~3 J/cm^2. A line of spots was ablated from the edge to the core with a spot size of 40 μm and a spacing of 40 μm. Before data collection, a cleaning run (pre-ablation) was performed across the same trajectory with a larger (80 μm) spot size. We measured a large suite of potentially informative analytes including lithium, sodium, magnesium, potassium, calcium, manganese, zinc, strontium, and barium (^{7}Li, ^{23}Na, ^{24}Mg, ^{39}K, ^{43}Ca, ^{44}Ca, ^{55}Mn, ^{66}Zn, ^{88}Sr, and ^{138}Ba, respectively). Data were reduced relative to NIST 612 using Iolite (Paton et al., 2011) and ^{43}Ca as the internal standard using the Trace Element data reduction schema following standard best practices (Longerich et al., 1996; Jochum et al., 2011). Otolith aragonite was assumed to contain 38.8 wt% Ca (e.g., Hüssy et al., 2016). NIST 610 and 612 glasses were measured prior to and between each sample and used as external reference materials to correct for instrument drift. Element-specific limits of detection were calculated as 3 times the standard deviation of the element-specific background value. Measured concentrations of an element below its respective detection limit were set to zero, indicating negligible abundance. Elements (X) were then ratioed to calcium $X/^{43}Ca$ and expressed in μmol/mol.

Statistical Analyses

Estimates of vaterite composition based on digital image analysis and XRD were compared by linear regression. Linear models were used to compare vaterite composition and asymmetry among cultured and wild fish. The presence of vaterite was compared between cultured and wild fish by logistic regression. The effects of hatchery conditions on vaterite and asymmetry in cultured fish were each compared by linear models including the fixed effects of temperature, feed, and their interaction, with fish size as a covariate. The effects of hatchery conditions on the presence of vaterite were examined by logistic regression as a function of the fixed effects of temperature, feed, and their interaction, with fish size included as a covariate.

Results

Validation

Raman spectroscopy displayed distinct peaks at 267, 300, 740, 750, 1075,1090 cm^{-1} and 705, 1085cm^{-1} for vaterite and aragonite, respectively (Figure 5-2.) showing agreement with Nehrke et al. (2012) and XRD. However, we also observed high variability at spectra 155 and 206 cm^{-1} and thus were excluded from the analysis. Calcite peak of wavelength 282 cm^{-1} was observed in 3 otoliths (Figure 5-4). However, these peaks are considered to be vaterite as we did not observe an additional calcite peak at 711 cm^{-1}. Therefore, there is no evidence for calcite development in Delta Smelt otoliths. Additional peaks not known to be $CaCO_3$ polymorphs were also observed due to contamination by binding resin (Jolivet et al., 2013). Comparison of XRD and visual analysis of vaterite prevalence showed a strong linear relationship ($p< 0.01$; $R^2 = 0.84$; Table 5-2.). An identification threshold of 10% prevalence is observed (Figure 5-5.), however, 6 samples were identified as aragonite by both visual and XRD. This suggests that the threshold seen is due to detection limitation on XRD rather than visual identification of vaterite.

Otolith Abnormalities

Vaterite formation was found to be significantly higher in cultured fish ($p<0.001$). Fish length was also found to influence the formation of vaterite ($p<0.01$), although it did not affect the prevalence of vaterite ($p>0.05$). Cultured fish were found to have vaterite in 50.2% (120/239) of otoliths, compared to just 0.9% (2/221) of wild fish otoliths (Table 5-1) while also showing higher prevalence with an average of 5.03% and 0.03% vaterite, respectively. Overall, 27 cultured and 1 wild fish otolith contained significant amounts of vaterite. Analysis of the treatment effects on vaterite development suggested that neither treatment affected vaterite formation. While hatchery treatments did have a slight significant effect on the presence of vaterite ($p<0.05$, Table 5-3) treatments were not significant when considering the random tank effect ($p>0.05$; Table 5-4).

The difference in otolith asymmetry was statistically significant ($p<0.05$; Table 5-3) between wild (0.36%) and cultured (1.20%) fish. In cultured fish, the formation of vaterite corresponded with higher degrees of asymmetry ($p<0.001$). Moreover, neither feed nor temperature affected otolith asymmetry ($p>0.05$; Table 5-3.). In contrast to vaterite, fish length did not affect asymmetry ($p>0.05$).

Otolith Chemistry

Chemical composition of the otolith varied between aragonite and vaterite. Regions visually identified as vaterite saw enriched levels of $Mg/^{43}Ca$ and $Mn/^{43}Ca$ and depleted levels of $Na/^{43}Ca$, $Ba/^{43}Ca$, and $Sr/^{43}Ca$, while $^{44}Ca/^{43}Ca$ remained consistent in comparison to aragonite. ^{7}Li, ^{39}K, and ^{66}Zn were found to be below detection levels. $Mg/^{43}Ca$ and $Mn/^{43}Ca$ concentrations were on average 4.6x and 2.4x greater in vaterite, while $Sr/^{43}Ca$, $Ba/^{43}Ca$, and $Sr/^{43}Ca$ were 2x, 14x, and 7.6x lower in vaterite otoliths, respectively (Figure 5-7.; Table 5-5.). Similar trends were seen in Tzeng et al. (2017), supporting the abnormal polymorph seen as vaterite. We did however see a slight disparity between visual identification and chemistry on otolith aragonite-vaterite edge in categories III and IV (Figure 5-6.).

Discussion

Summary of Main Findings

Here, we quantified the frequency and severity of developmental anomalies in Delta Smelt otoliths (*Hypomesus transpacificus*), a critically endangered estuarine fish that is endemic to the San Francisco Estuary (SFE). To our knowledge, this is the first study to combine and contrast visual, geochemical, and structural approaches to quantifying vaterite in fish otoliths, and the first to examine vestibular abnormalities in Delta Smelt. Our results confirm the presence of vaterite in cultured Delta Smelt, which can readily be observed as an irregular transparent zone in the otolith and is enriched in Mg and Mn, depleted in Ba, Sr, and Na, and is readily confirmed as vaterite (versus calcite or aragonite) using XRD or Raman spectroscopy.

Otoliths of cultured Delta Smelt were 50 times more likely to contain vaterite (>1%) and 20 times more likely to contain large (>15%) amounts of vaterite. Similarly, cultured fish exhibited 3 times greater asymmetry than wild fish. Larger, faster-growing cultured fish were more likely to exhibit vateritic otoliths, but not increased asymmetry. Short-term exposure to variation in temperature and feed did not appear to influence vaterite formation or asymmetry. Together, these results indicate that cultured Delta Smelt exhibit a significantly higher frequency of vestibular abnormalities which are known to reduce the fitness and survival of fishes (Anken et al., 2017; Oxman et al., 2007; Reimer et al., 2016). Such hatchery effects on otolith development could have important implications for captive culture practices and the supplementation of the wild Delta Smelt population with cultured individuals.

Validation – XRD & Raman

Vaterite in otoliths has been quantified using visual (Strong et al. 1986; Brown et al. 2013; Bowen II et al. 1999; Sweeting et al. 2004), structural (Gauldie, 1993), or geochemical analysis (Budnik et al., 2020). Here, visual identification of vaterite was highly correlated with results based on XRD, Raman, and geochemical approaches, indicating that visual identification is a reliable technique to identify and quantify vaterite in Delta Smelt otoliths. For example, 83% of the variation in bulk vaterite content estimated by XRD could be described by visual 2D estimates. Cross referencing spatial patterns in vaterite composition using both Raman spectroscopy and LA-ICPMS with those determined by image analysis further validated the approach. Variation in elemental concentrations as the laser transitioned from aragonite to vaterite regions of the otolith matched expected patterns based on the literature (Tomás, 2003; Tzeng et al., 2007). Results from Raman spectroscopy identified regions with both aragonite and vaterite signals (Figure 5-2), suggesting that visual transitions on the aragonite edge, e.g., of category III and IV otoliths (Melancon et al., 2005), are more gradual than they appear visually (Tomás and Geffen, 2003).

Treatment Effects

Although the experiment for cultured fish was not originally designed to assess vaterite formation, nevertheless, we examined evidence for the 60-day treatment effects on asymmetry and vaterite. While temperature has been shown to be correlated with the formation of vaterite (Gauldie, 1986; Reimer et al., 2017), we have not seen the same pattern in Delta Smelt ($p>0.05$). On the other hand, starvation, though speculated to contribute to vaterite growth (Budnik et al., 2020), has been shown to slow otolith growth but not result in the formation of vaterite (Guibbolini et al., 2006). Here, we observed a slight influence of starvation treatment on vaterite presence ($p<0.05$) in Delta Smelt, but this influence was not significant when accounting for tank effects ($p>0.05$). This lack of response

to temperature and food limitation could be due to the short treatment period; for example, a longer treatment period might result in significant treatment effects. Similarly, neither experimental treatment affected otolith asymmetry ($p>0.05$); however, the presence of vaterite in a fish's otoliths significantly increased the amount of asymmetry ($p<0.05$). This is likely due to the partial replacement of aragonite with the less dense vaterite polymorph, leading to larger otolith volume (Kamhi, 1963; Tomás and Geffen, 2003).

Causes of Vaterite Formation

While the causes of vaterite formation in otoliths is not extensively understood, otolith biomineralization is linked to energy availability (Fablet et al., 2011). Fast growing fish have been associated with the formation of vaterite (Reimer et al., 2017), which are assumed to have more energy. This is suspected to increase the transport of inorganic carbon (HCO_3^-) thus lowering the $[Ca^{2+}]/[CO_3^{2-}]$ ratio in the endolymph to favor vaterite formation (Reimer et al., 2017). Additionally, environmental stress such as handling stress (Bowen II et al., 1999), temperature (Gauldie, 1996), and density effects (Austad et al., 2021) are known to be associated with vaterite formation, while calcite formation has been induced by high pCO_2 conditions (Coll-Lladó et al., 2021). Diversion of energy expenditures to combat effects of stress could have resulted in changes to the endolymph $[Ca^{2+}]/[CO_3^{2-}]$ ratio (Grosell, 2019; Payan et al., 2004). Formation and biomineralization of otoliths is also shown to be induced by genetics (Hughes et al., 2004; Söllner et al., 2003) and the otolith protein matrix (Falini et al., 2005; Ren et al., 2013). Hughes et al. (2004) prevented the formation of otolith in zebrafish when the gene *otop1* was inhibited, thus demonstrating the importance of genetic expression and the protein matrix. Furthermore, organic matrix macromolecule-64 (*OMM-64*) can inhibit aragonite formation and promote vaterite when in the presence of Mg^{2+} and absence of *Otolin-1* (Poznar et al., 2020); however, when in contact with *Otolin-1*, aragonite is formed (Tohse et al., 2009). Changes in the *Otolin-1* and *OMM-64* ratio resulting from stress or fast growth could potentially induce a switch to vaterite formation.

Vaterite and Asymmetry Observed in Other Species

The prevalence of vateritic otoliths in cultured (50%) and wild (0.95%) Delta Smelt was similar to values observed in cultured and wild populations of other species. For example, Reimer et al. (2016) described the prevalence of vaterite in cultured Coho salmon (52 - 56%), herring (14 - 60%), rainbow trout (50%), and lake trout (48%). As for Delta Smelt, wild populations exhibited much less vaterite in their otoliths, including Coho salmon (1 – 12%), herring (5 - 6%), rainbow trout (5%), and lake trout (24%) (Reimer et al., 2016); however these values were often much higher than the 0.95% observed in wild Delta Smelt. Overall, vaterite presence is on average 10.4 times higher in cultured fish than wild fish, with up to 91% vaterite prevalence in certain species (Reimer et al., 2016; Tomás and Geffen, 2003). Otolith asymmetry in Delta Smelt was relatively low (0.36% - 1.2%), whereas prior estimates globally ranged from 1.25% - 4.66% , with an average of 2.77% (Mahé et al., 2019). Based on fluctuating asymmetry, hatchery fish have been shown to exhibit up to 3-fold greater asymmetry than wild fish (Koeberle et al., 2020), though this is not consistent for all species (Geladakis et al., 2021). Similarly, hatchery Delta Smelt exhibited 3-4 times higher asymmetry than wild fish, however, even the cultured values remained relatively low.

Consequences of Otolith Abnormalities

The effects of otolith anomalies on fitness have not been studied extensively, but could have implications for conservation (Reimer et al. 2017). For example, the development of vateritic otoliths does not appear to be reversible (Reimer et al. 2016) and is correlated with several other

developmental abnormalities including fewer lateral line neuromasts, smaller brain weight, and reduced olfactory bulb volume (Brown et al., 2013). In Norwegian Atlantic salmon, for example, higher frequencies of vaterite correspond with lower return rates, possibly due to reduced otolith function, behavioral alteration, and navigational impairment (Austad et al., 2021; Oxman et al., 2007; Reimer et al., 2016; Vignon and Aymes, 2020). Consequently, a decrease in sensory function could lead to increased mortality due to predation (Hung et al., 2019). Vaterite otolith impairments are suggested to be disproportionally more apparent in smaller fishes (Kondrachuk 2003; Reimer et al. 2016; Vignon and Aymes 2020). However, the effects of vaterite development on fish survival ultimately remain unclear as the extent of impact could vary with different life-stages (Delaval et al., 2021). As for otolith symmetry, asymmetrical development can impair hearing (Lychakov and Rebane, 2005) and lead to abnormal swimming behaviors (Anken et al. 2017), each of which can affect fitness.

Here we documented the prevalence of otolith anomalies in Delta Smelt, a critically endangered estuarine fish currently supported by a conservation hatchery. While the cause of these developmental abnormalities is not fully understood, otoliths with severe asymmetry or vaterite were common in cultured fish but rarely observed in the wild population. This suggests that either hatchery conditions increase otolith abnormalities in cultured fish, or that such abnormalities negatively affect fitness and survival, thus leading to strong selection in the wild. Further studies are needed to identify causal mechanisms of vaterite formation in Delta Smelt and how such abnormalities might affect the hatchery population and the effectiveness of population supplementation efforts.

References

Abràmoff, M.D., Magalhães, P.J., Ram, S.J., 2004. Image Processing with ImageJ 11, 36–42.

Anken, R., Knie, M., Hilbig, R., 2017. Inner Ear Otolith Asymmetry in Late-Larval Cichlid Fish (Oreochromis mossambicus , Perciformes) Showing Kinetotic Behaviour Under Diminished Gravity. Sci. Rep. 7, 15630. https://doi.org/10.1038/s41598-017-15927-z

Austad, B., Vøllestad, L.A., Foldvik, A., 2021. Frequency of vateritic otoliths and potential consequences for marine survival in hatchery-reared Atlantic salmon. J. Fish Biol. 98, 1401–1409. https://doi.org/10.1111/jfb.14683

Borchers, H.W., 2021. Practical Numerical Math Functions (pracma).

Bowen II, C.A., Bronte, C.R., Argyle, R.L., Adams, J.V., Johnson, J.E., 1999. Vateritic Sagitta in Wild and Stocked Lake Trout: Applicability to Stock Origin. Trans. Am. Fish. Soc. 128, 929–938. https://doi.org/10.1577/1548-8659(1999)128<0929:VSIWAS>2.0.CO;2

Brown, A.D., Sisneros, J.A., Jurasin, T., Nguyen, C., Coffin, A.B., 2013. Differences in Lateral Line Morphology between Hatchery- and Wild-Origin Steelhead. PLOS ONE 8, e59162. https://doi.org/10.1371/journal.pone.0059162

Budnik, R.R., Farver, J.R., Gagnon, J.E., Miner, J.G., 2020. Trash or treasure? Use of sagittal otoliths partially composed of vaterite for hatchery stock discrimination in steelhead. Can. J. Fish. Aquat. Sci. 77, 276–284. https://doi.org/10.1139/cjfas-2018-0387

California Department of FIsh and Wildlife, 2021. State and Federally Listed Endangered and Threatened Animals of California 31.

Campana, S.E., 2005. Otolith science entering the 21st century. Mar. Freshw. Res. 56, 485. https://doi.org/10.1071/MF04147

Campana, S.E., 1999. Chemistry and composition of fish otoliths:pathways, mechanisms and applications. Mar. Ecol. Prog. Ser. 188, 263–297. https://doi.org/10.3354/meps188263

Carlström, D., 1963. A CRYSTALLOGRAPHIC STUDY OF VERTEBRATE OTOLITHS. Biol. Bull. 125, 441–463. https://doi.org/10.2307/1539358

Coll-Lladó, C., Mittermayer, F., Webb, P.B., Allison, N., Clemmesen, C., Stiasny, M., Bridges, C.R., Göttler, G., Garcia de la serrana, D., 2021. Pilot study to investigate the effect of long-term exposure to high pCO2 on adult cod (Gadus morhua) otolith morphology and calcium carbonate deposition. Fish Physiol. Biochem. 47, 1879–1891. https://doi.org/10.1007/s10695-021-01016-6

Delaval, A., Solås, M.R., Skoglund, H., Salvanes, A.G.V., 2021. Does Vaterite Otolith Deformation Affect Post-Release Survival and Predation Susceptibility of Hatchery-Reared Juvenile Atlantic Salmon? Front. Vet. Sci. 8, 1066. https://doi.org/10.3389/fvets.2021.709850

Fablet, R., Pecquerie, L., Pontual, H. de, Høie, H., Millner, R., Mosegaard, H., Kooijman, S.A.L.M., 2011. Shedding Light on Fish Otolith Biomineralization Using a Bioenergetic Approach. PLOS ONE 6, e27055. https://doi.org/10.1371/journal.pone.0027055

Falini, G., Fermani, S., Vanzo, S., Miletic, M., Zaffino, G., 2005. Influence on the Formation of Aragonite or Vaterite by Otolith Macromolecules. Eur. J. Inorg. Chem. 2005, 162–167. https://doi.org/10.1002/ejic.200400419

Gauldie, R.W., 1996. Effects of temperature and vaterite replacement on the chemistry of metal ions in the otoliths of <I>Oncorhynchus tshawytscha. Can. J. Fish. Aquat. Sci. 53, 2015–2026. https://doi.org/10.1139/cjfas-53-9-2015

Gauldie, R.W., 1993. Polymorphic crystalline structure of fish otoliths. J. Morphol. 218, 1–28. https://doi.org/10.1002/jmor.1052180102

Gauldie, R.W., 1986. Vaterite otoliths from chinook salmon (*Oncorhynchus tshawytscha*). N. Z. J. Mar. Freshw. Res. 20, 209–217. https://doi.org/10.1080/00288330.1986.9516145

Geladakis, G., Somarakis, S., Koumoundouros, G., 2021. Differences in otolith shape and fluctuating-asymmetry between reared and wild gilthead seabream (Sparus aurata Linnaeus, 1758). J. Fish Biol. 98, 277–286. https://doi.org/10.1111/jfb.14578

Grosell, M., 2019. 4 - CO2 and calcification processes in fish, in: Grosell, M., Munday, P.L., Farrell, A.P., Brauner, C.J. (Eds.), Fish Physiology, Carbon Dioxide. Academic Press, pp. 133–159. https://doi.org/10.1016/bs.fp.2019.07.002

Guibbolini, M., Borelli, G., Mayer-Gostan, N., Priouzeau, F., De Pontual, H., Allemand, D., Payan, P., 2006. Characterization and variations of organic parameters in teleost fish endolymph during day–night cycle, starvation and stress conditions. Comp. Biochem. Physiol. A. Mol. Integr. Physiol. 145, 99–107. https://doi.org/10.1016/j.cbpa.2006.05.003

Hammock, B.G., Ramírez-Duarte, W.F., Garcia, P.A.T., Schultz, A.A., Avendano, L.I., Hung, T.-C., White, J.R., Bong, Y.-T., Teh, S.J., 2020. The health and condition responses of Delta Smelt to fasting: A time series experiment. PLOS ONE 15, e0239358. https://doi.org/10.1371/journal.pone.0239358

Hobbs, J.A., Moyle, P.B., Fangue, N.A., Fangue, N., University of California, Davis, 2017. Is Extinction Inevitable for Delta Smelt and Longfin Smelt? An Opinion and Recommendations for Recovery. San Franc. Estuary Watershed Sci. 15. https://doi.org/10.15447/sfews.2017v15iss2art2

Hughes, I., Blasiole, B., Huss, D., Warchol, M.E., Rath, N.P., Hurle, B., Ignatova, E., David Dickman, J., Thalmann, R., Levenson, R., Ornitz, D.M., 2004. Otopetrin 1 is required for otolith formation in the zebrafish Danio rerio. Dev. Biol. 276, 391–402. https://doi.org/10.1016/j.ydbio.2004.09.001

Hung, T., Rosales, M., Kurobe, T., Stevenson, T., Ellison, L., Tigan, G., Sandford, M., Lam, C., Schultz, A., Teh, S., 2019. A pilot study of the performance of captive-reared delta smelt Hypomesus transpacificus in a semi-natural environment. J. Fish Biol. 95, 1517–1522. https://doi.org/10.1111/jfb.14162

Igathinathane, C., Pordesimo, L.O., Columbus, E.P., Batchelor, W.D., Methuku, S.R., 2008. Shape identification and particles size distribution from basic shape parameters using ImageJ. Comput. Electron. Agric. 63, 168–182. https://doi.org/10.1016/j.compag.2008.02.007

Jolivet, A., Fablet, R., Bardeau, J.-F., de Pontual, H., 2013. Preparation techniques alter the mineral and organic fractions of fish otoliths: insights using Raman micro-spectrometry. Anal. Bioanal. Chem. 405, 4787–4798. https://doi.org/10.1007/s00216-013-6893-2

Kamhi, S.R., 1963. On the structure of vaterite CaCO3. Acta Crystallogr. 16, 770–772. https://doi.org/10.1107/S0365110X63002000

Kimmerer, W.J., Gartside, E., Orsi, J.J., 1994. Predation by an introduced clam as the likely cause of substantial declines in zooplankton of San Francisco Bay. Mar. Ecol. Prog. Ser. 113, 81–93.

Koeberle, A.L., Arismendi, I., Crittenden, W., Leer, D., Noakes, D.L.G., 2020. Fluctuating asymmetry of adult Chinook Salmon (Oncorhynchus tshawytscha) otoliths from wild and hatchery origins. Aquat. Ecol. 54, 431–446. https://doi.org/10.1007/s10452-019-09733-0

Kondrachuk, A.V., 2003. Mass and mechanical sensitivity of otoliths. Adv. Space Res., Space Life Sciences: Gravitational Biology: 2002 32, 1521–1526. https://doi.org/10.1016/S0273-1177(03)90390-5

Lessard, J., Cavallo, B., Anders, P., Sommer, T., Schreier, B., Gille, D., Schreier, A., Finger, A., Hung, T.-C., Hobbs, J., May, B., Schultz, A., Burgess, O., Clarke, R., 2018. Considerations for the Use of Captive-Reared Delta Smelt for Species Recovery and Research. San Franc. Estuary Watershed Sci. 16. https://doi.org/10.15447/sfews.2018v16iss3art3

Lewis, L.S., Denney, C., Willmes, M., Xieu, W., Fichman, R.A., Zhao, F., Hammock, B.G., Schultz, A.A., Fangue, N., Hobbs, J.A., 2021. Otolith-based approaches indicate strong effects of environmental variation on growth of a Critically Endangered estuarine fish. Mar. Ecol. Prog. Ser. 676, 37–56.

Lindberg, J.C., Tigan, G., Ellison, L., Rettinghouse, T., Nagel, M.M., Fisch, K.M., 2013. Aquaculture Methods for a Genetically Managed Population of Endangered Delta Smelt. North Am. J. Aquac. 75, 186–196. https://doi.org/10.1080/15222055.2012.751942

Lychakov, D.V., Rebane, Y.T., 2005. Fish otolith mass asymmetry: morphometry and influence on acoustic functionality. Hear. Res. 201, 55–69. https://doi.org/10.1016/j.heares.2004.08.017

Macdonald, J.I., McNeil, D.G., Crook, D.A., 2012. Asteriscus v. lapillus: comparing the chemistry of two otolith types and their ability to delineate riverine populations of common carp Cyprinus carpio. J. Fish Biol. 81, 1715–1729. https://doi.org/10.1111/j.1095-8649.2012.03443.x

Mahé, K., Ider, D., Massaro, A., Hamed, O., Jurado-Ruzafa, A., Gonçalves, P., Anastasopoulou, A., Jadaud, A., Mytilineou, C., Elleboode, R., Ramdane, Z., Bacha, M., Amara, R., de Pontual, H., Ernande, B., 2019. Directional bilateral asymmetry in otolith morphology may affect fish stock discrimination based on otolith shape analysis. ICES J. Mar. Sci. 76, 232–243. https://doi.org/10.1093/icesjms/fsy163

Melancon, S., Fryer, B.J., Ludsin, S.A., Gagnon, J.E., Yang, Z., 2005. Effects of crystal structure on the uptake of metals by lake trout (*Salvelinus namaycush*) otoliths. Can. J. Fish. Aquat. Sci. 62, 2609–2619. https://doi.org/10.1139/f05-161

Moyle, P.B., Brown, L.R., Durand, J.R., Hobbs, J.A., 2016. Delta Smelt: Life History and Decline of a Once-Abundant Species in the San Francisco Estuary. San Franc. Estuary Watershed Sci. 14. https://do10.15447/sfews.2016v14iss2art6

Moyle, P.B., Hobbs, J.A., Durand, J.R., 2018. Delta Smelt and Water Politics in California. Fisheries 43, 42–50. https://doi.org/10.1002/fsh.10014

Nehrke, G., Poigner, H., Wilhelms-Dick, D., Brey, T., Abele, D., 2012. Coexistence of three calcium carbonate polymorphs in the shell of the Antarctic clam *Laternula elliptica*. Geochem. Geophys. Geosystems 13, Q05014. https://doi.org/10.1029/2011GC003996

Oxman, D.S., Barnett-Johnson, R., Smith, M.E., Coffin, A., Miller, D.L., Josephson, R., Popper, A.N., 2007. The effect of vaterite deposition on sound reception, otolith morphology, and inner ear sensory epithelia in hatchery-reared Chinook salmon (*Oncorhynchus tshawytscha*). Can. J. Fish. Aquat. Sci. 64, 1469–1478. https://doi.org/10.1139/f07-106

Panfili, J., Durand, J.-D., Diop, K., Gourène, B., Simier, M., 2005. Fluctuating asymmetry in fish otoliths and heterozygosity in stressful estuarine environments (West Africa). Mar. Freshw. Res. 56, 505–516. https://doi.org/10.1071/MF04138

Payan, P., Pontual, H.D., Edeyer, A., Borelli, G., Boeuf, G., Mayer-Gostan, N., 2004. Effects of stress on plasma homeostasis, endolymph chemistry, and check formation during otolith growth in rainbow trout 61, 9.

Poznar, M., Stolarski, J., Sikora, A., Mazur, M., Olesiak-Bańska, J., Brach, K., Ożyhar, A., Dobryszycki, P., 2020. Fish Otolith Matrix Macromolecule-64 (OMM-64) and Its Role in Calcium Carbonate Biomineralization. Cryst. Growth Des. 20, 5808–5819. https://doi.org/10.1021/acs.cgd.0c00413

Pracheil, B.M., Chakoumakos, B.C., Feygenson, M., Whitledge, G.W., Koenigs, R.P., Bruch, R.M., 2017. Sturgeon and paddlefish (Acipenseridae) sagittal otoliths are composed of the calcium carbonate polymorphs vaterite and calcite. J. Fish Biol. 90, 549–558. https://doi.org/10.1111/jfb.13085

Reimer, T., Dempster, T., Wargelius, A., Fjelldal, P.G., Hansen, T., Glover, K.A., Solberg, M.F., Swearer, S.E., 2017. Rapid growth causes abnormal vaterite formation in farmed fish otoliths. J. Exp. Biol. 220, 2965–2969. https://doi.org/10.1242/jeb.148056

Reimer, T., Dempster, T., Warren-Myers, F., Jensen, A.J., Swearer, S.E., 2016. High prevalence of vaterite in sagittal otoliths causes hearing impairment in farmed fish. Sci. Rep. 6, 25249. https://doi.org/10.1038/srep25249

Ren, D., Feng, Q., Bourrat, X., 2013. The co-effect of organic matrix from carp otolith and microenvironment on calcium carbonate mineralization. Mater. Sci. Eng. C 33, 3440–3449. https://doi.org/10.1016/j.msec.2013.04.031

Söllner, C., Burghammer, M., Busch-Nentwich, E., Berger, J., Schwarz, H., Riekel, C., Nicolson, T., 2003. Control of Crystal Size and Lattice Formation by Starmaker in Otolith Biomineralization. Science. https://doi.org/10.1126/science.1088443

Sommer, T., Armor, C., Baxter, R., Breuer, R., Brown, L., Chotkowski, M., Culberson, S., Feyrer, F., Gingras, M., Herbold, B., Kimmerer, W., Mueller-Solger, A., Nobriga, M., Souza, K., 2007. The Collapse of Pelagic Fishes in the Upper San Francisco Estuary: El Colapso de los Peces Pelagicos en La Cabecera Del Estuario San Francisco. Fisheries 32, 270–277. https://doi.org/10.1577/1548-8446(2007)32[270:TCOPFI]2.0.CO;2

Strong, M.B., Neilson, J.D., Hunt, J.J., 1986. Aberrant Crystallization of Pollock (*Pollachius virens*) Otoliths. Can. J. Fish. Aquat. Sci. 43, 1457–1463. https://doi.org/10.1139/f86-180

Sweeting, R.M., Beamish, R.J., Neville, C.M., 2004. Crystalline otoliths in teleosts: Comparisons between hatchery and wild coho salmon (Oncorhynchus kisutch) in the Strait of Georgia. Rev. Fish Biol. Fish. 14, 361–369. https://doi.org/10.1007/s11160-005-3793-3

Tohse, H., Saruwatari, K., Kogure, T., Nagasawa, H., Takagi, Y., 2009. Control of Polymorphism and Morphology of Calcium Carbonate Crystals by a Matrix Protein Aggregate in Fish Otoliths. Cryst. Growth Des. 9, 4897–4901. https://doi.org/10.1021/cg9006857

511 Tomás, J., 2003. Morphometry and composition of aragonite and vaterite otoliths of deformed
512 laboratory reared juvenile herring from two populations. J. Fish Biol. 63, 1383–1401.
513 https://doi.org/10.1111/j.1095-8649.2003.00245.x
514 Tomás, J., Geffen, A.J., 2003. Morphometry and composition of aragonite and vaterite otoliths of
515 deformed laboratory reared juvenile herring from two populations. J. Fish Biol. 63, 1383–
516 1401. https://doi.org/10.1111/j.1095-8649.2003.00245.x
517 Tzeng, W., Chang, C., Wang, C., Shiao, J., Iizuka, Y., Yang, Y., You, C., Ložys, L., 2007.
518 Misidentification of the migratory history of anguillid eels by Sr/Ca ratios of vaterite
519 otoliths. Mar. Ecol. Prog. Ser. 348, 285–295. https://doi.org/10.3354/meps07022
520 US Fish and Wildlife, 1993. Endangered and threatened wildlife and plants: Determination of
521 threatened status for the delta smelt. US Dep. Inter. Fish Wildl. Serv. 58.
522 USFWS, Johnston, C., Durkacz, S., Mckenzie, R., Speegle, J., Mahardja, B., Perales, B., Bridgman,
523 D., Erly, K., 2020. Interagency Ecological Program and US Fish and Wildlife Service: San
524 Francisco Estuary Enhanced Delta Smelt Monitoring Program data, 2016-2020.
525 Vignon, M., Aymes, J.-C., 2020. Functional effect of vaterite – the presence of an alternative
526 crystalline structure in otoliths alters escape kinematics of the brown trout. J. Exp. Biol. 223.
527 https://doi.org/10.1242/jeb.222034
528 Winder, M., Jassby, A.D., 2011. Shifts in Zooplankton Community Structure: Implications for Food
529 Web Processes in the Upper San Francisco Estuary. Estuaries Coasts 34, 675–690.
530 https://doi.org/10.1007/s12237-010-9342-x
531

532

Tables

Table 5-1. Number of samples (n) quantified to be in each vaterite category (I-IV) in cultured and wild fish.

Category	Cultured (n)	Wild (n)
I	119	219
II	93	1
III	15	0
IV	12	1
Total	239	221

Table 5-2. Statistical result of linear model examining the proportion of vaterite in each otolith as determined by digital image analysis versus the bulk proportion of vaterite based on X-ray diffraction (XRD) analysis.

	DF	SS	MS	F	P	R^2
XRD	1	5950.4	5950.4	114.6	<0.001	0.839
Residual	22	1141.3	51.9			
Total	23	7091.7				

Table 5-3. Results of generalized linear models examining variation in asymmetry and percent vaterite in otoliths of wild versus cultured Delta Smelt (i.e., origin), and among cultured Delta Smelt as functions of adult hatchery conditions (T-temperature, F-feed).

Analysis	Model	Null DF	Null Residual Deviance	Model DF	Model Residual Deviance	ΔDF	Deviance	P-value
Cultured versus Wild	Asymmetry[†] ~ Origin	207	81.186	206	79.076	1	2.110	0.019
	Vaterite(%) ~ Origin	207	0.202746	206	0.470538	1	126.263	<0.001
	Vaterite(0,1) ~ Origin	207	287.12	206	168.36	1	118.76	<0.001
Hatchery Conditions (Temp. & Feed)	Asymmetry[†] ~ T + F + T*F	118	45.303	115	44.448	3	0.855	0.529
	Vaterite(%) ~ T + F + T*F	238	0.264726	235	0.275736	3	6.8969	0.075
	Vaterite(0,1) ~ T + F + T*F	238	326.75	235	314.27	3	12.478	0.006

544 [†]square-root transformed

545 Table 5-4. Results of generalized linear models examining variation in asymmetry and
546 vaterite among cultured Delta Smelt as functions of adult hatchery conditions (T-
547 temperature, F-feed), and including a random tank effect.

548 When including the random tank effect in cultured fish, treatments no longer were significant (p>0.05).

Analysis	Model	Null DF	Null Residual Deviance	Model DF	Model Residual Deviance	ΔDF	Deviance	P-value
Hatchery Conditions (Temp. & Feed)	Asymmetry[†] ~ T + F + T*F	3	298.15	6	297.55	3	0.5995	0.896
	Vaterite(%) ~ T + F + T*F	3	1123.9	6	1119.7	3	4.2368	0.237
	Vaterite(0,1) ~ T + F + T*F	3	303.53	6	300.71	3	2.8145	0.4211

549 [†]square-root transformed

550 Table 5-5. Mean ± standard deviation of concentrations of each trace element in
551 relation to ^{43}Ca, measured in visually identified aragonite and vaterite regions of the
552 otolith (µmol/mol).

Trace Element/^{43}Ca ratio (µmol/mol)	Aragonite	Vaterite
Na:Ca	3012.59 ± 525.07	1464.98 ± 230.26
Mg:Ca	124.97 ± 147.40	630.10 ± 85.34
^{44}Ca:^{43}Ca	3.71E+05 ± 1.30E+04	3.71E+05 ± 9.60E+03
Mn:Ca	2.19 ± 1.86	5.18 ± 3.63
Sr:Ca	961.97 ± 260.70	130.31 ± 12.96
Ba:Ca	10.37 ± 3.83	0.73 ± 0.15

553

554

Figures

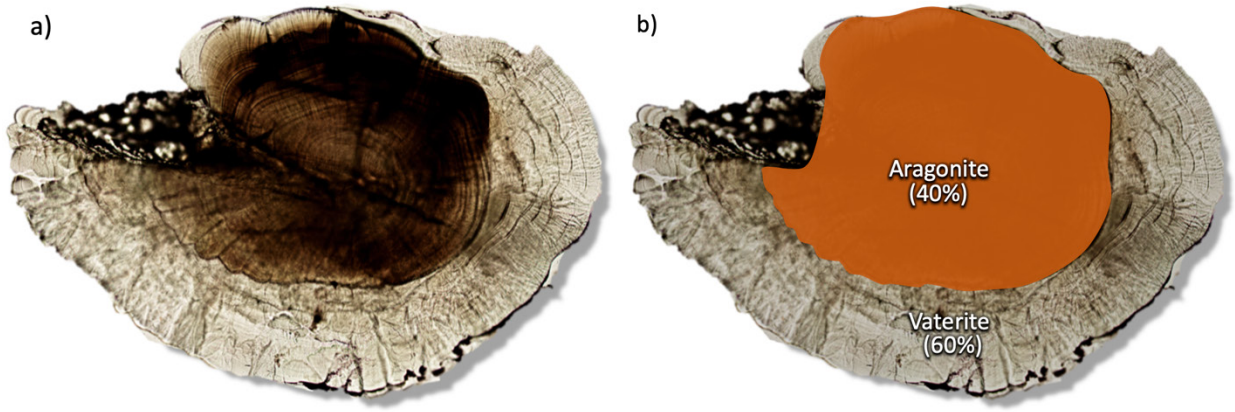

Figure 5-1. Example of a Delta Smelt sagittal otolith exhibiting vaterite (transparent area).

(a) Transmitted light image of a sagittally polished section. (b) The same image is sectioned and annotated to quantify the area of aragonitic and vateritic material.

Figure 5-2. Raman spectroscopy locations on Delta Smelt otoliths with different categories of vaterite prevalence (I-IV).

Spots indicate locations tested for CaCO3 polymorph. Color indicating polymorph identification as aragonite (red), vaterite (blue) or both (purple). Each spot is labeled with transect (A-E) and spot location (1-4).

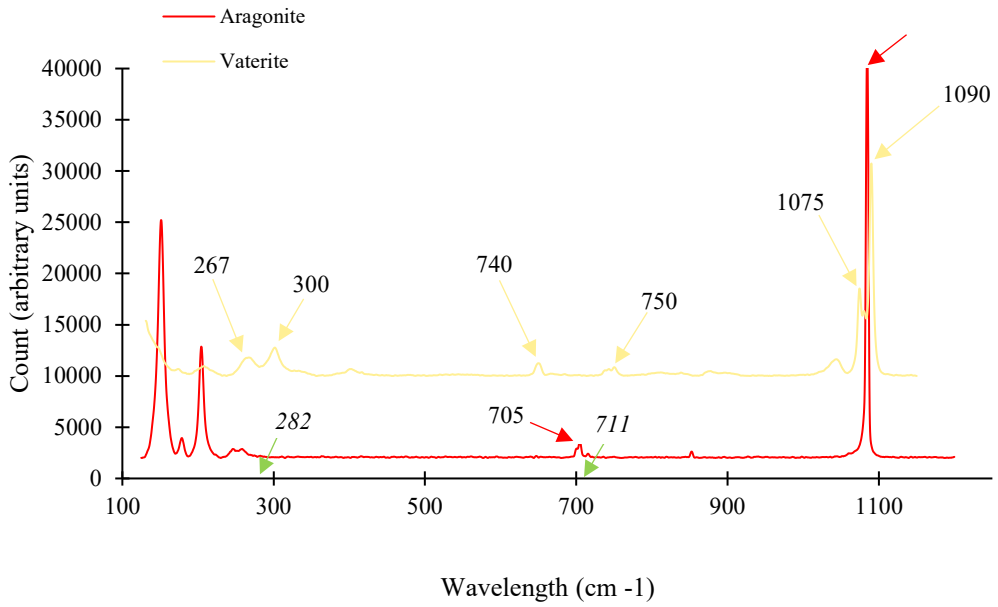

Figure 5-3. Raman spectra patterns of vaterite (blue), aragonite (red), and calcite (green; peaks not shown) between spectral range 125 – 1200 cm-1 denoted with wavelength (cm-1) distinguishing each polymorph.

Y-axis units are arbitrary, peaks are identified relative to background counts which are determined by the sample type and machine settings.

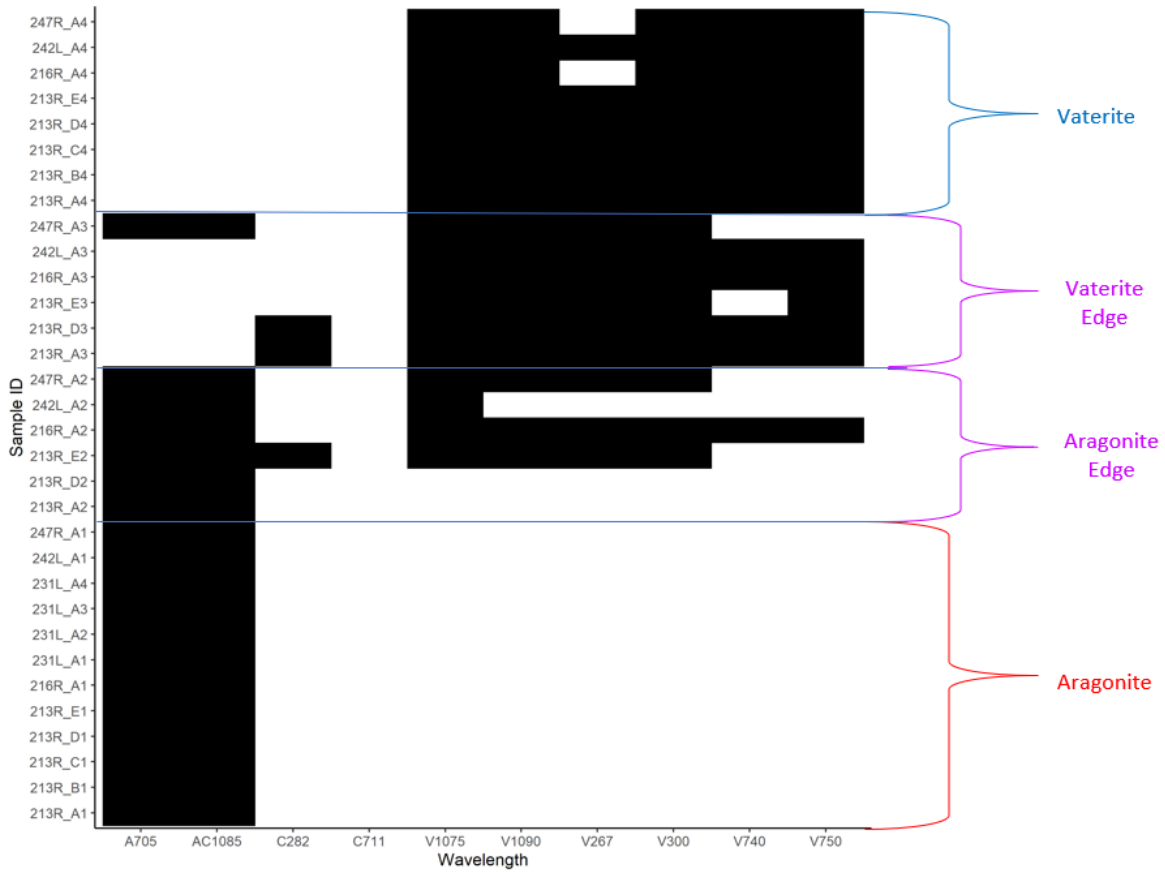

Figure 5-4. Presence of peaks at selected wavelength for each spot that has been identified as aragonite, aragonite edge, vaterite edge, and vaterite.

Denotation of polymorph as aragonite (A), calcite (C), and vaterite (V) is paired with its distinct peak at wavelength (cm^{-1}).

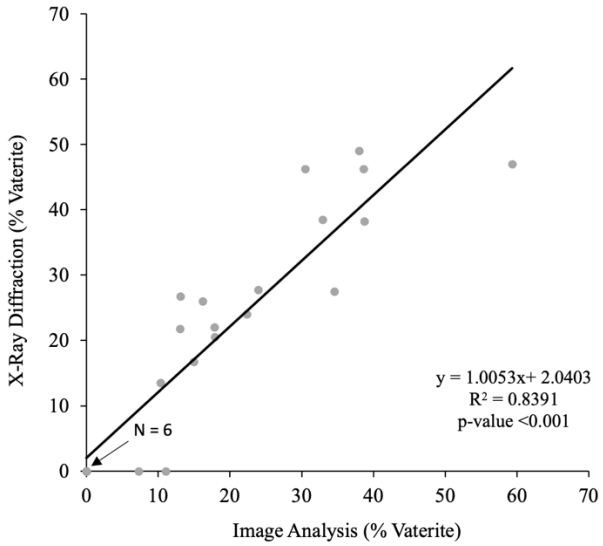

Figure 5-5. Scatter plot and results of a linear model contrasting estimates of vaterite prevalence based on X-ray diffraction (XRD) and digital image analysis.

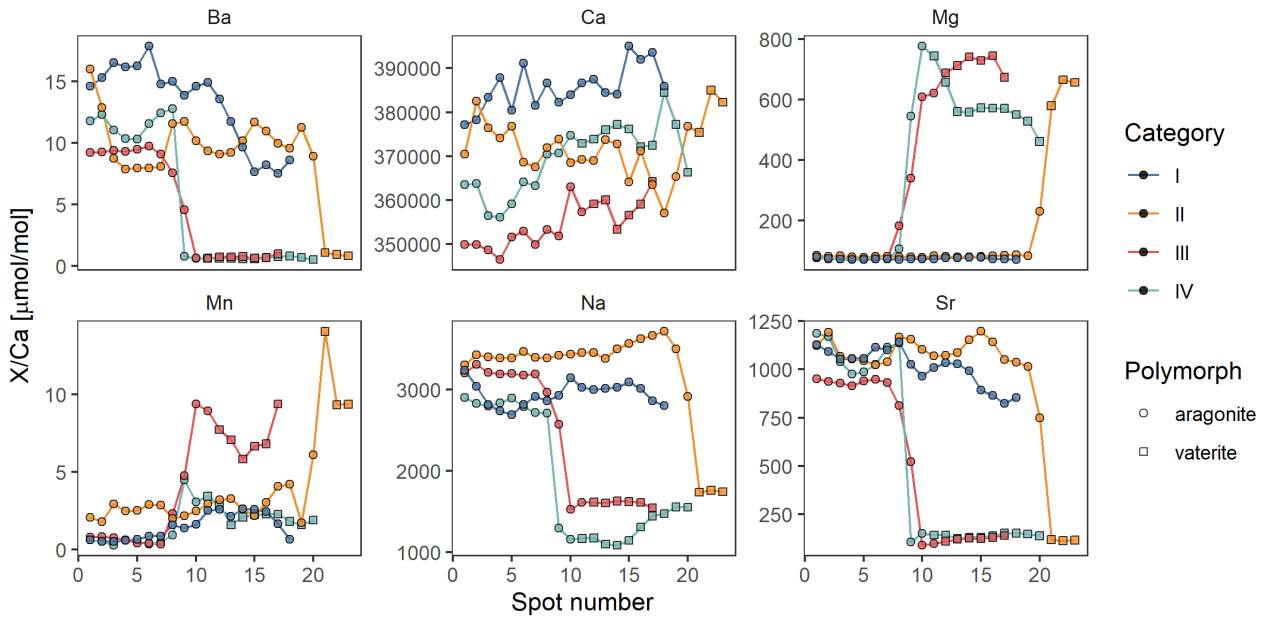

Figure 5-6. Chemical concentration of Ba^{137}, Mg^{24}, Mn^{55}, Na^{23}, Ca^{44} and Sr^{88} relative to Ca^{43} found between different CaCO3 polymorph aragonite (circle) and vaterite (square) in samples containing varying levels of vaterite replacement (I-IV).

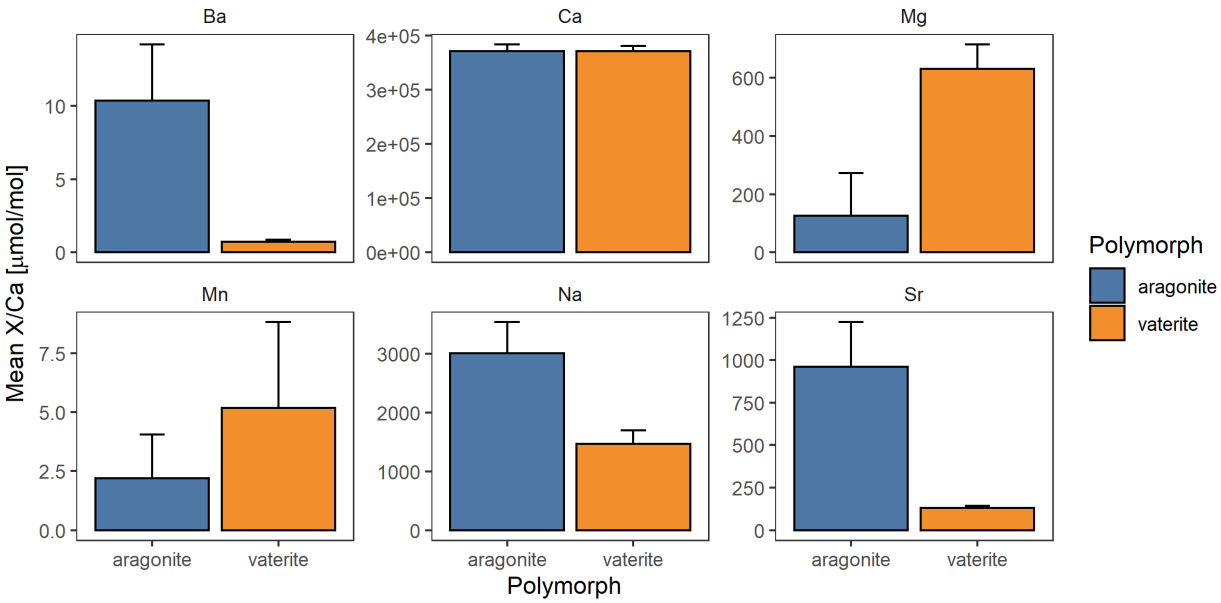

Figure 5-7. Average concentration and standard deviation (error bars) of Ba^{137}, Mg^{24}, Mn^{55}, Na^{23}, Ca^{44} and Sr^{88} relative to Ca^{43} between aragonite (blue) and vaterite (orange).

Chapter 6: Water Quality and Histopathology of Larval Delta Smelt

Marie E. Stillway[1], Shawn Acuña[2], Tien-Chieh Hung[3], Pramod Pandey[4], Swee J. Teh[1]

[1] School of Veterinary Medicine, Department of Anatomy, Physiology, and Cell Biology, Aquatic Health Program Laboratory, 1028 Veterinary Medicine Drive, University of California, Davis, California 95616, USA.

[2] Metropolitan Water District of Southern California, 1121 L Street, Suite 900, Sacramento 95814, USA

[3] Department of Biological and Agricultural Engineering, One Shields Avenue, University of California, Davis, California 95616, USA

[4] School of Veterinary Medicine, Department of Population Health and Reproduction, 1028 Veterinary Medicine Drive, University of California, Davis, California 95616, USA.

Abstract

Ambient samples were collected during the 2021 spring outflow as part of the Directed Outflow Project: Toe Drain (TD), Cache Slough (CS), Deep Water Ship Channel (DWSC), Sacramento River at Decker Island (SRD), Montezuma Slough (MS), and Grizzly Bay (GB), for use in larval Delta Smelt toxicity testing. Biomarkers included health and condition, RNA/DNA, contaminant exposure, and histopathology. Salinity was the greatest factor influencing health and condition of the larval Delta Smelt, with positive correlations in survival, condition factor, RNA/DNA, and glycogen stores, indicating that brackish water habitat can be beneficial to Delta Smelt health and survival at this sensitive life stage. The use of early life stage Delta Smelt demonstrated a heightened response in some biomarkers, namely condition factor and glycogen, and suggest that fish growth and energy usage is a sensitive endpoint. Analytical chemistry indicated a high frequency of fungicides used in agriculture, aligning with the dormant spray season and the land uses surrounding the study areas. Herbicides and insecticides were detected sporadically throughout the project period, continuing to follow the trend of chemical classes that have been observed in previous years. Chemical mixtures had the greatest acute effects on larval Smelt. Exposure 3 (April 9, 2021) had the highest number of contaminants for the TD (10), CS (4), DWSC (3), and SRD (3), and where mortality ranged from 35-41%. Severe gill lesions were observed in Delta Smelt exposed to water collected from CS during Exposure 5 (May 7, 2021), reduced condition factor and increased glycogen depletion throughout the study period, which suggest that CS continues to pose problems for Delta Smelt residing in or slated to be supplemented within that area. Results of this study strengthen our understanding of the drivers impacting Delta Smelt within the Delta during the spring outflow period, especially in terms of spawning success and subsequent rearing which takes place during this important time period.

Introduction

Increasing outflow has long been suggested as an action to improve the habitat for Delta Smelt (*Hypomesus transpacificus*), but the relationship between Delta Smelt abundance and outflow have been mixed (CSD 2018), and contaminants may be confounding the hypothesized relationship between outflow and abundance. Our previous studies have demonstrated that the Toe Drain in the Deep Water Ship Channel, Cache Slough, the Sacramento River at Decker Island, and the Sacramento River at Isleton, consistently caused a higher prevalence and severity of gill lesions in sub-adult Delta Smelt exposed to these waters during the fall months, regardless of outflow actions. These locations are within the North Delta Arc and lower Sacramento River, representing areas currently used in the Delta Smelt Supplementation Strategy. In this toxicity study we focused on a specific seasonal outflow during the spring of 2021, in one of the driest water years on record (CDWR 2021), to characterize the amount and types of contaminants to which early life-stage Delta Smelt would potentially be exposed during a critical life stage. The goal of this study was to provide crucial water quality and contaminant data, which can be used to infer the success of future Delta Smelt supplementation actions, especially those anticipated to occur post-adult release. Our study objective to identify toxic water sources can help inform managers on whether currently mandated flow actions are successful in increasing Delta Smelt health and abundance and can be used as a mechanism to determine ideal habitat areas for subsequent Delta Smelt supplementations.

Materials and Methods

Sampling Design and Water Collections

Water collections took place every two weeks from March to May in 2021, from fixed sampling sites in each of the five areas of the Enhanced Delta Smelt Monitoring Program (EDSM; Table 6-1, Figure 6-1) and included the following sites: 1) Toe Drain [TD], 2) Cache Slough [CS], 3) Deep Water Ship Channel [DWSC], 4) Sacramento River at Decker Island [SRD], 5) Montezuma Slough [MS], and 6) Grizzly Bay [GB]. Sites were chosen to strategically cover the areas of the Bay-Delta based on prior distribution of Delta Smelt, delta-wide hydrology, and potential habitats located in the North Delta Arc, one of the proposed locations for the upcoming Delta Smelt Supplementation Strategy.

Table 6-1. Summary of events and test initiation dates

Test Exposure	Collection Dates	Initiation Date	Age of Delta Smelt (dph)
1	March 8, 9, 2021	March 12, 2021	55
2	March 22, 23, 2021	March 26, 2021	69
3	April 5, 6, 2021	April 9, 2021	83
4	April 20, 22, 2021	April 23, 2021	97
5	May 4, 6, 2021	May 7, 2021	111

The use of fixed sampling locations was chosen to make spatial and temporal comparisons over the course of multiple project years. For each site, 15 gallons of water was collected by boat via bilge pump as sub-surface grabs, in three 20-L (5-gallon) low-density polyethylene cubitainers (I-CHEM,

Fisher Scientific). Plastic cubitainers were selected as sample collection containers to avoid using large glass containers on the boats due to breakage and safety concerns. Additional sub-samples were collected in 1L glass amber bottles (I-CHEM, Fisher Scientific) and 1L plastic (HDPE) bottles (I-CHEM, Fisher Scientific) for water quality measurements and chemical analyses.

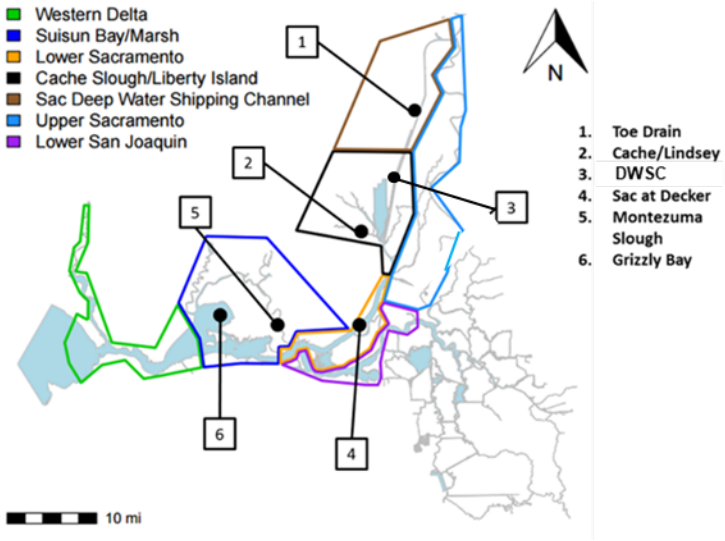

Figure 6-1. Map of study area with delineated sample collection areas (technical assistance from Lara Mitchell, USFWS).

Chemical Analyses

Water samples collected for organic/inorganic analyses were delivered to the Pandey lab at UC Davis, Department of Population Health and Reproduction. Analyses included Gas Chromatography Triple Quadrupole Mass Screening (GC-TQ-MS-MS) for targeted analyses. Inorganics (metals) analysis samples were analyzed via Agilent 7800 ICP-MS for: silver, arsenic, cadmium, copper, manganese, nickel, lead, zinc, aluminum, selenium, chromium, and mercury.

Instrumentation

For pesticide analyses in water samples, a gas chromatograph (GC) (Thermo Scientific™ TRACE™ 1310 Gas Chromatograph); Triple Quadrupole MS-MS (Thermo Scientific™ TSQ™ 8000 Gas Chromatograph/Triple Quadrupole Mass Spectrometer); an autosampler (Thermo Scientific™ TriPlus™ RSH autosampler) was used. Details of the instrument parameters are shown in Table S6 (supplemental information). To separate the analytes from water samples, a capillary column (Thermo TG-5MS; ID 0.25 mm; length 30 m; film 0.25µ; Temp -60 to 330/350°C) was used. The carrier and collision gases were helium (99.999% purity) and argon (99.999% purity), respectively. Carrier gas flow rate was set to 1.2 mL/min. In GC, a programmed Temperature Vaporization (PTV) injector was used to inject the samples, and temperature of injector was set to 200°C. Injection mode in PTV was splitless and injection volume was 1.5 µL using 10 µL syringe in autosampler. The GC column temperature ramps were set as initial temperature of 60°C, held for 2 min, increased at a rate of 18°C/min to 300°C and held for 10 min. The MS was operated in electron ionization mode at 70 eV of ionization energy and 50 uA emission current. The temperature of the ion source and transfer line temperatures were set at 300 and 250°C, respectively. The mass spectra and retention time of all 30 OCP analytes were acquired in SIM scan mode (50-

500). The GC-MS/MS data acquisition was done using Xcaliber Software (Thermo Scientific™ Xcalibur™ Data system). Good signal to noise ratios (3:1) were used for determining the limit of detection. The limit of detection was determined to be 0.05 ppb. GC-MS-MS polarity was positive, and ion source type was EI. Fore line pressure was 68 mTorr. Carrier gas mode was set to constant flow. Tune and air/water spectra check was performed to check functionality of instruments.

Sample extraction

The method used for pesticide analysis in this study was built on previously published methods (Hladik 2008; Hladik and McWayne, 2012; USGS 2020; EL-Saejd et al., 2020; Hladik and Calhoun, 2012). Water samples of 240 mL was measured using measuring cylinders. Sample extraction was done using solid phase extraction (SPE), which is a technique designed for selective sample extraction and preparation, and purification. The SPE is useful for extracting analytes from large volumes of samples, when analyte concentrations in original samples is in low quantity. When analyzing environmental water samples, SPE is often used prior to the sample analysis using GC and HPLC. Details of SPE conditions are shown in Figure S1 supplemental information. Prior to extraction, SPE cartridge (Oasis ® HLC 6 cc (500 mg) was conditioned using 10 mL of ethyl acetate (EtOAc) (Sigma-Aldrich, USA). Subsequently the SPE cartridge was equilibrated with 10 mL of HPLC grade water (Sigma-Aldrich, USA). Once the cartridge was conditioned and equilibrated, 240 mL of water sample was loaded. The water was passed slowly (1-2 mL/min) under vacuum. After 240 mL of sample passed through, the cartridge was dried under slow vacuum. Afterwards, 4 mL of methanol was passed through the cartridge to elute the analytes, and elution was collected in 10 mL falcon tube (Fisher Scientific). To evaporate elution, an evaporator (Thermo Scientific™ Reacti-Vap™ Evaporators) was used, and reconstitution was done using 200 µL of acetonitrile (ACN).

Standard calibration and quality control

To quantify the analytes in water, a series of pesticide standards: GC Multiresidue Pesticide Kit (Restek; Catalog #32562); and comprehensive GC/LC Pesticide Kit (Agilent Technologies; AGPSM-100) were used to develop calibration curves and relationships between peak area and concentrations of analytes. The solutions with spiked standard with concentrations of 0 ppb (0 ppt); 0.05 ppb (50 ppt); 0.1 ppb (100 ppb); 1 ppb (1000 ppt); 6 ppb (6,000 ppt); and 10 ppb (10,000 ppt) were prepared in HPLC grade water. Spike solutions were prepared using the water of the original samples. All of these standards and spike solutions were processed through SPE extraction, and elution was reconstituted in ACN solution (200 µL). Reconstituted ACN solution was used for analysis using GC-MS-MS. Calibration curve (linear) of various concentrations resulted in R^2 value of 0.99 (peak area versus analyte concentrations). Each standard was run in triplicate during method development. All samples were run in duplicate. After every five injections of samples, two standards followed by a blank were injected to verify the chromatograph and to control and maintain the quality of analysis. Prior to running the samples, same day instrument calibration was performed, and quality control was implemented to maintain the data integrity and robustness of the analysis.

Metals analyses

To analyze metals in water, EPA 200 Series Methods was used using Agilent 7800 ICP-MS. The ICP-MS is often used for metal analysis in water analysis. It is a well-accepted technique for routine trace element analysis across a wide range of applications and sample matrices. The ICP-MS was equipped with Agilent Chiller (G3292A), SPS 4 Autosampler, foreline pump (Agilent DS 402), and data system (PC, Monitor, Printer). The Agilent Chiller (G3292A) was used for the chilling

requirement of water. Argon gas (99.999%) was used as an ionizing gas, and helium (99.999%) was used as cell gas. Multiple analyses of trace analytes can be conducted in a single run in ppt to ppm ranges. The software used for this analysis is ICP-MS mass hunter. Spike samples and standards were used to verify the analysis and quantify the trace elements in water samples.

Delta Smelt Toxicity Testing

Larval Delta Smelt were obtained from and tested at the UC Davis Fish Conservation and Culture Laboratory (FCCL; Byron, CA) to minimize transport and acclimation stressors to the fish. Most toxicity studies use the same age of fish for each experiment within a project or timeline, allowing for repeated comparisons to be made across experimental trials. Vendors or hatcheries providing fish for toxicity studies will have multiple groups (cohorts) from various hatch dates in order to supply fish at a specific age at any given time. However, due to the timing of this project, only one cohort of Delta Smelt were available for toxicity testing, as there were no other fish born within FCCL that would meet the age requirements of the study. We therefore used the same cohort of fish during the entire project period, with fish age increasing with the duration of the project. Fish used for experiments were all selected from the January 14, 2021 hatch date cohort. Smelt for each toxicity exposure were selected based on similar size representative of fish age. Fish used in Exposure 1 were 55 days post hatch (dph) and were in the late larval stage of development. Fish in the last toxicity exposure were 111 dph and were considered in the sub-juvenile life stage. Smelt used for toxicity experiments were sacrificed at the end of each exposure for sub-lethal analyses and were not returned to the original culture. All fish were used once in the experiments.

Toxicity tests were 7-days in duration, using a static renewal water exchange system with temperature control. Experimental replicates consisted of four 12-L black plastic buckets outfitted with a PVC standpipe, aeration, and lids (Encore Plastics, Lowe's), and approximately 10 L of ambient water per replicate. Lids were loosely placed on top of the replicate buckets to block out light but allowed room for constant aeration of the replicates. Each replicate contained 20 Delta Smelt for a total of 80 fish per treatment. Ambient and control exposure waters were renewed every 48-h by releasing water from the standpipe through a valve built in below each replicate bucket and replaced with fresh ambient water. This method of water renewal was designed to reduce stress to the fish. Fish were fed once daily with newly hatched *Artemia* nauplii at a target density of 1-3 nauplii/mL.

Ambient water from the California Aqueduct, used for routine fish culturing practices after basic water treatment processes including solids removal and UV disinfection, was used as the primary control. A secondary, "High Salinity" control (HSC) was included, adjusted with Instant Ocean® to match the site with the highest salinity (GB), in order to elucidate salinity stressors on Delta Smelt, if present. Test temperature was maintained at a constant 16 ± 2°C via a temperature-controlled water bath. Mortality and abnormal swimming behavior were visually monitored once daily by FCCL staff, including the removal of dead fish if observed. At the end of the 7-day exposure, surviving fish were euthanized with an overdose of tricaine methane sulfonate, flash-frozen in liquid nitrogen and preserved according to procedures outlined in Teh et al. (2020) for histopathological analyses.

Indicators of General Fish Condition

Gross measurement and weights were used to determine condition factor (CF) in fish (Goede 1989; Schmitt et al. 1999; Schmitt and Dethloff 2000). CF is a measure of "plumpness" and was defined as body weight in grams x 100 / length in cm^3. CF across sites and exposures was analyzed with a one-way ANOVA followed by a Tukey's multiple comparison test. Salinity effects on CF were analyzed

with a Welch's t-test. Significance was set with an alpha level of 0.05. These analyses were performed using GraphPad PRISM 9.0.0.

RNA/DNA

Short-term growth was evaluated by measuring the RNA/DNA ratio. Growing involves synthesis of molecules to build up tissue which is manifested in higher synthesis of RNA for synthesis of protein, e.g. muscle. As the quantity of DNA per cell remains relatively constant, changes in the quantity of RNA per cell indicates different growth rate. RNA/DNA ratio is a sensitive indicator of growth rate after short exposure to adverse conditions such as contaminants (Bisbal and Bengston, 1995; McLaughlin et al., 1995; Chicharo et al. 1998). RNA-DNA ratio in muscle was measured using the ethidium bromide fluorometric technique (Caldarone et al., 2001). Briefly, sample protein from muscle was dissociated from nucleic acid and the fluorophore ethidium bromide (DNA staining dye) was used to measure total nucleic acids. RNase was added to digest RNA to differentiate RNA from DNA.

An ANCOVA was performed on the RNA/DNA results, with site, fork length, days post hatch, water temperature, and salinity as predictor variables. Fork length, days post hatch, and water temperature were treated as continuous variables, while site and salinity were treated as categorical variables. Salinity was treated as a categorical variable because we observed a similarly sized improvement in survival in all brackish water tests, and therefore suspected that growth would also be elevated. 'Trial' was included as a categorical variable initially but was not significant and was removed. Therefore, it was appropriate to group each of the five trials together. A plot of the residuals revealed no violations of ANCOVA assumptions. The analysis was performed using JMP 16.

Histopathology

Histopathology was performed on gill and liver tissues of Delta Smelt. Tissues were fixed in 10% neutral buffered formalin and were processed according to Teh at al. (1997). Briefly, tissues were embedded in paraffin, sectioned at 3-μm thickness and stained with hematoxylin and eosin. Liver and gill lesions were evaluated using the criteria as described in Teh et al. (2020). Lesions were scored semi-quantitatively based on a scale of 0-3, where 0 = not present, 1 = mild, 2 = moderate, and 3 = severe, in the livers and gills of each fish. To assess the overall health condition of liver and gill, a histopathological index was developed by averaging the sum of the lesion scores in each organ. The average summed lesion score represents the degree of damage to the liver and gill, with higher scores indicating a higher degree of damage.

Statistical comparisons were made on average summed lesion scores of liver and gill with a Kruskal-Wallis Rank Sum test, followed by pairwise comparisons using a Wilcoxon Rank Sum test with continuity corrections. Significance was set with an alpha level of 0.05. Summed lesion scores for the liver do not include glycogen depletion, as it is not considered a lesion and is more indicative of a nutrition metric (Hammock et al. 2015). Glycogen was analyzed separately using the same analyses. Statistical analyses were conducted using R v.4.0.3.

Results

2021 Water Year and Spring Outflow

The 2021 California water year was the second driest on record, with only 11.9 inches of rain and snow recorded (CDWR 2021). This lack of precipitation in combination with higher than normal temperatures in the winter and spring fueled a snow drought in the Sierras (http://www.drought.gov) and resulted in low runoff during the spring outflow (Figure 6-2). Figures 6-3 through 6-7 depict average daily discharge at USGS gauge sites representative of sample collection areas, which were generated using the USGS Surface-Water Daily Data for the Nation (https://nwis.waterdata.usgs.gov/nwis/dv).

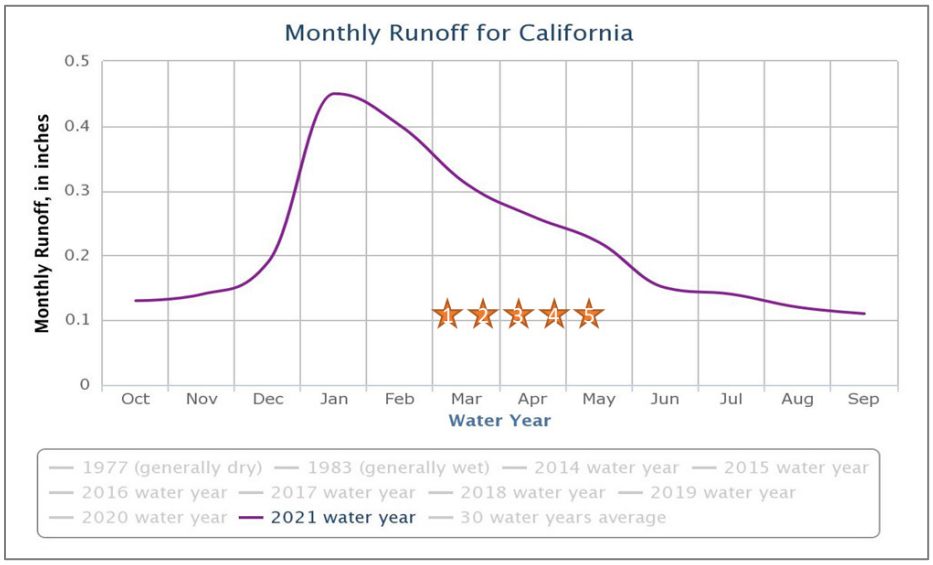

Figure 6-2. Graph of monthly runoff totals for California during the 2021 water year.

Orange stars indicate Delta smelt toxicity exposures. Graph obtained from www.ca.water.usgs.gov_california-drought.

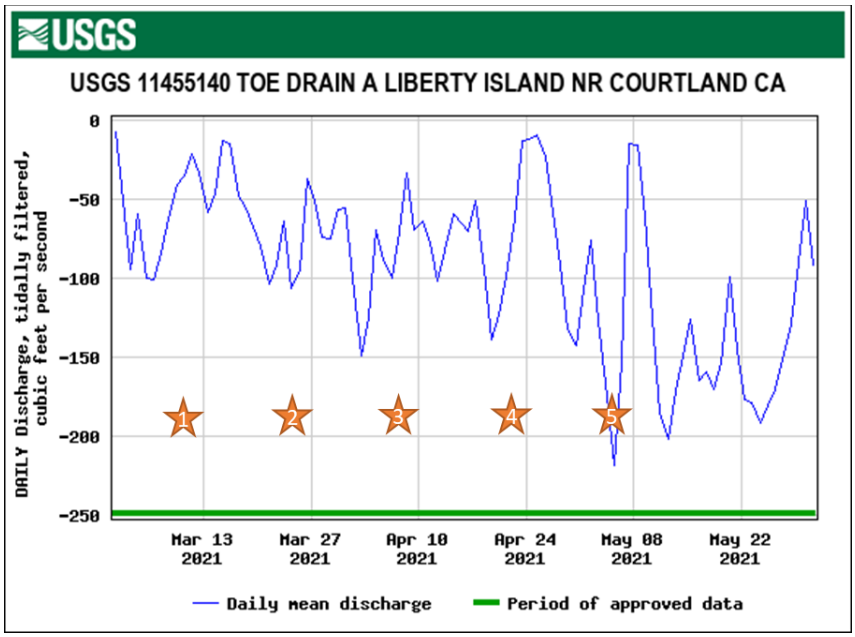

Figure 6-3. Graph of mean daily discharge for USGS site 11455140 Toe Drain at Liberty Island, CA.

Graph depicts flows influencing water quality at Site 1: Toe Drain, during the 2021 spring outflow. Orange stars indicate Delta Smelt toxicity exposures.

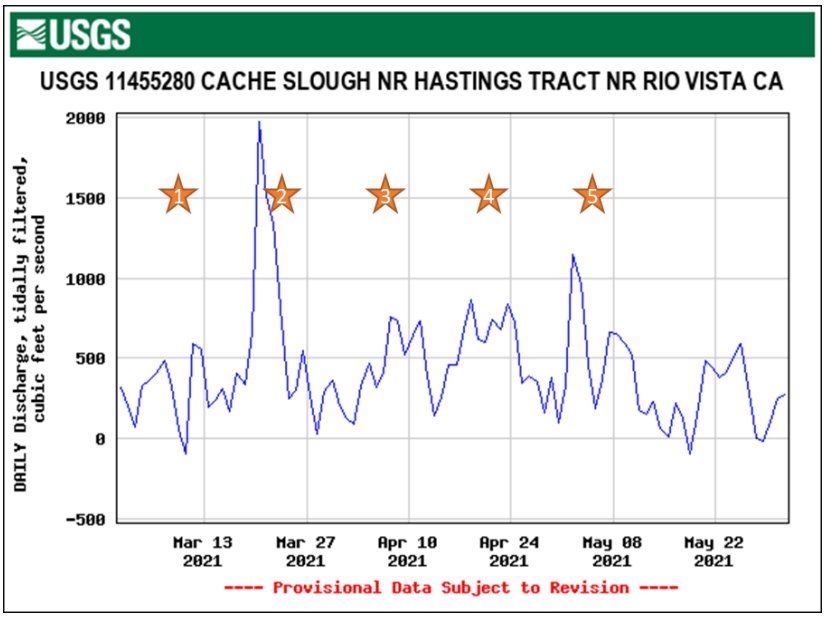

Figure 6-4. Graph of mean daily discharge for USGS site 11455280 Cache Slough near Hasting's Tract, CA.

Graph depicts flows influencing water quality at Site 2: Cache Slough, during the 2021 spring outflow. Orange stars indicate Delta Smelt toxicity exposures.

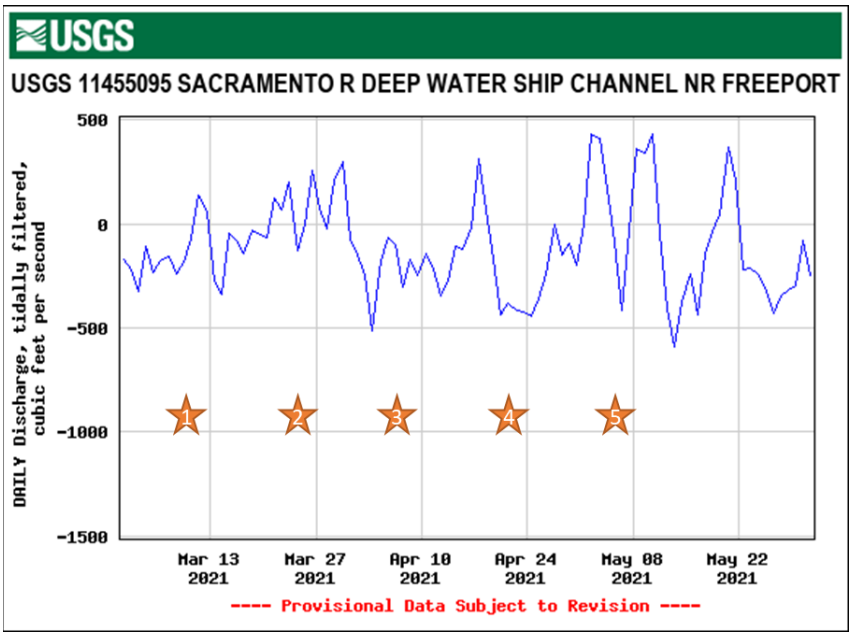

Figure 6-5. Graph of mean daily discharge for USGS site 11455095 Sacramento River Deep Water Ship Channel, CA.

Graph depicts flows influencing water quality at Site 3: Deep Water Ship Channel, during the 2021 spring outflow. Orange stars indicate Delta Smelt toxicity exposures.

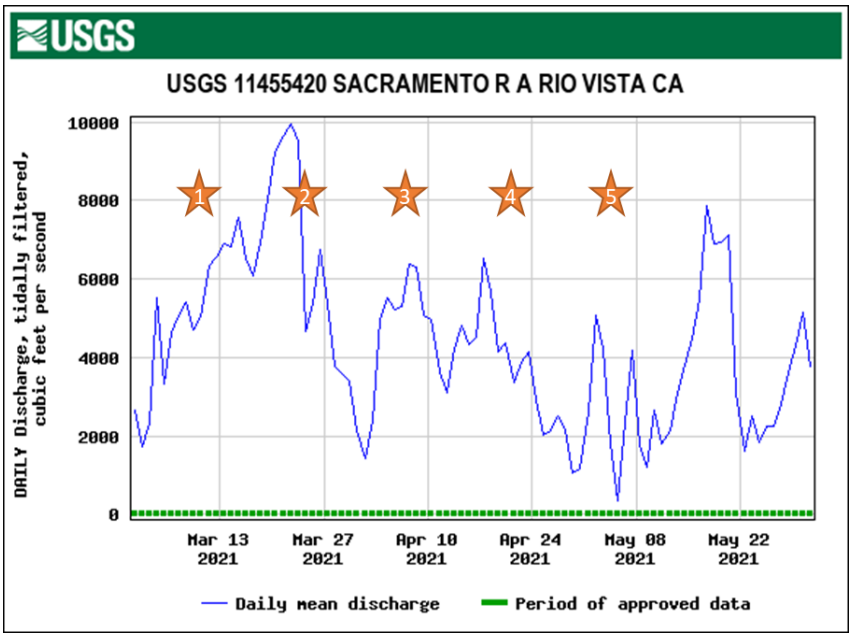

Figure 6-6. Graph of mean daily discharge for USGS site 11455420 Sacramento River at Rio Vista, CA.

Graph depicts flows influencing water quality at Site 4: Sacramento River at Decker Island, during the 2021 spring outflow. Orange stars indicate Delta Smelt toxicity exposures.

Analytical Chemistry

Water samples used in toxicity tests were analyzed for dissolved metals and organic chemicals. There were 145 detections of metals and 49 detections of organics across the study period. Of the metals, manganese was detected in 100% of the samples collected and made up 21% of all metal detections. Aluminum was detected in 93% of samples, copper was detected in 87% of samples, and chromium was detected in 80% of samples collected. Aluminum consistently had the highest concentrations of the detected metals, for example, 1,700 µg/L (Exposure 5 in GB), 1,100 µg/L, and 1,000 µg/L (SRD and TD, respectively, both during Exposure 3; see tables below).

For the organics, fungicides were the most frequently detected compound, being 61% of organic detections, followed by herbicides (29%), and insecticides (10%). Of those, the fungicide metconazole had the highest frequency of detections (77%) and made up 47% of all organic detections. The herbicide fluridone was the second most frequently detected compound (23%) and made up 14% of all detections (see tables below).

Water collected from the TD during Exposure 3 (initiated April 9, 2021), had the highest number of organic detections (n=10) with concentrations ranging from 0.08 µg/L of pyrimethanil at the lowest, to a max of 0.548 µg/L of 2-phenylphenol. Fluridone had the highest concentrations during the study, detected in the TD (Exposure 3) at 3.3 µg/L and in CS (Exposure 1) at 1.1 µg/L.

Table 6-2. Summary of trace metals analysis for Site 1: Toe Drain, for the duration of the study period.

Analyte	Reporting Limit (µg/L)	Exposure 1 3/12/21	Exposure 2 3/26/21	Exposure 3 4/9/21	Exposure 4 4/26/21	Exposure 5 5/7/21
Aluminum	20	**180**	**320**	**1000**	**150**	**650**
Arsenic	2.0	**6.3**	**3.5**	ND	ND	4.5
Cadmium	0.5	ND	ND	ND	ND	ND
Chromium	1.0	**1.6**	**1.4**	**4.3**	**1.2**	**3.0**
Copper	2.0	**3.9**	**2.5**	**3.5**	**2.2**	**3.1**
Lead	5.0	ND	ND	ND	ND	ND
Manganese	2.0	**21**	**38**	**50**	**8.8**	**30**
Mercury	0.2	ND	ND	ND	ND	ND
Nickel	2.0	**6.0**	**5.1**	**6.6**	**2.7**	**5.6**
Silver	0.5	ND	ND	ND	ND	ND
Zinc	10	ND	ND	ND	ND	ND

Detections are **bolded**.

Table 6-3. Summary of organic analyses detections for Site 1: Toe Drain, for the duration of the study period.

Analyte	Reporting Limit (µg/L)	Exposure 1 3/12/21	Exposure 2 3/26/21	Exposure 3 4/9/21	Exposure 4 4/26/21	Exposure 5 5/7/21
Fludioxonil	0.040	**0.042**	ND	ND	ND	ND
Fluridone	0.040	ND	**3.301**	**0.461**	ND	**0.561**
Metconazole	0.040	ND	**0.603**	**0.152**	**0.066**	**0.125**
Pyrimethanil	0.040	ND	ND	**0.080**	ND	ND
Cyprodinil	0.040	ND	ND	**0.086**	ND	ND
Paclobutrazol	0.040	ND	ND	**0.102**	ND	ND
Flutriafol	0.040	ND	ND	**0.049**	ND	ND
Deltamethrin	0.040	ND	ND	**0.114**	ND	ND
DEET	0.040	ND	ND	**0.242**	ND	ND
Metolachlor	0.040	ND	ND	**0.428**	ND	**0.546**
2-Phenylphenol	0.040	ND	ND	**0.548**	ND	ND

Only detected analytes are presented. Detections are **bolded**.

Table 6-4. Summary of trace metals analysis for Site 2: Cache Slough, for the duration of the study period.

Analyte	Reporting Limit (µg/L)	Exposure 1 3/12/21	Exposure 2 3/26/21	Exposure 3 4/9/21	Exposure 4 4/26/21	Exposure 5 5/7/21
Aluminum	20	**80**	**65**	**64**	**30**	**130**
Arsenic	2.0	**3.1**	ND	ND	ND	**2.7**
Cadmium	0.5	ND	ND	ND	ND	ND
Chromium	1.0	**1.5**	ND	ND	**1.1**	**1.4**
Copper	2.0	ND	ND	**2.2**	**2.0**	**2.2**
Lead	5.0	ND	ND	ND	ND	ND
Manganese	2.0	**6.3**	**5.5**	**7.7**	**12**	**16**
Mercury	0.2	**0.2**	ND	ND	ND	ND
Nickel	2.0	ND	ND	ND	ND	ND
Silver	0.5	ND	ND	ND	ND	ND
Zinc	10	ND	ND	ND	ND	ND

Detections are **bolded**.

281 Table 6-5. Summary of organic analyses detections for Site 2: Cache Slough, for the
282 duration of the study period.

Analyte	Reporting Limit (µg/L)	Exposure 1 3/12/21	Exposure 2 3/26/21	Exposure 3 4/9/21	Exposure 4 4/26/21	Exposure 5 5/7/21
Fluridone	0.040	**1.099**	ND	**0.335**	**0.322**	**0.335**
Metconazole	0.040	ND	**0.569**	**0.282**	**0.072**	**0.132**
DEET	0.040	ND	ND	**0.598**	ND	ND
Metolachlor	0.040	ND	ND	**0.296**	ND	ND

283 Only detected analytes are presented. Detections are **bolded**.

284 Table 6-6. Summary of trace metals analysis for Site 3: Deep Water Ship Channel, for the
285 duration of the study period.

Analyte	Reporting Limit (µg/L)	Exposure 1 3/12/21	Exposure 2 3/26/21	Exposure 3 4/9/21	Exposure 4 4/26/21	Exposure 5 5/7/21
Aluminum	20	**130**	**110**	**150**	**57**	**400**
Arsenic	2.0	**3.4**	ND	ND	ND	ND
Cadmium	0.5	ND	ND	ND	ND	ND
Chromium	1.0	**1.6**	ND	**1.5**	ND	**2.4**
Copper	2.0	**2.1**	ND	**2.3**	**2.0**	**2.3**
Lead	5.0	ND	ND	ND	ND	ND
Manganese	2.0	**4.6**	**7.7**	**6.6**	**5.4**	**14**
Mercury	0.2	ND	ND	ND	ND	ND
Nickel	2.0	ND	ND	ND	ND	**2.3**
Silver	0.5	ND	ND	ND	ND	ND
Zinc	10	ND	ND	ND	ND	ND

286 Detections are **bolded**.

287 Table 6-7. Summary of organics analysis detections for Site 3: Deep Water Ship Channel,
288 for the duration of the study period.

Analyte	Reporting Limit (µg/L)	Exposure 1 3/12/21	Exposure 2 3/26/21	Exposure 3 4/9/21	Exposure 4 4/26/21	Exposure 5 5/7/21
Metconazole	0.040	ND	**0.647**	**0.222**	**0.065**	**0.175**
DEET	0.040	ND	ND	**0.519**	ND	ND
Metolachlor	0.040	ND	ND	**0.381**	ND	ND

289 Only detected analytes are presented. Detections are **bolded**.

290 Table 6-8. Summary of trace metals analysis for Site 4: Sacramento River at Decker
291 Island, for the duration of the study period.

Analyte	Reporting Limit (µg/L)	Exposure 1 3/12/21	Exposure 2 3/26/21	Exposure 3 4/9/21	Exposure 4 4/26/21	Exposure 5 5/7/21
Aluminum	20	**440**	**78**	**1100**	**480**	**840**
Arsenic	2.0	**3.9**	ND	ND	ND	**2.6**
Cadmium	0.5	ND	ND	ND	ND	ND
Chromium	1.0	**2.4**	ND	**3.7**	**1.4**	**3.6**
Copper	2.0	**5.2**	ND	**6.4**	**3.5**	**6.1**
Lead	5.0	ND	ND	ND	ND	ND
Manganese	2.0	**9.4**	**4.4**	**26**	**12**	**23**
Mercury	0.2	ND	ND	ND	ND	ND
Nickel	2.0	**2.6**	ND	**3.8**	**2.7**	**4.0**
Silver	0.5	ND	ND	ND	ND	ND
Zinc	10	ND	ND	ND	ND	ND

292 Detections are **bolded**.

293 Table 6-9. Summary of organic analysis detections for Site 4: Sacramento River at Decker
294 Island, for the duration of the study period.

Analyte	Reporting Limit (µg/L)	Exposure 1 3/12/21	Exposure 2 3/26/21	Exposure 3 4/9/21	Exposure 4 4/26/21	Exposure 5 5/7/21
Metconazole	0.040	ND	**0.369**	**0.209**	**0.067**	**0.141**
DEET	0.040	ND	ND	**0.491**	ND	ND
Metolachlor	0.040	ND	ND	**0.342**	ND	ND

295 Only detected analytes are presented. Detections are **bolded**.

296 Table 6-10. Summary of trace metals analysis for Site 5: Montezuma Slough, for the
297 duration of the study period.

Analyte	Reporting Limit (µg/L)	Exposure 1 3/12/21	Exposure 2 3/26/21	Exposure 3 4/9/21	Exposure 4 4/26/21	Exposure 5 5/7/21
Aluminum	20	**480**	**250**	**450**	ND	**790**
Arsenic	2.0	**5.3**	**3.0**	ND	ND	**5.0**
Cadmium	0.5	ND	ND	ND	ND	ND
Chromium	1.0	**2.3**	ND	**2.8**	**2.6**	**3.6**
Copper	2.0	**12**	**8.3**	**14**	**5.7**	**17**
Lead	5.0	ND	ND	ND	ND	ND
Manganese	2.0	**9.9**	**7.8**	**10**	**11**	**22**
Mercury	0.2	ND	ND	ND	ND	ND

Analyte	Reporting Limit (µg/L)	Exposure 1 3/12/21	Exposure 2 3/26/21	Exposure 3 4/9/21	Exposure 4 4/26/21	Exposure 5 5/7/21
Nickel	2.0	**3.7**	**2.7**	**4.1**	**3.7**	**7.0**
Silver	0.5	ND	ND	ND	ND	ND
Zinc	10	ND	ND	ND	ND	ND

Detections are **bolded**.

Table 6-11. Summary of organic analysis detections for Site 5: Montezuma Slough, for the duration of the study period.

Analyte	Reporting Limit (µg/L)	Exposure 1 3/12/21	Exposure 2 3/26/21	Exposure 3 4/9/21	Exposure 4 4/26/21	Exposure 5 5/7/21
Metconazole	0.040	ND	**0.562**	**0.158**	**0.057**	**0.129**
DEET	0.040	ND	ND	ND	ND	ND
Metolachlor	0.040	ND	ND	ND	ND	ND
Desmetryn	0.040	ND	ND	ND	ND	**0.722**

Only detected analytes are presented. Detections are **bolded**.

Table 6-12. Summary of trace metals analysis for Site 6: Grizzly Bay, for the duration of the study period.

Analyte	Reporting Limit (µg/L)	Exposure 1 3/12/21	Exposure 2 3/26/21	Exposure 3 4/9/21	Exposure 4 4/26/21	Exposure 5 5/7/21
Aluminum	20	**870**	**310**	**480**	ND	**1700**
Arsenic	2.0	**8.9**	**7.3**	**4.8**	ND	**9.7**
Cadmium	0.5	ND	ND	ND	ND	ND
Chromium	1.0	**3.7**	**1.5**	**3.5**	**4.4**	**6.3**
Copper	2.0	**40**	**42**	**39**	**11**	**54**
Lead	5.0	ND	ND	ND	ND	ND
Manganese	2.0	**21**	**9.9**	**10**	**19**	**54**
Mercury	0.2	ND	ND	ND	ND	ND
Nickel	2.0	**8.8**	**6.0**	**8.3**	**7.1**	**17**
Silver	0.5	ND	ND	ND	ND	ND
Zinc	10	**2.8**	ND	ND	ND	ND

Detections are **bolded**.

Table 6-13. Summary of organics analysis detections for Site 6: Grizzly Bay, for the duration of the study period.

Analyte	Reporting Limit (µg/L)	Exposure 1 3/12/21	Exposure 2 3/26/21	Exposure 3 4/9/21	Exposure 4 4/26/21	Exposure 5 5/7/21
Metconazole	0.040	ND	**0.387**	**0.102**	ND	**0.114**
Cyprodinil	0.040	ND	ND	ND	ND	**0.052**
Desmetryn	0.040	ND	ND	ND	ND	**0.874**

Only detected analytes are presented. Detections are **bolded**.

Table 6-14. Summary of trace metals analysis for the Control, for the duration of the study period.

Analyte	Reporting Limit (µg/L)	Exposure 1 3/12/21	Exposure 2 3/26/21	Exposure 3 4/9/21	Exposure 4 4/26/21	Exposure 5 5/7/21
Aluminum	20	**210**	**180**	**310**	**500**	**430**
Arsenic	2.0	**3.0**	**2.1**	ND	ND	ND
Cadmium	0.5	ND	ND	ND	ND	ND
Chromium	1.0	**1.9**	ND	**2.5**	**2.4**	**3.3**
Copper	2.0	**4.2**	**4.7**	**5.5**	**5.8**	**4.4**
Lead	5.0	ND	ND	ND	ND	ND
Manganese	2.0	**27**	**27**	**51**	**30**	**25**
Mercury	0.2	ND	ND	ND	ND	ND
Nickel	2.0	**2.6**	**3.0**	**2.7**	**3.1**	**2.4**
Silver	0.5	ND	ND	ND	ND	ND
Zinc	10	ND	ND	ND	ND	ND

Detections are **bolded**.

Table 6-15. Summary of organics analysis detections for the Control for the duration of the study period.

Analyte	Reporting Limit (µg/L)	Exposure 1 3/12/21	Exposure 2 3/26/21	Exposure 3 4/9/21	Exposure 4 4/26/21	Exposure 5 5/7/21
Atrazine	0.040	ND	**0.226**	ND	ND	ND
Flutriafol	0.040	ND	**0.103**	ND	ND	ND
Fludioxonil	0.040	ND	**0.050**	ND	ND	ND
Flusilazole	0.040	ND	**0.076**	ND	ND	ND
Hexazinone	0.040	ND	**0.071**	ND	ND	ND
Metconazole	0.040	ND	**0.401**	**0.179**	**0.074**	**0.111**
Metolachlor	0.040	ND	ND	**0.697**	**0.202**	ND

Only detected analytes are presented. Detections are **bolded**.

Survival

Delta Smelt in the standard control had poor survival in Exposures 1, 2, and 3; however, smelt survival improved in Exposures 4 and 5. This made statistical comparisons difficult, in that most comparisons between fish in ambient waters and the standard control were not significant, or fish exposed to ambient water collections did significantly better than those in the standard control. Salinity had a significant effect on survival (Welch's t-test t: 9.299, df: 136.8, P<0.0001). Smelt exposed to the HSC (salinity adjusted to match that of GB), consistently exhibited robust survival in all exposures. Likewise, Delta Smelt exposed to waters collected from GB and MS, the two site locations with the highest salinities, also exhibited high survival in all exposures.

One cohort of fish was used for the entire project, with fish starting at 55 days post hatch (dph) for Exposure 1 and increasing in age with each subsequent exposure test. Fish in the beginning of the project were small enough to escape from the replicate containers during the water acclimation and renewal processes, which resulted in fewer fish available to run sub-lethal analyses and to determine survival calculations. Because of this, fish that were deemed 'lost' were removed from the analyses and not included in survival totals. This became less of an issue as the project progressed, for as fish grew in size, fewer fish were missing from the replicate buckets, generally being too large to escape. Summary tables with four and seven-day Delta Smelt survival are outlined in Tables 6-16 through 6-20. Seven-day smelt survival for the toxicity exposures are outlined in Figures 6-7 through 6-11. Tables outlining the toxicity test water quality parameters are summarized in Supplemental Information.

Table 6-16. Summary of results of a chronic 7-day toxicity test initiated on March 12, 2021, examining the toxicity of Delta surface water to Delta Smelt (*Hypomesus transpacificus*).

Treatment	4-day Survival (%) Mean	4-day Survival (%) Standard Deviation	4-day Survival (%) Standard Error	7-day Survival (%) Mean	7-day Survival (%) Standard Deviation	7-day Survival (%) Standard Error
Control	86.6	14.15	7.08	50.6	37.40	18.70
High Salinity Control	94.1	8.32	4.16	91.2	10.19	5.09
Site 1 - Toe Drain	91.8	8.47	4.24	83.3	10.06	5.03
Site 2 - Cache Slough	97.5	5.00	2.50	56.8	32.26	16.13
Site 3 - Deep Water Ship Channel	93.6	5.20	2.60	64.1	19.43	9.71
Site 4 - Sac River at Decker Island	89.9	7.40	3.70	84.6	17.86	8.93
Site 5 - Montezuma Slough	100.0	0.00	0.00	93.9	4.85	2.43
Site 6 - Grizzly Bay	96.4	7.14	3.57	91.0	7.24	3.62

Smelt were 55 dph at test initiation for Exposure 1.

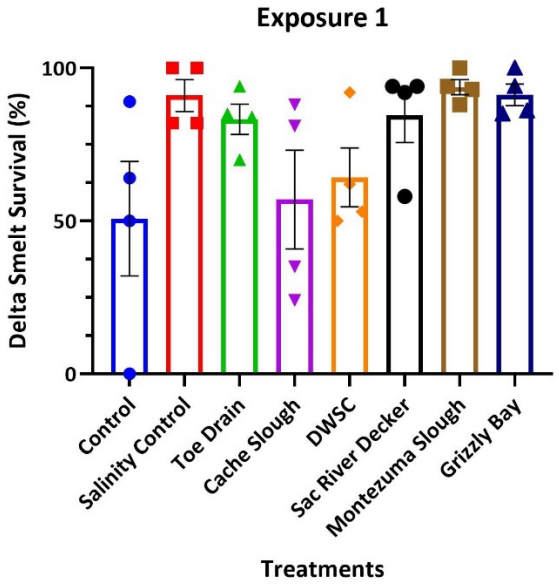

Figure 6-7. Summary of 7-day survival of Delta Smelt exposed to ambient surface waters collected from the Delta on March 8 and 9, 2021.

Individual data points represent survival of smelt in each of four test replicates. Error bars are standard error.

Table 6-17. Summary of results of a chronic 7-day toxicity test initiated on March 26, 2021, examining the toxicity of Delta surface water to Delta Smelt (*Hypomesus transpacificus*).

Treatment	4-day Survival (%) Mean	4-day Survival (%) Standard Deviation	4-day Survival (%) Standard Error	7-day Survival (%) Mean	7-day Survival (%) Standard Deviation	7-day Survival (%) Standard Error
Control	78.9	13.23	6.62	51.5	26.66	13.33
High Salinity Control	96.9	3.66	1.83	94.6	3.91	1.95
Site 1 - Toe Drain	78.6	12.70	6.35	65.8	16.81	8.41
Site 2 - Cache Slough	78.9	15.45	7.72	60.4	27.49	13.74
Site 3 - Deep Water Ship Channel	87.3	9.78	4.89	62.1	8.53	4.26
Site 4 - Sac River at Decker Island	84.5	10.46	5.23	72.7	22.70	11.35
Site 5 - Montezuma Slough	90.4	10.75	5.37	76.9	15.11	7.55
Site 6 - Grizzly Bay	95.3	9.38	4.69	95.3	9.38	4.69

Smelt were 69 dph at test initiation for Exposure 2.

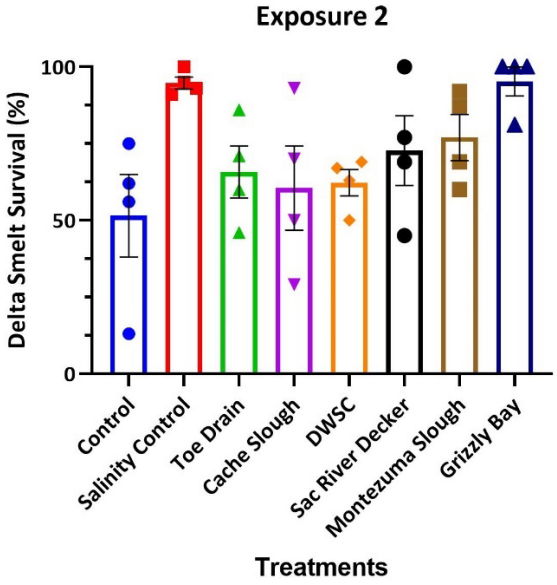

Figure 6-8. Summary of 7-day survival of Delta Smelt exposed to ambient surface waters collected from the Delta on March 22 and 23, 2021.

Individual data points represent survival of smelt in each of four test replicates. Error bars are standard error.

Table 6-18. Summary of results of a chronic 7-day toxicity test initiated on April 9, 2021, examining the toxicity of Delta surface water to Delta Smelt (*Hypomesus transpacificus*).

Treatment	4-day Survival (%) Mean	4-day Survival (%) Standard Deviation	4-day Survival (%) Standard Error	7-day Survival (%) Mean	7-day Survival (%) Standard Deviation	7-day Survival (%) Standard Error
Control	49.4	28.86	14.43	22.9	24.46	12.23
High Salinity Control	98.8	2.50	1.25	98.8	2.38	1.19
Site 1 - Toe Drain	76.2	10.57	5.28	60.8	13.13	6.56
Site 2 - Cache Slough	81.7	11.06	5.53	65.4	22.33	11.17
Site 3 - Deep Water Ship Channel	78.8	20.20	10.10	58.9	23.44	11.72
Site 4 - Sac River at Decker Island	83.8	10.95	5.48	59.8	17.07	8.53
Site 5 - Montezuma Slough	97.2	5.56	2.78	90.4	9.57	4.79
Site 6 - Grizzly Bay	100.0	0.00	0.00	84.3	4.98	2.49

Smelt were 83 dph at test initiation for Exposure 3.

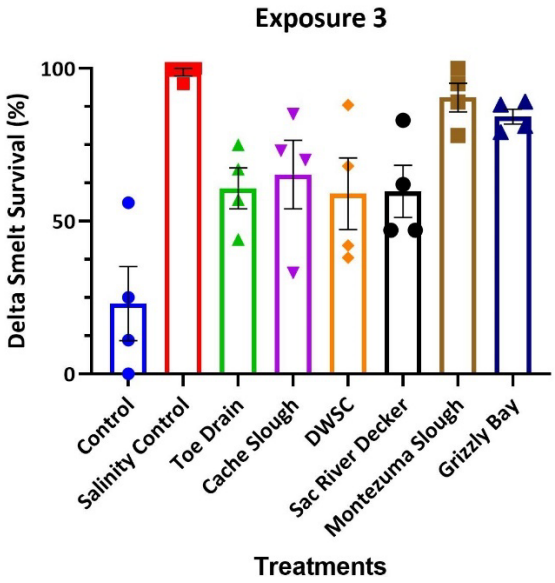

Figure 6-9. Summary of 7-day survival of Delta Smelt exposed to ambient surface waters collected from the Delta on April 5 and 6, 2021.

Individual data points represent survival of smelt in each of four test replicates. Error bars are standard error.

Table 6-19. Summary of results of a chronic 7-day toxicity test initiated on April 23, 2021, examining the toxicity of Delta surface water to Delta Smelt.

Treatment	4-day Survival (%) Mean	4-day Survival (%) Standard Deviation	4-day Survival (%) Standard Error	7-day Survival (%) Mean	7-day Survival (%) Standard Deviation	7-day Survival (%) Standard Error
Control	88.6	9.35	4.67	82.2	6.15	3.08
High Salinity Control	100.0	0.00	0.00	98.8	2.50	1.25
Site 1 - Toe Drain	93.6	4.93	2.46	88.4	4.96	2.48
Site 2 - Cache Slough	86.8	16.30	8.15	73.0	24.94	12.47
Site 3 - Deep Water Ship Channel	88.7	7.43	3.71	76.2	19.23	9.61
Site 4 - Sac River at Decker Island	93.5	6.44	3.22	88.4	4.41	2.20
Site 5 - Montezuma Slough	89.5	8.61	4.30	89.5	8.61	4.30
Site 6 - Grizzly Bay	92.8	4.90	2.45	92.8	4.90	2.45

Smelt were 97 dph at test initiation for Exposure 4.

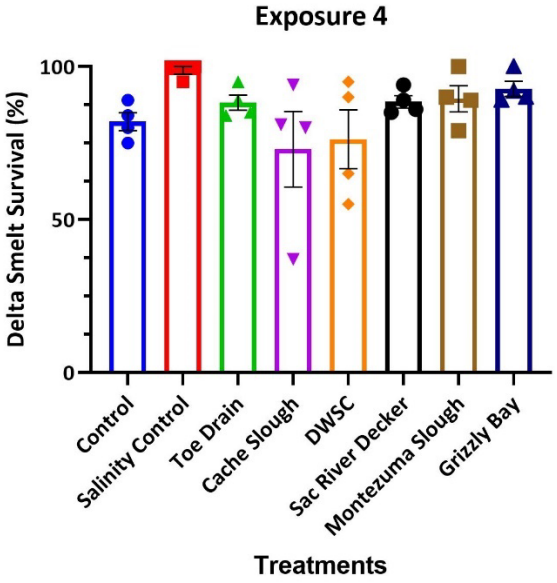

Figure 6-10. Summary of 7-day survival of Delta Smelt exposed to ambient surface waters collected from the Delta on April 20 and 22, 2021.

Individual data points represent survival of smelt in each of four test replicates. Error bars are standard error.

Table 6-20. Summary of results of a chronic 7-day toxicity test initiated on May 7, 2021, examining the toxicity of Delta surface water to Delta Smelt (*Hypomesus transpacificus*).

Treatment	4-day Survival (%) Mean	4-day Survival (%) Standard Deviation	4-day Survival (%) Standard Error	7-day Survival (%) Mean	7-day Survival (%) Standard Deviation	7-day Survival (%) Standard Error
Control	93.5	4.89	2.44	77.6	19.05	9.53
High Salinity Control	95.0	4.08	2.04	93.0	5.73	2.87
Site 1 - Toe Drain	91.3	7.50	3.75	84.4	7.01	3.51
Site 2 - Cache Slough	87.0	13.28	6.64	72.5	12.68	6.34
Site 3 - Deep Water Ship Channel	95.9	5.10	2.55	77.4	12.07	6.03
Site 4 - Sac River at Decker Island	86.1	15.50	7.75	72.1	27.19	13.59
Site 5 - Montezuma Slough	95.0	4.08	2.04	91.4	2.43	1.22
Site 6 - Grizzly Bay	97.9	4.17	2.08	96.5	4.17	2.08

Smelt were 111 dph at test initiation for Exposure 5.

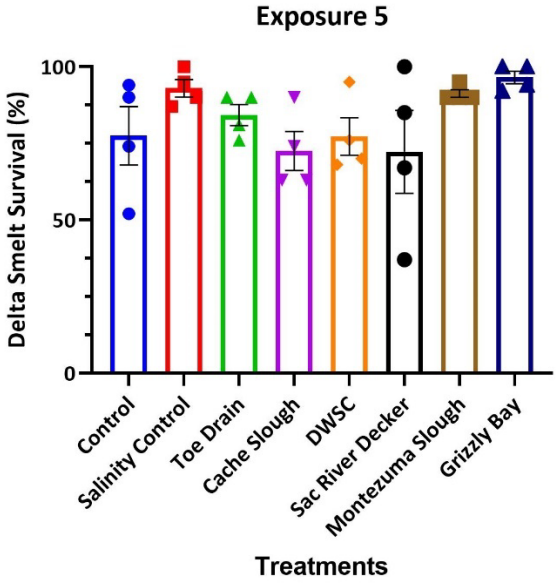

Figure 6-11. Summary of 7-day survival of Delta Smelt exposed to ambient surface waters collected from the Delta on May 4 and 6, 2021.

Individual data points represent survival of smelt in each of four test replicates. Error bars are standard error.

Condition Factor

We observed significant differences in condition factor (CF) in most of the toxicity exposures and among sites (Table 6-21). Smelt in the HSC had significantly higher CF when compared to those exposed to the TD (P=0.0178) and CS (P=0.0158) in Exposure 1 (Figure 6-12), the DWSC in

Exposure 2 (P=0.0464; Figure 6-13) and in Exposure 4 (P=0.0285; Figure 6-15), as well as SRD (P<0.0001) and GB (P=0.0005). Fish in the Control had significantly higher CF than those exposed to SRD (P=0.0030) and GB (P=0.0022) in Exposure 4. In Exposure 5 (Figure 6-16), fish exposed to MS had significantly higher CF than those in the Control (P=0.0366) and the DWSC (P=0.0182).

Salinity had a significant effect on CF in that fish exposed to brackish water sites (MS, GB, HSC) were significantly plumper than those fish exposed to freshwater sites (Welch's t-test t: 4.335, df: 810.8, P<0.0001). Considering the high survival of smelt observed in the HSC throughout the project, it is not surprising that those fish also exhibited significantly higher CF than fish exposed to ambient waters. Additionally, we observed a positive correlation between CF and time, indicating that fish plumpness increased with age (Figure 6-17).

Table 6-21. Summary of significant differences in Condition Factor over the course of the project.

Exposure	One-way ANOVA	P-value	Tukey's Significant Comparisons	> or <	Region	P-value
1	$F_{7, 170} = 3.697$	0.0010	Salinity Control	>	Toe Drain	0.0178
				>	Cache Slough	0.0158
2	$F_{7, 173} = 2.677$	0.0118	Salinity Control	>	DWSC	0.0464
3	$F_{7, 173} = 0.8935$	0.5129	None			
4	$F_{7,184} = 6.004$	<0.0001	Control	>	Sac River Decker	0.0003
				>	Grizzly Bay	0.0022
			Salinity Control	>	DWSC	0.0285
				>	Sac River Decker	<0.0001
				>	Grizzly Bay	0.0005
5	$F_{7,185} = 2.654$	0.0122	Montezuma Sl.	>	Control	0.0366
				>	DWSC	0.0182

Data were analyzed with a one-way ANOVA followed by a post hoc Tukey's multiple comparison test.

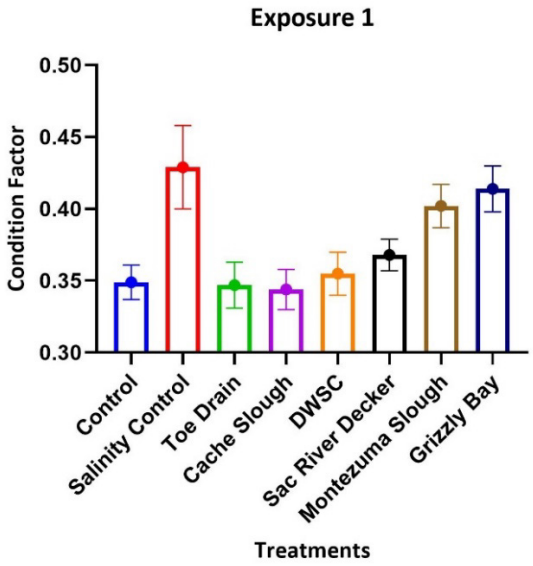

Figure 6-12. Summary of Condition Factor of Delta Smelt in Exposure 1, initiated March 12, 2021.

Error bars indicate standard error.

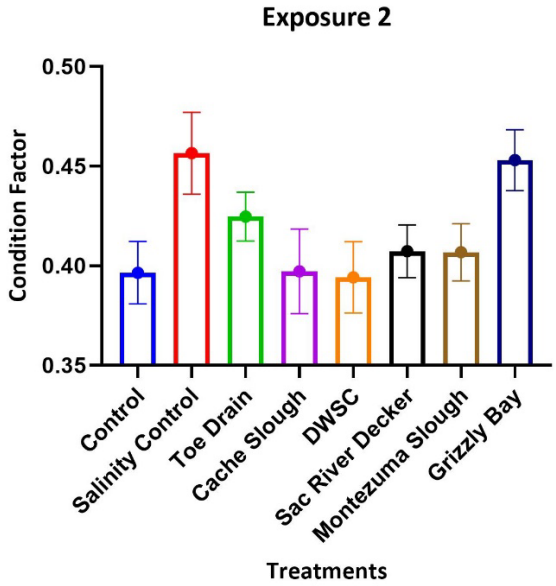

Figure 6-13. Summary of Condition Factor of Delta Smelt in Exposure 2, initiated March 26, 2021.

Error bars indicate standard error.

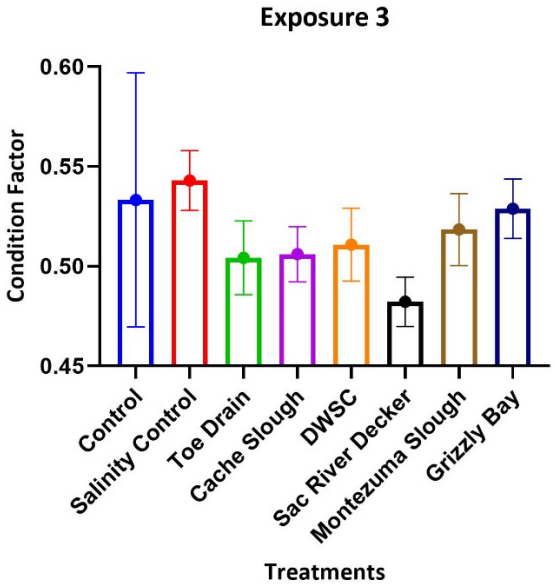

Figure 6-14. Summary of Condition Factor of Delta Smelt in Exposure 3, initiated April 9, 2021.

Error bars indicate standard error.

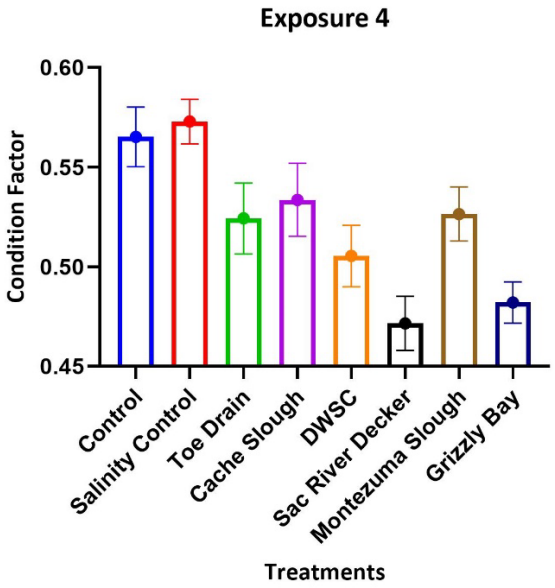

Figure 6-15. Summary of Condition Factor of Delta Smelt in Exposure 4, initiated April 23, 2021.

Error bars indicate standard error.

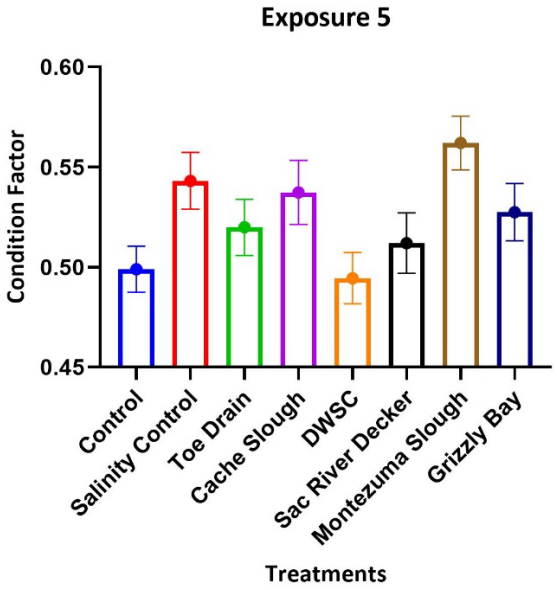

405

406 Figure 6-16. Summary of Condition Factor of Delta Smelt in Exposure 5, initiated May 7,
407 2021.

408 Error bars indicate standard error.

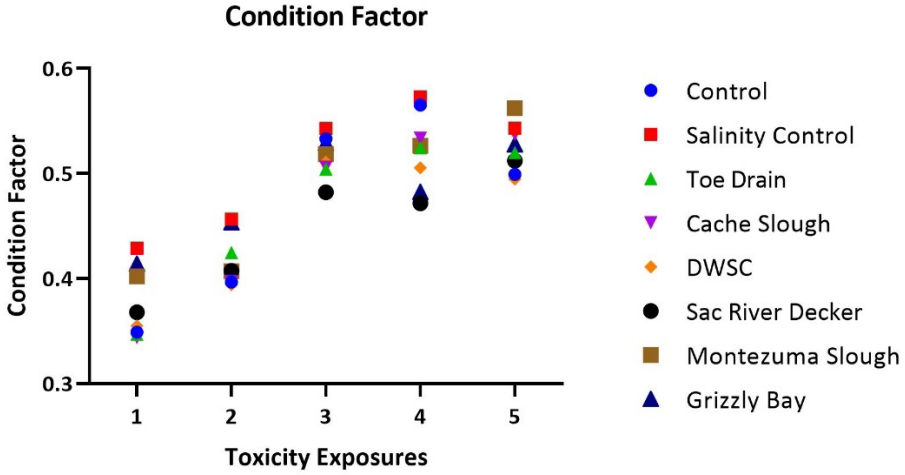

409

410 Figure 6-17. Summary of Condition Factor of Delta Smelt across the project period.

411 **RNA/DNA**

412 There was a significant effect of fork length and salinity, with RNA/DNA increasing substantially
413 with fork length (Figure 6-18; ANCOVA, $F_{1, 392} = 88.8$, $P < 0.0001$), and in brackish water (Figure 6-
414 19; ANCOVA, $F_{1, 392} = 6.4$, $P = 0.0121$). Site was not significant (ANCOVA, $F_{7, 392} = 1.0098$, $P =$
415 0.4237), nor was days post hatch (ANCOVA, $F_{1, 392} = 0.08$, $P = 0.7758$) or water temperature
416 (ANCOVA, $F_{1, 392} = 0.4641$, $P = 0.4961$). We note that water temperature varied minimally during

the experiment, so it is unsurprising that it did not affect RNA/DNA. RNA/DNA was elevated in the brackish treatments (i.e., GB, MS, HSC, and SRD to a lesser extent; Table 6-22), but this was likely a product of elevated salinity because the effect was lost when the salinity dummy variable was included in the model (Figure 6-20).

Table 6-22. RNA/DNA and mean salinity by treatment.

Site Number	Site Name	RNA/DNA	Mean Salinity (ppt)
C	Low Salinity Control	0.922	0.275
1	Toe Drain	0.977	0.238
2	Cache Slough	1.035	0.099
3	DWSC	0.868	0.098
4	Sac River @ Decker	0.986	0.586
5	Montezuma Slough	1.039	2.208
6	Grizzly Bay	1.172	7.060
HSC	High Salinity Control	1.118	6.855

Note that RNA/DNA increases with increased salinity.

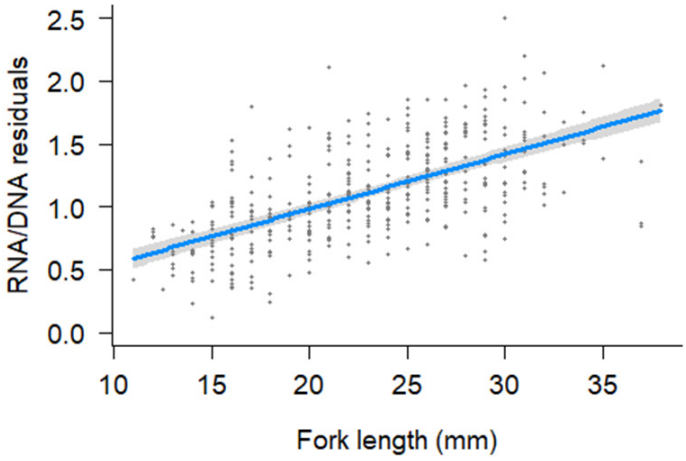

Figure 6-18. Partial residuals of the RNA/DNA model as a function of fork length.

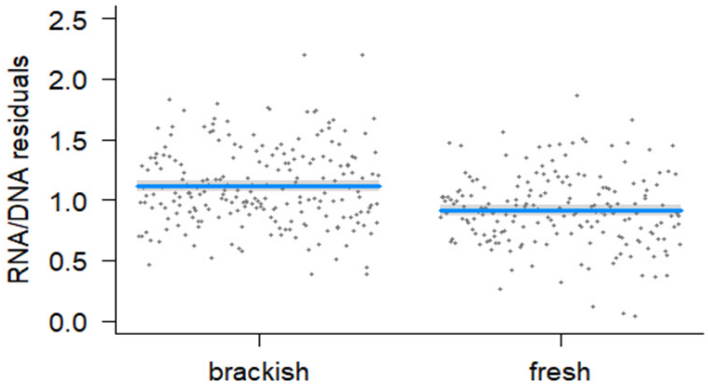

Figure 6-19. Partial residuals for the RNA/DNA model as a function of salinity (fresh or brackish).

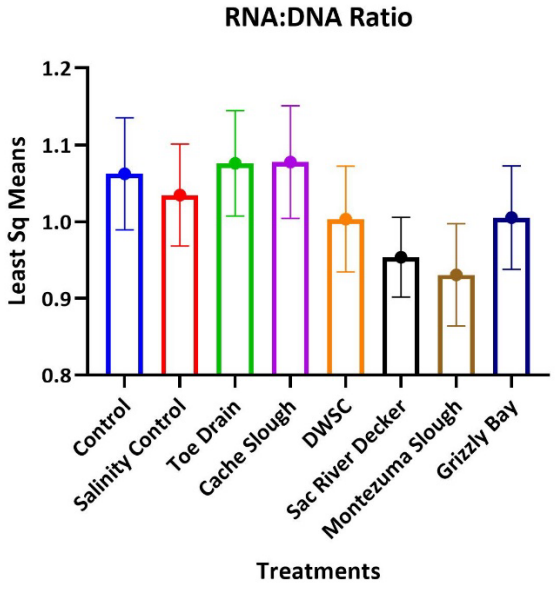

Figure 6-20. Least Squares Means from the ANCOVA fit to the RNA/DNA results.

The figure shows that most of the variation detected in RNA/DNA among stations (Table 6-17) is explained by differences in salinity and fish size.

Histopathology

Histopathology analyses indicate that fish were in good condition for the majority of the project, with very few significant lesions observed in liver or gills (Supplemental Information). There were no significant differences observed in liver lesions (Kruskal-Wallis X^2: 5.8223, df: 7, P=0.5606), with most livers having an absence of lesions entirely. In the gills, fish exposed to water collected from CS during Exposure 5 exhibited significantly higher severe gill lesions than all other sites (Kruskal-Wallis X^2: 61.753, df: 7, P<0.0001). Three out of 12 fish had moderate epithelial cell necrosis (25%) and four out of 12 fish (33%) had severe epithelial cell hyperplasia in the gills (Table 6-23; Figures 6-21 through 6-23).

Table 6-23. Statistical comparisons made for significant gill lesions observed in Delta Smelt exposed to water collected from CS in Exposure 5, initiated May 7, 2021. Site Name: Cache Slough

Wilcoxon rank sum Comparison	P-value
Control	0.0022
Salinity Control	0.0011
Toe Drain	0.0047
Deep Water Ship Channel	0.0011
Sacramento River Decker Island	0.0010
Montezuma Slough	0.0012
Grizzly Bay	0.0011

Figure 6-21. Severe fusion of primary (Box A) and secondary (Box B) lamella in larval Delta Smelt exposed to water collected from Cache Slough in Exposure 5, initiated May 7, 2021, at 40x magnification.

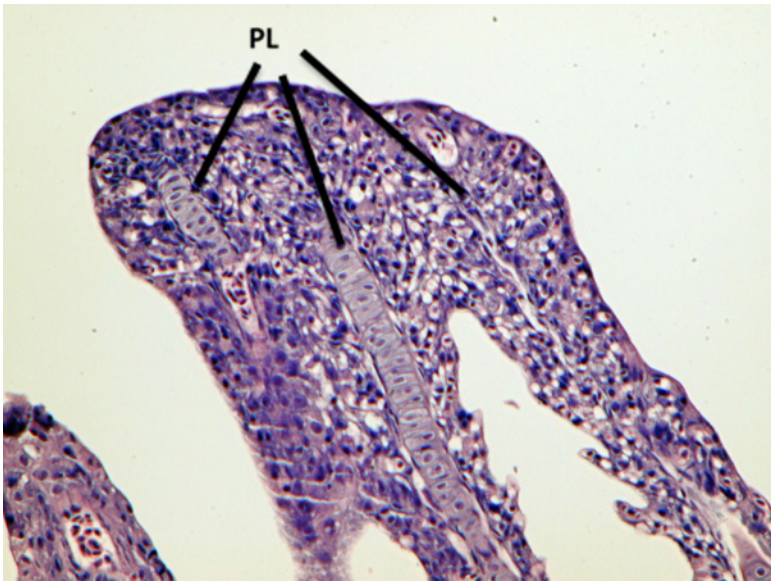

Figure 6-22. Higher magnification (200x) of Box A, showing severe epithelial cell hyperplasia, resulting in fusion of the three primary lamellae (PL).

Figure 6-23. Higher magnification (200x) of Box B, showing severe epithelial cell hyperplasia, resulting in extensive fusion of secondary lamellae (SL).

The obliteration of secondary lamella results in loss of surface area and therefore gas exchange. CS: cell swelling. CN: cell necrosis.

Glycogen

We saw significant differences in glycogen depletion in Delta Smelt by site (Kruskal-Wallis X^2: 57.541, df:7, P<0.0001) and by exposure (Kruskal-Wallis X^2: 52.135, df:4, P<0.0001). Overall, we observed a lower prevalence of glycogen depletion in Delta Smelt exposed to waters collected for Exposure 1 and a higher prevalence of glycogen depletion in Delta Smelt exposed to waters collected for Exposure 2. Salinity also had a significant effect on glycogen (Kruskal-Wallis X^2: 44.93,

464 df: 1, P<0.0001), where smelt in brackish water sites (i.e., MS, GB) had significantly less glycogen
465 depletion than fish exposed to freshwater sites (P<0.0001). A summary of statistical analyses is
466 outlined in Tables 6-24 and 6-25, and glycogen depletion in smelt for all exposures are outlined in
467 Figure 6-24.

468 Table 6-24. Summary of significant differences in Glycogen Depletion by Site during the
469 course of the project.

Kruskal-Wallis	Wilcoxon rank sum test comparisons	> or <	Region	P-value
X^2: 57.541, df: 7, P<0.0001	Grizzly Bay	<	Control	0.00541
		<	Cache Slough	0.00053
		<	DWSC	0.00020
	Montezuma Slough	<	Control	<0.0001
		<	Cache Slough	<0.0001
		<	DWSC	<0.0001
	Salinity Control	<	Control	<0.0001
		<	Cache Slough	<0.0001
		<	DWSC	<0.0001
	Sac River Decker	>	Grizzly Bay	0.01654
		>	Montezuma Slough	0.00036
		>	Salinity Control	0.00089
	Toe Drain	<	Control	0.03198
		<	Cache Slough	0.00448
		<	DWSC	0.00101
		>	Montezuma Slough	0.01550
		>	Salinity Control	0.04770

470

471 Table 6-25. Summary of significant differences in Glycogen Depletion by Exposure
472 during the course of the project.

Kruskal-Wallis	Wilcoxon rank sum test comparisons	> or <	Exposure	P-value
X^2: 52.135, df: 4, P<0.0001	Exposure 2	>	Exposure 1	<0.0001
	Exposure 3	>	Exposure 1	0.00043
		<	Exposure 2	0.01285
	Exposure 4	<	Exposure 2	<0.0001
		<	Exposure 3	0.01941
	Exposure 5	>	Exposure 1	0.00053
		<	Exposure 2	<0.0001

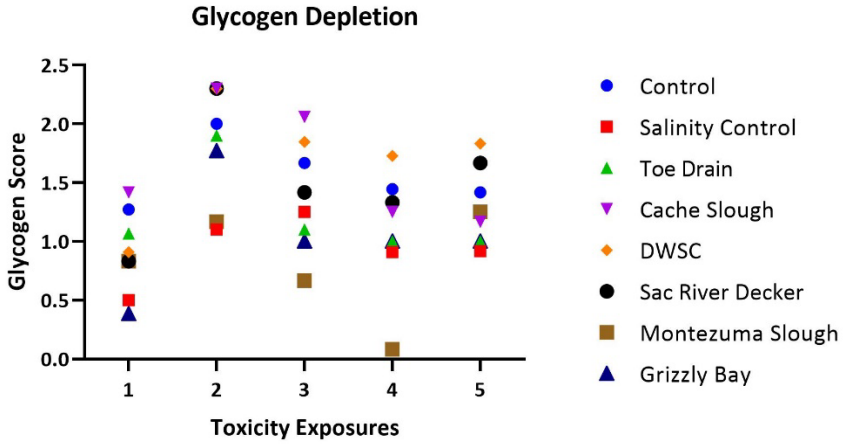

Figure 6-24. Summary of Glycogen Depletion observed in Delta Smelt across the project period.

The higher the glycogen score, the more depleted glycogen stores were in the liver.

Discussion

Results from this study indicate that surviving Delta Smelt exposed to Bay-Delta waters collected during the 2021 spring outflow were generally in good condition. There were no significant lesions observed in any of the livers of Delta Smelt used in this project, and there was one instance where significant lesions were observed in the gills. This project year was the first where we evaluated the water quality of Bay-Delta waters collected during the spring outflow with late-larval stage Delta Smelt used in the toxicity exposures. This differed from previous project years that were conducted during the summer and fall periods, which used sub-adult Delta Smelt, based on the life stage of fish anticipated to be present in the Delta during this time. To our knowledge this is the first study to utilize one cohort of fish for the entire project, all selected from the January 14, 2021 hatch date, with fish becoming progressively older as the project period progressed. Delta Smelt are widely known to be delicate and sensitive to both handling stress and environmental factors (Teh et al. 2020, Hobbs et al. 2019, Moyle et al. 2016), especially during the younger life stages (Linberg et al. 2013) and as such, this was the first instance where mortality was observed in the toxicity exposures.

The highest mortality was observed in the standard control, especially during the first three toxicity exposures where the youngest fish were used. This mortality was likely due to stress, as fish in the HSC exhibited high survival during the entire study period, with no more than 10% mortality observed. The use of salt as a stress reducer in the transport of teleost fish is common in aquaculture (Tacchi et al., 2015; Sampaio and Freire 2016); therefore, it is likely that the added salt in the HSC contributed to the high survival of the larval Smelt, as the water source and treatment was the same between both controls. Smelt survival improved in the standard control in Exposures 4 and 5, when they entered into the sub-juvenile life stage at 97 and 111 dph, respectively. We observed low survival in fish exposed to ambient waters across the study period, including fish exposed to CS (57%) and DWSC (64%) in Exposure 1, TD (66%), CS (60%), DWSC (62%), SRD (73%), and MS (77%) in Exposure 2, TD (61%), CS (65%), DWSC (59%), SRD (60%) in Exposure 3, CS (73%) and DWSC (76%) in Exposure 4, and CS (73%), DWSC (77%), and SRD (72%) in Exposure 5. Salinity

had a significant effect on survival, as larval Smelt exposed to the brackish water sites (MS, GB) typically had survival above 80%, with the exception of fish exposed to MS in Exposure 2, which had 77% survival.

In addition to survival, salinity had significant effects on CF, RNA/DNA, and glycogen. Fish exposed to brackish water sites were significantly plumper, had higher RNA/DNA ratios, and their livers were more glycogen rich than those fish exposed to freshwater sites. Taken together, fish had higher survival, were larger and had a more efficient short-term energy growth rate when exposed to brackish water sites, indicating that brackish water habitat can be beneficial to Delta Smelt in the larval rearing stages in the wild (Hobbs et al. 2019). The significant differences observed in CF among sites during this study period demonstrate that late-larval and early juvenile stages of fish have a particularly responsive growth rate at this time and further supports these biomarkers as sensitive endpoints which can be used to evaluate Delta Smelt health and condition during this integral life stage.

The surviving larval Smelt from the toxicity exposures were in good condition in that lesions were completely absent from all fish livers, and gill lesions were generally absent with the exception of fish exposed to water collected from CS during Exposure 5. The combination of high mortality and good liver/gill condition may be due to the hardiness of the fish which survived, where stronger fish survived the toxicity tests and the weaker fish did not (Teh et al. 2020). The lack of lesions in liver and gills of fish appear to follow the trend of improved condition in fish during severe drought conditions, where Teh et al. (2020) found that the lowest liver lesion scores were observed in fish collected during the peak of the drought in 2015/2016 (Teh et al. 2020). With this past water year being the second driest on record (CDWR 2021) coupled with the lack of outflow present during this study period, our data appear to support that hypothesis.

Analytical chemistry indicates a high detection frequency of fungicides used in agriculture, especially those used on stone fruit trees and post-harvest treatment, which would align with the dormant spray season and the land uses surrounding the study areas. Herbicides and insecticides were detected sporadically throughout the project period, continuing to follow the trend of chemical classes that have been observed in our previous project years. It appears that chemical mixtures had the greatest acute effects on smelt. Exposure 3 (initiated April 9, 2021) had the highest number of contaminants for the TD (10), CS (4), DWSC (3), and SRD (3), and where smelt mortality ranged from 35-41%. Interestingly, we observed severe gill lesions in Delta Smelt exposed to water collected from CS during Exposure 5 (initiated May 7, 2021), in which fluridone and metconazole were detected in concentrations below ng/L and all dissolved metals detections were in the low µg/L range. There was a slight increase in discharge measured at the USGS gauge near Hasting's Tract in Cache Slough during the week of sample collection, which may have contained contaminant(s) that were not included in the suite of organics we measured. The gills are the first route of exposure to water-borne contaminants and are quick to respond to stressors (Teh et al. 2020), therefore it is possible that the fish which survived Exposure 5 had a quick but significant negative response to a stressor(s) that cannot be explained through analytical chemistry alone. However, because Delta Smelt exposed to water from Cache Slough in this study exhibited elevated and significant gill lesions, reduced condition factor, and increased glycogen depletion, it demonstrates that this location continues to potentially pose problems for Delta Smelt residing in or slated to be supplemented within that area.

Conclusion

This study was the first of its kind to evaluate the water quality and toxicity of Bay-Delta waters during the spring outflow period to late-larval stage Delta Smelt. The use of early life stage Delta Smelt demonstrated a heightened response in some biomarkers, namely condition factor and glycogen, and indicate that larval growth and energy usage is a sensitive endpoint. Due to the delicate nature of Delta Smelt during this life stage, we observed instances of increased mortality that is usually absent in later life stage Delta Smelt during these toxicity exposures. Salinity was the greatest factor influencing health and condition of the Delta Smelt used in this study, with positive correlations in survival, condition factor, RNA/DNA, and glycogen stores, indicating that brackish water habitat can be beneficial to Delta Smelt health and survival at this sensitive life stage. The abundance of healthy fish observed in this study could be due to: 1) the short exposure period, where the fish did not have the chance to develop liver lesions due to chronic stress/contaminant exposure; 2) the potential for the weaker, more susceptible fish to die off during the initial toxicity exposure, leaving the healthier fish for sub-lethal analyses (Teh et al. 2020); and/or 3) a decreased contaminant load due to low outflow in a particularly dry water year (CDWR 2021; Teh et al. 2020; Grant et al. 2003; Sansalone and Buchberger, 1997). With Delta Smelt supplementations to occur in the North Delta Arc and lower Sacramento River, where many of these sites are located, it is important to understand what contaminants are present in these waters, and to what effect exposure to these contaminants may have on Delta Smelt. The results from this study indicate that contaminant mixtures caused acute negative effects in larval Smelt exposed to waters collected from the Toe Drain, Cache Slough, Deep Water Ship Channel, and the Sacramento River at Decker Island, where more than a quarter of fish in these waters succumbed to mortality during Exposure 3. Moreover, Delta Smelt exposed to water collected from Cache Slough exhibited severe gill lesions in Exposure 5, and reduced condition factor, RNA/DNA, and glycogen stores across the study period, indicating continued toxicity at this site. These results strengthen our understanding of the drivers impacting Delta Smelt within the Delta during the spring outflow period, especially in terms of spawning success and subsequent rearing which takes place during this important life stage.

Acknowledgements

Funding for this study was provided by the State Water Contractors, Contract No. 21-13, in conjunction with the Metropolitan Water District of Southern California and, as part of the larger Directed Outflow Project. Delta Smelt and testing facilities were provided by the UC Davis Fish Conservation and Culture Laboratory. The authors would like to thank Luke Ellison and Troy Stevenson for their assistance with the toxicity tests, and to the field staff of ICF for the water collections.

References

Bisbal, G., & Bengston, D. (1995). Development of the digestive tract in larval summer flounder. *Journal of Fish Biology*, 47(2), 277-291. doi:10.1006/jfbi.1995.0133.

Caldarone E.M., Wagner M., St. Onge-Burns J., Buckley L.J. (2001) Protocol and guide for estimating nucleic acids in larval fish using a fluorescence microplate reader. Northeast Fisheries Science Center Reference Document 01-11. Available at http://www.nefsc.noaa.gov/publications/crd/crd0111/crd0111.pdf.

587 CDWR. (2021) Water Year 2021: An Extreme Year. California Department of Water Resources,
588 Sacramento, CA. https://water.ca.gov/drought.
589 Chícharo M.A., Chícharo L., López-Jamar E., Valdes L., Ré P. (1998) Estimation of starvation and
590 diel variation of the RNA/DNA ratios of field caught *Sardina pilchardus* larvae off north of
591 Spain. *Mar. Ecol. Prog. Ser.* 164: 273–283.
592 EL-Saeid, M.H. and Alghamdi, A.G., 2020, Identification of Pesticide Residues and Prediction of
593 Their Fate in Agricultural Soil. *Water, Air, & Soil Pollution*, *231*, pp.1-10.
594 Grant S.B., Rekhi N.V., Pise N.R., Reeves R.L., Matsumoto M., Wistrom A., Moussa L., Bay S.,
595 Kayhanian M. (2003) A review of the contaminants and toxicity associated with particles in
596 stormwater runoff. Technical Report prepared for the California Department of
597 Transportation. CTSW-RT-03-059-73.15. Regents of the University of California.
598 Goede R.W. (1989) Fish health/condition assessment procedures. Logan (UT): Utah Division of
599 Wildlife Resources, Fisheries Experiment Station.
600 Hammock B.G., Hobbs J.A., Slater S.B., Acuña S., Teh S.J. (2015) Contaminant and food limitation
601 stress in an endangered estuarine fish. *Science of the total environment* 532: 316-326.
602 Hladik, M.L., and McWayne, M.M. (2012) Methods of analysis—Determination of pesticides in
603 sediment using gas chromatography/mass spectrometry: U.S. Geological Survey Techniques
604 and Methods 5–C3, 18 p., https://doi.org/10.3133/tm5C3.
605 Hladik, M.L., and Calhoun, D.L. (2012) Analysis of the herbicide diuron, three diuron degradates,
606 and six neonicotinoid insecticides in water—Method details and application to two Georgia
607 streams: U.S. Geological Survey Scientific Investigations Report 2012–5206, 10 p.,
608 https://doi.org/10.3133/sir20125206.
609 Hobbs J.A., Lewis L.S., Wilmes M., Denney C., Bush E. (2019) Complex life histories discovered in
610 a critically endangered fish. *Scientific Reports*. 9:16772. https://doi.org/10.1038/s41598-019-
611 52273-8.
612 Linberg J.C., Tigan G., Ellison L., Rettinghouse T., Nagel M.M., Fisch K.M. (2013) Aquaculture
613 Methods for a Genetically Managed Population of Endangered Delta Smelt. N. Am. J.
614 Aquaculture. 75:2, 186-196. http://dx.doi.org/10.1080/15222055.2012.751942.
615 Mclaughlin, R.L., Ferguson, M.M., & Noakes, D.L. (1995) Concentrations of nucleic acids and
616 protein as indices of nutritional status for recently emerged brook trout (*Salvelinus fontinalis*).
617 *Canadian Journal of Fisheries and Aquatic Sciences,* 52(4), 848-854. doi:10.1139/f95-084.
618 Moyle P.D., Brown L.R., Durand J.R., Hobbs, J.A. (2016) Delta Smelt: Life History and Decline of a
619 Once-Abundant Species in the San Francisco Estuary. The State of Bay-Delta Science 2016:
620 Part 1. Special Issue, San Francisco Estuary and Watershed Science. 14(2):6. doi:
621 http://dx.doi.org/10.15447/sfews.2016v14iss2art6.
622 Sampaio F.D.F. and Friere C.A. (2016) An overview of stress physiology of fish transport: changes
623 in water quality as a function of transport duration. *Fish and Fisheries*. 17: 1055-1072. DOI:
624 10.111/faf.12158.
625 Sansalone, J.J., Buchberger, S.G. (1997) Partitioning and first flush of metals in urban roadway storm
626 water. *J. Environ. Eng.* 123: 134–143.
627 Schmitt C.J., Blazer V.S., Dethloff G.M., Tillitt D.E., Gross T.S., Bryant W.L., DeWeese L.R., Smith
628 S.B., Goede R.W., Bartish T.M, Kubiak T.J. (1999) Biomonitoring of Environmental Status
629 and Trends (BEST) Program: Field Procedures for Assessing the Exposure of Fish to
630 Environmental Contaminants. United States Geological Survey. Information and
631 Technology Report USGS/BRD/ITR 1999-0007.

Schmitt C.J., Dethloff G.M., eds. (2000) Biomonitoring of Environmental Status and Trends (BEST) Program: Selected Methods for Monitoring Chemical Contaminants and Their Effects in Aquatic Ecosystems. United States Geological Survey. Information and Technology Report USGS/BRD/ITR—2000-005.

Tacchi L., Lowrey L., Musharrafieh R., Crossey K., Larrogoite E.T., Salinas I. (2014) Effects of transportation stress and addition of salt to transport water on the skin mucosal homeostatsis of rainbow trout (*Oncorhynchus mykiss*). *Aquaculture*. 435: 120-127. doi: 10.1016/j.aquaculture.2014.09.027

Teh S.J., Adams S.M, Hinton D.E. (1997) Histopathologic biomarkers in feral freshwater fish populations exposed to different types of contaminant stress. Aq. Toxiol. 37(1): 51-70. https://doi.org/10.1016/S0166-445X(96)00808-9.

Teh S.J., Schultz A.A., Ramírez Duarte W., Acuña S., Barnard D.M., Baxter R.D., Triana Garcia P.A.T., Hammock B.G. (2020) Histopathological assessment of seven year-classes of Delta Smelt. *Sci. Tot. Environ.* 726: 138333. https://doi.org/10.1016/j.scitotenv.2020.138333.

USGS. (2020) Pesticide concentrations associated with augmented flow pulses in the Yolo Bypass and Cache Slough Complex, California. Open File Report 2020-1076. U.S. Department of the Interior, U.S. Geological Survey. Prepared in cooperation with the California Department of Water Resources and the State and Federal Contractors Water Agency. https://pubs.usgs.gov/of/2020/1076/ofr20201076.pdf (accessed on 10/16/2021).

Supplemental Information

Table 6-S1. Summary of water quality measurements taken during a 7-day larval Delta Smelt toxicity exposure initiated on March 12, 2021.

Treatment	Temperature (°C) Min	Temperature (°C) Max	Temperature (°C) Ave	SC (µS/cm)	DO (mg/L) Min	DO (mg/L) Max	DO (mg/L) Ave	pH Min	pH Max	pH Ave
Control	15.2	17.6	16.1	638	9.42	11.37	10.13	7.65	8.66	8.05
High Salinity Control	15.1	16.8	15.8	12760	8.74	9.92	9.26	7.58	8.43	7.94
Site 1: Toe Drain	14.9	16.5	15.5	823	8.81	11.75	9.85	8.06	8.23	8.14
Site 2: Cache Slough	14.6	16.4	15.4	283	9.39	11.05	9.99	7.67	8.06	7.91
Site 3: Deep Water Ship Channel	14.5	16.3	15.3	258	8.92	11.80	10.25	7.84	7.99	7.93
Site 4: Sac River at Decker Is.	14.6	16.4	15.3	1316	9.78	10.95	10.16	7.49	7.98	7.75
Site 5: Montezuma Slough	14.5	16.4	15.3	3824	9.17	10.70	9.88	7.64	7.85	7.75
Site 6: Grizzly Bay	14.7	16.3	15.3	12707	9.41	9.70	9.51	7.45	7.93	7.71

Treatment	Initial Hardness (as $CaCO_3$) (mg/L)	Initial Alkalinity (as $CaCO_3$) (mg/L)	Initial Total Ammonia (mg/L)	Initial Unionized Ammonia (mg/L)	Day 4 Final Total Ammonia (mg/L)	Day 4 Final Unionized Ammonia (mg/L)	Day 7 Final Total Ammonia (mg/L)	Day 7 Final Unionized Ammonia (mg/L)	Day 7 Final Nitrate (mg/L)	Day 7 Final Nitrite (mg/L)
Control	88	86	0.02	0.003	0.47	0.005	0.93	0.019	0.84	0.174
High Salinity Control	1400	98	0.01	0.001	0.36	0.004	0.68	0.006	1.07	0.079
Site 1: Toe Drain	268	268	0.04	0.002	0.44	0.013	1.14	0.045	1.12	0.207
Site 2: Cache Slough	108	102	0.00	0.000	0.29	0.007	0.84	0.026	1.48	0.443
Site 3: Deep Water Ship Channel	88	94	0.13	0.002	0.36	0.008	0.88	0.023	1.16	0.644
Site 4: Sac River at Decker Is.	180	88	0.11	0.001	0.31	0.007	0.83	0.013	0.91	0.680
Site 5: Montezuma Slough	400	88	0.13	0.002	0.36	0.006	1.01	0.011	1.08	0.460
Site 6: Grizzly Bay	1360	98	0.15	0.002	0.41	0.007	0.88	0.005	0.97	0.358

657 Table 6-S2. Summary of water quality measurements taken during a 7-day larval Delta Smelt toxicity exposure initiated on
658 March 26, 2021.

Treatment	Temperature (°C) Min	Temperature (°C) Max	Temperature (°C) Ave	SC (µS/cm)	DO (mg/L) Min	DO (mg/L) Max	DO (mg/L) Ave	pH Min	pH Max	pH Ave
Control	15.4	16.0	15.8	659	8.45	11.32	9.71	8.00	8.17	8.08
High Salinity Control	15.3	16.1	15.8	10690	7.88	10.37	9.20	7.86	8.05	7.94
Site 1: Toe Drain	15.4	16.2	15.9	689	8.34	10.53	9.26	8.28	8.39	8.33
Site 2: Cache Slough	15.5	16.0	15.8	290	8.79	9.84	9.28	8.03	8.61	8.23
Site 3: Deep Water Ship Channel	15.4	16.1	15.8	242	8.45	9.95	9.27	7.98	8.04	8.01
Site 4: Sac River at Decker Is.	15.3	16.1	15.8	362	9.26	10.12	9.46	7.88	8.03	7.96
Site 5: Montezuma Slough	15.3	16.1	15.8	2169	8.65	10.19	9.40	7.89	7.97	7.94
Site 6: Grizzly Bay	15.5	16.0	15.8	10490	8.62	9.99	9.33	7.75	8.04	7.89

659

Treatment	Initial Hardness (as $CaCO_3$) (mg/L)	Initial Alkalinity (as $CaCO_3$) (mg/L)	Initial Total Ammonia (mg/L)	Initial Unionized Ammonia (mg/L)	Day 4 Final Total Ammonia (mg/L)	Day 4 Final Unionized Ammonia (mg/L)	Day 7 Final Total Ammonia (mg/L)	Day 7 Final Unionized Ammonia (mg/L)	Day 7 Final Nitrate (mg/L)	Day 7 Final Nitrite (mg/L)
Control	148	86	0.06	0.002	0.68	0.017	0.87	0.026	1.55	0.092
High Salinity Control	1200	88	0.02	0.001	0.43	0.007	0.76	0.011	1.09	0.035
Site 1: Toe Drain	240	246	0.06	0.003	0.62	0.033	0.76	0.047	0.89	0.082
Site 2: Cache Slough	96	108	0.03	0.003	0.55	0.016	0.72	0.021	0.69	0.055
Site 3: Deep Water Ship Channel	88	86	0.13	0.003	0.63	0.016	0.79	0.023	1.23	0.170
Site 4: Sac River at Decker Is.	88	78	0.13	0.002	0.62	0.015	0.79	0.022	1.03	0.124
Site 5: Montezuma Slough	240	84	0.13	0.002	0.56	0.013	0.69	0.015	1.82	0.168
Site 6: Grizzly Bay	1160	92	0.24	0.005	0.48	0.008	0.55	0.006	0.71	0.061

660 Table 6-S3. Summary of water quality measurements taken during a 7-day larval Delta Smelt toxicity exposure initiated on
661 April 9, 2021.

Treatment	Temperature (°C) Min	Temperature (°C) Max	Temperature (°C) Ave	SC (µS/cm)	DO (mg/L) Min	DO (mg/L) Max	DO (mg/L) Ave	pH Min	pH Max	pH Ave
Control	16.0	16.4	16.2	666	8.24	9.94	9.07	7.88	8.14	7.99
High Salinity Control	15.8	16.4	16.1	11326	8.33	10.19	9.24	7.98	8.04	8.01
Site 1: Toe Drain	15.9	16.5	16.2	541	8.19	9.86	8.76	8.00	8.27	8.16
Site 2: Cache Slough	15.8	16.5	16.1	252	8.19	9.83	9.05	7.95	8.27	8.10
Site 3: Deep Water Ship Channel	15.9	16.4	16.1	232	8.28	10.12	9.09	7.80	7.98	7.91
Site 4: Sac River at Decker Is.	15.9	16.4	16.1	1459	8.23	9.96	9.08	7.85	8.01	7.91
Site 5: Montezuma Slough	15.9	16.4	16.2	4087	8.28	10.19	9.37	7.75	7.98	7.87
Site 6: Grizzly Bay	15.8	16.7	16.3	11252	8.24	9.91	9.10	7.71	7.92	7.82

662
663

Treatment	Initial Hardness (as $CaCO_3$) (mg/L)	Initial Alkalinity (as $CaCO_3$) (mg/L)	Initial Total Ammonia (mg/L)	Initial Unionized Ammonia (mg/L)	Day 4 Final Total Ammonia (mg/L)	Day 4 Final Unionized Ammonia (mg/L)	Day 7 Final Total Ammonia (mg/L)	Day 7 Final Unionized Ammonia (mg/L)	Day 7 Final Nitrate (mg/L)	Day 7 Final Nitrite (mg/L)
Control	152	112	0.17	0.006	0.63	0.015	0.59	0.012	1.08	0.098
High Salinity Control	1120	98	0.17	0.003	0.47	0.010	0.73	0.016	2.05	0.290
Site 1: Toe Drain	156	146	0.11	0.003	0.60	0.029	0.75	0.031	0.84	0.298
Site 2: Cache Slough	80	90	0.07	0.002	0.61	0.031	0.85	0.020	0.90	0.156
Site 3: Deep Water Ship Channel	88	76	0.09	0.002	0.70	0.019	0.88	0.021	1.25	0.262
Site 4: Sac River at Decker Is.	176	72	0.10	0.002	0.52	0.014	0.73	0.013	2.08	0.157
Site 5: Montezuma Slough	400	78	0.09	0.002	0.48	0.011	0.64	0.008	1.57	0.092
Site 6: Grizzly Bay	1200	76	0.26	0.004	0.53	0.009	0.67	0.007	1.07	0.149

664 Table 6-S4. Summary of water quality measurements taken during a 7-day larval Delta Smelt toxicity exposure initiated on
665 April 23, 2021.

Treatment	Temperature (°C) Min	Temperature (°C) Max	Temperature (°C) Ave	SC (µS/cm)	DO (mg/L) Min	DO (mg/L) Max	DO (mg/L) Ave	pH Min	pH Max	pH Ave
Control	15.9	16.3	16.1	605	9.16	10.08	9.50	7.94	8.28	8.06
High Salinity Control	15.9	16.2	16.1	11372	9.23	10.62	9.85	7.80	7.99	7.92
Site 1: Toe Drain	15.9	16.1	16.0	321	8.91	10.52	9.56	8.09	8.38	8.20
Site 2: Cache Slough	15.8	16.0	15.9	207	8.97	10.31	9.51	7.92	8.37	8.09
Site 3: Deep Water Ship Channel	15.9	16.0	16.0	226	9.00	10.50	9.53	7.95	8.18	8.03
Site 4: Sac River at Decker Is.	15.8	16.1	16.0	1475	9.43	10.68	9.69	7.85	7.96	7.89
Site 5: Montezuma Slough	15.9	16.2	16.0	4763	9.00	10.66	9.59	7.66	7.94	7.82
Site 6: Grizzly Bay	15.9	16.2	16.0	11410	9.07	10.89	9.68	7.62	7.95	7.80

666

Treatment	Initial Hardness (as $CaCO_3$) (mg/L)	Initial Alkalinity (as $CaCO_3$) (mg/L)	Initial Total Ammonia (mg/L)	Initial Unionized Ammonia (mg/L)	Day 4 Final Total Ammonia (mg/L)	Day 4 Final Unionized Ammonia (mg/L)	Day 7 Final Total Ammonia (mg/L)	Day 7 Final Unionized Ammonia (mg/L)	Day 7 Final Nitrate (mg/L)	Day 7 Final Nitrite (mg/L)
Control	140	92	0.10	0.005	0.55	0.012	0.70	0.016	3.82	0.321
High Salinity Control	1160	128	0.08	0.002	0.43	0.008	0.61	0.008	1.33	0.081
Site 1: Toe Drain	116	120	0.05	0.003	0.56	0.020	0.89	0.029	0.89	0.090
Site 2: Cache Slough	76	80	0.02	0.001	0.58	0.014	0.86	0.019	0.40	0.079
Site 3: Deep Water Ship Channel	68	76	0.04	0.002	0.55	0.013	0.89	0.021	0.61	0.078
Site 4: Sac River at Decker Is.	184	78	0.08	0.001	0.53	0.012	0.84	0.015	1.42	0.071
Site 5: Montezuma Slough	380	82	0.11	0.002	0.54	0.009	0.70	0.007	0.51	0.061
Site 6: Grizzly Bay	1080	76	0.30	0.005	0.36	0.005	0.57	0.005	2.18	0.169

667 Table 6-S5. Summary of water quality measurements taken during a 7-day larval Delta Smelt toxicity exposure initiated on
668 May 7, 2021.

Treatment	Temperature (°C) Min	Temperature (°C) Max	Temperature (°C) Ave	SC (µS/cm)	DO (mg/L) Min	DO (mg/L) Max	DO (mg/L) Ave	pH Min	pH Max	pH Ave
Control	16.1	17.2	16.8	530	8.32	9.91	9.14	7.84	8.00	7.94
High Salinity Control	16.4	17.2	16.8	15990	8.49	10.12	9.43	7.90	7.98	7.95
Site 1: Toe Drain	16.5	17.2	16.9	377	8.23	9.77	8.99	8.06	8.15	8.10
Site 2: Cache Slough	16.1	17.3	16.9	191	8.05	8.99	8.45	7.80	8.14	7.92
Site 3: Deep Water Ship Channel	16.3	17.3	16.9	201	8.27	9.59	8.82	7.87	7.99	7.95
Site 4: Sac River at Decker Is.	16.3	17.3	16.9	1538	8.26	9.95	9.04	7.86	7.88	7.87
Site 5: Montezuma Slough	16.3	17.5	17.0	6067	8.24	9.74	9.10	7.84	7.92	7.88
Site 6: Grizzly Bay	16.5	17.5	17.1	16050	8.23	10.45	9.30	7.74	7.85	7.79

669

Treatment	Initial Hardness (as $CaCO_3$) (mg/L)	Initial Alkalinity (as $CaCO_3$) (mg/L)	Initial Total Ammonia (mg/L)	Initial Unionized Ammonia (mg/L)	Day 4 Final Total Ammonia (mg/L)	Day 4 Final Unionized Ammonia (mg/L)	Day 7 Final Total Ammonia (mg/L)	Day 7 Final Unionized Ammonia (mg/L)	Day 7 Final Nitrate (mg/L)	Day 7 Final Nitrite (mg/L)
Control	132	94	0.04	0.001	0.79	0.016	1.11	0.029	1.61	0.378
High Salinity Control	1920	146	0.06	0.001	0.64	0.013	0.76	0.013	0.35	0.049
Site 1: Toe Drain	140	144	0.07	0.002	1.03	0.034	1.52	0.061	0.23	0.107
Site 2: Cache Slough	88	76	0.04	0.001	1.01	0.019	1.48	0.029	0.00	0.068
Site 3: Deep Water Ship Channel	68	76	0.04	0.001	1.01	0.022	1.27	0.036	0.30	0.138
Site 4: Sac River at Decker Is.	216	74	0.07	0.001	0.87	0.017	1.07	0.022	0.53	0.123
Site 5: Montezuma Slough	1000	82	0.14	0.003	0.85	0.015	0.99	0.017	0.36	0.117
Site 6: Grizzly Bay	1800	96	0.17	0.002	0.73	0.010	0.77	0.009	0.23	0.212

670

671 Table 6-S6. GC/MS/MS parameters used for detection of pesticides in water samples.

GC-MS/MS Method Parameters	Descriptions
Gas Chromatograph (GC) Type	Thermo Scientific™ TRACE™ 1310 Gas Chromatograph.
Mass Spectrometer (MS) Type	Thermo Scientific™ TSQ™ 8000 Gas Chromatograph/Triple Quadrupole Mass Spectrometer
Autosampler Type	Thermo Scientific™ TriPlus™ RSH autosampler
Ion source	Thermo Scientific™ ExtractaBrite™ Electron Ionization (EI) source
Software	Thermo Scientific™ Xcalibur™ Data system, common platform for all Thermo Scientific MS systems
Injector Type	Programmed Temperature Vaporization (PTV) injector
GC Column	Thermo TG-5MS; ID 0.25 mm; length 30 m; film 0.25µ; Temp -60 to 330/350 ºC
Carrier Gas	Helium (99.999%)
Collision Gas	Argon (99.999%)
Inlet Temperature	200 °C
Injection Mode	Splitless
Carrier mode	Constant flow
Carrier flow rate	1.2 mL/min
temperature ramps	60 °C (2 min); Rate 18 °C/min; 300 °C (10 min)
Solid phase extraction kit	Oasis
Injection syringe	10 µL
MS transfer line temperature	250 °C
MS Mode SIM Range	50 - 500
Electron Lens Voltage	5 V
Electron Energy	70 eV
Emission Current	50 uA
Ion source temperature	300 °C
Polarity	Positive
Ion source type	EI
Fore line pressure	68 mTorr

672

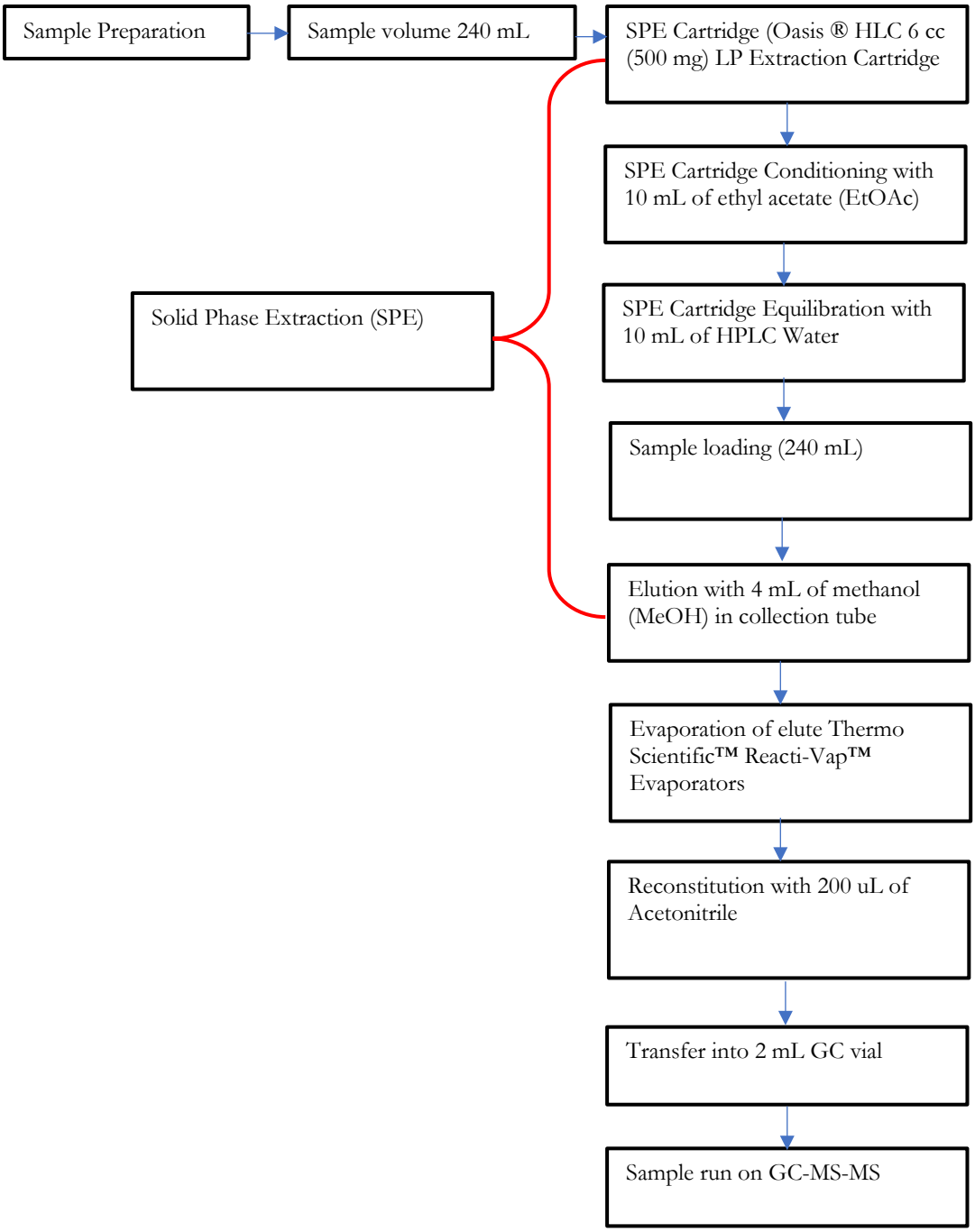

673

674

675 Figure 6-S1. Sample preparation and solid phase extraction (SPE) of water samples.

676 Table 6-S7. Individual histopathology scores for the liver and gills of Delta Smelt in Exposure 1 initiated March 12, 2021.

Site	Liver GD	Liver LIP	Liver SCN	Liver INF	Liver MA	Liver SC	Gills ANU	Gills GCN	Gills CCH	Gills MCH	Gills ECH	Gills SLE	Gills P	Gills GINF	Gills F
C-1	0	0	0	0	0	0	0	0	0	0	0	0	0	0	0
C-2	0	0	0	0	0	0	0	0	0	0	0	0	0	0	0
C-3	1	0	0	0	0	0	0	0	0	0	0	0	0	0	0
C-4	2	0	0	0	0	0	0	0	0	0	0	0	0	0	0
C-5	1	0	0	0	0	0	0	0	0	0	0	0	0	0	0
C-6	1	0	0	0	0	0	0	0	0	0	0	0	0	0	0
C-7	2	0	0	0	0	0	0	0	0	0	0	0	0	0	0
C-8	1	0	0	0	0	0	0	0	0	0	0	0	0	0	0
C-9	2	0	0	0	0	0	0	0	0	0	0	0	0	0	0
C-10	2	0	0	0	0	0	0	0	0	0	0	0	0	0	0
C-11	2	0	0	0	0	0	0	0	0	0	0	0	0	0	0
HSC-1	0	0	0	0	0	0	0	0	0	0	0	0	0	0	0
HSC-2	0	0	0	0	0	0	0	0	0	0	0	0	0	0	0
HSC-3	0	0	0	0	0	0	0	0	0	0	0	0	0	0	0
HSC-4	2	0	0	0	0	0	0	0	0	0	0	0	0	0	0
HSC-5	1	0	0	0	0	0	0	0	0	0	0	0	0	0	0
HSC-6	1	0	0	0	0	0	0	0	0	0	0	0	0	0	0
HSC-7	0	0	0	0	0	0	0	0	0	0	0	0	0	0	0
HSC-8	0	0	0	0	0	0	0	0	0	0	0	0	0	0	0
HSC-9	0	0	0	0	0	0	0	0	0	0	0	0	0	0	0
HSC-10	0	0	0	0	0	0	0	0	0	0	0	0	0	0	0
HSC-11	0	0	0	0	0	0	0	0	0	0	0	0	0	0	0
HSC-12	2	0	0	0	0	0	0	0	0	0	0	0	0	0	0
TD-1	2	0	0	0	0	0	0	0	0	0	0	0	0	0	0

Site	Liver GD	Liver LIP	Liver SCN	Liver INF	Liver MA	Liver SC	Gills ANU	Gills GCN	Gills CCH	Gills MCH	Gills ECH	Gills SLE	Gills P	Gills GINF	Gills F
TD-2	2	0	0	0	0	0	0	0	0	0	0	0	0	0	0
TD-3	2	0	0	0	0	0	0	0	0	0	0	0	0	0	0
TD-3	2	0	0	0	0	0	0	0	0	0	0	0	0	0	0
TD-4	2	0	0	0	0	0	0	0	0	0	0	0	0	0	0
TD-5	2	0	0	0	0	0	0	0	0	0	0	0	0	0	0
TD-6	2	0	0	0	0	0	0	0	0	0	0	0	0	0	0
TD-7	0	0	0	0	0	0	0	0	0	0	0	0	0	0	0
TD-8	0	0	0	0	0	0	0	0	0	0	0	0	0	0	0
TD-9	0	0	0	0	0	0	0	0	0	0	0	0	0	0	0
TD-10	0	0	0	0	0	0	0	0	0	0	0	0	0	0	0
TD-11	0	0	0	0	0	0	0	0	0	0	0	0	0	0	0
TD-12	2	0	0	0	0	0	0	0	0	0	0	0	0	0	0
CS-1	2	0	0	0	0	0	0	0	0	0	0	0	0	0	0
CS-2	1	0	0	0	0	0	0	0	0	0	0	0	0	0	0
CS-3	2	0	0	0	0	0	0	0	0	0	0	0	0	0	0
CS-4	2	0	0	0	0	0	0	0	0	0	0	0	0	0	0
CS-5	1	0	0	0	0	0	0	0	0	0	0	0	0	0	0
CS-6	0	0	0	0	0	0	0	0	0	0	0	0	0	0	0
CS-7	0	0	0	0	0	0	0	0	0	0	0	0	0	0	0
CS-8	3	0	0	0	0	0	0	0	0	0	0	0	0	0	0
CS-9	2	0	0	0	0	0	0	0	0	0	2	0	0	0	0
CS-10	2	0	0	0	0	0	0	0	0	0	2	0	0	0	0
CS-11	2	0	0	0	0	0	0	0	0	0	2	0	0	0	0
CS-12	0	0	0	0	0	0	0	0	0	0	0	0	0	0	0
DWSC-1	1	0	0	0	0	0	0	0	0	0	0	0	0	0	0

Site	Liver GD	Liver LIP	Liver SCN	Liver INF	Liver MA	Liver SC	Gills ANU	Gills GCN	Gills CCH	Gills MCH	Gills ECH	Gills SLE	Gills P	Gills GINF	Gills F
DWSC-2	1	0	0	0	0	0	0	0	0	0	0	0	0	0	0
DWSC-3	0	0	0	0	0	0	0	0	0	0	0	0	0	0	0
DWSC-4	0	0	0	0	0	0	0	0	0	0	0	0	0	0	0
DWSC-5	0	0	0	0	0	0	0	0	0	0	0	0	0	0	0
DWSC-6	2	0	0	0	0	0	0	0	0	0	0	0	0	0	0
DWSC-7	1	0	0	0	0	0	0	0	0	0	0	0	0	0	0
DWSC-8	1	0	0	0	0	0	0	0	0	0	0	0	0	0	0
DWSC-9	1	0	0	0	0	0	0	0	0	0	0	0	0	0	0
DWSC-10	2	0	0	0	0	0	0	0	0	0	0	0	0	0	0
DWSC-11	1	0	0	0	0	0	0	0	0	0	0	0	0	0	0
SRD-1	1	0	0	0	0	0	0	0	0	0	0	0	0	0	0
SRD-2	0	0	0	0	0	0	0	0	0	0	0	0	0	0	0
SRD-3	0	0	0	0	0	0	0	0	0	0	0	0	0	0	0
SRD-4	0	0	0	0	0	0	0	0	0	0	0	0	0	0	0
SRD-5	2	0	0	0	0	0	0	0	0	0	0	0	0	0	0
SRD-6	1	0	0	0	0	0	0	0	0	0	0	0	0	0	0
SRD-7	2	0	0	0	0	0	0	0	0	0	0	0	0	0	0
SRD-8	2	0	0	0	0	0	0	0	0	0	0	0	0	0	0
SRD-9	2	0	0	0	0	0	0	0	0	0	0	0	0	0	0
SRD-10	0	0	0	0	0	0	0	0	0	0	0	0	0	0	0
SRD-11	0	0	0	0	0	0	0	0	0	0	0	0	0	0	0
SRD-12	0	0	0	0	0	0	0	0	0	0	0	0	0	0	0
MS-1	0	0	0	0	0	0	0	0	0	0	0	0	0	0	0
MS-2	0	0	0	0	0	0	0	0	0	0	0	0	0	0	0
MS-3	0	0	0	0	0	0	0	0	0	0	0	0	0	0	0

Site	Liver GD	Liver LIP	Liver SCN	Liver INF	Liver MA	Liver SC	Gills ANU	Gills GCN	Gills CCH	Gills MCH	Gills ECH	Gills SLE	Gills P	Gills GINF	Gills F
MS-4	2	0	0	0	0	0	0	0	0	0	0	0	0	0	0
MS-5	2	0	0	0	0	0	0	0	0	0	0	0	0	0	0
MS-6	3	0	0	0	0	0	0	0	0	0	0	0	0	0	0
MS-7	0	0	0	0	0	0	0	0	0	0	0	0	0	0	0
MS-8	2	0	0	0	0	0	0	0	0	0	0	0	0	0	0
MS-9	0	0	0	0	0	0	0	0	0	0	0	0	0	0	0
MS-10	0	0	0	0	0	0	0	0	0	0	0	0	0	0	0
MS-11	0	0	0	0	0	0	0	0	0	0	0	0	0	0	0
MS-12	0	0	0	0	0	0	0	0	0	0	0	0	0	0	0
GB-1	0	0	0	0	0	0	0	0	0	0	0	0	0	0	0
GB-2	3	0	0	0	0	0	0	0	0	0	0	0	0	0	0
GB-3	0	0	0	0	0	0	0	0	0	0	0	0	0	0	0
GB-4	0	0	0	0	0	0	0	0	0	0	0	0	0	0	0
GB-5	0	0	0	0	0	0	0	0	0	0	0	0	0	0	0
GB-6	0	0	0	0	0	0	0	0	0	0	0	0	0	0	0
GB-7	0	0	0	0	0	0	0	0	0	0	0	0	0	0	0
GB-8	0	0	0	0	0	0	0	0	0	0	0	0	0	0	0
GB-9	1	0	0	0	0	0	0	0	0	0	0	0	0	0	0
GB-10	0	0	0	0	0	0	0	0	0	0	0	0	0	0	0
GB-11	0	0	0	0	0	0	0	0	0	0	0	0	0	0	0
GB-12	0	0	0	0	0	0	0	0	0	0	0	0	0	0	0

677 (GD) glycogen depletion, (LIP) lipidosis, (SCN) single cell necrosis, (INF) liver inflammation, (MA) macrophage aggregate, (SC) sinusoidal congestion, (ANU)
678 aneurysm, (GCN) epithelial cell necrosis, (CCH) Ionocyte hyperplasia, (MCH) mucus cell hyperplasia, (ECH) epithelial cell hyperplasia, (SLE) secondary lamella edema,
679 (GINF) gill inflammation.

680

681 Table 6-S8. Individual histopathology scores for the liver and gills of Delta Smelt in Exposure 2 initiated March 26, 2021.

Site	Liver GD	Liver LIP	Liver SCN	Liver INF	Liver MA	Liver SC	Gills ANU	Gills GCN	Gills CCH	Gills MCH	Gills ECH	Gills SLE	Gills P	Gills GINF	Gills F
C-1	1	0	0	0	0	0	0	0	0	0	0	0	0	0	0
C-2	1	0	0	0	0	0	0	0	0	0	0	0	0	0	0
C-3	1	0	0	0	0	0	0	0	0	0	0	0	0	0	0
C-4	2	0	0	0	0	0	0	0	0	0	0	0	0	0	0
C-5	3	0	0	0	0	0	0	0	0	0	0	0	0	0	0
C-6	3	0	0	0	0	0	0	0	0	0	0	0	0	0	0
C-7	2	0	0	0	0	0	0	0	0	0	0	0	0	0	0
C-8	3	0	0	0	0	0	0	0	0	0	0	0	0	0	0
C-9	2	0	0	0	0	0	0	0	0	0	0	0	0	0	0
HSC-1	1	0	0	0	0	0	0	0	0	0	0	0	0	0	0
HSC-2	1	0	0	0	0	0	0	0	0	0	0	0	0	0	0
HSC-3	0	0	0	0	0	0	0	0	0	0	0	0	0	0	0
HSC-4	3	0	0	0	0	0	0	0	0	0	0	0	0	0	0
HSC-5	2	0	0	0	0	0	0	0	0	0	0	0	0	0	0
HSC-6	1	0	0	0	0	0	0	0	0	0	0	0	0	0	0
HSC-7	0	0	0	0	0	0	0	0	0	0	0	0	0	0	0
HSC-8	2	0	0	0	0	0	0	0	0	0	0	0	0	0	0
HSC-9	1	0	0	0	0	0	0	0	0	0	0	0	0	0	0
HSC-10	0	0	0	0	0	0	0	0	0	0	0	0	0	0	0
TD-1	1	0	0	0	0	0	0	0	0	0	0	0	0	0	0
TD-2	2	0	0	0	0	0	0	0	0	0	0	0	0	0	0
TD-3	3	0	0	0	0	0	0	0	0	0	0	0	0	0	0
TD-3	3	0	0	0	0	0	0	0	0	0	0	0	0	0	0
TD-4	2	0	0	0	0	0	0	0	0	0	0	0	0	0	0
TD-5	1	0	0	0	0	0	0	0	0	0	0	0	0	0	0

Site	Liver GD	Liver LIP	Liver SCN	Liver INF	Liver MA	Liver SC	Gills ANU	Gills GCN	Gills CCH	Gills MCH	Gills ECH	Gills SLE	Gills P	Gills GINF	Gills F
TD-6	1	0	0	0	0	0	0	0	0	0	0	0	0	0	0
TD-7	2	0	0	0	0	0	0	0	0	0	0	0	0	0	0
TD-8	2	0	0	0	0	0	0	0	0	0	0	0	0	0	0
TD-9	2	0	0	0	0	0	0	0	0	0	0	0	0	0	0
TD-10	1	0	0	0	0	0	0	0	0	0	0	0	0	0	0
CS-1	2	0	0	0	0	0	0	0	0	0	0	0	0	0	0
CS-2	3	0	0	0	0	0	0	0	0	0	0	0	0	0	0
CS-3	3	0	0	0	0	0	0	0	0	0	0	0	0	0	0
CS-4	2	0	0	0	0	0	0	0	0	0	0	0	0	0	0
CS-5	2	0	0	0	0	0	0	0	0	0	0	0	0	0	0
CS-6	3	0	0	0	0	0	0	0	0	0	0	0	0	0	0
CS-7	2	0	0	0	0	0	0	0	0	0	0	0	0	0	0
CS-8	2	0	0	0	0	0	0	0	0	0	0	0	0	0	0
CS-9	2	0	0	0	0	0	0	0	0	0	2	0	0	0	0
CS-10	2	0	0	0	0	0	0	0	0	0	2	0	0	0	0
DWSC-1	2	0	0	0	0	0	0	0	0	0	0	0	0	0	0
DWSC-2	3	0	0	0	0	0	0	0	0	0	0	0	0	0	0
DWSC-3	3	0	0	0	0	0	0	0	0	0	0	0	0	0	0
DWSC-4	3	0	0	0	0	0	0	0	0	0	0	0	0	0	0
DWSC-5	1	0	0	0	0	0	0	0	0	0	0	0	0	0	0
DWSC-6	2	0	0	0	0	0	0	0	0	0	0	0	0	0	0
DWSC-7	2	0	0	0	0	0	0	0	0	0	0	0	0	0	0
DWSC-8	1	0	0	0	0	0	0	0	0	0	0	0	0	0	0
DWSC-9	3	0	0	0	0	0	0	0	0	0	0	0	0	0	0
DWSC-10	3	0	0	0	0	0	0	0	0	0	0	0	0	0	0
SRD-1	2	0	0	0	0	0	0	0	0	0	0	0	0	0	0
SRD-2	3	0	0	0	0	0	0	0	0	0	0	0	0	0	0

Site	Liver GD	Liver LIP	Liver SCN	Liver INF	Liver MA	Liver SC	Gills ANU	Gills GCN	Gills CCH	Gills MCH	Gills ECH	Gills SLE	Gills P	Gills GINF	Gills F
SRD-3	2	0	0	0	0	0	0	0	0	0	0	0	0	0	0
SRD-4	3	0	0	0	0	0	0	0	0	0	0	0	0	0	0
SRD-5	2	0	0	0	0	0	0	0	0	0	0	0	0	0	0
SRD-6	2	0	0	0	0	0	0	0	0	0	0	0	0	0	0
SRD-7	1	0	0	0	0	0	0	0	0	0	0	0	0	0	0
SRD-8	2	0	0	0	0	0	0	0	0	0	0	0	0	0	0
SRD-9	3	0	0	0	0	0	0	0	0	0	0	0	0	0	0
SRD-10	3	0	0	0	0	0	0	0	0	0	0	0	0	0	0
MS-1	0	0	0	0	0	0	0	0	0	0	0	0	0	0	0
MS-2	2	0	0	0	0	0	0	0	0	0	0	0	0	0	0
MS-3	2	0	0	0	0	0	0	0	0	0	0	0	0	0	0
MS-4	0	0	0	0	0	0	0	0	0	0	0	0	0	0	0
MS-5	0	0	0	0	0	0	0	0	0	0	0	0	0	0	0
MS-6	1	0	0	0	0	0	0	0	0	0	0	0	0	0	0
MS-7	0	0	0	0	0	0	0	0	0	0	0	0	0	0	0
MS-8	0	0	0	0	0	0	0	0	0	0	0	0	0	0	0
MS-9	2	0	0	0	0	0	0	0	0	0	0	0	0	0	0
MS-10	2	0	0	0	0	0	0	0	0	0	0	0	0	0	0
MS-11	3	0	0	0	0	0	0	0	0	0	0	0	0	0	0
MS-12	2	0	0	0	0	0	0	0	0	0	0	0	0	0	0
GB-1	3	0	0	0	0	0	0	0	0	0	0	0	0	0	0
GB-2	2	0	0	0	0	0	0	0	0	0	0	0	0	0	0
GB-3	2	0	0	0	0	0	0	0	0	0	0	0	0	0	0
GB-4	2	0	0	0	0	0	0	0	0	0	0	0	0	0	0
GB-5	2	0	0	0	0	0	0	0	0	0	0	0	0	0	0
GB-6	2	0	0	0	0	0	0	0	0	0	0	0	0	0	0
GB-7	0	0	0	0	0	0	0	0	0	0	0	0	0	0	0

Site	Liver GD	Liver LIP	Liver SCN	Liver INF	Liver MA	Liver SC	Gills ANU	Gills GCN	Gills CCH	Gills MCH	Gills ECH	Gills SLE	Gills P	Gills GINF	Gills F
GB-8	0	0	0	0	0	0	0	0	0	0	0	0	0	0	0
GB-9	0	0	0	0	0	0	0	0	0	0	0	0	0	0	0
GB-10	3	0	0	0	0	0	0	0	0	0	0	0	0	0	0
GB-11	2	0	0	0	0	0	0	0	0	0	0	0	0	0	0
GB-12	2	0	0	0	0	0	0	0	0	0	0	0	0	0	0

682 (GD) glycogen depletion, (LIP) lipidosis, (SCN) single cell necrosis, (INF) liver inflammation, (MA) macrophage aggregate, (SC) sinusoidal congestion, (ANU)
683 aneurysm, (GCN) epithelial cell necrosis, (CCH) Ionocyte hyperplasia, (MCH) mucus cell hyperplasia, (ECH) epithelial cell hyperplasia, (SLE) secondary lamella edema,
684 (GINF) gill inflammation.

685

686 Table 6-S9. Individual histopathology scores for the liver and gills of Delta Smelt in Exposure 3 initiated April 9, 2021.

Site	Liver GD	Liver LIP	Liver SCN	Liver INF	Liver MA	Liver SC	Gills ANU	Gills GCN	Gills CCH	Gills MCH	Gills ECH	Gills SLE	Gills P	Gills GINF	Gills F
C-1	1	0	0	0	0	0	0	0	0	0	0	0	0	0	0
C-2	1	0	0	0	0	0	0	0	0	0	0	0	0	0	0
C-3	0	0	0	0	0	0	0	0	0	0	0	0	0	0	0
C-4	2	0	0	0	0	0	0	0	0	0	0	0	0	0	0
C-5	3	0	0	0	0	0	0	0	0	0	0	0	0	0	0
C-6	2	0	0	0	0	0	0	0	0	0	0	0	0	0	0
C-7	1	0	0	0	0	0	0	0	0	0	0	0	0	0	0
C-8	2	0	0	0	0	0	0	0	0	0	0	0	0	0	0
C-9	3	0	0	0	0	0	0	0	0	0	0	0	0	0	0
HSC-1	2	0	0	0	0	0	0	0	0	0	0	0	0	0	0
HSC-2	3	0	0	0	0	0	0	0	0	0	0	0	0	0	0
HSC-3	2	0	0	0	0	0	0	0	0	0	0	0	0	0	0
HSC-4	0	0	0	0	0	0	0	0	0	0	0	0	0	0	0
HSC-5	1	0	0	0	0	0	0	0	0	0	0	0	0	0	0
HSC-6	1	0	0	0	0	0	0	0	0	0	0	0	0	0	0
HSC-7	2	0	0	0	0	0	0	0	0	0	0	0	0	0	0
HSC-8	1	0	0	0	0	0	0	0	0	0	0	0	0	0	0
HSC-9	0	0	0	0	0	0	0	0	0	0	0	0	0	0	0
HSC-10	1	0	0	0	0	0	0	0	0	0	0	0	0	0	0
HSC-11	2	0	0	0	0	0	0	0	0	0	0	0	0	0	0
HSC-12	0	0	0	0	0	0	0	0	0	0	0	0	0	0	0
TD-1	2	0	0	0	0	0	0	0	0	0	0	0	0	0	0
TD-2	1	0	0	0	0	0	0	0	0	0	0	0	0	0	0
TD-3	0	0	0	0	0	0	0	0	0	0	0	0	0	0	0
TD-3	1	0	0	0	0	0	0	0	0	0	0	0	0	0	0
TD-4	0	0	0	0	0	0	0	0	0	0	0	0	0	0	0

Site	Liver GD	Liver LIP	Liver SCN	Liver INF	Liver MA	Liver SC	Gills ANU	Gills GCN	Gills CCH	Gills MCH	Gills ECH	Gills SLE	Gills P	Gills GINF	Gills F
TD-5	0	0	0	0	0	0	0	0	0	0	0	0	0	0	0
TD-6	2	0	0	0	0	0	0	0	0	0	0	0	0	0	0
TD-7	2	0	0	0	0	0	0	0	0	0	0	0	0	0	0
TD-8	2	0	0	0	0	0	0	0	0	0	0	0	0	0	0
TD-9	1	0	0	0	0	0	0	0	0	0	0	0	0	0	0
TD-10	2	0	0	0	0	0	0	0	0	0	0	0	0	0	0
CS-1	3	0	0	0	0	0	0	0	0	0	0	0	0	0	0
CS-2	2	0	0	0	0	0	0	0	0	0	0	0	0	0	0
CS-3	2	0	0	0	0	0	0	0	0	0	0	0	0	0	0
CS-4	3	0	0	0	0	0	0	0	0	0	0	0	0	0	0
CS-5	3	0	0	0	0	0	0	0	0	0	0	0	0	0	0
CS-6	3	0	0	0	0	0	0	0	0	0	0	0	0	0	0
CS-7	1	0	0	0	0	0	0	0	0	0	0	0	0	0	0
CS-8	2	0	0	0	0	0	0	0	0	0	0	0	0	0	0
CS-9	2	0	0	0	0	0	0	0	0	0	2	0	0	0	0
CS-10	3	0	0	0	0	0	0	0	0	0	2	0	0	0	0
CS-11	2	0	0	0	0	0	0	0	0	0	2	0	0	0	0
CS-12	1	0	0	0	0	0	0	0	0	0	0	0	0	0	0
DWSC-1	1	0	0	0	0	0	0	0	0	0	0	0	0	0	0
DWSC-2	2	0	0	0	0	0	0	0	0	0	0	0	0	0	0
DWSC-3	2	0	0	0	0	0	0	0	0	0	0	0	0	0	0
DWSC-4	1	0	0	0	0	0	0	0	0	0	0	0	0	0	0
DWSC-5	0	0	0	0	0	0	0	0	0	0	0	0	0	0	0
DWSC-6	2	0	0	0	0	0	0	0	0	0	0	0	0	0	0
DWSC-7	2	0	0	0	0	0	0	0	0	0	0	0	0	0	0
DWSC-8	2	0	0	0	0	0	0	0	0	0	0	0	0	0	0
DWSC-9	3	0	0	0	0	0	0	0	0	0	0	0	0	0	0

Site	Liver GD	Liver LIP	Liver SCN	Liver INF	Liver MA	Liver SC	Gills ANU	Gills GCN	Gills CCH	Gills MCH	Gills ECH	Gills SLE	Gills P	Gills GINF	Gills F
DWSC-10	2	0	0	0	0	0	0	0	0	0	0	0	0	0	0
DWSC-11	2	0	0	0	0	0	0	0	0	0	0	0	0	0	0
DWSC-12	2	0	0	0	0	0	0	0	0	0	0	0	0	0	0
SRD-1	0	0	0	0	0	0	0	0	0	0	0	0	0	0	0
SRD-2	3	0	0	0	0	0	0	0	0	0	0	0	0	0	0
SRD-3	1	0	0	0	0	0	0	0	0	0	0	0	0	0	0
SRD-4	3	0	0	0	0	0	0	0	0	0	0	0	0	0	0
SRD-5	0	0	0	0	0	0	0	0	0	0	0	0	0	0	0
SRD-6	1	0	0	0	0	0	0	0	0	0	0	0	0	0	0
SRD-7	2	0	0	0	0	0	0	0	0	0	0	0	0	0	0
SRD-8	0	0	0	0	0	0	0	0	0	0	0	0	0	0	0
SRD-9	3	0	0	0	0	0	0	0	0	0	0	0	0	0	0
SRD-10	3	0	0	0	0	0	0	0	0	0	0	0	0	0	0
SRD-11	0	0	0	0	0	0	0	0	0	0	0	0	0	0	0
SRD-12	1	0	0	0	0	0	0	0	0	0	0	0	0	0	0
MS-1	0	0	0	0	0	0	0	0	0	0	0	0	0	0	0
MS-2	0	0	0	0	0	0	0	0	0	0	0	0	0	0	0
MS-3	2	0	0	0	0	0	0	0	0	0	0	0	0	0	0
MS-4	2	0	0	0	0	0	0	0	0	0	0	0	0	0	0
MS-5	0	0	0	0	0	0	0	0	0	0	0	0	0	0	0
MS-6	1	0	0	0	0	0	0	0	0	0	0	0	0	0	0
MS-7	0	0	0	0	0	0	0	0	0	0	0	0	0	0	0
MS-8	1	0	0	0	0	0	0	0	0	0	0	0	0	0	0
MS-9	0	0	0	0	0	0	0	0	0	0	0	0	0	0	0
GB-1	0	0	0	0	0	0	0	0	0	0	0	0	0	0	0
GB-2	0	0	0	0	0	0	0	0	0	0	0	0	0	0	0
GB-3	3	0	0	0	0	0	0	0	0	0	0	0	0	0	0

Site	Liver GD	Liver LIP	Liver SCN	Liver INF	Liver MA	Liver SC	Gills ANU	Gills GCN	Gills CCH	Gills MCH	Gills ECH	Gills SLE	Gills P	Gills GINF	Gills F
GB-4	0	0	0	0	0	0	0	0	0	0	0	0	0	0	0
GB-5	0	0	0	0	0	0	0	0	0	0	0	0	0	0	0
GB-6	2	0	0	0	0	0	0	0	0	0	0	0	0	0	0
GB-7	2	0	0	0	0	0	0	0	0	0	0	0	0	0	0
GB-8	0	0	0	0	0	0	0	0	0	0	0	0	0	0	0
GB-9	2	0	0	0	0	0	0	0	0	0	0	0	0	0	0

687 (GD) glycogen depletion, (LIP) lipidosis, (SCN) single cell necrosis, (INF) liver inflammation, (MA) macrophage aggregate, (SC) sinusoidal congestion, (ANU)
688 aneurysm, (GCN) epithelial cell necrosis, (CCH) Ionocyte hyperplasia, (MCH) mucus cell hyperplasia, (ECH) epithelial cell hyperplasia, (SLE) secondary lamella edema,
689 (GINF) gill inflammation.

690 Table 6-S10. Individual histopathology scores for the liver and gills of Delta Smelt in Exposure 4 initiated April 23, 2021.

Site	Liver GD	Liver LIP	Liver SCN	Liver INF	Liver MA	Liver SC	Gills ANU	Gills GCN	Gills CCH	Gills MCH	Gills ECH	Gills SLE	Gills P	Gills GINF	Gills F
C-1	1	0	0	0	0	0	0	0	0	0	0	0	0	0	0
C-2	2	0	0	0	0	0	0	0	0	0	0	0	0	0	0
C-3	2	0	0	0	0	0	0	0	0	0	0	0	0	0	0
C-4	0	0	0	0	0	0	0	0	0	0	0	0	0	0	0
C-5	2	0	0	0	0	0	0	0	0	0	0	0	0	0	0
C-6	1	0	0	0	0	0	0	0	0	0	0	0	0	0	0
C-7	2	0	0	0	0	0	0	0	0	0	0	0	0	0	0
C-8	1	0	0	0	0	0	0	0	0	0	0	0	0	0	0
C-9	2	0	0	0	0	0	0	0	0	0	0	0	0	0	0
HSC-1	1	0	0	0	0	0	0	0	0	0	0	0	0	0	0
HSC-2	1	0	0	0	0	0	0	0	0	0	0	0	0	0	0
HSC-3	2	0	0	0	0	0	0	0	0	0	0	0	0	0	0
HSC-4	0	0	0	0	0	0	0	0	0	0	0	0	0	0	0
HSC-5	1	0	0	0	0	0	0	0	0	0	0	0	0	0	0
HSC-6	2	0	0	0	0	0	0	0	0	0	0	0	0	0	0
HSC-7	1	0	0	0	0	0	0	0	0	0	0	0	0	0	0
HSC-8	0	0	0	0	0	0	0	0	0	0	0	0	0	0	0
HSC-9	1	0	0	0	0	0	0	0	0	0	0	0	0	0	0
HSC-10	0	0	0	0	0	0	0	0	0	0	0	0	0	0	0
HSC-11	1	0	0	0	0	0	0	0	0	0	0	0	0	0	0
TD-1	1	0	0	0	0	0	0	0	0	0	0	0	0	0	0
TD-2	1	0	0	0	0	0	0	0	0	0	0	0	0	0	0
TD-3	1	0	0	0	0	0	0	0	0	0	0	0	0	0	0
TD-3	0	0	0	0	0	0	0	0	0	0	0	0	0	0	0
TD-4	1	0	0	0	0	0	0	0	0	0	0	0	0	0	0
TD-5	1	0	0	0	0	0	0	0	0	0	0	0	0	0	0

Site	Liver GD	Liver LIP	Liver SCN	Liver INF	Liver MA	Liver SC	Gills ANU	Gills GCN	Gills CCH	Gills MCH	Gills ECH	Gills SLE	Gills P	Gills GINF	Gills F
TD-6	2	0	0	0	0	0	0	0	0	0	0	0	0	0	0
TD-7	1	0	0	0	0	0	0	0	0	0	0	0	0	0	0
TD-8	1	0	0	0	0	0	0	0	0	0	0	0	0	0	0
TD-9	0	0	0	0	0	0	0	0	0	0	0	0	0	0	0
TD-10	1	0	0	0	0	0	0	0	0	0	0	0	0	0	0
TD-11	2	0	0	0	0	0	0	0	0	0	0	0	0	0	0
TD-12	1	0	0	0	0	0	0	0	0	0	0	0	0	0	0
CS-1	2	0	0	0	0	0	0	0	0	0	0	0	0	0	0
CS-2	1	0	0	0	0	0	0	0	0	0	0	0	0	0	0
CS-3	0	0	0	0	0	0	0	0	0	0	0	0	0	0	0
CS-4	1	0	0	0	0	0	0	0	0	0	0	0	0	0	0
CS-5	1	0	0	0	0	0	0	0	0	0	0	0	0	0	0
CS-6	3	0	0	0	0	0	0	0	0	0	0	0	0	0	0
CS-7	1	0	0	0	0	0	0	0	0	0	0	0	0	0	0
CS-8	1	0	0	0	0	0	0	0	0	0	0	0	0	0	0
CS-9	1	0	0	0	0	0	0	0	0	0	2	0	0	0	0
CS-10	1	0	0	0	0	0	0	0	0	0	2	0	0	0	0
CS-11	1	0	0	0	0	0	0	0	0	0	2	0	0	0	0
CS-12	2	0	0	0	0	0	0	0	0	0	0	0	0	0	0
DWSC-1	2	0	0	0	0	0	0	0	0	0	0	0	0	0	0
DWSC-2	2	0	0	0	0	0	0	0	0	0	0	0	0	0	0
DWSC-3	1	0	0	0	0	0	0	0	0	0	0	0	0	0	0
DWSC-4	1	0	0	0	0	0	0	0	0	0	0	0	0	0	0
DWSC-5	na	0	0	0	0	0	0	0	0	0	0	0	0	0	0
DWSC-6	2	0	0	0	0	0	0	0	0	0	0	0	0	0	0
DWSC-7	2	0	0	0	0	0	0	0	0	0	0	0	0	0	0
DWSC-8	3	0	0	0	0	0	0	0	0	0	0	0	0	0	0

Site	Liver GD	Liver LIP	Liver SCN	Liver INF	Liver MA	Liver SC	Gills ANU	Gills GCN	Gills CCH	Gills MCH	Gills ECH	Gills SLE	Gills P	Gills GINF	Gills F
DWSC-9	1	0	0	0	0	0	0	0	0	0	0	0	0	0	0
DWSC-10	2	0	0	0	0	0	0	0	0	0	0	0	0	0	0
DWSC-11	1	0	0	0	0	0	0	0	0	0	0	0	0	0	0
DWSC-12	2	0	0	0	0	0	0	0	0	0	0	0	0	0	0
SRD-1	2	0	0	0	0	0	0	0	0	0	0	0	0	0	0
SRD-2	2	0	0	0	0	0	0	0	0	0	0	0	0	0	0
SRD-3	2	0	0	0	0	0	0	0	0	0	0	0	0	0	0
SRD-4	1	0	0	0	0	0	0	0	0	0	0	0	0	0	0
SRD-5	2	0	0	0	0	0	0	0	0	0	0	0	0	0	0
SRD-6	1	0	0	0	0	0	0	0	0	0	0	0	0	0	0
SRD-7	1	0	0	0	0	0	0	0	0	0	0	0	0	0	0
SRD-8	1	0	0	0	0	0	0	0	0	0	0	0	0	0	0
SRD-9	0	0	0	0	0	0	0	0	0	0	0	0	0	0	0
SRD-10	1	0	0	0	0	0	0	0	0	0	0	0	0	0	0
SRD-11	2	0	0	0	0	0	0	0	0	0	0	0	0	0	0
SRD-12	1	0	0	0	0	0	0	0	0	0	0	0	0	0	0
MS-1	0	0	0	0	0	0	0	0	0	0	0	0	0	0	0
MS-2	0	0	0	0	0	0	0	0	0	0	0	0	0	0	0
MS-3	0	0	0	0	0	0	0	0	0	0	0	0	0	0	0
MS-4	0	0	0	0	0	0	0	0	0	0	0	0	0	0	0
MS-5	0	0	0	0	0	0	0	0	0	0	0	0	0	0	0
MS-6	0	0	0	0	0	0	0	0	0	0	0	0	0	0	0
MS-7	0	0	0	0	0	0	0	0	0	0	0	0	0	0	0
MS-8	0	0	0	0	0	0	0	0	0	0	0	0	0	0	0
MS-9	0	0	0	0	0	0	0	0	0	0	0	0	0	0	0
MS-10	0	0	0	0	0	0	0	0	0	0	0	0	0	0	0
MS-11	0	0	0	0	0	0	0	0	0	0	0	0	0	0	0

Site	Liver GD	Liver LIP	Liver SCN	Liver INF	Liver MA	Liver SC	Gills ANU	Gills GCN	Gills CCH	Gills MCH	Gills ECH	Gills SLE	Gills P	Gills GINF	Gills F
MS-12	1	0	0	0	0	0	0	0	0	0	0	0	0	0	0
GB-1	2	0	0	0	0	0	0	0	0	0	0	0	0	0	0
GB-2	1	0	0	0	0	0	0	0	0	0	0	0	0	0	0
GB-3	0	0	0	0	0	0	0	0	0	0	0	0	0	0	0
GB-4	0	0	0	0	0	0	0	0	0	0	0	0	0	0	0
GB-5	1	0	0	0	0	0	0	0	0	0	0	0	0	0	0
GB-6	1	0	0	0	0	0	0	0	0	0	0	0	0	0	0
GB-7	2	0	0	0	0	0	0	0	0	0	0	0	0	0	0
GB-8	2	0	0	0	0	0	0	0	0	0	0	0	0	0	0
GB-9	1	0	0	0	0	0	0	0	0	0	0	0	0	0	0
GB-10	0	0	0	0	0	0	0	0	0	0	0	0	0	0	0
GB-11	0	0	0	0	0	0	0	0	0	0	0	0	0	0	0
GB-12	2	0	0	0	0	0	0	0	0	0	0	0	0	0	0

691 (GD) glycogen depletion, (LIP) lipidosis, (SCN) single cell necrosis, (INF) liver inflammation, (MA) macrophage aggregate, (SC) sinusoidal congestion, (ANU)
692 aneurysm, (GCN) epithelial cell necrosis, (CCH) Ionocyte hyperplasia, (MCH) mucus cell hyperplasia, (ECH) epithelial cell hyperplasia, (SLE) secondary lamella edema,
693 (GINF) gill inflammation.

694 Table 6-S11. Individual histopathology scores for the liver and gills of Delta Smelt in
695 Exposure 5 initiated May 7, 2021.

Site	LiverGD	Liver LIP	Liver SCN	Liver INF	Liver MA	Liver SC	Gills ANU	Gills GCN	Gills CCH	Gills MCH	Gills ECH	Gills SLE	GillsP	Gills GINF	GillsF
C-1	0	0	0	0	0	0	0	0	0	0	0	0	0	0	0
C-2	1	0	0	0	0	0	0	0	0	0	0	0	0	0	0
C-3	2	0	0	0	0	0	0	0	0	0	0	0	0	0	0
C-4	2	0	0	0	0	0	0	0	0	0	0	0	0	0	0
C-5	2	0	0	0	0	0	0	0	0	0	0	0	0	0	0
C-6	1	0	0	0	0	0	0	0	0	0	0	0	0	0	0
C-7	2	0	0	0	0	0	0	0	0	0	0	0	0	0	0
C-8	1	0	0	0	0	0	0	0	0	0	0	0	0	0	0
C-9	2	0	0	0	0	0	0	0	0	0	0	0	0	0	0
C-10	1	0	0	0	0	0	0	0	0	0	0	0	0	0	0
C-11	1	0	0	0	0	0	0	0	0	0	0	0	0	0	0
C-12	2	0	0	0	0	0	0	0	0	0	0	0	0	0	0
HSC-1	1	0	0	0	0	0	0	0	0	0	0	0	0	0	0
HSC-2	1	0	0	0	0	0	0	0	0	0	0	0	0	0	0
HSC-3	1	0	0	0	0	0	0	0	0	0	0	0	0	0	0
HSC-4	0	0	0	0	0	0	0	0	0	0	0	0	0	0	0
HSC-5	1	0	0	0	0	0	0	0	0	0	0	0	0	0	0
HSC-6	1	0	0	0	0	0	0	0	0	0	0	0	0	0	0
HSC-7	2	0	0	0	0	0	0	0	0	0	0	0	0	0	0
HSC-8	1	0	0	0	0	0	0	0	0	0	0	0	0	0	0
HSC-9	1	0	0	0	0	0	0	0	0	0	0	0	0	0	0
HSC-10	1	0	0	0	0	0	0	0	0	0	0	0	0	0	0
HSC-11	0	0	0	0	0	0	0	0	0	0	0	0	0	0	0
HSC-12	1	0	0	0	0	0	0	0	0	0	0	0	0	0	0
TD-1	0	0	0	0	0	0	0	0	0	3	0	0	0	0	0
TD-2	1	0	0	0	0	0	0	0	0	3	0	0	0	0	0
TD-3	1	0	0	0	0	0	0	2	0	0	0	0	0	0	0
TD-3	1	0	0	0	0	0	0	0	0	0	0	0	0	0	0
TD-4	1	0	0	0	0	0	0	0	0	0	0	0	0	0	0
TD-5	2	0	0	0	0	0	0	0	0	0	0	0	0	0	0
TD-6	1	0	0	0	0	0	0	0	0	0	0	0	0	0	0
TD-7	1	0	0	0	0	0	0	0	0	2	0	0	0	0	0
TD-8	1	0	0	0	0	0	0	0	0	0	0	0	0	0	0
TD-9	1	0	0	0	0	0	0	0	0	0	0	0	0	0	0

Site	Liver GD	Liver LIP	Liver SCN	Liver INF	Liver MA	Liver SC	Gills ANU	Gills GCN	Gills CCH	Gills MCH	Gills ECH	Gills SLE	Gills P	Gills GINF	Gills F
TD-10	1	0	0	0	0	0	0	2	0	3	0	0	0	0	0
TD-11	1	0	0	0	0	0	0	1	0	0	0	0	0	0	0
TD-12	0	0	0	0	0	0	0	2	0	3	0	0	0	0	0
CS-1	1	0	0	0	0	0	0	0	0	0	0	0	0	0	0
CS-2	1	0	0	0	0	0	0	0	0	0	0	0	0	0	0
CS-3	1	0	0	0	0	0	0	0	0	0	0	0	0	0	0
CS-4	1	0	0	0	0	0	0	0	0	0	0	0	0	0	0
CS-5	1	0	0	0	0	0	0	0	0	0	0	0	0	0	0
CS-6	1	0	0	0	0	0	0	0	0	0	0	0	0	0	0
CS-7	2	0	0	0	0	0	0	0	0	0	0	0	0	0	0
CS-8	1	0	0	0	0	0	0	0	0	0	0	0	0	0	0
CS-9	1	0	0	0	0	0	0	0	0	0	2	0	0	0	0
CS-10	1	0	0	0	0	0	0	0	0	0	2	0	0	0	0
CS-11	1	0	0	0	0	0	0	0	0	0	2	0	0	0	0
CS-12	2	0	0	0	0	0	0	0	0	0	0	0	0	0	0
DWSC-1	2	0	0	0	0	0	0	0	0	0	0	0	0	0	0
DWSC-2	2	0	0	0	0	0	0	0	0	0	0	0	0	0	0
DWSC-3	3	0	0	0	0	0	0	0	0	0	0	0	0	0	0
DWSC-4	1	0	0	0	0	0	0	0	0	0	0	0	0	0	0
DWSC-5	2	0	0	0	0	0	0	0	0	0	0	0	0	0	0
DWSC-6	1	0	0	0	0	0	0	0	0	0	0	0	0	0	0
DWSC-7	2	0	0	0	0	0	0	0	0	0	0	0	0	0	0
DWSC-8	2	0	0	0	0	0	0	0	0	0	0	0	0	0	0
DWSC-9	2	0	0	0	0	0	0	0	0	0	0	0	0	0	0
DWSC-10	2	0	0	0	0	0	0	0	0	0	0	0	0	0	0
DWSC-11	2	0	0	0	0	0	0	0	0	0	0	0	0	0	0
DWSC-12	1	0	0	0	0	0	0	0	0	0	0	0	0	0	0
SRD-1	2	0	0	0	0	0	0	0	0	0	0	0	0	0	0
SRD-2	1	0	0	0	0	0	0	0	0	0	0	0	0	0	0
SRD-3	2	0	0	0	0	0	0	0	0	0	0	0	0	0	0
SRD-4	3	0	0	0	0	0	0	0	0	0	0	0	0	0	0
SRD-5	1	0	0	0	0	0	0	0	0	0	0	0	0	0	0
SRD-6	2	0	0	0	0	0	0	0	0	0	0	0	0	0	0
SRD-7	1	0	0	0	0	0	0	0	0	0	0	0	0	0	0
SRD-8	1	0	0	0	0	0	0	0	0	0	0	0	0	0	0
SRD-9	2	0	0	0	0	0	0	0	0	0	0	0	0	0	0

Site	Liver GD	Liver LIP	Liver SCN	Liver INF	Liver MA	Liver SC	Gills ANU	Gills GCN	Gills CCH	Gills MCH	Gills ECH	Gills SLE	Gills P	Gills GINF	Gills F
SRD-10	2	0	0	0	0	0	0	0	0	0	0	0	0	0	0
SRD-11	1	0	0	0	0	0	0	0	0	0	0	0	0	0	0
SRD-12	2	0	0	0	0	0	0	0	0	0	0	0	0	0	0
MS-1	2	0	0	0	0	0	0	0	0	0	0	0	0	0	0
MS-2	0	0	0	0	0	0	0	0	0	0	0	0	0	0	0
MS-3	2	0	0	0	0	0	0	0	0	0	0	0	0	0	0
MS-4	1	0	0	0	0	0	0	0	0	0	0	0	0	0	0
MS-5	0	0	0	0	0	0	0	0	0	0	0	0	0	0	0
MS-6	1	0	0	0	0	0	0	0	0	0	0	0	0	0	0
MS-7	2	0	0	0	0	0	0	0	0	0	0	0	0	0	0
MS-8	1	0	0	0	0	0	0	0	0	0	0	0	0	0	0
MS-9	2	0	0	0	0	0	0	0	0	0	0	0	0	0	0
MS-10	1	0	0	0	0	0	0	0	0	0	0	0	0	0	0
MS-11	1	0	0	0	0	0	0	0	0	0	0	0	0	0	0
MS-12	2	0	0	0	0	0	0	0	0	0	0	0	0	0	0
GB-1	2	0	0	0	0	0	0	0	0	0	0	0	0	0	0
GB-2	1	0	0	0	0	0	0	0	0	0	0	0	0	0	0
GB-3	1	0	0	0	0	0	0	0	0	0	0	0	0	0	0
GB-4	1	0	0	0	0	0	0	0	0	0	0	0	0	0	0
GB-5	0	0	0	0	0	0	0	0	0	0	0	0	0	0	0
GB-6	1	0	0	0	0	0	0	0	0	0	0	0	0	0	0
GB-7	1	0	0	0	0	0	0	0	0	0	0	0	0	0	0
GB-8	1	0	0	0	0	0	0	0	0	0	0	0	0	0	0
GB-9	2	0	0	0	0	0	0	0	0	0	0	0	0	0	0
GB-10	0	0	0	0	0	0	0	0	0	0	0	0	0	0	0
GB-11	1	0	0	0	0	0	0	0	0	0	0	0	0	0	0
GB-12	1	0	0	0	0	0	0	0	0	0	0	0	0	0	0

(GD) glycogen depletion, (LIP) lipidosis, (SCN) single cell necrosis, (INF) liver inflammation, (MA) macrophage aggregate, (SC) sinusoidal congestion, (ANU) aneurysm, (GCN) epithelial cell necrosis, (CCH) Ionocyte hyperplasia, (MCH) mucus cell hyperplasia, (ECH) epithelial cell hyperplasia, (SLE) secondary lamella edema, (GINF) gill inflammation

This page intentionally left blank

Chapter 7: Patterns and Predictors of Condition Indices in a Critically Endangered Fish

Authors:

Bruce G. Hammock*[,a], Rosemary Hartman[b], Randy A. Dahlgren[c], Catherine Johnston[d], Tomofumi Kurobe[a], Peggy W. Lehman[b], Levi S. Lewis[e], Erwin Van Nieuwenhuyse[f], Wilson F. Ramírez-Duarte[g], Andrew A. Schultz[f], Swee J. Teh[a]

[a]Department of Anatomy, Physiology, and Cell Biology, University of CA, Davis, USA

[b]California Department of Water Resources, West Sacramento, CA, USA

[c]Department of Land, Air, Water, Resources, University of California, Davis, CA, USA

[d]U.S. Fish and Wildlife Service, Lodi, CA, USA

[e]Department of Wildlife, Fish, and Conservation Biology, University of CA, Davis, USA

[f]Science Division, U.S. Bureau of Reclamation Bay-Delta Office, Sacramento, CA, USA

[g]Grupo de Investigación en Sanidad de Organismos Acuáticos, Instituto de Acuicultura de los Llanos, Universidad de los Llanos, Villavicencio, Meta, Colombia

Keywords: Hepatosomatic index; condition factor; estuary; outflow; chlorophyll *a*; temperatura, Delta Smelt

*Corresponding author: brucehammock@gmail.com

Abstract

Condition indices are key predictors of health and fitness in wild fish populations. Variation in body condition, therefore, can be used to identify stressful conditions that may impact endangered species, such as California's endemic Delta Smelt (*Hypomesus transpacificus* McAllister, 1963). Here, we examined spatiotemporal variation in the condition indices of >1600 Delta Smelt collected over nine years (2011-2019), a period characterized by tremendous variability in hydrodynamic and water quality conditions. The population exhibited low hepatosomatic index (HSI) and condition factor (CF) during September/October/November (fall), and both condition indices declined over the nine-year study during fall. HSI was positively correlated with indicators of pelagic productivity (e.g., Chlorophyll *a*, zooplankton biomass, and proximity to tidal wetlands), whereas CF was negatively correlated with temperature, peaking at a relatively cool 10-13 °C. In sum, seasonal and interannual variation in body condition corresponded strongest with pelagic productivity and water temperature, with little correlation to freshwater outflow. Management actions that increase pelagic productivity,

restore and freshen productive wetlands during late summer-fall, and reduce water temperatures overall are likely to benefit condition indices and, therefore, fitness of the Delta Smelt population.

Introduction

Estuaries occur where freshwater from rivers and streams tidally mixes with salt water from the ocean. These ecosystems are typically hotspots for productivity (Hopkinson & Smith, 2005), but also anthropogenic influence, leading to declines in many estuarine fishes. These declines are often attributed to some combination of anthropogenic stressors, including overfishing, freshwater abstraction, climate change, contaminants, invasive species, eutrophication, and habitat loss (e.g., Africa [Guastella, 1994; Baird et al., 1996; James et al., 2018], North America [Hughes et al., 2002; Kemp et al., 2005; Buchheister et al., 2013], South America [Belarmino et al., 2021], Australia [Cottingham et al., 2018]). Thus, understanding the causes of the declines in estuarine fishes, and how those declines can be reversed, are major goals of scientists and managers.

The San Francisco Estuary and Sacramento-San Joaquin Delta of North America (SFE) has many of these same stressors, including freshwater abstraction by pumping plants in the South Delta, contaminants, loss of tidal wetland, and invasive species (Nichols et al., 1986; Kuivila & Moon, 2004), although notably not eutrophication despite high nutrient concentrations (Jassby, 2008). Together, these perturbations are thought to suppress abundance of pelagic fishes (Feyrer et al., 2007, Sommer et al., 2007). One such species is the Delta Smelt (*Hypomesus transpacificus*, McAllister 1963), a small, mostly annual osmerid that is endemic to the SFE (Bennett, 2005). The species spawns in the spring, and has freshwater, brackish water, and migratory phenotypes (Hobbs et al., 2019). Previously one of the most abundant pelagic fishes in the SFE (Moyle et al., 2016), it is currently listed under the California Endangered Species Act and the US Endangered Species Act (USFWS, 1993; California Fish and Game Commission, 2009). Given its historical abundance and small size it was likely an important prey species for SFE fishes, but is too uncommon to meaningfully contribute to the SFE foodweb today (Moyle et al., 2016; Figure 7-1A). The species' habitat overlaps with the largest source of fresh water in California, so water resource management within the SFE aims to prevent further declines in abundance (Moyle et al., 2018). Like many imperiled species, much of the information on the habitat requirements of Delta Smelt is based on its distribution (Jarnevich et al., 2015). However, determining habitat quality based on distribution can be misleading because detrimental habitat is frequently occupied (Weldon & Haddad 2005; Faldyn et al., 2018; Hale et al. 2018), and otherwise high-quality habitat may be unoccupied due to biotic interactions or limited dispersal (Guisan & Thuiller, 2005).

Current information on suitable habitat for Delta Smelt focuses on salinity, temperature, and turbidity, with much of this information coming from abundance and distribution surveys. Delta Smelt occur almost entirely at salinities below 15 (Feyrer et al., 2007), and 90% of the population occurs below a salinity of 7 (Bennett, 2005). The species rarely occurs above 25 °C (Sommer & Mejia, 2013), and the critical thermal maxima of hatchery fish ranges from 24-29 °C, depending on acclimation temperature and life stage (Komoroske et al., 2014). Delta Smelt abundance peaks at turbidities above 12 NTU (Sommer & Mejia, 2013), perhaps because foraging success is improved (Hasenbein et al., 2016), predation risk is lowered (Ferrari et al., 2014), or behavioral changes associated with higher turbidity increase the efficiency of sampling gear. Indeed, stimulating feeding of larval Delta Smelt in culture requires inputs of phytoplankton, which is used to increase turbidity up to 9 NTU (Baskerville-Bridges & Lindberg, 2004; Tigan et al., 2020). However, stomach fullness

in juveniles through adults is not influenced by a wide range of turbidities (0-80 NTU), only shows a small decrease at turbidities above 80 NTU, and Delta Smelt do not require increased turbidity in culture to feed after the larval stage (Baskerville-Bridges & Lindberg, 2004; Hasenbein et al., 2016; Hammock et al., 2019A; Tigan et al., 2020). Thus, the decrease in catch at low turbidity may be unrelated to foraging.

Freshwater outflow is not well correlated with abundance of Delta Smelt (Stevens & Miller, 1983; Dege & Brown, 2004), but there are hints that it is important to the species. A recent study showed that spring recruitment and survival of subsequent life-stages of Delta Smelt were positively correlated with greater outflow (Polansky et al., 2020). However, out of five previous droughts, Delta Smelt abundance rebounded following only two, with warm water temperatures possibly preventing population rebounds following the other three (Mahardja et al., 2021). For example, abundance estimates reached historical lows during a recent, severe drought in California (2012-16), and abundance remained low during the subsequent wet period (Teh et al., 2020; Figs. 1A, 1B). Periods of low outflow are thought to stress the population because the volume of physically suitable habitat becomes restricted by encroaching salinity (Moyle et al., 1992; Bennett, 2005; Feyrer et al., 2011). As the salinity field shifts upstream of the confluence of the Sacramento and San Joaquin rivers, Delta Smelt rapidly loses access to the more seaward portions of its range, including the relatively intact habitat of Suisun Marsh (Moyle, 1992; Feyrer et al., 2011; Figure 7-2). Consequently, late summer into fall may represent a seasonal bottleneck for the species as freshwater flows reach their annual nadir and access to seaward habitat is lost, particularly during droughts.

While multiple stressors are thought to have contributed to the decline of Delta Smelt (Sommer et al., 2007), food limitation may be a primary factor (Maunder & Deriso, 2011; Hamilton & Murphy, 2018). The species' decline, like other pelagic fishes, has roughly coincided with negative exponential declines in primary and secondary pelagic productivity in the SFE (Winder & Jassby 2011; Moyle et al., 2016; Hammock et al., 2019B). Calanoid copepods are a major prey item for Delta Smelt (Nobriga, 2002; Slater & Baxter, 2014), and summer to fall survival is correlated with calanoid copepod biomass (Kimmerer, 2008). Declines in productivity and introductions of invasive zooplankton have caused Delta Smelt to rely on smaller, potentially less nutritious prey items in the fall (Winder & Jassby, 2011; Slater & Baxter, 2014). Several observational studies show that stomach fullness of Delta Smelt varies regionally, increases with mesozooplankton abundance, and increases with tidal wetland proximity, indicating that individuals would consume more prey if conditions were more suitable or prey more available (Hammock et al., 2015; 2017; 2019A).

While much is known regarding the environmental conditions associated with Delta Smelt abundance, far less is known regarding the influence of environmental conditions on Delta Smelt condition. Here, we used a nine-year collection of Delta Smelt to examine spatio-temporal patterns and predictors of the species' condition throughout the upper SFE. The study period encompassed a wide range in hydrologic conditions in California, from wet years (2011, 2017, 2019) to critically dry (2014-15), based on classifications by California Department of Water Resources (Figure 7-1B). The study has two major objectives. In objective one, we describe the influence of region, season, and year-class on condition of Delta Smelt collected from 2011 through 2019 (i.e., spatio-temporal models). Based on previous studies, we hypothesized that Delta Smelt condition would vary regionally, and be lowest during fall and during drought years (Bennett, 2005; Feyrer et al., 2011; Hammock et al., 2015). In objective two, we explore the predictors of Delta Smelt condition to better understand its spatio-temporal drivers (i.e., environmental models). We hypothesized that

Delta Smelt would exhibit relatively poor condition at temperatures above ~20 °C, at low turbidities (<12 NTU), and in fresh water, where foraging is depressed much of the year (Bennett, 2005; Sommer & Mejia, 2013; Hasenbein et al., 2016; Hammock et al., 2017; 2019A, Lewis et al., 2021). We further hypothesized that Delta Smelt condition would decline with decreased phytoplankton abundance, decreased zooplankton biomass, greater distance to tidal wetlands, and under low outflow conditions (Bennett, 2005; Feyrer, 2011; Hammock et al., 2017; 2019A). By quantifying how Delta Smelt condition varies in space and time, and in relation to environmental variation, we aim to inform management efforts to conserve the species. Proposed and ongoing efforts include fall reservoir releases to shift the salinity field seaward, tidal wetland restoration to improve habitat quality and prey availability, and operation of salinity control gates to freshen Suisun Marsh, a region relatively rich in tidal wetlands (Brown, 2003; USFWS, 2008; CNRA, 2016; USFWS, 2019; Sommer et al., 2020).

Materials and Methods

We focused on two indicators of Delta Smelt condition: Hepatosomatic index (HSI; the percentage of body weight comprised by the liver) and Condition factor (CF; body weight divided by fork length cubed; Bolger & Connolly, 1989). We examine HSI and CF for four main reasons. First, both variables are widely used indicators of the general condition of fish, with HSI generally indicating the availability of shorter-term energy reserves (i.e., liver glycogen), protein, and lipid, and CF generally associated with muscle, protein and mesenteric fat (Boujard & Leatherland, 1992; Zamal & Ollevier, 1995; De Pedro et al., 2003; Hards et al., 2019). Second, in a recent experiment on cultured Delta Smelt, HSI was the most sensitive to fasting of the many biomarkers examined, becoming significantly depressed after four days without food at 15.9 °C, and CF was also relatively sensitive to food limitation, becoming significantly depressed after 7 days of fasting (Hammock et al., 2020). The relative sensitivities of these indices make them ideal for assessing environmental conditions, because individuals have less time for movement to homogenize their responses to local conditions. Third, other known stressors in the SFE, such as contaminants and adverse water temperatures, are also known to affect HSI and CF, hence HSI and CF are considered good indicators of general habitat suitability (Bolger & Connolly, 1989; Verma et al., 2019; Morrison et al., 2020). Finally, HSI and CF can correlate with survival, reproductive fitness, and growth, such that changes in both metrics are likely to influence abundance (e.g., Ruthsatz et al., 2018).

HSI and CF were calculated from Delta Smelt collected during fish monitoring surveys conducted by California Department of Fish and Wildlife (CDFW) and United States Fish and Wildlife Service (USFWS). CDFW provided our study with fish at juvenile through adult life-stages throughout the study, from August 2011 through December 2019, collected during three surveys: Fall Midwater Trawl, Spring Kodiak Trawl, and Summer Townet Survey (Honey et al., 2004; Feyrer et al., 2007; Sommer & Mejia, 2013; Damon et al., 2016). However, Delta Smelt became nearly undetectable by CDFW surveys beginning in 2014. Consequently, USFWS began their own, more intensive effort in 2017, the Enhanced Delta Smelt Monitoring survey (EDSM; USFWS et al., 2020). EDSM specifically targets Delta Smelt and provided our study with juvenile through sub-adult life stages from August through November 2017, and July through November 2018 and 2019. Thus, sharply declining abundance led to low sample sizes through the middle of the study (2014-2016), before increasing with the addition of the EDSM samples in 2017 (e.g., annual fall sample sizes in Table 7-1). Together, these surveys covered most of the contemporary range of Delta Smelt.

CDFW and USFWS preserved Delta Smelt using the same method, so although gear types varied among the four surveys it is unlikely that fish condition was affected. Moreover, focusing on a single survey was not an option due to the limited number of fish available from any single survey. Individuals that were caught in trawls were wrapped in labeled aluminum foil packets and immediately frozen in Dewar flasks of liquid nitrogen onboard survey boats. Water temperature, turbidity, specific conductivity, and GPS coordinates were recorded during the trawls and associated with individual fish in a relational database. Dewar flasks were transported to University of California, Davis (UCD) for subsequent measurement and dissection of fish as they thawed (5-10 min per fish; Teh et al., 2016). Each fish was measured for fork length and weighed on an analytical balance. The liver was excised and weighed. HSI was calculated as $HSI = {W_l}/{W_b} \times 100$ and CF was calculated as $CF = {W_b}/{L^3} \times 100$, where W_l is liver weight (mg), W_b is the body weight (mg), and L is the fork length (mm).

Statistical Analysis

To avoid conflating habitat quality with reproductive maturity, all female fish collected during January, February, and March were excluded from analyses (females collected from June-December were left in the analyses; Figure 1-S1). These exclusions eliminated a clear relationship between HSI and fork length (Figure 7-S1C). One fish with a liver enlarged by a tumor was also excluded. In the resulting dataset, HSI and CF were poorly correlated (Figure 7-S2) and therefore provide unique information and required separate analyses. The analyses of HSI and CF were divided into two parts: spatio-temporal and environmental models. The spatio-temporal models are purely descriptive, whereas the environmental models attempt to characterize the mechanisms underlying the spatio-temporal patterns in HSI and CF. Individuals in the dataset ranged in fork length from 21 to 90 mm and females ranged in sexual maturity from immature to early vitellogenic stage (males were not assessed for sexual maturity; Kurobe et al., 2016).

Spatio-temporal Models

Fish were divided into five regions, four seasons, and nine year-classes based on collection location and date. These categories were kept coarse to maintain a sufficient number of samples within each category (e.g., season rather than month; Table 7-S1). The regions analyzed encompass the bulk of the range of Delta Smelt and were described and justified previously (Hammock et al., 2015; Teh et al., 2020). The regions include the Cache Slough Complex, Sacramento River Deep Water Ship Channel (SRDWSC), the confluence of the Sacramento and San Joaquin rivers (the Confluence), Suisun Marsh, and Suisun Bay (Figure 7-2). Briefly, the Cache Slough Complex is a freshwater, relatively shallow area in the North Delta. The SRDWSC is also fresh, and was constructed to allow shipping to access the Port of Sacramento. The Confluence ranges from fresh to brackish and deep to shallow depending on the tide, freshwater outflow and location. Suisun Marsh is a brackish region with relatively intact tidal wetland habitat. Suisun Bay is an open water, brackish region that has both deep and shallow areas. Fish were divided into seasons based on collection date (summer: June-August, fall: September-November, winter: December-February, and spring: March-May). Year-classes began in June (juveniles) and ended the following May (adults), except in a few cases where adult fish from the previous year-class were collected in June (Damon et al., 2016). Large differences in size made these year-class classifications clear. Larvae were not collected as part of this study.

HSI and CF were compared among regions and seasons with mixed model ANOVAs fit to the entire dataset (HSI ~ region + season and CF ~ region + season). Year-class was included as the

random effect in both models to account for possible year effects and sample size imbalance among year-classes. Sample sizes were 1628 and 1749 for the HSI and CF ANOVAs, respectively. Year-class was analyzed separately using ANOVAs for both HSI and CF, using only fish collected during fall (HSI ~ year-class, CF ~ year-class). Only the fall model was fit to a subset of the data, all other models in this study were fit to the entire dataset. We focused on fall because this season is thought to be relatively stressful to Delta Smelt due to low-flow conditions (Moyle et al., 1992; Bennett, 2005; Feyrer et al., 2011), a hypothesis which was confirmed by the seasonal ANOVAs of the full dataset (Figure 7-3). We reasoned that if fall was generally stressful due to low flow, condition indices should improve during wet years. Residual plots were checked for conformity with test assumptions. Significant results for the ANOVAs ($P < 0.05$) were followed by Tukey Honestly Significant Difference (HSD) mean separations. ANOVAs were performed using JMP Pro 15.

Environmental Models

To identify and quantify drivers of spatio-temporal variation in HSI and CF, a series of multiple regression models were compared. Predictors of HSI ($n = 1483$) and CF ($n = 1604$) used in the model comparisons included three variables recorded during trawls: salinity, water temperature, and turbidity. We also examined five additional variables: Chlorophyll *a* concentration (Chl *a*), zooplankton biomass, tidal wetland area, the X2 index (distance from the Golden Gate Bridge [Pacific Ocean] to the bottom isohaline of 2; Jassby et al., 1995), and fork length, which are described below. A correlation matrix of the predictor variables was examined to check for independence ($r < 0.53$ for all pairs), including the relationship between zooplankton biomass and Chl *a* ($r = 0.29$). The 'dredge' function from the R package MuMIn was used to fit all possible main effects models (Barton, 2020). Models were compared using Akaike information criterion corrected for small sample size (AIC_c; Burnham & Anderson, 2002). The five top-ranked HSI and CF models, plus the intercept model, are presented in the results. We also report the effect size for each predictor, the ΔAIC_c of the selected model with and without each predictor, and the p-value for each predictor. Effect sizes were calculated as the percent change in model prediction from the min to the max of each predictor, with the other predictors held constant. The error distributions were Gaussian. However, because HSI is a percentage and is therefore not normally distributed, we fit the same set of models to liver weight as the response variable (log_{10}-transformed), with individual body weight as a predictor. The HSI and liver weight model comparisons yielded nearly identical results, so the HSI model comparison is presented here.

Zooplankton biomass was estimated using zooplankton abundance data from five sources: Environmental Monitoring Program Zooplankton Survey, 20-mm Survey, Summer Townet Survey, Fall Midwater Trawl, and a UCD/United States Bureau of Reclamation (USBR) project that monitored zooplankton in the SRDWSC. The first four datasets were merged following Bashevkin et al. (2020) and then combined with the UCD/USBR-SRDWSC data. See Kayfetz et al. (2020) for full details of the collection and enumeration methods for the first four datasets, but in brief: A 160-µm mesh zooplankton net was mounted on a steel sled and towed obliquely through the water column for ten minutes at sites throughout the SFE. Samples were preserved in formalin and all zooplankton were identified to the lowest feasible taxon at the CDFW Laboratory in Stockton, CA. Samples were identified in 1-mL aliquots on Sedgewick-rafter slides with a concentration of 200-400 organisms per slide. Between 5 and 20 slides were processed per sample. Methods were similar for the UCD/USBR surveys. A vertical tow of the water column was made using a 150-µm mesh zooplankton tow net with a retrieval rate of ~0.33 m/s. Samples were preserved in Lugol's solution and zooplankton were identified to the lowest feasible taxon by BSA Environmental Services

(Beechwood, OH). Zooplankton identifications were made and abundances measured on three 1-ml aliquots using a Wilovert inverted microscope at 100× with a target tally of 200-400 specimens.

All zooplankton samples collected within a region over the course of a month were used to calculate a monthly regional mean of zooplankton biomass to use as an indicator of Delta Smelt prey availability (Figure 7-2). Zooplankton biomass only included taxa common in Delta Smelt diets; all copepods and Cladocera were included, while barnacle nauplii, rotifers, and crab zoea were excluded (Slater & Baxter, 2014). Abundance was converted to biomass (mg carbon) by multiplying by life-stage specific factors from the literature (references and conversion factors in Kayfetz et al., 2020). We note that the estimates of zooplankton biomass leave out important prey for which data were less available, such as amphipods, mysids, and larval fish (Hammock et al., 2019A). Therefore, it is only a proxy for prey availability, and likely is more applicable to younger, more zooplanktivorous fish than for older fish that eat larger prey in addition to zooplankton.

Tidal wetland area was defined as the area of tidal wetlands within a 2-km radius from where each fish was collected and was calculated using ArcGIS as described in Hammock et al. (2019A). The X2 index data were downloaded from the California Department of Water Resources Dayflow website: https://data.cnra.ca.gov/dataset/dayflow. Of the eight predictors examined, the X2 index is under the greatest human control and is therefore of particular interest to scientists and managers. X2 declines with increased flow as the salinity field shifts seaward. Its position is regulated for several reasons, including to avoid contaminating freshwater exports with saltwater from the Pacific Ocean, and to benefit native fishes, including Delta Smelt (Gartrell et al., 2017). Fork length was included as a possible predictor in the CF model comparison to ensure that seasonal changes were not simply due to CF changing with maturation. To ensure that any influence of X2 was not obscured by its inclusion in a complex model (e.g., if X2 appeared less important because tidal wetland area was included in the same model), we also fit HSI and CF to X2 individually (see Supplemental Results).

Chl *a* was measured monthly throughout the range of Delta Smelt by a variety of projects. We merged these data to create a 'Chl *a* index' variable. For 94% of the fish in our analysis, we obtained Chl *a* specific to the five regions in our study (Figure 7-2), measured during the same month as the fish were collected. The data sources were the Discrete Water Quality Environmental Monitoring Program (IEP, 2020), the UCD/USBR-SRDWSC project (which has paired Chl *a* and zooplankton data), and the Liberty Island Study of primary productivity in tidal wetlands by P. Lehman (CA Department of Water Resources). In cases with multiple Chl *a* measurements collected from the same region and month, the measurements were averaged. For the remaining 6% of fish, which were collected in the Cache Slough Complex and the SRDWSC where Chl *a* was not routinely measured, an average of the freshwater Chl *a* measurements by EMP was used (salinity < 0.55), specific to the month of collection. We ran the model comparisons both with and without the 6% of fish lacking associated Chl *a* data and obtained nearly identical results; thus, we present the results that include all fish.

In preliminary analyses, water temperature, salinity, turbidity, and X2 were modeled both as continuous variables and binned in several different ways to account for potential nonlinearities and thresholds. The most predictive variables (lowest AIC_c), and what we present here, were water temperature divided into six bins (7-10, 10-13, 13-16, 16-19, 19-22, and 22-26 °C), salinity divided into fresh and brackish bins (< or >0.55 salinity), turbidity divided into two bins (< or > 80 NTU), and X2 divided into two bins (< and > 80 km). The salinity threshold was used in previous Delta Smelt studies, including as a predictor of foraging success by Hammock et al. (2017) and as a cutoff

between fresh and brackish water life history strategies by Hobbs et al. (2019). The thresholds for turbidity and X2 were initially selected because Delta Smelt foraging success declines at high turbidity (>80 NTU; Hasenbein et al., 2016; Hammock et al., 2019A), and Delta Smelt habitat availability has an inflection point at 80 km (i.e., physical habitat volume declines rapidly above an X2 of 80 km, and vice versa; Feyrer et al., 2011). Chl *a*, fork length, and zooplankton biomass were modeled as continuous, linear predictors.

Zooplankton data were unavailable for 102 fish collected in the SRDWSC and the Cache Slough Complex. Analyses run with and without the zooplankton biomass variable yielded nearly identical results for the other variables. Therefore, the analysis with zooplankton biomass (and without the 102 fish) is presented here. These exclusions left sample sizes of 1483 and 1604 Delta Smelt for the HSI and CF model comparisons, respectively.

Results

Spatio-temporal Models

There were significant differences in HSI among the five regions (ANOVA, $F_{4, 1611} = 11.73$, $P < 0.0001$; Figure 7-4A). The highest HSI means occurred in the Cache Slough Complex and Suisun Marsh, with an intermediate mean in the SRDWSC, and the lowest means in the Confluence and Suisun Bay (Figure 7-4A). The difference between the highest and lowest regional means was 24%. There was also a significant effect of season on HSI (ANOVA, $F_{3, 1570} = 30.16$, $P < 0.0001$; Figure 7-3). Delta Smelt exhibited the lowest mean HSI during fall, an intermediate value in winter, and the highest values in spring and summer. The difference between the highest and lowest mean was 30.0% (i.e., between spring and fall).

There were significant differences among regions in CF (ANOVA, $F_{4, 1722} = 6.32$, $P < 0.0001$; Figure 7-4B), which exhibited a similar pattern to HSI. The highest CF means were observed in the Cache Slough Complex and Suisun Marsh, the SRDWSC and Suisun Bay means were intermediate, and the Confluence had the lowest mean CF (Figure 7-4B). The difference between the highest and the lowest regional mean was 5.6%. There was also a significant effect of season on CF (ANOVA, $F_{3, 1671} = 4.72$, $P = 0.0028$; Figure 7-3), with fish collected during summer and fall having the lowest and next lowest CFs, respectively. Fish collected from winter and spring had the highest CFs. The difference between the highest (spring) and lowest (summer) mean was 8.0%.

Fall HSI showed significant variation among year classes (ANOVA, $F_{8, 365} = 6.76$, $P < 0.0001$), as did CF (ANOVA, $F_{8, 369} = 22.86$, $P < 0.0001$). However, fish collected during drier years did not display poorer condition than in other years (Table 7-2). For example, the 2019/20 year-class, classified as 'wet', had the lowest mean HSI and CF of any year. While the highest CF did occur in 2011/12, a wet year, the highest HSI occurred in 2012/13, a below normal year. Rather than responding to water year type, fall HSI and CF instead declined steadily over the nine-year study (Figure 1-7-1C). The difference between the highest mean fall HSI (2012-13 year-class) and the lowest (2019-20) was 57%. Fall CF also declined over the nine-year study, and the difference between the highest mean fall CF (2011-12 year-class) and the lowest (2019-20) was 10.3%.

Environmental Models

The top-ranked HSI model included seven predictor variables (Table 7-3). Chl *a*, the predictor with the largest effect size, was associated with a 54% increase in HSI (Table 7-4). HSI also increased

substantially with zooplankton biomass (39%) and tidal wetland area (22%; Table 7-4). Temperature was the fourth most important predictor, with the highest HSI occurring between 10 and 13 °C, and the lowest between 16 and 19 °C (Figure 7-5; Table 7-4). HSI also decreased at turbidities over 80 NTU, in brackish habitat (>0.55 salinity), and at X2 >80 km (i.e., HSI declined under low outflow conditions). These last three variables had relatively small effect sizes (<10%, Table 7-4, Figure 7-S3).

There was parity among the top-ranked CF models, so we selected the most parsimonious of the five highest-ranked models, namely the second ranked model (Table 7-5). Temperature and Chl *a* were by far the most important predictors, accounting for effect sizes of 13.0 and 7.8%, respectively (Table 7-4). CF peaked at 10-13 °C and increased with Chl *a*. CF also increased with tidal wetland area, but to a lesser extent (Figure 7-6; Table 7-4). CF was higher under lower outflow conditions (X2 >80; Figure 7-6D), the opposite of X2's influence on HSI. Fork length was not a significant predictor of CF (Figure 7-S4).

Habitat Characterization

Means by region, season, and year-class (during fall only) of the four most important HSI and CF predictors are presented in Table 7-1, including Chl *a*, water temperature, zooplankton biomass, and tidal wetland area. These means reflect what the fish were experiencing at the time of collection, and do not necessarily represent the region, season or year-class overall. Notable results include relatively high Chl *a* and zooplankton biomass and low temperature during fall 2012, a period that coincided with collections of relatively good condition fish (Figure 7-1C, Table 7-1). Summer and fall, the seasons with the worst condition fish, had considerably higher temperatures and lower Chl *a* concentrations than spring, when fish were in relatively good condition (Figure 7-3).

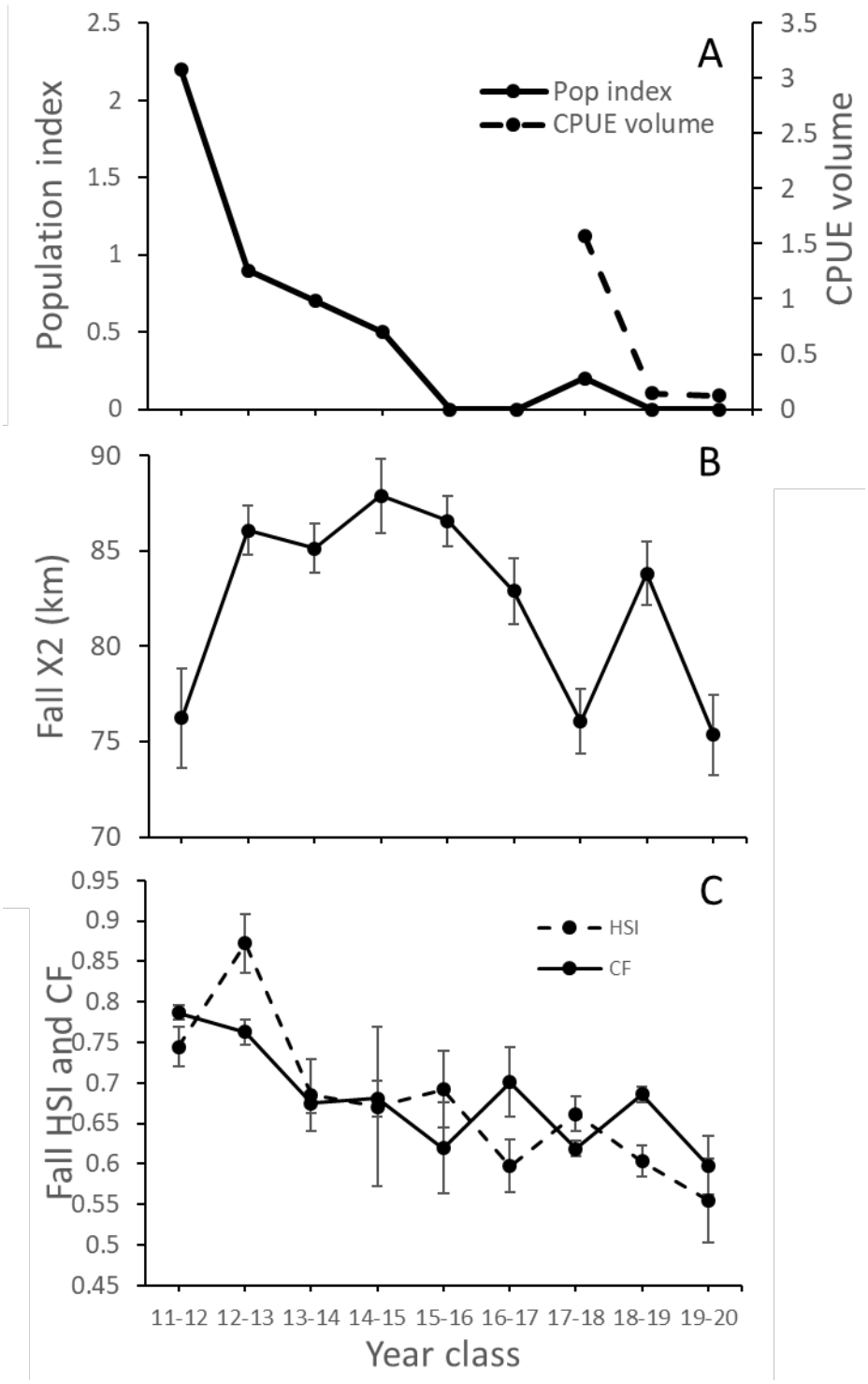

Figure 7-1. Delta Smelt abundance estimates (panel A), mean fall X2 (distance from the Pacific Ocean to the bottom isohaline of 2; panel B), and HSI and CF (panel C) during fall, by year-class (fall includes September, October, November).

Nomenclature 11-12 is the 2011-12 year-class, 12-13 is the 2012-13 year-class, etc. (e.g., 11-12 refers to the year-class of Delta Smelt that hatched in 2011 and reached sexual maturity in 2012). The solid line in panel A is the Delta Smelt

population index, calculated from CDFW's Fall Midwater Trawl (details in Miller et al., 2012; https://www.dfg.ca.gov/delta/data/townet/indices.asp?species=3). The dashed line in panel A is Delta Smelt catch per unit effort (water volume sampled, in units of m^3 × 10,000) calculated from USFWS Kodiak trawls (Enhanced Delta Smelt Monitoring Program [EDSM]). Note: EDSM's CPUE values and CDFW's population index in Panel A are not directly comparable. EDSM's sampling effort is more intensive, so the survey detects Delta Smelt even when CDFW's population index is zero. The three lowest X2 values in panel B correspond to three years classified as 'wet' by CA Department of Water Resources. The two highest values of X2 correspond to 'critically dry' years (2014-15 and 2015-16; https://cdec.water.ca.gov/reportapp/javareports?name=WSIHIST). For panel C, n = 131, 34, 11, 8, 5, 7, 81, 98, and 13 for each year-class (fall). Error bars are ±SD in panel B and ±SE in panel C.

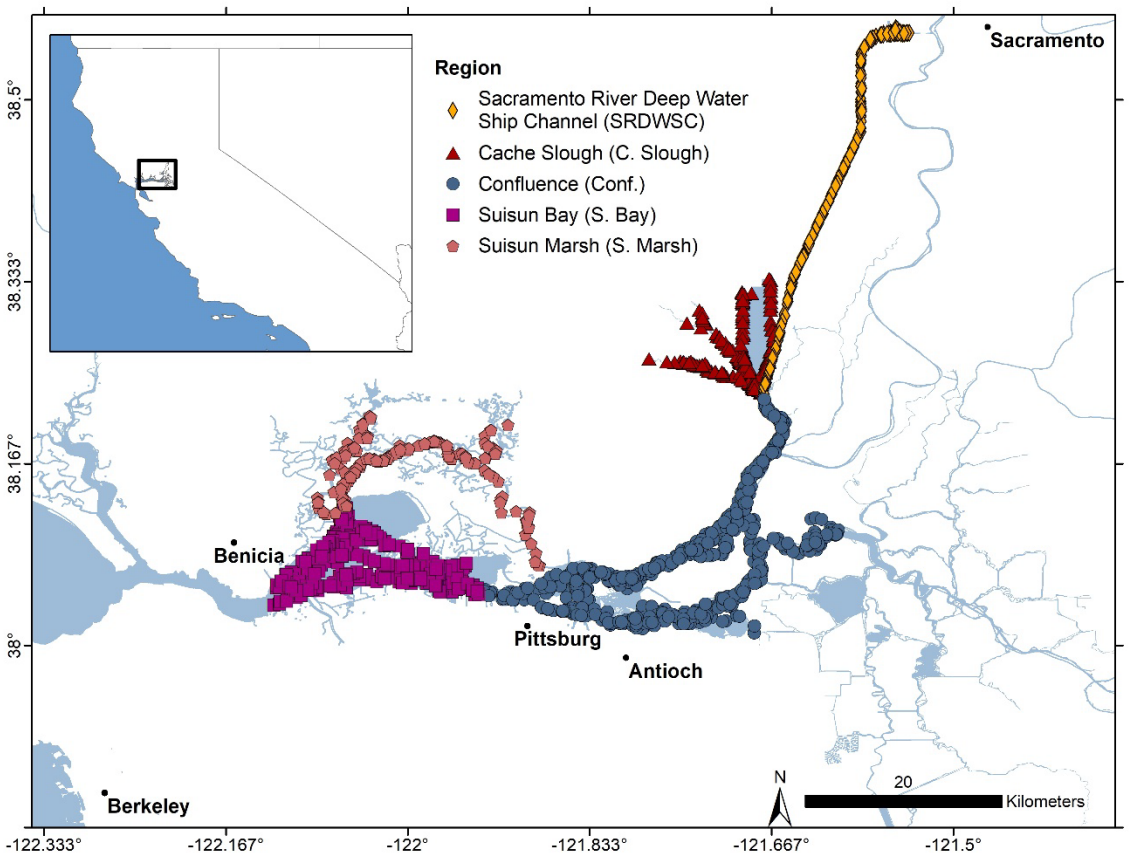

Figure 7-2. Study area within the Sacramento-San Joaquin Delta and San Francisco Estuary (SFE; CA, USA).

The map depicts the five regions from which Delta Smelt were collected and compared in terms of HSI and CF. Each point represents an EDSM trawl site. CDFW fish were collected from the same five regions.

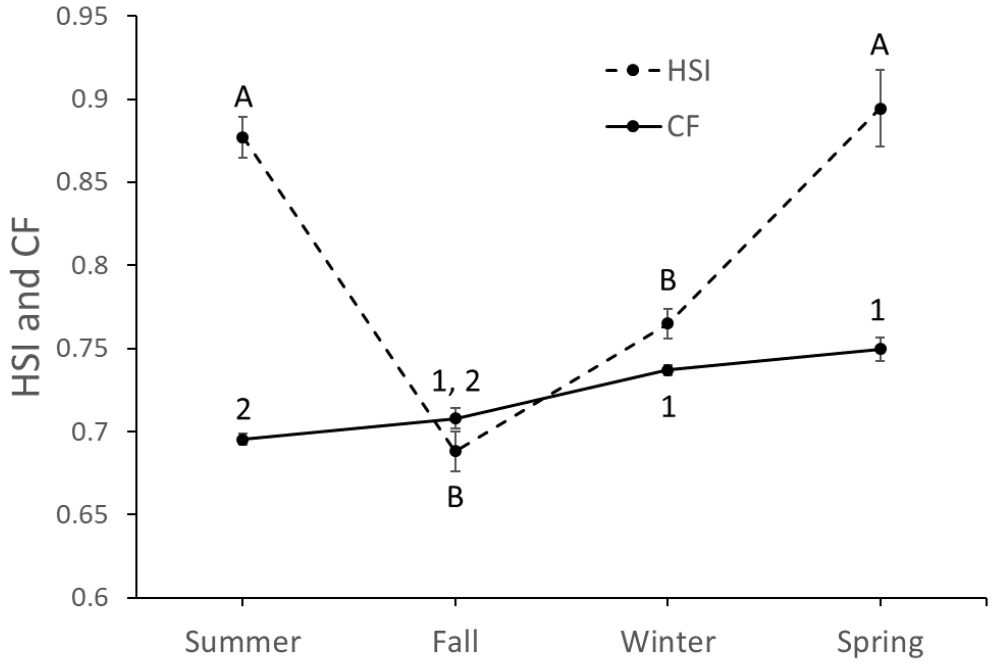

Figure 7-3. Hepatosomatic index (HSI: dashed line) and condition factor (CF: solid line) by season, averaged across years.

For HSI, n = 491, 374, 603, and 160 for each season, left to right. For CF, n = 607, 378, 603, and 161, left to right. Differing letters represent significantly different HSI means and differing numbers represent significantly different CF means ($P < 0.05$; Tukey HSD).

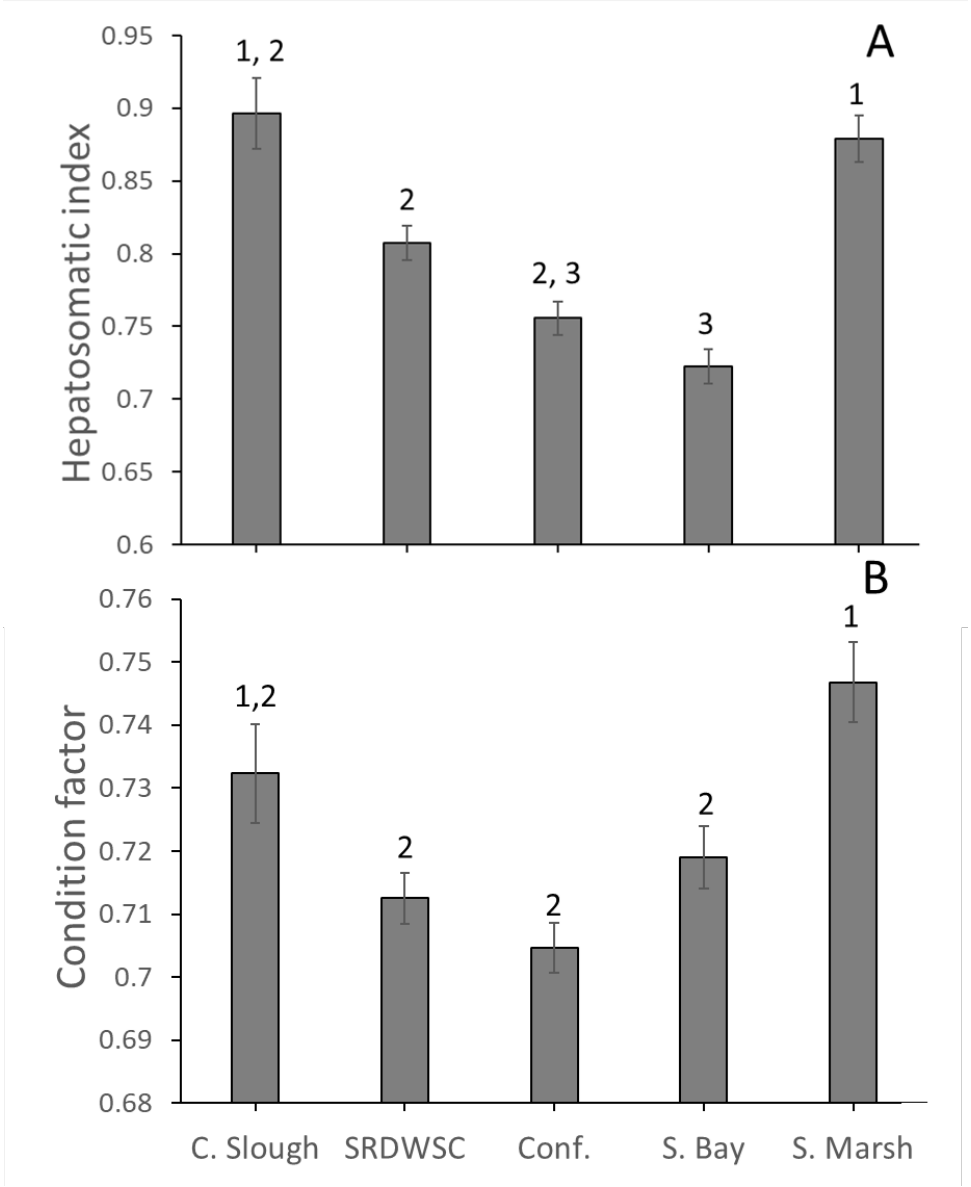

Figure 7-4. Mean (±SE) HSI (panel A) and CF (panel B) by region, averaged across all seasons.

For HSI, sample sizes for each region were 126, 533, 461, 293, and 215, left to right. For CF, sample sizes for each region were 130, 577, 520, 304, and 218, left to right. Note that only 5 of the 126 fish collected from the Cache Slough Complex were from the fall, the season with the lowest mean HSI (Figure 7-3). Differing numbers above the bars denote significant differences based on Tukey HSD tests.

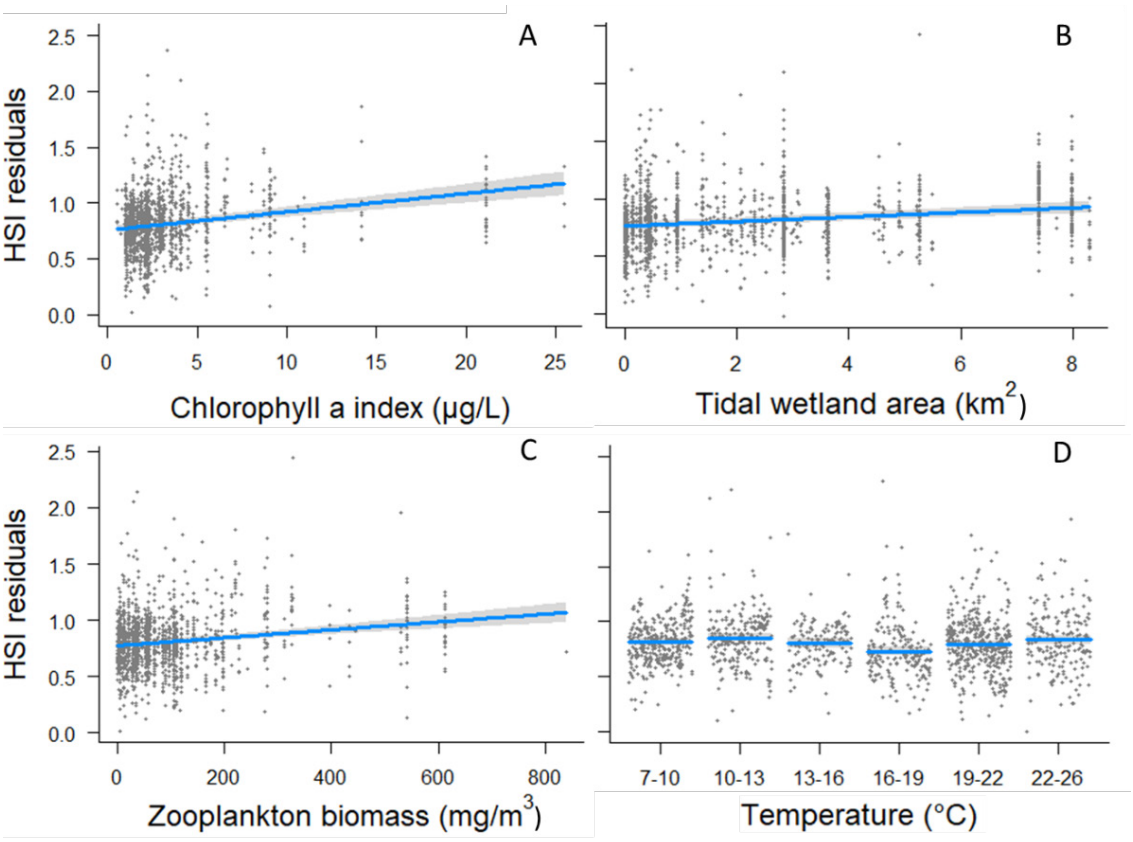

Figure 7-5. Partial residuals from the selected (top-ranked) environmental HSI model (Table 7-3).

Fish from all seasons were included in the analysis. The four variables with the largest effect sizes are presented here; the other three variables are displayed in Figure 7-S3 (effect sizes in Table 7-4). The shaded regions are 95% confidence intervals of the model. Water temperature was binned to capture possible nonlinearities.

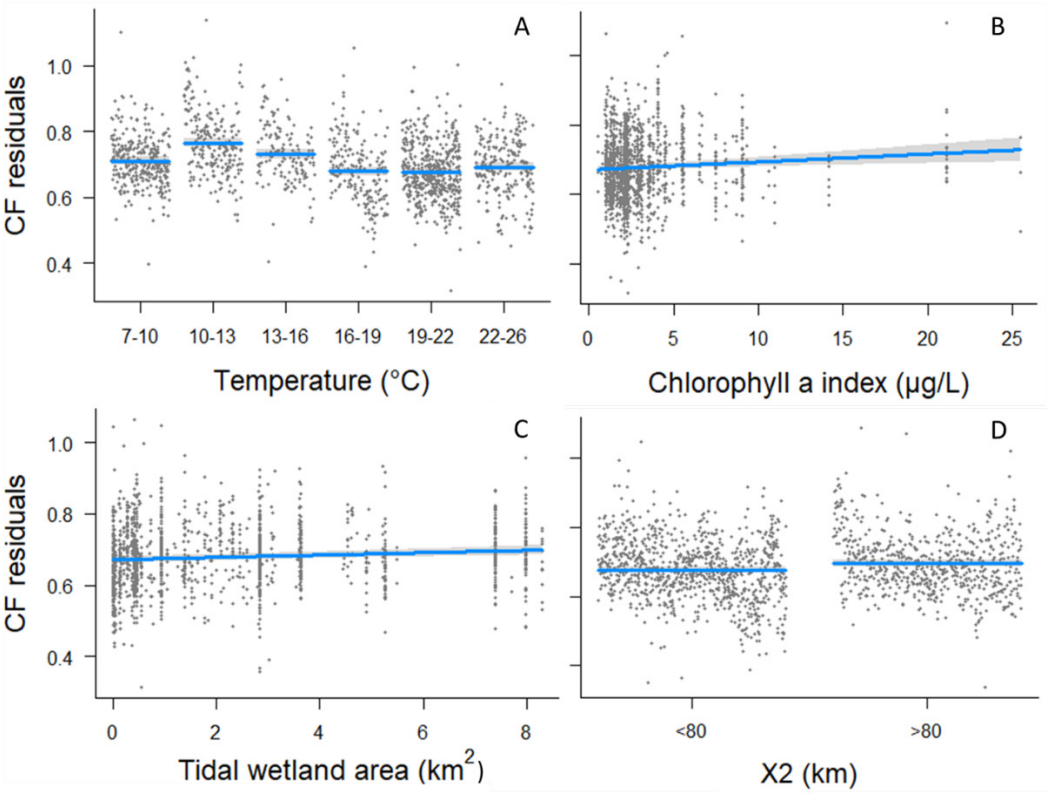

405

406 Figure 7-6. Partial residuals for each variable in the selected (2nd ranked) environmental
407 CF model (Table 7-5).

408 Fish from all seasons were included in this analysis. The shaded regions are 95% confidence intervals of the model.
409 Temperature was binned to detect possible nonlinearities, and X2 was binned because Delta Smelt habitat volume
410 shrinks rapidly above an X2 of 80 km. Effect sizes are in Table 7-4.

411

Table 7-1. Mean Chl *a* (µg/L), water temperature (Temp; °C), zooplankton biomass density (Zoop; mg/m^3), tidal wetland area (TW; km^2), and sample size (after removal of sexually mature females) by region, season, and year-class (YC).

The year-class data only include fish collected during fall (September-November), while the regional and seasonal means include all data. Note that the means represent the average conditions that the fish were experiencing at collection, and do not necessarily represent the region, seasons, and years overall. Water temperature was measured during trawls and tidal wetland area was estimated using ArcGIS (Hammock et al., 2019A). Chl *a* and zooplankton biomass were not measured during trawls, but obtained from ancillary studies.

Region/Season/Year-class	Chl *a*	Temp	Zoop	TW	n
C. Slough	4.4	16.8	109.7	0.5	126
SRDWSC	3.7	16.9	150.2	1.7	533
Conf.	2.7	15.1	155.5	1.6	461
Suisun Bay	2.2	16.8	71.4	2.2	292
Suisun Marsh	3.0	13.6	20.3	6.8	215
Summer	3.8	21.5	232.1	1.7	490
Fall	3.3	18.1	83.1	1.9	374
Winter	1.9	9.7	16.7	3.1	603
Spring	4.5	13.9	74.2	2.6	160
11-12	2.4	17.3	43.2	3.1	121
12-13	13.6	17.0	198.2	2.0	34
13-14	1.9	17.6	104.6	2.4	11
14-15	2.9	21.1	219.6	0.5	8
15-16	2.1	22.2	178.0	0.4	5
16-17	1.5	16.9	35.9	0.6	7
17-18	2.1	17.9	139.1	1.9	81
18-19	2.2	19.4	120.6	0.6	98
19-20	2.7	19.4	120.6	1.4	13

Table 7-2. Fall HSI and CF mean comparisons following the significant ANOVA.

The water year type refers to CA Department of Water Resources water year classifications for the Sacramento River Valley. Year-classes with the same letter are not significantly different (Tukey HSD).

Year-class	Water year type	HSI	HSI group	CF	CF group
2011-12	Wet	0.744	A, B	0.786	A
2012-13	Below normal	0.872	A	0.763	A, B
2013-14	Dry	0.685	A, B, C	0.675	B, C, D
2014-15	Critically dry	0.670	A, B, C	0.680	A, B, C, D
2015-16	Critically dry	0.692	A, B, C	0.619	B, C, D
2016-17	Below normal	0.597	A, B, C	0.701	A, B, C, D
2017-18	Wet	0.662	B, C	0.619	D
2018-19	Below normal	0.603	C	0.686	C
2019-20	Wet	0.555	B, C	0.598	C, D

Table 7-3. Comparison of the top five environmental HSI models, plus the intercept model.

The first-ranked model was selected. Chl *a* is chlorophyll *a* as a continuous variable, 'Sal' is a dummy variable for salinity (< or >0.55), 'Temp' is temperature bin (7-10, 10-13, 13-16, 16-19, 19-22, 22-26 °C), 'Turb' is a dummy variable for turbidity (< or >80 NTU), 'TW' is tidal wetland area, 'X2' is a dummy variable for the X2 index (< or >80 km), and 'Z' is zooplankton biomass.

Model	df	ΔAIC_c	Weight
~Chl *a* + Sal + Temp + Turb + TW + X2 + Z	13	0.00	0.76
~Chl *a* + Sal + Temp + TW + X2 + Z	12	2.47	0.22
~Chl *a* + Sal + Temp + Turb + TW + Z	12	9.64	0.01
~Chl *a* + Sal + Temp + TW + Z	11	10.21	0.00
~Chl *a* + Temp Turb + TW + Z	12	11.53	0.00
~Intercept	2	206.5	<0.0001

df degrees of freedom, ΔAIC_c difference between model of interest and top-ranked model in Akaike Information Criterion Units corrected for small sample size, *Weight* AIC_c weight.

Table 7-4. Effect size, ΔAIC_c, and p-value for each variable in the selected environmental HSI and CF models.

Effect sizes were calculated as the percent change in model prediction from the min to the max of each predictor, with the other predictors held constant. ΔAIC_c is the difference in AIC_c between the selected model with and without each variable. Chl *a* is chlorophyll *a* as a continuous variable, 'Zoop' is zooplankton biomass density, 'Wetlands' is tidal wetland area, Temp is temperature bin (7-10, 10-13, 13-16, 16-19, 19-22, 22-26 °C), 'Turb' is a turbidity dummy variable (< or >80 NTU) , 'Sal' is a salinity dummy variable for fresh vs brackish (< or >0.55), and 'X2' is a dummy variable for the X2 index (< or >80 km). The sign in parentheses indicates the sign of each parameter, if applicable.

Effect size, ΔAIC_c, P-value	**Response**	**Chl *a***	**Zoop**	**Wetlands**	**Temp**	**Turb**	**Sal**	**X2**
Effect size	HSI	54.3 (+)	38.7 (+)	21.9 (+)	16.9 (NA)	8.6 (-)	7.7 (-)	6.3 (-)
ΔAIC_c	HSI	52.2	27.8	41.0	19.2	2.5	11.5	9.6
P-value	HSI	<0.0001	<0.0001	<0.0001	<0.0001	0.0102	0.0002	<0.0001
Effect size	CF	7.8 (+)	-	3.7 (+)	13.0 (NA)	-	-	2.8 (+)
ΔAIC_c	CF	7.1	-	10.5	163.7	-	-	16.0
P-value	CF	0.0002	-	0.0025	<0.0001	-	-	<0.0001

Table 7-5. Model comparison of the top five environmental CF models, plus the intercept model.

The second-ranked model was selected. Chl *a* is chlorophyll *a* as a continuous variable, 'Sal' is a dummy variable for salinity (< or >0.55), 'Temp' is temperature bin (7-10, 10-13, 13-16, 16-19, 19-22, 22-26 °C), 'Turb' is a dummy variable for turbidity (< or >80 NTU), 'TW' is tidal wetland area, 'X2' is a dummy variable for the X2 index (< or >80 km), and 'Z' is zooplankton biomass.

Model	**df**	**ΔAIC_c**	**Weight**
~Chl *a* + Temp + TW + X2 + Z	11	0.00	0.21
~Chl *a* + Temp + TW + X2	10	0.37	0.18
~Chl *a* + Sal + Temp + TW + X2 + Z	12	0.39	0.18
~Chl *a* + Sal + Temp + TW + X2	11	0.82	0.14
~Chl *a* + Temp + TW + X2 + Z +Turb	12	1.93	0.08
~Intercept	2	204.7	<0.0001

df degrees of freedom, *ΔAIC_c* difference between model of interest and top-ranked model in Akaike Information Criterion Units corrected for small sample size, *Weight* AIC_c weight.

Discussion

Delta Smelt is nearing extinction in the wild, and a large body of work suggests that food limitation is a major contributor to its decline (Kimmerer, 2008; Maunder & Deriso, 2011; Hamilton & Murphy, 2018). In a recent laboratory study, HSI and CF responded relatively rapidly to food limitation in Delta Smelt, and are therefore sensitive metrics for evaluating the quality of habitat

from which individuals are collected (Hammock et al., 2020). In objective one of our study, we assessed the spatio-temporal variation in HSI and CF of more than 1600 Delta Smelt collected over nine years (2011-2019). Relatively poor condition indices were observed in Suisun Bay and the Confluence (Figure 7-4), and during fall (Figure 7-3). Relatively good condition indices were observed in Suisun Marsh and C. Slough (Figure 7-4), and during spring (Figure 7-3). We also observed a steady decline in both HSI and CF during fall over the nine-year study, a period of tremendous hydrologic variability (Figs. 1B, C). Given that HSI and CF are tightly coupled to fitness and survival (e.g., Robinson et al., 2008; Mion et al., 2018), which dictate the population dynamics of fishes (Maunder & Starr, 2003; Rose et al., 2013), the downward trajectory in both condition indices is alarming.

In objective two, we identified and quantified predictors of HSI and CF using model comparisons. Conditions that were most strongly associated with improved Delta Smelt condition indices were high Chl *a*, low water temperature (10-13 °C), high zooplankton biomass, and proximity to tidal wetlands (Figs. 5 and 6). The range in condition indices of wild Delta Smelt observed in this study are likely to be ecologically meaningful because the range in HSI and CF of wild fish spanned roughly 2/3 of the difference between fully-fed and severely-starved hatchery Delta Smelt (i.e., fasted three weeks at 15.9 °C; Hammock et al., 2020). We note that although HSI varied more than CF with its predictors (i.e., the effect sizes were larger; Table 4), the HSI results should not be considered more important because a far smaller change in CF than HSI indicates an equivalent level of starvation (Hammock et al., 2020). For example, 21 days of fasting resulted in significant declines in both HSI and CF, but the effect sizes were 131% and 32%, respectively (Hammock et al., 2020). Although turbidities less than 80 NTU improved HSI somewhat, we found no change in HSI and CF from 0 - 80 NTU. The 0 - 80 NTU turbidity range also did not influence Delta Smelt foraging success (Hammock et al., 2019A), suggesting that the decline in catch at turbidities below 12 NTU is unrelated to stressors that affect condition indices, such as food limitation (Sommer & Mejia, 2013).

The regional patterns we observed in HSI and CF are consistent with previous studies. Hammock et al. (2015) reported depressed stomach fullness, RNA-DNA ratio in muscle, HSI, and CF in Suisun Bay and the Confluence, whereas fish collected from Suisun Marsh had relatively good nutritional and condition indices. Here we observed this same pattern in HSI and CF (Figure 7-4), but over more years and seven times the sample size. Hobbs et al. (2006) also reported better Delta Smelt feeding success in the north of Suisun Bay, near Suisun Marsh. The Cache Slough Complex appeared to be beneficial to Delta Smelt condition, which is consistent with several studies indicating that the region is an important area for Delta Smelt and other native fishes due to its relatively high productivity, zooplankton abundance and historical spawning of Delta Smelt (Sommer et al., 2011; Sommer & Mejia, 2013; Kimmerer et al., 2018A). The model comparison suggests that causes for regional differences may include low Chl *a* in Suisun Bay and the Confluence, and low zooplankton biomass in Suisun Bay (Table 1). Although zooplankton biomass was even lower in Suisun Marsh (Table 1), this may have been offset by lower water temperature and the prevalence of tidal wetlands in the region, which improves foraging success of Delta Smelt (Table 1, Bever et al., 2016; Hammock et al., 2019A; Sommer et al., 2020). For example, tidal wetlands provide key nursery habitat for larval fishes, an important prey item for Delta Smelt that was not captured by our zooplankton biomass metric (Beck et al., 2001; Hammock et al., 2019A).

Although our results are consistent with the hypothesis of a survival bottleneck during summer into fall (Figure 7-3), they are less consistent with the proposed mechanism of decreased access to more

seaward habitat (Moyle et al., 1992; Bennett, 2005; USFWS, 2008; Feyrer et al., 2011). As outflow declines, salt water encroaches on the seaward portions of Delta Smelt habitat, restricting the species to more channelized habitat upstream (Feyrer et al., 2011). This mechanism is the basis for targeting late summer and fall with several management actions designed to benefit the species, including reservoir releases and freshening Suisun Marsh with tidally timed salinity control gate operations (Sommer et al., 2020). In our study, while an improvement in HSI for fish collected in fresh water was observed, the effect size was modest (Table 4). In addition, X2 had only a minor influence on HSI and CF and its effects were in opposing directions, even when X2 was used as the only predictor (Figs. 6D and S3D, Supplemental Results). In addition, despite the tremendous range in hydrologic conditions in the SFE during the study, HSI and CF steadily declined (Figure 7-1). In fact, fall 2019 exhibited both the lowest X2 (wettest conditions) and poorest condition Delta Smelt in our study (Figure 7-1). Rather than being driven by low outflow, the modeling results suggest that fall condition indices of Delta Smelt declined over the nine-year study due to some combination of low pelagic productivity and high water temperatures.

The lack of a clear relationship between X2 and Delta Smelt condition is consistent with other studies that found an unclear or inconsistent relationship between Delta Smelt population indices and outflow or X2 (e.g., Stevens & Miller, 1983; Kimmerer, 2002; Dege & Brown, 2004; Bennett, 2005; Miller et al., 2012). However, our results present an apparent paradox. While X2 does not correlate with Delta Smelt condition, two variables with well established relationships to X2 did correlate with improved condition: collection from Suisun Marsh and proximity to tidal wetlands. That is, Delta Smelt have greater access to Suisun Marsh and tidal wetlands as outflow increases, but X2 had little overall influence on condition, even when modeled on its own. One possibility is that while high outflow provides Delta Smelt access to higher quality habitat, it may also reduce phytoplankton and zooplankton abundance by advection. Another possibility is that low X2 increases accessibility to both high and low quality habitat, possibly offsetting the benefits of low X2 to Delta Smelt. In any case, our results suggest that low flow is not the primary driver of poor condition indices of Delta Smelt during summer and fall. Instead, the seasonal analysis, in combination with the environmental modeling, suggests that the poor CF during summer was driven largely by high water temperature, whereas poor HSI during fall was driven more by food web related factors (Chl *a*, zooplankton, and tidal wetland access). We note, however, that abundance of Delta Smelt is generally suppressed during dry years (Figure 7-1), suggesting that increased flow may benefit Delta Smelt abundance, even if it does not appear to improve condition.

None of the predictors of HSI and CF is necessarily causative, but Chl *a* seems especially likely to be a proxy for another key variable. Condition indices may have increased with Chl *a* because the chronically low secondary productivity of the SFE was stimulated by increased phytoplankton concentrations, leading to improved foraging success and condition. For example, increased productivity is thought to explain the positive relationship between Chl *a* and larval abundance of another osmerid endemic to the SFE, the Longfin Smelt (*Spirinchus thaleichthys* Ayres, 1860; Grimaldo et al., 2017). However, the relationship between Chl *a* and zooplankton is complex. While zooplankton generally increases with Chl *a* in other systems (McCauley & Kalff 1981; Yuan & Pollard, 2018), Chl *a* is a poor predictor of zooplankton biomass in the SFE (Montgomery et al., 2015; Kimmerer et al., 2018B), and a poor predictor of production for some of the major copepods that make up Delta Smelt diets (Kimmerer et al., 2014; Slater & Baxter 2014; Jungbluth et al., 2021). Moreover, Chl *a* was a stronger predictor of HSI and CF than zooplankton biomass (Table 4), suggesting that stimulation of secondary productivity is not the primary cause for the association between Chl *a* and condition indices. Another possibility is that the energetic costs for Delta Smelt

546 decline with longer residence times, and longer residence times also favor phytoplankton. For
547 example, many fish avoid fast water to reduce energy expenditure (Bisson et al. 1988; Korman &
548 Campana, 2009), including migrating Delta Smelt (Bennett & Burau 2015; Bever et al., 2016).
549 Elevated phytoplankton levels may also improve foraging success and condition, as they do for
550 larval Delta Smelt in captivity (Baskerville-Bridges & Lindberg 2004; Bennett & Burau, 2015; Tigan
551 et al., 2020). Thus, elevated phytoplankton, or the conditions associated with it, appear to confer
552 substantial benefit to Delta Smelt, but the reasons remain unclear.

553 Water temperature was the most important predictor of CF, peaking in the 10-13 °C range, likely
554 because metabolic demand of Delta Smelt was low. Delta Smelt also exhibited the highest HSI at
555 10-13 °C, although the differences in model predictions across the temperature range were small.
556 Lewis et al. (2021) largely corroborates our temperature results, reporting that Delta Smelt growth
557 peaked in the 12-13 °C range, and declined rapidly over 20 °C. However, Lewis et al. (2021) does
558 not corroborate the small but surprising secondary peak in HSI at 22-26 °C, which is likely due to
559 another, unknown variable associated with summer, rather than a direct benefit of high water
560 temperature on HSI (Figure 7-5D). The far more pronounced influence of temperature on CF may
561 be due to differences in the biochemical pathways underlying short versus long-term energy storage.
562 It may indicate an evolutionary strategy that favors lipid accumulation in muscle and mesenteric fat,
563 and muscle growth over liver glycogen accumulation at low temperatures. For example, evidence of
564 increased energy substrate mobilization (i.e., amino acids) was reported in salmonid species after
565 prolonged exposure to high temperatures, which could be an indication of enhanced protein
566 catabolism (Liu et al., 2019) or a reflection of increased lipolysis or decreased lipid accumulation in
567 muscle and mesenteric adipose tissue, as showed for Atlantic Salmon exposed to high water
568 temperature (Kullgren et al., 2013). Given that optimal body condition occurred at 10-13 °C, which
569 is 10-15 °C below the critical thermal maximum of hatchery Delta Smelt (Komoroske et al., 2014), it
570 is likely that greater foraging success would increase the optimal temperature range of wild Delta
571 Smelt, as in other fishes (e.g., Lusardi et al., 2019). Under the current, oligotrophic conditions of the
572 SFE, however, water temperatures above 13 °C depressed Delta Smelt body condition (Figure 7-
573 6A).

574 Assuming that poor fall condition indices lead to depressed abundance, our study is more consistent
575 with bottom-up rather than top-down causes of Delta Smelt declines. Predators, parasites, or disease
576 could have depressed Delta Smelt condition directly or indirectly, but there is no evidence that any
577 of these factors became progressively more pronounced during the study, and parasites and
578 parasitoids are rare in wild Delta Smelt (He & Kitchell, 1990; Foott & Bigelow, 2010; Teh et al.,
579 2020). Entrainment in the South Delta pumps, another top-down effect, could not have caused the
580 steady, nine-year decline in fall HSI and CF (Grimaldo et al., 2021; Korman et al., 2021). However,
581 the pumping plants may contribute to depressed condition indices via bottom-up effects if water
582 exports suppress phytoplankton abundance (Hammock et al., 2019B). Contaminants, another
583 stressor for Delta Smelt (Kuivila & Moon, 2004; Teh et al., 2020), could depress condition indices
584 (e.g., Verma et al., 2019). However, liver condition of Delta Smelt improved substantially from 2011-
585 16 (Teh et al., 2020), even as fall condition indices and overall abundance of Delta Smelt declined
586 (Figs. 1A, C). In addition, the strongest evidence for contaminants in the SFE comes from the
587 Cache Slough Complex (Werner et al., 2000; Kuivila & Moon, 2004; Weston et al., 2014; 2019),
588 which was highly underrepresented during fall in our study. The best fall condition indices occurred
589 in 2012 during a period of relatively high phytoplankton and low water temperature for our Delta
590 Smelt collections (Figure 7-1C; Table 1). More recently, fall conditions were generally characterized
591 by low Chl *a* and high water temperature (e.g., 2015-16, Table 1). Thus, our results suggest that low

Chl *a* and high water temperatures have contributed substantially to declines in Delta Smelt condition indices.

Management Implications

The downward trajectory in fall condition indices and abundance shows a species at increasing risk of extinction, but there may be ways to improve environmental conditions for Delta Smelt. Our results are consistent with the USFWS Biological Opinion and CDFW Incidental Take Permit that specifically target fall for management actions to benefit the species (USFWS, 2019; CDFW, 2020). Increasing Chl *a* appears to be a promising option to improve conditions for Delta Smelt because it was associated with the largest improvement in HSI, and the second largest improvement in CF (Figs. 5A and 6B). In addition, increasing Chl *a* may increase zooplankton biomass (Williams & Poulet 1986; Mozetič et al., 2012), which was also associated with improved HSI (Figure 7-5C). However, the success of management actions to increase Chl *a* likely depend on the composition of the primary producer community, and the method used. For example, stimulating primary production with nutrient addition may not improve conditions for Delta Smelt if the primary producers are toxic or provide poor quality food for zooplankton (Cloern, 2018; Ger et al., 2018). The cyanobacterium *Microcystis* has increased within the SFE since 1999, and fish exposed to the microcystin toxins it produces exhibit reductions in condition indices (Lehman et al., 2010; Acuña et al., 2012A; 2012B; 2020). Moreover, the correlation between Delta Smelt and Chl *a* concentration may not represent a food web link. For example, perhaps Delta Smelt and phytoplankton both benefit from longer hydrologic residence times, and phytoplankton does not provide a benefit itself. In this case, nutrient additions would not be expected to benefit Delta Smelt, even if they stimulate phytoplankton growth. Thus, understanding why Chl *a* correlates with improved condition indices, and whether primary producer community structure explains additional variation in condition indices, are key next steps.

Multiple outflow-related actions geared toward benefitting Delta Smelt habitat and ultimately its population are ongoing or planned (USFWS, 2008; CNRA, 2016; USFWS, 2019). Operation of the salinity control gates to freshen Suisun Marsh should benefit Delta Smelt, because the region is associated with improved condition indices, as is fresh water itself (Figs. 4, S3; Sommer et al., 2020). We found little evidence that fall reservoir releases would benefit Delta Smelt because X2 had little net influence on the condition indices, and the poorest condition fish occurred during the fall with the lowest X2 (Figure 7-1). This stated, high outflow years with low fall X2 may produce system-wide beneficial effects beyond the scope of our study (IEP-MAST, 2015). Potential for flow actions to have the desired ecological effects may increase the more their design mirrors the natural seasonal hydrograph that the system's native biota evolved with, and fall historically was the period of the year when flow was lowest (Propst & Gido, 2004; Kiernan at al., 2012; Schultz et al., 2019). While it is uncertain to what extent managers can influence water temperature (Sommer et al., 2020), especially in a warming world, management actions to decrease water temperature during summer would almost certainly improve Delta Smelt CF (Figure 7-3, Table 4). Finally, our results suggest that efforts to restore tidal wetland in the SFE should benefit Delta Smelt condition (Brown, 2003).

Conclusions

This study examined the predictors of HSI and CF of more than 1600 Delta Smelt collected over nine years (2011-2019), a period of tremendous variability in hydrodynamic and water quality conditions. The population exhibited low HSI and CF during September/October/November,

supporting the long-standing hypothesis that the species is disproportionately stressed during fall. Chlorophyll *a*, zooplankton biomass, and proximity to tidal wetlands were all positively associated with HSI. Water temperature was the strongest predictor of CF, with condition peaking at 10-13 °C, and exhibiting its worst level during summer. X2, a correlate of outflow, was a poor predictor of Delta Smelt condition overall. Our results therefore suggest that the condition of Delta Smelt during fall declined over the nine-year study largely due to a combination of low pelagic productivity and high water temperatures. Management actions to increase primary and secondary pelagic productivity, freshen Suisun Marsh during late summer and fall, restore tidal wetlands, and decrease water temperature should benefit condition indices of Delta Smelt, and therefore population fitness.

Declarations

Funding: Funding was provided by US Bureau of Reclamation R17AC00129, US Geological Survey G15AS00018, and CDFW Ecosystem Restoration Program E1183004.

Conflicts of Interest: The authors have no conflict of interest to declare.

Availability of data and code: Data and code are available upon request from the corresponding author.

Acknowledgments

We are grateful to the CDFW, USFWS, UCD and CDWR staff and scientists who conducted trawls, measured water quality, identified zooplankton and provided our study with specimens. We also thank Ching Teh, and numerous UCD scientists and staff who assisted with this project. The views expressed are those of the authors and do not represent the official opinion of any employer, institution or government agency.

References

Acuña, S., D. Baxa & S. Teh, 2012A. Sublethal dietary effects of microcystin producing Microcystis on threadfin shad, *Dorosoma petenense*. Toxicon 60:1191-1202.

Acuña, S., D.-F. Deng, P. Lehman & S. Teh, 2012B. Sublethal dietary effects of Microcystis on Sacramento splittail, *Pogonichthys macrolepidotus*. Aquatic Toxicology 110:1-8.

Acuña, S., D. Baxa, P. Lehman, F. C. Teh, D. F. Deng & S. Teh, 2020. Determining the exposure pathway and impacts of Microcystis on threadfin shad, *Dorosoma petenense*, in San Francisco Estuary. Environmental Toxicology and Chemistry 39:787-798.

Baird, D., J. Marais & C. Daniel, 1996. Exploitation and conservation of angling fish in two South African estuaries. Aquatic Conservation: Marine and Freshwater Ecosystems 6:319-330.

Barton, K. 2009. MuMIn: multi-model inference. http://r-forge. r-project. org/projects/mumin/.

Bashevkin, S.M., R. Hartman, M. Thomas, A. Barros, C. Burdi, A. Hennessy, T. Tempel & K. Kayfetz, 2020. Interagency Ecological Program: Zooplankton abundance in the Upper San Francisco Estuary from 1972-2018, an integration of 5 long-term monitoring programs ver 1. Environmental Data Initiative. https://doi.org/10.6073/pasta/0c400c670830e4c8f7fd45c187efdcb9 (Accessed 2020-09-23).

672 Baskerville-Bridges, B. & C. Lindberg, 2004. The effect of light intensity, alga concentration, and
673 prey density on the feeding behavior of Delta Smelt larvae. Pages 219-227 *in* American
674 Fisheries Society Symposium. CiteSeerX.
675 Beck, M. W., K. L. Heck Jr, K. W. Able, D. L. Childers, D. B. Eggleston, B. M. Gillanders, B.
676 Halpern, C. G. Hays, K. Hoshino & T. J. Minello, 2001. The identification, conservation,
677 and management of estuarine and marine nurseries for fish and invertebrates: A better
678 understanding of the habitats that serve as nurseries for marine species and the factors that
679 create site-specific variability in nursery quality will improve conservation and management
680 of these areas. BioScience 51:633-641.
681 Bennett, W. A., 2005. Critical assessment of the delta smelt population in the San Francisco Estuary,
682 California. San Francisco Estuary and Watershed Science 3.
683 Bennett, W. & J. R. Burau, 2015. Riders on the storm: Selective tidal movements facilitate the
684 spawning migration of threatened Delta Smelt in the San Francisco Estuary. Estuaries and
685 Coasts 38:826-835.
686 Bever, A. J., M. L. MacWilliams, B. Herbold, L. R. Brown & F. V. Feyrer, 2016. Linking
687 hydrodynamic complexity to Delta Smelt (*Hypomesus transpacificus*) distribution in the San
688 Francisco Estuary, USA. San Francisco Estuary and Watershed Science 14.
689 Bisson, P. A., K. Sullivan & J. L. Nielsen, 1988. Channel hydraulics, habitat use, and body form of
690 juvenile coho salmon, steelhead, and cutthroat trout in streams. Transactions of the
691 American Fisheries Society 117:262-273.
692 Bolger, T. & P. Connolly, 1989. The selection of suitable indices for the measurement and analysis
693 of fish condition. Journal of Fish Biology 34:171-182.
694 Boujard, T. & J. Leatherland, 1992. Circadian pattern of hepatosomatic index, liver glycogen and
695 lipid content, plasma non-esterified fatty acid, glucose, T3, T4, growth hormone and cortisol
696 concentrations in *Oncorhynchus mykiss* held under different photoperiod regimes and fed using
697 demand-feeders. Fish Physiology and Biochemistry 10:111-122.
698 Brown, L. R., 2003. Will tidal wetland restoration enhance populations of native fishes? San
699 Francisco Estuary and Watershed Science 1.
700 Buchheister, A., C. F. Bonzek, J. Gartland & R. J. Latour, 2013. Patterns and drivers of the demersal
701 fish community of Chesapeake Bay. Marine Ecology Progress Series 481:161-180.
702 Burnham, K. P. & D. R. Anderson, 2002. Model selection and multimodel inference: A practical
703 information-theoretic approach. New York: Springer Verlag.
704 California Fish and Game Commission, 2009. Final statement of reasons for regulatory action,
705 Amend Title 14, CCR, Section 670.5, Re: Uplisting the Delta Smelt to endangered species
706 status. California Fish and Game Commission, Sacramento, CA.
707 Cottingham, A., P. Huang, M. R. Hipsey, N. G. Hall, E. Ashworth, J. Williams & I. C. Potter, 2018.
708 Growth, condition, and maturity schedules of an estuarine fish species change in estuaries
709 following increased hypoxia due to climate change. Ecology and Evolution 8:7111-7130.
710 CDFW, 2020. Incidental Take Permit for Long-Term Operation of the State Water Project in the
711 Sacramento-San Joaquin Delta. https://water.ca.gov/-/media/DWR-Website/Web-
712 Pages/Programs/State-Water-Project/Files/ITP-for-Long-Term-SWP-Operations.pdf
713 Cloern, J. E., 2018. Why large cells dominate estuarine phytoplankton. Limnology and
714 Oceanography 63:S392-S409.
715 CNRA 2016. Delta Smelt Resiliency Strategy July 2016.
716 https://resources.ca.gov/CNRALegacyFiles/docs/Delta-Smelt-Resiliency-Strategy-
717 FINAL070816.pdf

718 Belarmino E., E. B., M. F. de Nóbrega, A. M. Grimm, M. da Silva Copertino, J. P. Vieira & A. M.
719 Garcia, 2021. Long-term trends in the abundance of an estuarine fish and relationships with
720 El Niño climatic impacts and seagrass meadows reduction. Estuarine, Coastal and Shelf
721 Science:107565.
722 Damon, L. J., S. B. Slater, R. D. Baxter & R. W. Fujimura, 2016. Fecundity and reproductive
723 potential of wild female Delta Smelt in the upper San Francisco Estuary, California.
724 California Fish and Game 102:188-210.
725 De Pedro, N., M. Delgado, B. Gancedo & M. Alonso-Bedate, 2003. Changes in glucose, glycogen,
726 thyroid activity and hypothalamic catecholamines in tench by starvation and refeeding.
727 Journal of Comparative Physiology B 173:475-481.
728 Dege, M. & L. R. Brown, 2003. Effect of outflow on spring and summertime distribution and
729 abundance of larval and juvenile fishes in the upper San Francisco Estuary. Pages 49-66 *in*
730 American Fisheries Society Symposium. CiteSeerX.
731 Faldyn, M. J., M. D. Hunter & B. D. Elderd, 2018. Climate change and an invasive, tropical
732 milkweed: An ecological trap for monarch butterflies. Wiley Online Library.
733 Ferrari, M. C., L. Ranåker, K. L. Weinersmith, M. J. Young, A. Sih & J. L. Conrad, 2014. Effects of
734 turbidity and an invasive waterweed on predation by introduced largemouth bass.
735 Environmental Biology of Fishes 97:79-90.
736 Feyrer, F., M. L. Nobriga & T. R. Sommer, 2007. Multidecadal trends for three declining fish
737 species: Habitat patterns and mechanisms in the San Francisco Estuary, California, USA.
738 Canadian Journal of Fisheries and Aquatic Sciences 64:723-734.
739 Feyrer, F., K. Newman, M. Nobriga & T. Sommer, 2011. Modeling the effects of future outflow on
740 the abiotic habitat of an imperiled estuarine fish. Estuaries and Coasts 34:120-128.
741 Foott, J. S. & J. Bigelow, 2010. Pathogen survey, gill Na-K-ATPase activity, and leukocyte profile of
742 adult Delta Smelt. California Fish and Game 96:223-231.
743 Gartrell, G., J. Mount, E. Hanak & B. Gray, 2017. A new approach to accounting for environmental
744 water. Public Policy Institute of California. San Francisco, CA
745 Ger, K. A., S. J. Teh, D. V. Baxa, S. Lesmeister & C. R. Goldman, 2010. The effects of dietary
746 *Microcystis aeruginosa* and microcystin on the copepods of the upper San Francisco Estuary.
747 Freshwater Biology 55:1548-1559.
748 Ger, K. A., T. G. Otten, R. DuMais, T. Ignoffo & W. Kimmerer, 2018. *In situ* ingestion of
749 Microcystis is negatively related to copepod abundance in the upper San Francisco Estuary.
750 Limnology and Oceanography 63:2394-2410.
751 Grimaldo, L., F. Feyrer, J. Burns & D. Maniscalco, 2017. Sampling uncharted waters: Examining
752 rearing habitat of larval longfin smelt (*Spirinchus thaleichthys*) in the upper San Francisco
753 Estuary. Estuaries and Coasts 40:1771-1784.
754 Grimaldo, L. F., W. E. Smith & M. L. Nobriga, 2021. Re-examining factors that affect Delta Smelt
755 (*Hypomesus transpacificus*) entrainment at the State Water Project and Central Valley Project in
756 the Sacramento–San Joaquin Delta. San Francisco Estuary and Watershed Science 19.
757 Guastella, L. A., 1994. A quantitative assessment of recreational angling in Durban Harbour, South
758 Africa. South African Journal of Marine Science 14:187-203.
759 Guisan, A. & W. Thuiller, 2005. Predicting species distribution: Offering more than simple habitat
760 models. Ecology Letters 8:993-1009.
761 Hale, R., R. Coleman, M. Sievers, T. R. Brown & S. E. Swearer, 2018. Using conservation behavior
762 to manage ecological traps for a threatened freshwater fish. Ecosphere 9:e02381.
763 Hamilton, S. A. & D. D. Murphy, 2018. Analysis of limiting factors across the life cycle of Delta
764 Smelt (*Hypomesus transpacificus*). Environmental Management 62:365–382.

765 Hammock, B. G., J. A. Hobbs, S. B. Slater, S. Acuña & S. J. Teh, 2015. Contaminant and food
766 limitation stress in an endangered estuarine fish. Science of the Total Environment 532:316-
767 326.
768 Hammock, B. G., S. B. Slater, R. D. Baxter, N. A. Fangue, D. Cocherell, A. Hennessy, T. Kurobe, C.
769 Y. Tai & S. J. Teh, 2017. Foraging and metabolic consequences of semi-anadromy for an
770 endangered estuarine fish. PLoS One 12:e0173497.
771 Hammock, B. G., R. Hartman, S. B. Slater, A. Hennessy & S. J. Teh, 2019A. Tidal wetlands
772 associated with foraging success of Delta Smelt. Estuaries and Coasts 42:857-867.
773 Hammock, B. G., S. P. Moose, S. S. Solis, E. Goharian & S. J. Teh, 2019B. Hydrodynamic modeling
774 coupled with long-term field data provide evidence for suppression of phytoplankton by
775 invasive clams and freshwater exports in the San Francisco Estuary. Environmental
776 Management 63:703-717.
777 Hammock, B. G., W. F. Ramírez-Duarte, P. A. Triana Garcia, A. A. Schultz, L. I. Avendano, T.-C.
778 Hung, J. R. White, Y.-T. Bong & S. J. Teh, 2020. The health and condition responses of
779 Delta Smelt to fasting: A time series experiment. PLoS One 15:e0239358.
780 Hards, A. R., M. A. Gray, S. C. Noël & R. A. Cunjak, 2019. Utility of condition indices as predictors
781 of lipid content in slimy sculpin (*Cottus cognatus*). Diversity 11:71.
782 Hasenbein, M., N. A. Fangue, J. Geist, L. M. Komoroske, J. Truong, R. McPherson & R. E.
783 Connon, 2016. Assessments at multiple levels of biological organization allow for an
784 integrative determination of physiological tolerances to turbidity in an endangered fish
785 species. Conservation Physiology 4.
786 He, X. & J. F. Kitchell, 1990. Direct and indirect effects of predation on a fish community: A whole-
787 lake experiment. Transactions of the American Fisheries Society 119:825-835.
788 Hobbs, J., W. Bennett & J. Burton, 2006. Assessing nursery habitat quality for native smelts
789 (Osmeridae) in the low-salinity zone of the San Francisco estuary. Journal of Fish Biology
790 69:907-922.
791 Hobbs, J. A., L. S. Lewis, M. Willmes, C. Denney & E. Bush, 2019. Complex life histories
792 discovered in a critically endangered fish. Scientific Reports 9:1-12.
793 Honey, K., R. Baxter, Z. Hymanson, T. Sommer, M. Gingras & P. Cadrett, 2004. IEP long-term fish
794 monitoring program element review. State of California, Department of Water Resources,
795 Interagency Ecological Program.
796 Hopkinson, C. & E. M. Smith, 2005. Estuarine respiration: An overview of benthic, pelagic, and
797 whole system respiration. Respiration in Aquatic Ecosystems, Chapter 8:122-146.
798 Hughes, J. E., L. A. Deegan, J. C. Wyda, M. J. Weaver & A. Wright, 2002. The effects of eelgrass
799 habitat loss on estuarine fish communities of southern New England. Estuaries 25:235-249.
800 IEP-MAST, R. Baxter, L. R. Brown, G. Castillo, L. Conrad, S. Culberson, M. Dekar, F. Feyrer, L.
801 Grimaldo, T. Hunt, J. Kirsch, A. Mueller-Solger, S. Slater, T. Sommer & K. Souza, 2015. An
802 updated conceptual model for Delta Smelt: Our evolving understanding of an estuarine fish.
803 Interagency Ecological Program, Sacramento, CA.
804 Interagency Ecological Program (IEP), S. Lesmeister & M. Martinez, 2020. Interagency Ecological
805 Program: Discrete water quality monitoring in the Sacramento-San Joaquin Bay-Delta,
806 collected by the Environmental Monitoring Program, 2000-2018. ver 2. Environmental Data
807 Initiative. https://doi.org/10.6073/pasta/a215752cb9ac47f9ed9bb0fdb7fc7c19
808 James, N. C., P. D. Cowley & A. K. Whitfield, 2018. The marine fish assemblage of the East
809 Kleinemonde Estuary over 20 years: Declining abundance and nursery function? Estuarine,
810 Coastal and Shelf Science 214:64-71.

811 Jarnevich, C. S., T. J. Stohlgren, S. Kumar, J. T. Morisette & T. R. Holcombe, 2015. Caveats for
812 correlative species distribution modeling. Ecological Informatics 29:6-15.
813 Jassby, A. D., W. J. Kimmerer, S. G. Monismith, C. Armor, J. E. Cloern, T. M. Powell, J. R. Schubel
814 & T. J. Vendlinski, 1995. Isohaline position as a habitat indicator for estuarine populations.
815 Ecological Applications 5:272-289.
816 Jassby, A., 2008. Phytoplankton in the upper San Francisco Estuary: Recent biomass trends, their
817 causes, and their trophic significance. San Francisco Estuary and Watershed Science **6**.
818 Jungbluth, M., C. Lee, C. Patel, T. Ignoffo, B. Bergamaschi & W. Kimmerer, 2021. Production of
819 the copepod *Pseudodiaptomus forbesi* is not enhanced by ingestion of the diatom *Aulacoseira*
820 *granulata* during a bloom. Estuaries and Coasts 44:1083-1099.
821 Kayfetz, K., S. M. Bashevkin, M. Thomas, R. Hartman, C. E. Burdi, A. Hennessy, T. Tempel & A.
822 Barros, 2020. Zooplankton Integrated Dataset Metadata Report. IEP Technical Report 93.
823 California Department of Water Resources, Sacramento, California.
824 Kemp, W. M., W. R. Boynton, J. E. Adolf, D. F. Boesch, W. C. Boicourt, G. Brush, J. C. Cornwell,
825 T. R. Fisher, P. M. Glibert & J. D. Hagy, 2005. Eutrophication of Chesapeake Bay: Historical
826 trends and ecological interactions. Marine Ecology Progress Series 303:1-29.
827 Kiernan, J. D., P. B. Moyle & P. K. Crain, 2012. Restoring native fish assemblages to a regulated
828 California stream using the natural flow regime concept. Ecological Applications 22:1472-
829 1482.
830 Kimmerer, W., 2002. Effects of freshwater flow on abundance of estuarine organisms: Physical
831 effects or trophic linkages? Marine Ecology Progress Series 243:39-55.
832 Kimmerer, W. J., 2008. Losses of Sacramento River Chinook salmon and delta smelt to entrainment
833 in water diversions in the Sacramento-San Joaquin Delta. San Francisco Estuary and
834 Watershed Science 6.
835 Kimmerer, W. J., T. R. Ignoffo, A. M. Slaughter & A. L. Gould, 2014. Food-limited reproduction
836 and growth of three copepod species in the low-salinity zone of the San Francisco Estuary.
837 Journal of Plankton Research 36:722-735.
838 Kimmerer, W., T. R. Ignoffo, B. Bemowski, J. Modéran, A. Holmes & B. Bergamaschi, 2018A.
839 Zooplankton dynamics in the Cache Slough Complex of the Upper San Francisco Estuary.
840 San Francisco Estuary and Watershed Science 16.
841 Kimmerer, W. J., T. R. Ignoffo, K. R. Kayfetz & A. M. Slaughter, 2018B. Effects of freshwater flow
842 and phytoplankton biomass on growth, reproduction, and spatial subsidies of the estuarine
843 copepod *Pseudodiaptomus forbesi*. Hydrobiologia 807:113-130.
844 Komoroske, L., R. E. Connon, J. Lindberg, B. Cheng, G. Castillo, M. Hasenbein & N. Fangue, 2014.
845 Ontogeny influences sensitivity to climate change stressors in an endangered fish.
846 Conservation Physiology 2.
847 Korman, J., E. S. Gross & L. F. Grimaldo, 2021. Statistical evaluation of behavior and population
848 dynamics models predicting movement and proportional entrainment loss of adult Delta
849 Smelt in the Sacramento–San Joaquin River Delta. San Francisco Estuary and Watershed
850 Science 19.
851 Korman, J. & S. E. Campana, 2009. Effects of hydropeaking on nearshore habitat use and growth of
852 age-0 rainbow trout in a large regulated river. Transactions of the American Fisheries Society
853 138:76-87.
854 Kuivila, K. M. & G. E. Moon, 2004. Potential exposure of larval and juvenile delta smelt to
855 dissolved pesticides in the Sacramento-San Joaquin Delta, California. Pages 229-242 *in*
856 American Fisheries Society Symposium. American Fisheries Society.

857 Kullgren, A., F. Jutfelt, R. Fontanillas, K. Sundell, L. Samuelsson, K. Wiklander, P. Kling, W.
858 Koppe, D. J. Larsson & B. T. Björnsson, 2013. The impact of temperature on the
859 metabolome and endocrine metabolic signals in Atlantic salmon (*Salmo salar*). Comparative
860 Biochemistry and Physiology Part A: Molecular & Integrative Physiology 164:44-53.
861 Kurobe, T., M. O. Park, A. Javidmehr, F. C. Teh, S. C. Acuña, C. J. Corbin, A. Conley, W. A.
862 Bennett & S. J. Teh, 2016. Assessing oocyte development and maturation in the threatened
863 Delta Smelt, *Hypomesus transpacificus*. Environmental Biology of Fishes 99:423-432.
864 Lehman, P., S. J. Teh, G. Boyer, M. Nobriga, E. Bass & C. Hogle, 2010. Initial impacts of *Microcystis*
865 *aeruginosa* blooms on the aquatic food web in the San Francisco Estuary. Hydrobiologia
866 637:229-248.
867 Lewis, L.S., C. Denney, M. Willmes, W. Xieu, R. Fichman, F. Zhao, B. Hammock, A. Schultz, N.A.
868 Fangue & J.A. Hobbs, 2021 (in press). Otolith-based approaches indicate strong effects of
869 environmental variation on growth of a critically endangered estuarine fish. Marine Ecology
870 Progress Series. https://www.int-res.com/prepress/m13848.html
871 Liu, Y., J. Liu, S. Ye, D. P. Bureau, H. Liu, J. Yin, Z. Mou, H. Lin & F. Hao, 2019. Global metabolic
872 responses of the lenok (*Brachymystax lenok*) to thermal stress. Comparative Biochemistry and
873 Physiology Part D: Genomics and Proteomics 29:308-319.
874 Lusardi, R. A., B. G. Hammock, C. A. Jeffres, R. A. Dahlgren & J. D. Kiernan, 2020. Oversummer
875 growth and survival of juvenile coho salmon (*Oncorhynchus kisutch*) across a natural gradient
876 of stream water temperature and prey availability: An *in situ* enclosure experiment. Canadian
877 Journal of Fisheries and Aquatic Sciences 77:413-424.
878 Mahardja, B., V. Tobias, S. Khanna, L. Mitchell, P. Lehman, T. Sommer, L. Brown, S. Culberson &
879 J. L. Conrad, 2021. Resistance and resilience of pelagic and littoral fishes to drought in the
880 San Francisco Estuary. Ecological Applications 31(2).
881 Maunder, M. & P. Starr, 2003. Fitting fisheries models to standardised CPUE abundance indices.
882 Fisheries Research 63:43-50.
883 Maunder, M. N. & R. B. Deriso, 2011. A state–space multistage life cycle model to evaluate
884 population impacts in the presence of density dependence: Illustrated with application to
885 delta smelt (*Hyposmesus transpacificus*). Canadian Journal of Fisheries and Aquatic Sciences
886 68:1285-1306.
887 McCauley, E. & J. Kalff, 1981. Empirical relationships between phytoplankton and zooplankton
888 biomass in lakes. Canadian Journal of Fisheries and Aquatic Sciences 38:458-463.
889 Miller, W. J., B. F. J. Manly, D. D. Murphy, D. Fullerton & R. R. Ramey, 2012. An investigation of
890 factors affecting the decline of Delta Smelt (*Hypomesus transpacificus*) in the Sacramento-San
891 Joaquin Estuary. Reviews in Fisheries Science 20:1-19.
892 Mion, M., A. Thorsen, F. Vitale, J. Dierking, J. Herrmann, B. Huwer, B. von Dewitz & M. Casini,
893 2018. Effect of fish length and nutritional condition on the fecundity of distressed Atlantic
894 cod *Gadus morhua* from the Baltic Sea. Journal of Fish Biology 92:1016-1034.
895 Montgomery, J., J. Durand & P. Moyle, 2015. Zooplankton biomass and chlorophyll-a trends in the
896 North Delta Arc: Two consecutive drought years. IEP Newsletter 28:14-23.
897 Morrison, S. M., T. E. Mackey, T. Durhack, J. D. Jeffrey, L. M. Wiens, N. J. Mochnacz, C. T. Hasler,
898 E. C. Enders, J. R. Treberg & K. M. Jeffries, 2020. Sub-lethal temperature thresholds
899 indicate acclimation and physiological limits in brook trout *Salvelinus fontinalis*. Journal of Fish
900 Biology 97:583-587.
901 Moyle, P. B., B. Herbold, D. E. Stevens & L. W. Miller, 1992. Life history and status of delta smelt
902 in the Sacramento-San Joaquin Estuary, California. Transactions of the American Fisheries
903 Society 121:67-77.

Moyle, P. B., L. R. Brown, J. R. Durand & J. A. Hobbs, 2016. Delta smelt: Life history and decline of a once-abundant species in the San Francisco Estuary. San Francisco Estuary and Watershed Science 14.

Moyle, P. B., J. A. Hobbs & J. R. Durand, 2018. Delta Smelt and water politics in California. Fisheries 43:42-50.

Mozetič, P., J. Francé, T. Kogovšek, I. Talaber & A. Malej, 2012. Plankton trends and community changes in a coastal sea (northern Adriatic): Bottom-up vs. top-down control in relation to environmental drivers. Estuarine, Coastal and Shelf Science 115:138-148.

Nobriga, M. L, 2002. Larval delta smelt diet composition and feeding incidence: Environmental and ontogenetic influences. California Fish and Game 88:149-164.

Polansky, L., K. B. Newman & L. Mitchell, 2021. Improving inference for nonlinear state-space models of animal population dynamics given biased sequential life stage data. Biometrics 77:352-361.

Propst, D. L. & K. B. Gido, 2004. Responses of native and nonnative fishes to natural flow regime mimicry in the San Juan River. Transactions of the American Fisheries Society, 133:922-931.

Robinson, M., L. Gomez-Raya, W. Rauw & M. Peacock, 2008. Fulton's body condition factor K correlates with survival time in a thermal challenge experiment in juvenile Lahontan cutthroat trout (*Oncorhynchus clarki henshawi*). Journal of Thermal Biology 33:363-368.

Rose, K. A., W. J. Kimmerer, K. P. Edwards & W. A. Bennett, 2013. Individual-based modeling of Delta Smelt population dynamics in the upper San Francisco Estuary: I. Model description and baseline results. Transactions of the American Fisheries Society 142:1238-1259.

Ruthsatz, K., K. H. Dausmann, C. Drees, L. I. Becker, L. Hartmann, J. Reese, N. M. Sabatino, M. A. Peck & J. Glos, 2018. Altered thyroid hormone levels affect body condition at metamorphosis in larvae of *Xenopus laevis*. Journal of Applied Toxicology 38:1416-1425.

Schultz, A. A., L. Grimaldo, J. Hassrick, A. Kalmbach, A. Smith, O. Townes, D. Barnard & J. Brandon, 2019. Effect of Isohaline (X2) and Region on Delta Smelt Habitat, Prey and Distribution During the Summer and Fall: Insights into Managed Flow Actions in a Highly Modified Estuary. Pages 237-301 in A. A. Schultz, editor. Directed Outflow Project: Technical Report 1. U.S. Bureau of Reclamation, Bay-Delta Office, Mid-Pacific Region, Sacramento, CA. November 2019, 318 pp.

Slater, S. B. & R. D. Baxter, 2014. Diet, prey selection, and body condition of age-0 Delta Smelt, *Hypomesus transpacificus*, in the Upper San Francisco Estuary. San Francisco Estuary and Watershed Science 12.

Sommer, T., C. Armor, R. Baxter, R. Breuer, L. Brown, M. Chotkowski, S. Culberson, F. Feyrer, M. Gingras & B. Herbold, 2007. The collapse of pelagic fishes in the upper San Francisco Estuary. Fisheries 32:270-277.

Sommer, T., F. H. Mejia, M. L. Nobriga, F. Feyrer & L. Grimaldo, 2011. The spawning migration of delta smelt in the upper San Francisco Estuary. San Francisco Estuary and Watershed Science 9.

Sommer, T. & F. Mejia, 2013. A place to call home: A synthesis of Delta Smelt habitat in the upper San Francisco Estuary. San Francisco Estuary and Watershed Science 11.

Sommer, T., R. Hartman, M. Koller, M. Koohafkan, J. L. Conrad, M. MacWilliams, A. Bever, C. Burdi, A. Hennessy & M. Beakes, 2020. Evaluation of a large-scale flow manipulation to the upper San Francisco Estuary: Response of habitat conditions for an endangered native fish. PLoS One 15:e0234673.

Stevens, D. E. & L. W. Miller, 1983. Effects of river flow on abundance of young Chinook salmon, American shad, longfin smelt, and delta smelt in the Sacramento-San Joaquin River system. North American Journal of Fisheries Management 3:425-437.

Teh, S. J., D. V. Baxa, B. G. Hammock, S. A. Gandhi & T. Kurobe, 2016. A novel and versatile flash-freezing approach for evaluating the health of Delta Smelt. Aquatic Toxicology 170:152-161.

Teh, S. J., A. A. Schultz, W. R. Duarte, S. Acuña, D. M. Barnard, R. D. Baxter, P. A. T. Garcia & B. G. Hammock, 2020. Histopathological assessment of seven year-classes of Delta Smelt. Science of the Total Environment 726:138333.

Tigan, G., W. Mulvaney, L. Ellison, A. Schultz & T.-C. Hung, 2020. Effects of light and turbidity on feeding, growth, and survival of larval Delta Smelt (*Hypomesus transpacificus*, Actinopterygii, Osmeridae). Hydrobiologia 847:2883-2894.

USFWS, 1993. Final Rule: Endangered and threatened wildlife and plants; determination of threatened status for the Delta smelt. Federal Register 58:12854-12864.

USFWS, 2008. Biological Opinion on the Coordinated Operations of the Central Valley Project and State Water Project in California. https://www.fws.gov/sfbaydelta/Documents/SWP-CVP_OPs_BO_12-15_final_signed.pdf

USFWS, 2019. Biological opinion for the reinitiation of consultation on the coordinated operations of the Central Valley Project and State Water Project. https://www.fws.gov/sfbaydelta/cvp-swp/documents/10182019_ROC_BO_final.pdf

USFWS, C. Johnston, S. Durkacz, R. McKenzie, J. Speegle, B. Mahardja, B. Perales, D. Bridgman & K. Erly, 2020. Interagency Ecological Program and US Fish and Wildlife Service: San Francisco Estuary Enhanced Delta Smelt Monitoring Program data, 2016-2020 ver 3. Environmental Data Initiative. https://doi.org/10.6073/pasta/764f27ff6b0a7b11a487a71c90397084

Verma, A. K. & S. Prakash, 2019. Impact of arsenic on haematology, condition factor, hepatosomatic and gastrosomatic index of a fresh water catfish, *Mystus vittatus*. International Journal on Biological Sciences 10:49-54.

Werner, I., L. A. Deanovic, V. Connor, V. de Vlaming, H. C. Bailey & D. E. Hinton, 2000. Insecticide-caused toxicity to *Ceriodaphnia dubia* (CLADOCERA) in the Sacramento–San Joaquin River delta, California, USA. Environmental Toxicology and Chemistry 19:215-227.

Weston, D. P., A. M. Asbell, S. A. Lesmeister, S. J. Teh & M. J. Lydy, 2014. Urban and agricultural pesticide inputs to a critical habitat for the threatened delta smelt (*Hypomesus transpacificus*). Environmental Toxicology and Chemistry 33:920-929.

Weston, D. P., C. Moschet & T. M. Young, 2019. Chemical and toxicological effects on Cache Slough after storm-driven contaminant inputs. San Francisco Estuary and Watershed Science 17:3.

Weldon, A. J. & N. M. Haddad, 2005. The effects of patch shape on Indigo Buntings: Evidence for an ecological trap. Ecology 86:1422-1431.

Williams, R. & S. Poulet, 1986. Relationship between the zooplankton, phytoplankton, particulate matter and dissolved free amino acids in the Celtic Sea. Marine Biology 90:279-284.

Winder, M. & A. D. Jassby, 2011. Shifts in zooplankton community structure: Implications for food web processes in the upper San Francisco Estuary. Estuaries and Coasts 34:675-690.

Yuan, L. L. & A. I. Pollard, 2018. Changes in the relationship between zooplankton and phytoplankton biomasses across a eutrophication gradient. Limnology and Oceanography 63:2493-2507.

995 Zamal, H. & F. Ollevier, 1995. Effect of feeding and lack of food on the growth, gross biochemical
996 and fatty acid composition of juvenile catfish. Journal of Fish Biology 46:404-414.
997

998

999 This page intentionally left blank

1000

Chapter 8: Spatial Differences in Lower Trophic Communities in an Artificial Backwater Channel in the Sacramento-San Joaquin River Delta during the Fall Season

Authors:

Calvin Y. Lee[1*], April G. Smith[1], Andrew J. Kalmbach[1]

[1] ICF, 201 Mission Street, Suite 1500, San Francisco, CA 94105 USA

[*] Corresponding author: Calvin.Lee@icf.com

Keywords: Mesozooplankton, Phytoplankton, Food-web, Community relationships

Abstract

Delta Smelt were once prevalent throughout Suisun Bay and the Sacramento San Joaquin River Delta in California, USA but are now at risk of extinction. Multiple factors such as habitat alteration, invasive species and decreased zooplankton abundances have contributed to the decline of Delta Smelt. However, there are still regions where Delta Smelt are often found. One of these areas, the Sacramento Deep Water Ship Channel (SDWSC) is a long artificial channel that now serves as a terminal channel habitat with characteristics important for Delta Smelt such as relatively high zooplankton biomass, locally high turbidity, and daily thermal stratification, which can provide a temperature refuge during summer months. The SDWSC can be divided into different subregions based on turbidity and specific conductance (and by proxy water residence time) characteristics. In this study, we asked if there were different zooplankton and phytoplankton communities in different regions of the SDWSC and what factors determined the distribution and community composition of the mesoplankton community using a Non-Metric Multidimensional Scaling (NMDS) approach. Previous studies have shown environmental properties such as turbidity and water residence times can have an important ecological effect on the phytoplankton and invertebrate community. We found that mesozooplankton communities differed from each other upstream and downstream of the maximum turbidity zone, with the maximum turbidity zone acting as an intermediary between the two. The highest average mesozooplankton biomass was concentrated in the uppermost high conductivity regions of the SDWSC. *Psuedodiaptomus forbesi* were found throughout the SDWSC while cladocerans and *Sinocalanus doerrii* were found in the upper portions of the SDWSC. Chlorophyll-*a*, nutrients, and specific conductance were important in determining the distribution of zooplankton. Phytoplankton communities also differed in the SDWSC, with the abundance of diatoms dominating downstream of the maximum turbidity zone and decreasing upstream. None of the phytoplankton taxonomic groups we examined were important factors in determining zooplankton communities, which may be due to several factors related to the timing of sample collection and differences among phytoplankton species composition in cell size and quality as prey.

Introduction

The San Francisco Bay Estuary (the estuary) and Sacramento San Joaquin Delta (the delta) have undergone many anthropogenic changes in the last century and a half. The current state of the estuary and delta has been altered from large swaths of tidal marshes to a series of dredged channels and diked wetlands, losing much of the habitat complexity that previously existed (Whipple 2012, Moyle et al. 2010). Alongside habitat loss, the region suffers from invasion of non-native species, changes in flow regimes, increased contaminant loads, declines in planktonic prey, and altered nutrient loads (such as discharge of ammonia) that have modified food webs for native fish species (Mount et al. 2012, Winder and Jassby 2011, Gilbert et al. 2011, Kimmerer 2002, Cohen and Carlton 1998). Collectively, these factors have led to the decline of populations of native fishes such as the Delta Smelt (*Hypomesus transpacificus*) (Moyle et al. 2016).

The Delta Smelt is a small, planktivorous, euryhaline fish with a mostly annual life cycle endemic to the estuary and delta. While traditionally thought of as a semi-anadromous species, Delta Smelt utilize multiple life history strategies including resident populations that stay and reproduce in brackish or freshwater habitat (Hobbs et al. 2019). Having multiple life history strategies can improve resilience of a species when habitats become degraded (Hobbs et al. 2019, Kerr and Secor 2010). While much of the estuary and delta have become unsuitable for Delta Smelt, certain regions are considered contemporary "hot spots" for populations of Delta Smelt given the altered environment (Moyle et al. 2016, Sommer and Mejia 2013, Merz et al. 2011). Even though considered hotspots, conditions within these areas are not always ideal for Delta Smelt due to factors including high water temperatures and levels of contaminants (Hammock et al. 2015). However, some habitat components benefit Delta Smelt such as high turbidity and abundant zooplankton prey (Kimmerer et al. 2018, Sommer and Mejia 2013).

The Sacramento Deep Water Ship Channel (SDWSC) is one such hotspot for Delta Smelt (Feyrer et al. 2017, Baxter et al. 2010). Within the SDWSC are areas with different turbidity and water residence times that create regions of varying environmental properties affecting both zooplankton and phytoplankton. (Young et al. 2021, Feyrer et al. 2017, Downing et al. 2016, Gross et al. 2019). Zooplankton densities were observed to be higher at or near the turbidity maximum in the SDWSC and other estuaries (Feyrer et al. 2017, Roman et al. 2005, Suzuki et al. 2009). Phytoplankton derived and allochthonous organic matter tend to become entrapped in the turbidity maximum zone which may be important for zooplankton communities (Keller et al. 2014, Suzuki et al. 2012, Etcheber et al. 2007, Islam et al. 2006). Higher chlorophyll-*a* concentrations have been found adjacent to or at the turbidity maximum in other systems which can also benefit zooplankton (Keller et al. 2014, Suzuki et al. 2012). In addition, water residence time has been observed to be important in determining phytoplankton biomass and taxa composition; longer residence times can allow for the accumulation of phytoplankton biomass unless suppressed by grazing (Stumpner 2020, Kimmerer and Thompson 2014, Lucas and Thompson 2012, Wan et al. 2013).

Zooplankton biomass and growth has been correlated to phytoplankton community structure and chlorophyll-*a* (a proxy for phytoplankton biomass) in the estuary (Montgomery 2017, Cloern & Dufford 2005, Müller-Solger et al. 2002, Lehman 2000, Orsi and Mecum 1986). In the SDWSC, the phytoplankton community may exert influence on the zooplankton through various bottom-up effects. For example, the size of phytoplankton cells, resistance to grazing, and toxicity can affect zooplankton community compositions (Murrell and Lores 2004, Roy et al. 2007). Zooplankton have

also been observed to show selectively towards a food source (Harfmann et al. 2019, Ger et al. 2019, Ger et al. 2010, Müller-Solger et al. 2002).

Different portions of the SDWSC have environmental properties that can affect the phytoplankton community; the upper reaches of the SDWSC have higher specific conductance due to evaporation, which indicates longer water residence times (Gross et al. 2019, Downing et al. 2016). High water residence times have been associated with higher chlorophyll-*a* levels and variable effects on nutrient (phosphorous, ammonium and nitrogen) levels (Stumpner et al. 2020, Downing et al. 2016, Friedl and Wüest 2002). Along with water residence time, nutrients and light also influence phytoplankton abundances in the estuary and delta (Dahm et al. 2016, Wilkerson et al. 2006). Phytoplankton in the SDWSC may be limited by nitrogen (N) where concentrations are lower than phosphorous (P) and N:P ratios are found to be below the 16:1 Redfield ratio (Kalmbach et al. 2021). Nutrient limitation may affect phytoplankton abundance and community composition and thus available resources for mesozooplankton (Gilbert 2010).

Understanding the food resources available to zooplankton and how they affect the distribution and composition of the zooplankton community is important when Delta Smelt are reliant on zooplankton and may preferentially consume certain zooplankton species over others or derive greater nutritional value from certain prey (Slater et al. 2019, Slater and Baxter 2014). To understand what food resources are available for Delta Smelt in the SDWSC and what environmental properties are driving their food sources distribution we sought to answer three questions. 1. Does zooplankton species composition differ among the turbidity/conductivity subregions of the SDWSC? 2. What environmental properties are present in the different subregions of the SDWSC and are these correlated with the zooplankton community? 3. Does the phytoplankton community and/or density appear to be a driver in the zooplankton community and if so, what environmental conditions predict phytoplankton distribution?

Methods

Study Area

The Sacramento Deep Water Ship Channel (SDWSC) is a 43-mile artificial canal in the Delta that was built in 1963 and runs from the Sacramento River to the Port of Sacramento (Figure 8-1). The SDWSC is approximately 30 feet deep with little shallow water habitat. The SDWSC is a terminal channel with the only major water inflow occurring at the southerly confluence with the Sacramento River, with artificial gates blocking separating the northern channel from the Sacramento River. There is some stormwater flow in the upstream end and agricultural runoff at multiple points along the channel (Young et al. 2021).

We divided the SDWSC into five regions using specific conductance and turbidity similar to Young et al. (2021). The zones run from the bottom to the top of the SDWSC and are referred to by their acronyms as described in Figure 8-2 or as regions when referring to all of them.

Field Data Collection

Sampling occurred in the fall of 2017 to 2020 from September through November throughout the SDWSC (Figure 8-1). Three random sites were sampled bi-weekly in 2017 and weekly from 2018-2020 alongside the U.S. Fish and Wildlife Service Enhanced Delta Smelt Monitoring (EDSM) program. Sites were randomly selected using a Generalized Random Tessellation Stratified (GRTS)

survey design (Starcevich et al. 2016; Stevens and Olsen 2004). The sites were later snapped to a polyline running up the center of the SDWSC that allowed us to use linear referencing to measure distances. The position of Coast Guard navigational markers used in previous studies were snapped to the same polyline for use as references to where random sites were in relation to the navigational markers (Feyrer et al. 2017, Young et al. 2021). Figures in this study use the relative position of data points to where channel markers are positioned.

At each site measurements of temperature (C), turbidity (NTU), specific conductance (µS/cm), and chlorophyll-*a* (µg/L) were taken using an EXO-2 multiparameter sonde (Yellow Springs Inc., Yellow Springs, Ohio USA). Water samples were collected from one meter beneath the surface of the water using a vacuum pump. From each water sample, 100 mL was filtered using a vacuum pump (filtration pressure was <10 mm Hg) through 0.2µm pore size, 47-mm diameter polycarbonate filters for nutrient analysis. The filtered water samples were later analyzed using colorimetric assays at the University of California, Davis for ammonium (NH_4^+, ppm), nitrate (NO_3^-, ppm), and phosphorus (PO_4^{3-}, ppm) (Doane and Horwáth 2003; Murphy and Riley 1962; Verdouw et al. 1978). Another 45 mL of the water sample was retained for phytoplankton identification and cell counts. The phytoplankton samples were stained and preserved with acidified Lugol's solution and stored in the dark until they could be processed by ICF (Lund et al. 1958). For each sample a 25-mL subsample was allowed to settle for at least 12 hours in Utermoehl settling chambers. Phytoplankton were identified via light microscopy to the genera level or best possible taxonomic level (Bellinger and Sigee 2015, Wehr et al. 2015, Tomas 1997).

Surface mesozooplankton were collected using a plankton ring net (20-cm diameter, 60-cm length, 150-µm mesh size) towed at a fixed depth of one meter for five minutes and preserved in 10% formalin. Samples were diluted so that the number of organisms in 1-mL of the sample was between 200-400 organisms. Between five and ten 1-mL subsamples were analyzed per sample, following methods described in the Interagency Ecological Program's Environmental Monitoring Program (Kayfetz et al. 2020), except that a maximum of 10 aliquot counts were used instead of 20 aliquot counts to account for higher sample densities. Higher densities were the result of the larger volume nets used in this study as outlined in Schultz et al. (2019). Individuals were identified to species and life stage (hereafter referred to as species). Biomass per unit volume (µg/m^3) was calculated by multiplying species-specific carbon content by the abundance value of each zooplankton taxa in the sample as outlined in Kayfetz et al. (2020) using values from Kayfetz et al. (2020) and Kimmerer et al. (2011).

Statistical Methods

Zooplankton community structure and biomass differences between the turbidity/conductivity subregions of the SDWSC were evaluated via non-parametric multidimensional scaling (NMDS) ordination using a Bray-Curtis dissimilarity matrix of 29 zooplankton species biomass (Oksanen et al. 2017). The dissimilarity matrix reduces dimensionality of a dataset and helps to characterize biomass, allowing for trends in the community composition to be described. We removed rare taxa from the dataset; species/life stage groups that occurred at five or fewer sites (Arscott et al 2006). Prior to calculating the dissimilarity matrix, zooplankton biomass was square root transformed followed by Wisconsin double standardization to equalize the effects of dominant sites or taxa on the ordination space. A two-dimensional solution was selected as the final solution with a stress of 0.23. We further investigated the relationship between zooplankton biomass and environmental properties, chlorophyll-*a*, and phytoplankton taxa. Phytoplankton taxa were binned into broader taxonomic groups according to Kalmbach et al. (2021) for statistical analysis. Phytoplankton data

were only available for 2017 to 2019. Initial analysis without 2020 zooplankton data did not show any significant correlation between phytoplankton taxa and zooplankton communities, hence for analyses moving forward 2020 zooplankton data were included. We used the ENVFIT function (Oksanen et al. 2017) to fit linear trends (vectors) to the ordination space. ENVFIT produces a goodness of fit statistic as well as a Monte Carlo randomization test p-value based on 9999 Permutations. All community analyses were completed using the "vegan" package in R (Oksanen et al. 2017).

To evaluate environmental differences between the subregions of the SDWSC we used an Analysis of Variance (ANOVA) to individually test if specific conductance, temperature, turbidity, ammonium, nitrate, phosphate, and chlorophyll-*a* varied by subregions. We followed this with pairwise comparison using estimated marginal means and a Bonferroni correction for multiple comparisons (emmeans package) using a p-value cutoff of 0.05 to denote a difference.

We used generalized additive models (GAMs) to test how chlorophyll-*a* varied with nitrate, ammonium, phosphate, temperature, and turbidity with the 'mgcv' package version 1.8-31 (Wood 2011). We fit GAMs with a Gaussian distribution as chlorophyll-*a* is normally distributed (Shapiro Wilks test p-value =0.11). We used a "shrinkage" version of thin plate spline smoothing functions which can penalize a curve, shrinking it to zero, eliminating the effect of noncontributing covariates on model predictions (Wood 2011). We let the smoothing function and the upper limit of the effective degrees of freedom vary with each water quality variable controlled by the degree of penalization associated with a Generalized Cross Validation Fit.

Results

A total of 127 samples were collected across 4 years in the SDWSC (Figure 8-1, Table 8-1). Sampling distribution was uneven across the entire SDWSC; the lowest portions of the SDWSC had the fewest samples taken across all four years (n = 11), the rest of the SDWSC was sampled more evenly (Table 1).

Zooplankton Community

We found 34 zooplankton taxa, of these, ten taxa/life history designations, hereafter referred to interchangeably as species or taxa, were found to have relatively high biomass: Daphniidae species, *Sinocalanus doerrii* adults and copepodites, *Psuedodiaptomus forbesi* adults and copepodites, adult and copepodite Cyclopoida species, *Bosmina longirostris*, *Daphnia* species, and Sididae species. Average biomass was the lowest in the low conductivity, low turbidity (LCLT) region and increased further up the SDWSC, with the highest average biomass in the high conductivity, low turbidity (HCLT) region (Figure 8-3). *P. forbesi* made up the largest proportion of mesozooplankton in the three lowermost regions of the SDWSC. *S. doerrii* made up the largest proportion of mesozooplankton in the two uppermost regions and was found less frequently downstream of the moderate conductivity, high turbidity (MCHT) subregion. The biomass and proportion of cladocerans (Daphniidae, *Daphnia* and Sididae species, and *B. longirostris*) gradually increased moving from lowermost to uppermost regions. Most cladocerans were not seen in the MCHT region except for Sididae. Much like *S. doerrii*, the highest proportion and biomass of cladocerans occurred in the HCLT region (Figure 8-3).

Analysis of the zooplankton community using NMDS revealed that conductivity, chlorophyll-*a,* nitrate, ammonium, and phosphate were the primary water quality variables correlated with the

ordination space of this zooplankton community (R^2 = 0.72, 0.53, 0.41, 0.23 and 0.22 respectively; permutation test P-value = 0.0001 for all variables) (Figure 8-4, Table 8-2). Specific conductance, chlorophyll-*a,* and phosphate increased along axis 1 while nitrate and ammonium decreased with axis 1. The subregions were also correlated with the ordination space for this zooplankton community separating along axis 1, but not axis 2 (R^2 = 0.54, permutation test p-value =0.0001). Total phytoplankton abundance, temperature, turbidity, year, year type, day of year, and individual phytoplankton taxa were either insignificant (Permutation test p-values> 0.05) or had low correlations with the ordination space (R^2< 0.12). No water quality or other variable measured in this study was associated strongly with axis 2 (Figure 8-4, Table 8-2).

The zooplankton assemblages in the lower reaches of the SDWSC were different from the upper reaches. The LCLT and low conductivity, moderate turbidity (LCMT) zones were different from the high conductivity, moderate turbidity (HCMT) and HCLT zones. The moderate conductivity, high turbidity (MCHT) zone acted as an intermediary between the upper and lower portions of the SDWSC (Figure 8-3). *P. forbesi* adults and copepodites comprised a large proportion of the community in the LCLT, LCMT, and MCHT zones, while Sididae, *S. doerrii* adults and copepodites, Daphniidae, *Daphnia* spp., and *B. longirostris* were more common in the HCMT and HCLT zones. (Figure 8-3 & Figure 8-4).

Environmental Conditions

All measured water quality variables except temperature significantly differed in mean values ($p < 0.05$), and all differed significantly in variance between the regions (F-test p-values <0.05) (Figure 8-5). We found that the subregions fell within three different significant groups based on specific conductance, with the two lowermost regions like each other (LCLT and LCMT), the mid region (MCHT) a second group, and the two uppermost regions (HCMT and HCLT) a third distinct group. Turbidity differed only in one region, with the MCHT region having significantly higher turbidity values than the other four regions. Chlorophyll-*a* and phosphate concentrations were significantly higher in the three uppermost regions (MCHT, HCMT, and HCLT) compared to the two lowermost regions. Ammonium and nitrate had similar patterns with the downstream regions having higher concentrations than the upstream regions. However, nitrates were high and similar to the downstream regions in the middle (MCHT) region, whereas ammonium was lower and similar to the upstream regions. Overall, the water quality conditions between the lowermost and uppermost regions are distinctly different, with the middle region (MCHT) intermediate between the two, except for turbidity.

Phytoplankton Community

Diatoms and cyanobacteria had much greater average abundance than dinoflagellates, green algae, cryptophytes, and other phytoplankton. Mean phytoplankton density was highest in the lowermost regions of the SDWSC (the LCLT and LCMT subregion), lowest in the middle region (MCHT region) and increased moving into the uppermost portions of the channel, but cell counts were never as high as in the LCLT and LCMT regions (Figure 8-6). Diatoms and cyanobacteria constituted most of the phytoplankton in the lower regions of the SDWSC. Diatom proportion decreased moving into the uppermost regions of the SDWSC while cyanobacteria proportion increased. Mean diatom and cyanobacteria abundance was lowest in the MCHT region. Dinoflagellates, green algae, and other phytoplankton were rare or not present throughout the SDWSC, while cryptophytes were occasionally encountered in high abundance.

We did not find evidence to support a correlation between individual phytoplankton taxa and the zooplankton community within the SDWSC in the fall (NMDS R^2 between 0.01 and 0.11, Table 8-2). However, we did find a strong statistical linkage driven by spatial variation of chlorophyll-*a* concentration and the zooplankton community (NMDS $R^2 = 0.53$, Table 8-2). We further investigated the environmental conditions which influence chlorophyll-*a*. Specific conductance was strongly correlated with chlorophyll-*a* with nearly four times the amount of chlorophyll-*a* found at moderate to high specific conductance (500 uS/cm) than at low values (<50 uS/cm). After this point, chlorophyll-*a* generally levelled off at just below 4 ug/l. While other water quality variables did influence chlorophyll-*a*, none were as strong as the relationship with specific conductance. Nitrates were negatively related to chlorophyll-*a* at low values, but positively correlated at high values, phosphate was slightly negatively related to chlorophyll-*a*, while turbidity was positively correlated (Figure 8-7, Table 8-3).

Discussion

In this study we were able to demonstrate that regions within the SDWSC have different environmental conditions, chlorophyll-*a* concentrations and mesozooplankton food resources available to Delta Smelt. We found that the moderate conductivity high turbidity (MCHT) region acted as an intermediary region between two distinct zooplankton communities found above and below it. The highest zooplankton biomass was seen in the uppermost regions of the SDWSC (HCMT and HCLT regions) where cladocerans (*Daphniidae and B. longirostris*,) and the calanoid copepod *S. doerrii* dominated the mesozooplankton community. The mesozooplankton community in the lowermost regions (LCLT and LCMT) were composed primarily of the calanoid copepod *P. forbesi*. Within the MCHT zone, the mesozooplankton community consisted of mostly the two calanoid copepod species.

The factors that mostly closely correlated with differences in the zooplankton community composition between subregions were conductivity subregion, chlorophyll-*a* and nitrate. The importance of chlorophyll-*a* in the analysis suggests phytoplankton biomass is important to zooplankton communities. Many of the significant environmental vectors were related to phytoplankton, such as, specific conductance, which was interpreted as a proxy for water residence time, nitrate constituents, and turbidity; however, none of the phytoplankton taxa examined were correlated with zooplankton communities. The scope of our study limited our ability to explore links between phytoplankton taxa and zooplankton communities. For example, our temporal resolution was unable to capture time lags between phytoplankton production and zooplankton biomass response. In addition, connections between phytoplankton and zooplankton communities are strongest during the spring-summer season when phytoplankton and zooplankton biomasses are at their peak (Merz et al. 2016).

Most zooplankton species found in the SDWSC are omnivores, not strict herbivores. For example, *Daphnia* species feed on both microzooplankton and phytoplankton (Gifford et al. 2007) and *P. forbesi* has been found to consume ciliates in addition to diatoms (Kayfetz and Kimmerer 2017, Bowen et al. 2015). While *S. doerrii* has been found to feed primarily on diatoms in the estuary, a related species, *Sinocalanus tenellus*, is known to consume nauplii, rotifers, cladocerans and even cannibalizes its own nauplii (Bollens et al. 2012, referenced in Winder and Jassby 2011, Orsi 1995, Hada and Uye 1991). Multiple trophic linkages may exist between the phytoplankton and

mesozooplankton community within the SDWSC rather than just one direct path from phytoplankton to mesozooplankton.

Microzooplankton were not examined as part of this study but could be an important component in explaining distribution of zooplankton species across the SDWSC. Microzooplankton are an important trophic link acting as grazers on phytoplankton and as food for mesozooplankton (Rollwagen-Bollens et al. 2011, Calbet 2008). Historically in the estuary, high densities of microzooplankton are associated with high concentrations of chlorophyll, so it is possible there would be higher densities of microzooplankton in the uppermost regions of the SDWSC (Ambler et al. 1985). Microzooplankton can benefit mesozooplankton by either concentrating multiple phytoplankton cells in one organism that is then consumed or serve as supplemental food in addition to phytoplankton (Gifford et al. 2007). The microzooplankton community has been identified as being understudied in the estuary and delta and is an important trophic link (Brown et al. 2016). A more targeted study of the microzooplankton community would provide better insight into this level of trophic linkage, as well as a study that includes detrital food sources.

Detritus was not measured as a mesozooplankton food source in our sampling but can be a supplemental source of nutrition for zooplankton communities. Isotope studies in the SDWSC show higher detrital organic material in the turbidity maximum zone (Young et al. 2021). We would expect detritus to be particularly important for invertebrate organisms in the MCHT zone, where allochthonous material can accumulate (Etcheber et al. 2007). Use of detrital food sources by mesozooplankton differs among taxa, and zooplankton can exhibit plasticity between feeding on live phytoplankton and detrital sources (Derisio et al. 2014, DeMott 1988). Similarly, the benefits of consuming detritus appear to differ (Harfmann et al. 2019, Müller-Solger et al. 2002). While detrital sources of food are abundant, phytoplankton biomass is considered to be more valuable to the zooplankton food web (Sobczak et al. 2005). Detrital food sources can be important for mysid shrimp and other suprabenthic invertebrates, a historically important supplemental prey item for Delta Smelt, with declining numbers in the estuary and delta (Jassby and Winder 2011, Feyrer et al. 2003, Fockedey and Mees 1999).

While we broadly interpreted chlorophyll-*a* as a proxy for phytoplankton biomass there are important caveats to consider. Phytoplankton community composition plays a key role in determining chlorophyll-*a* concentrations because different taxonomic groups of phytoplankton can have variable chlorophyll-*a* content (Kasprzak et al. 2008). In addition, the relationship between phytoplankton biomass and chlorophyll-*a* can vary due to factors like cell size, seasonality, available light, and nutrient concentrations, which could explain why we had higher chlorophyll-*a* measurements, but lower mean cell counts in certain subregions (Jakobsen and Markager 2016, Felip and Catalan 2000). Our results indicate that chlorophyll-*a* was an important factor in determining zooplankton communities which suggests biomass is an important factor. Individual phytoplankton taxa were not identified as important in our analysis. This could be an artifact of using cell density instead of biovolume, which may produce a different view of what phytoplankton taxa dominate a region. For example, smaller-celled phytoplankton may be more abundant but make up less of the biomass compared to larger but less abundant taxa. Studies integrating phytoplankton biomass alongside phytoplankton community composition data and chlorophyll-*a* measurements would provide more information on how phytoplankton and zooplankton biomass are related (Yuan and Pollard 2018).

The phytoplankton community changed numerically from diatom dominated to more cyanobacteria dominated with increasing residence time (specific conductance). A similar shift from larger-celled diatoms to smaller-celled cyanobacteria with increasing water residence times has been seen in other parts of the delta (Stumpner et al. 2020). Nitrogen limitation may have been a factor in the upper regions of the SDWSC as suggested by Kalmbach et al. (2021), where chlorophyll-*a* increased as nitrogen concentrations decreased, and phosphate remained high (Figure 8-5). Stumpner et al. (2020) found similar low-nitrogen high-chlorophyll dynamics in the highest water residence areas of the Cache Slough Complex, which may suggest a similar nutrient-phytoplankton relationship in that region. Observed patterns in the size and species composition of phytoplankton and mesozooplankton communities could also or instead be due to differences among zooplankton taxa in prey size selectivity. For example, multiple studies have shown that cladocerans prefer to feed on smaller phytoplankton particles, while calanoid copepods feed on larger phytoplankton cells and can be more selective about what they consume (Sommer and Sommer 2006, Yoshida et al. 2001, Lehmann 2000, DeMott 1988, Peters and Downing 1984). Toxicity may also play a role in determining the standing stock of phytoplankton. Zooplankton including *P. forbesi* have been shown to select against ingesting toxic *Microcystis* cells, a cyanobacteria genus responsible for recent blooms in the delta (Ger et al. 2019, Moni et al. 2011, Ger et al. 2010).

Our study not did directly measure phytoplankton cell size and we excluded picophytoplankton due to our identification methodology. Phytoplankton cell size can have important implications for trophic linkages in the zooplankton community. A study in the Cache Slough region of the delta found the phytoplankton community included the smaller picophytoplankton in areas with high water residence times, rather than the predicted large-celled diatoms (Stumpner et al. 2020). Despite our inability to report on this trophic linkage from the smaller components of the phytoplankton community, our phytoplankton community composition results (Figure 8-6) were similar to Stumpner et al. (2020) with lower diatom proportional abundance in the high conductivity zones. Phytoplankton communities dominated by smaller sized phytoplankton tend to contribute more to the microbial food web while larger-celled phytoplankton are directly fed upon by mesozooplankton (Marañón et al. 2009, Cloern and Dufford 2005). Cell size may affect zooplankton community composition by reflecting changing food resources available to zooplankton, routing energy and prey through different trophic pathways as well as zooplankton predators exerting influences on phytoplankton cell size (Murrell and Lores 2004, Cloern and Dufford 2005, Bergquist et al. 1985). This has important implications for the food resources available for zooplankton.

In the estuary, phytoplankton and zooplankton are well studied during their peak abundance seasons from spring to summer. In other aquatic ecosystems, phytoplankton and zooplankton communities exhibit seasonal variation and shifts in community composition (Li et al. 2019, Murrell and Lowes 2004). Zooplankton have demonstrated seasonal and spatial shifts in their diets, thus the importance of phytoplankton for different zooplankton species can change across seasons (Rautio et al. 2011, Taipale et al. 2009). Thus, examining if the zooplankton community changes from season to season can provide information on habitat quality within the SDWSC for resident populations of Delta Smelt present in the area throughout their life cycle (Merz et al. 2016). Our study focuses on the fall season, when zooplankton and phytoplankton are less abundant but is a crucial time for Delta Smelt breeding. The fall season is also when freshwater management actions to improve Delta Smelt habitat and prey quality and quantity occur (Hammock et al. 2022, Young et al. 2021, Hamock et al. 2019, Merz et al. 2016, Murphy and Hamilton 2013).

Conclusion

Multiple attributes go into defining a habitat "hot spot" for Delta Smelt populations given the altered ecosystem within the San Francisco Bay Estuary, such as prey availability, temperature, turbidity, contaminant levels, etc. (Kimmerer et al. 2018, Sommer and Mejia 2013). Understanding how environmental conditions influence the dynamics of the food web for Delta Smelt can help identify ecological processes that are important in creating the conditions in which abundant prey biomass co-occurs with other "hot spot" habitat conditions. Our finding that specific conductance (a proxy for water residence time) had the greatest influence on mesozooplankton community composition adds to other studies that suggest that water residence times could be important to habitat restoration efforts for Delta Smelt throughout the estuary. Specifically, we found that food resources (zooplankton populations) were highest in regions with the oldest water. We also found a positive correlation between zooplankton biomass and chlorophyll-*a*. Additionally, we found that chlorophyll-*a* was high in regions with high turbidity and phosphate but low nitrate, suggesting uptake of available nitrate by phytoplankton and that phosphate is not a limiting resource in the SDWSC. Future studies should consider other characteristics of the zooplankton food web such as phytoplankton biovolume, cell size distribution and microzooplankton abundance, which may also affect mesozooplankton abundance and community composition.

Acknowledgements

This work was conducted as part of the Interagency Ecological Program (IEP) annual work plan. Early reviews of related study plans were supported by the IEP Flow Alteration Project Work Team and the Collaborative Adaptive Management Team (special thanks to Larry Brown [USGS]), and USFWS, DWR, CDFW, and USBR. Permitting for this work was facilitated through CDFW, USWFS and IEP. This study was supported by the contribution of multiple IEP agency field sampling activities of fish and zooplankton (USFWS, DOP [USBR]), as well as informed by DWR DAYFLOW. Funding and contractual support was provided by USBR, DWR, State Water Contractors (special thanks to Jennifer Pierre) and State and Federal Contractors Water Agency (special thanks to Laura Valoppi). Nutrient samples were analyzed by Xien Wang, UC Davis. We acknowledge the support of many people from the Delta science community. Contributors from ICF include Jason Hassrick, Lenny Grimaldo, Colin Brennan, Rob Miller, Athena Maguire, Brandon Greco, Andrew Winston, Ramona Zeno, Jake Sousa, Angelina Ravani, Tim Carrara, Katherine Maniscalco, Donna Maniscalco, Eric Chapman, Teague Corning, Crystal Garcia, LuzMaria Soto, Rita Wilson, Amy Wong, Amy Lagerquist, Jamie Yin and Stephanie Owens. We thank Stephanie Durkacz, Catherine Johnston, and Lara Mitchell (USFWS) on timely guidance for site selection, coordination, and data; and Tom Philippi (National Park Service) for sampling and GRTS advice. Any use of trade, product, or firm names is for descriptive purposes only and does not imply endorsement by the U.S. Bureau of Reclamation or the U.S. Government. The views expressed are those of the authors and do not represent the official opinion of the U.S. Bureau of Reclamation.

References

Almén, A. K., & Tamelander, T. (2020). Temperature-related timing of the spring bloom and match between phytoplankton and zooplankton. Marine Biology Research, 16(8-9), 674-682.

418 Ambler, J. W., Cloern, J. E., & Hutchinson, A. (1985). Seasonal cycles of zooplankton from San
419 Francisco Bay. In *Temporal Dynamics of an Estuary: San Francisco Bay* (pp. 177-197). Springer,
420 Dordrecht.
421 Arhonditsis, G. B., Stow, C. A., Steinberg, L. J., Kenney, M. A., Lathrop, R. C., McBride, S. J., &
422 Reckhow, K. H. (2006). Exploring ecological patterns with structural equation modeling and
423 Bayesian analysis. Ecological Modelling, 192(3-4), 385-409.
424 Arscott, D. B., Jackson, J. K., & Kratzer, E. B. (2006). Role of rarity and taxonomic resolution in a
425 regional and spatial analysis of stream macroinvertebrates. *Journal of the North American*
426 *Benthological Society*, *25*(4), 977-997.
427 Baxter, R., Breuer, R., Brown, L., Conrad, L., Feyrer, F., Fong, S., Gehrts, K., Grimaldo, L., Herbold,
428 B., Hrodey, P., Mueller-Solger, A, Sommer, T., Souza, K. (2010). Interagency Ecological
429 Program 2010 pelagic organism decline work plan and synthesis of results. *Sacramento, CA:*
430 *Interagency Ecological Program for the San Francisco Estuary. Available online at:*
431 *https://www.waterboards.ca.gov/waterrights/water_issues/programs/bay_delta/docs/cmnt091412/sldmwa*
432 */baxter_etal_iep_2010.pdf. Last accessed Dec*, *6*, 2021.
433 Bellinger, E. G., & Sigee, D. C. (2015). Freshwater algae: identification, enumeration and use as
434 bioindicators. John Wiley & Sons.
435 Bergquist, A. M., Carpenter, S. R., & Latino, J. C. (1985). Shifts in phytoplankton size structure and
436 community composition during grazing by contrasting zooplankton assemblages 1. *Limnology*
437 *and Oceanography*, *30*(5), 1037-1045.
438 Brown, L. R., Kimmerer, W., Conrad, J. L., Lesmeister, S., & Mueller–Solger, A. (2016). Food webs
439 of the Delta, Suisun Bay, and Suisun Marsh: an update on current understanding and
440 possibilities for management. *San Francisco Estuary and Watershed Science*, *14*(3).
441 Bollens, S. M., Breckenridge, J. K., Cordell, J. R., Rollwagen-Bollens, G., & Kalata, O. (2012).
442 Invasive copepods in the Lower Columbia River Estuary: Seasonal abundance, co-
443 occurrence and potential competition with native copepods. *Aquatic Invasions*, *7*(2).
444 Bowen, A., Rollwagen-Bollens, G., Bollens, S. M., & Zimmerman, J. (2015). Feeding of the invasive
445 copepod Pseudodiaptomus forbesi on natural microplankton assemblages within the lower
446 Columbia River. *Journal of Plankton Research*, *37*(6), 1089-1094.
447 Calbet, A. (2008). The trophic roles of microzooplankton in marine systems. *ICES Journal of Marine*
448 *Science*, *65*(3), 325-331.
449 Calbet, A., & Saiz, E. (2005). The ciliate-copepod link in marine ecosystems. *Aquatic Microbial*
450 *Ecology*, *38*(2), 157-167.
451 Cloern, J. E., & Dufford, R. (2005). Phytoplankton community ecology: principles applied in San
452 Francisco Bay. *Marine Ecology Progress Series*, *285*, 11-28.
453 Cohen, A. N., & Carlton, J. T. (1998). Accelerating invasion rate in a highly invaded
454 estuary. *Science*, *279*(5350), 555-558.
455 Dahm, C. N., Parker, A. E., Adelson, A. E., Christman, M. A., & Bergamaschi, B. A. (2016).
456 Nutrient dynamics of the Delta: effects on primary producers. *San Francisco Estuary and*
457 *Watershed Science*, *14*(4).
458 DeMott, W. R. (1988). Discrimination between algae and artificial particles by freshwater and marine
459 copepods 1. *Limnology and Oceanography*, *33*(3), 397-408.
460 Derisio, C., Braverman, M., Gaitán, E., Hozbor, C., Ramírez, F., Carreto, J., ... & Mianzan, H.
461 (2014). The turbidity front as a habitat for Acartia tonsa (Copepoda) in the Río de la Plata,
462 Argentina-Uruguay. *Journal of Sea Research*, *85*, 197-204.

Downing, B. D., Bergamaschi, B. A., Kendall, C., Kraus, T. E., Dennis, K. J., Carter, J. A., & Von Dessonneck, T. S. (2016). Using continuous underway isotope measurements to map water residence time in hydrodynamically complex tidal environments. *Environmental science & technology*, *50*(24), 13387-13396.

Du, X., García-Berthou, E., Wang, Q., Liu, J., Zhang, T., & Li, Z. (2015). Analyzing the importance of top-down and bottom-up controls in food webs of Chinese lakes through structural equation modeling. *Aquatic Ecology*, *49*(2), 199-210.

Etcheber, H., Taillez, A., Abril, G., Garnier, J., Servais, P., Moatar, F., & Commarieu, M. V. (2007). Particulate organic carbon in the estuarine turbidity maxima of the Gironde, Loire and Seine estuaries: origin and lability. Hydrobiologia, 588(1), 245-259.

Felip, M., & Catalan, J. (2000). The relationship between phytoplankton biovolume and chlorophyll in a deep oligotrophic lake: decoupling in their spatial and temporal maxima. *Journal of Plankton Research*, *22*(1), 91-106.

Feyrer, F., B. Herbold, S.A. Matern, and P.B. Moyle. 2003. Dietary shifts in a stressed fish assemblage: consequences of a bivalve invasion in the San Francisco Estuary. Environmental Biology of Fishes 67: 277-288.

Feyrer, F., Slater, S. B., Portz, D. E., Odom, D., Morgan-King, T., & Brown, L. R. (2017). Pelagic nekton abundance and distribution in the northern Sacramento–San Joaquin Delta, California. *Transactions of the American Fisheries Society*, *146*(1), 128-135.

Fockedey, N., & Mees, J. (1999). Feeding of the hyperbenthic mysid Neomysis integer in the maximum turbidity zone of the Elbe, Westerschelde and Gironde estuaries. Journal of Marine Systems, 22(2-3), 207-228.

Friedl, G., & Wüest, A. (2002). Disrupting biogeochemical cycles-Consequences of damming. Aquatic Sciences, 64(1), 55-65.

Ger, K. A., Arneson, P., Goldman, C. R., & Teh, S. J. (2010). Species specific differences in the ingestion of Microcystis cells by the calanoid copepods Eurytemora affinis and Pseudodiaptomus forbesi. *Journal of plankton research*, *32*(10), 1479-1484.

Ger, K. A., Naus-Wiezer, S., De Meester, L., & Lürling, M. (2019). Zooplankton grazing selectivity regulates herbivory and dominance of toxic phytoplankton over multiple prey generations. *Limnology and Oceanography*, *64*(3), 1214-1227.

Gifford, S. M., Rollwagen-Bollens, G., & Bollens, S. M. (2007). Mesozooplankton omnivory in the upper San Francisco Estuary. *Marine Ecology Progress Series*, *348*, 33-46.

Glibert, P. M. (2010). Long-term changes in nutrient loading and stoichiometry and their relationships with changes in the food web and dominant pelagic fish species in the San Francisco Estuary, California. *Reviews in Fisheries Science*, *18*(2), 211-232.

Glibert, P. M., Fullerton, D., Burkholder, J. M., Cornwell, J. C., & Kana, T. M. (2011). Ecological stoichiometry, biogeochemical cycling, invasive species, and aquatic food webs: San Francisco Estuary and comparative systems. *Reviews in Fisheries Science*, *19*(4), 358-417.

Grace, J. B., Anderson, T. M., Olff, H., & Scheiner, S. M. (2010). On the specification of structural equation models for ecological systems. *Ecological Monographs*, *80*(1), 67-87.

Gross, E., Andrews, S., Bergamaschi, B., Downing, B., Holleman, R., Burdick, S., & Durand, J. (2019). The use of stable isotope-based water age to evaluate a hydrodynamic model. *Water*, *11*(11), 2207.

Hada, A., & Uye, S. I. (1991). Cannibalistic feeding behavior of the brackish-water copepod Sinocalanus tenellus. *Journal of Plankton research*, *13*(1), 155-166.

Hamilton, S. A., & Murphy, D. D. (2020). Use of affinity analysis to guide habitat restoration and enhancement for the imperiled delta smelt. *Endangered Species Research*, *43*, 103-120.

Hammock, B. G., Hartman, R., Slater, S. B., Hennessy, A., & Teh, S. J. (2019). Tidal wetlands associated with foraging success of Delta Smelt. *Estuaries and Coasts*, *42*(3), 857-867.

Hammock, B. G., Hartman, R., Dahlgren, R. A., Johnston, C., Kurobe, T., Lehman, P. W., ... & Teh, S. J. (2022). Patterns and predictors of condition indices in a critically endangered fish. Hydrobiologia, 849(3), 675-695.

Hammock, B. G., Hobbs, J. A., Slater, S. B., Acuña, S., & Teh, S. J. (2015). Contaminant and food limitation stress in an endangered estuarine fish. Science of the Total Environment, 532, 316-326.

Harfmann, J., Kurobe, T., Bergamaschi, B., Teh, S., & Hernes, P. (2019). Plant detritus is selectively consumed by estuarine copepods and can augment their survival. *Scientific reports*, *9*(1), 1-9.

Hobbs, J. A., Lewis, L. S., Willmes, M., Denney, C., & Bush, E. (2019). Complex life histories discovered in a critically endangered fish. *Scientific reports*, *9*(1), 1-12.

Hodapp, D., Meier, S., Muijsers, F., Badewien, T. H., & Hillebrand, H. (2015). Structural equation modeling approach to the diversity-productivity relationship of Wadden Sea phytoplankton. *Marine Ecology Progress Series*, *523*, 31-40.

Islam, M. S., Ueda, H., & Tanaka, M. (2006). Spatial and seasonal variations in copepod communities related to turbidity maximum along the Chikugo estuarine gradient in the upper Ariake Bay, Japan. Estuarine, Coastal and Shelf Science, 68(1-2), 113-126.

Jakobsen, H. H., & Markager, S. (2016). Carbon-to-chlorophyll ratio for phytoplankton in temperate coastal waters: Seasonal patterns and relationship to nutrients. *Limnology and Oceanography*, *61*(5), 1853-1868.

Kalmbach, A.K., D.M. Cox, C.Y. Lee, and A. Schultz. 2021. Comparison of Phytoplankton Community Structure and Nutrient Conditions in the Sacramento River Delta During a Fall Flow Action and Non-action Period. Pages 289-331 in A.A. Schultz, editor. Directed Outflow Project: Technical Report 2. U.S. Bureau of Reclamation, Bay-Delta Office, California-Great Basin Region, Sacramento, CA. March 2021, 349 pp.

Kayfetz, K., & Kimmerer, W. (2017). Abiotic and biotic controls on the copepod Pseudodiaptomus forbesi in the upper San Francisco Estuary. *Marine Ecology Progress Series*, *581*, 85-101.

Keller, D. P., Lee, D. Y., & Hood, R. R. (2014). Turbidity maximum entrapment of phytoplankton in the Chesapeake Bay. Estuaries and coasts, 37(2), 279-298.

Kasprzak, P., Padisak, J., Koschel, R., Krienitz, L., & Gervais, F. (2008). Chlorophyll a concentration across a trophic gradient of lakes: An estimator of phytoplankton biomass? *Limnologica*, *38*(3-4), 327-338.

Kayfetz, K., S.M. Bashevkin, M. Thomas, R. Hartman, C.E. Burdi, A. Hennessy, T. Tempel, A. Barros, and E. Burdi. 2020. Zooplankton Integrated Dataset Metadata Report. Delta Stewardship Council.

Keller, D. P., Lee, D. Y., & Hood, R. R. (2014). Turbidity maximum entrapment of phytoplankton in the Chesapeake Bay. *Estuaries and coasts*, *37*(2), 279-298.

Kerr, L. A., & Secor, D. H. (2010). Latent effects of early life history on partial migration for an estuarine-dependent fish. *Environmental Biology of Fishes*, *89*(3), 479-492.

Kimmerer, W. (2004). Open water processes of the San Francisco Estuary: from physical forcing to biological responses. *San Francisco Estuary and Watershed Science*, *2*(1).

Kimmerer, W. J. (2002). Effects of freshwater flow on abundance of estuarine organisms: physical effects or trophic linkages?. *Marine Ecology Progress Series*, *243*, 39-55.

Kimmerer, W., Ignoffo, T. R., Bemowski, B., Modéran, J., Holmes, A., & Bergamaschi, B. (2018). Zooplankton dynamics in the cache slough complex of the Upper San Francisco Estuary. San Francisco Estuary and Watershed Science, 16(3).

557 Kimmerer W, T.R. Ignoffo, and L. Sullivan L. 2011. Length, weight, carbon, and nitrogen content of
558 the common copepods in the San Francisco Estuary. Tiburon, CA: Romberg Tiburon
559 Center, San Francisco State University. Unpublished Manuscript.
560 Kimmerer, W. J., & Thompson, J. K. (2014). Phytoplankton growth balanced by clam and
561 zooplankton grazing and net transport into the low-salinity zone of the San Francisco
562 Estuary. Estuaries and Coasts, 37(5), 1202-1218.
563 Kruk, M., & Paturej, E. (2020). Indices of trophic and competitive relations in a planktonic network
564 of a shallow, temperate lagoon. A graph and structural equation modeling
565 approach. *Ecological Indicators*, *112*, 106007.
566 Lehman, P. W. (2000). Phytoplankton biomass, cell diameter, and species composition in the low
567 salinity zone of northern San Francisco Bay Estuary. *Estuaries*, *23*(2), 216-230.
568 Li, C., Feng, W., Chen, H., Li, X., Song, F., Guo, W., ... & Sun, F. (2019). Temporal variation in
569 zooplankton and phytoplankton community species composition and the affecting factors in
570 Lake Taihu—a large freshwater lake in China. Environmental Pollution, 245, 1050-1057.
571 Liu, X., & Georgakakos, A. P. (2021). Chlorophyll an estimation in lakes using multi-parameter
572 sonde data. *Water Research*, *205*, 117661.
573 Lucas, L. V., & Thompson, J. K. (2012). Changing restoration rules: Exotic bivalves interact with
574 residence time and depth to control phytoplankton productivity. Ecosphere, 3(12), 1-26.
575 Lund, J. W. G., Kipling, C., & Le Cren, E. D. (1958). The inverted microscope method of estimating
576 algal numbers and the statistical basis of estimations by counting. Hydrobiologia, 11(2), 143-
577 170.
578 Lv, H., Yang, J., Liu, L., Yu, X., Yu, Z., & Chiang, P. (2014). Temperature and nutrients are
579 significant drivers of seasonal shift in phytoplankton community from a drinking water
580 reservoir, subtropical China. Environmental Science and Pollution Research, 21(9), 5917-
581 5928.
582 Mahardja, B., Hobbs, J. A., Ikemiyagi, N., Benjamin, A., & Finger, A. J. (2019). Role of freshwater
583 floodplain-tidal slough complex in the persistence of the endangered delta smelt. *PloS*
584 *one*, *14*(1), e0208084.
585 Marañón, E., Steele, J., Thorpe, A., & Turekian, K. (2009). Phytoplankton size structure. *Elements of*
586 *physical oceanography: A derivative of the encyclopedia of ocean sciences*, *85*.
587 Merz, J. E., Bergman, P. S., Simonis, J. L., Delaney, D., Pierson, J., & Anders, P. (2016). Long-term
588 seasonal trends in the prey community of Delta Smelt (Hypomesus transpacificus) within the
589 Sacramento-San Joaquin Delta, California. Estuaries and Coasts, 39(5), 1526-1536.
590 Merz, J. E., Hamilton, S., Bergman, P. S., & Cavallo, B. (2011). Spatial perspective for delta smelt: a
591 summary of contemporary survey data. *California Fish and Game*, *97*(4), 164-189.
592 Mioni, C., Kudela, R., Baxa, D., Sullivan, M., Hayashi, K., Smythe, U. T., & White, C. (2011).
593 Harmful cyanobacteria blooms and their toxins in Clear Lake and the Sacramento-San
594 Joaquin Delta (California). Delta (California), 10, 058-150.
595 Montgomery, J. R. (2017). Food web dynamics in shallow tidal sloughs of the San Francisco Estuary.
596 M.S. Thesis. University of California, Davis.
597 Mount, J., Bennett, W., Durand, J., Fleenor, W., Hanak, E., Lund, J., & Moyle, P. (2012). Aquatic
598 ecosystem stressors in the Sacramento-San Joaquin Delta. San Francisco: Public Policy
599 Institute of California.
600 Moyle, P. B., Brown, L. R., Durand, J. R., & Hobbs, J. A. (2016). Delta smelt: life history and decline
601 of a once-abundant species in the San Francisco Estuary. *San Francisco Estuary and Watershed*
602 *Science*, *14*(2).
603 Moyle, P. B., Lund, J. R., Bennett, W. A., & Fleenor, W. E. (2010). Habitat variability and complexity
604 in the upper San Francisco Estuary. *San Francisco Estuary and Watershed Science*, *8*(3).

605 Müller-Solger, A. B., Jassby, A. D., & Müller-Navarra, D. C. (2002). Nutritional quality of food
606 resources for zooplankton (Daphnia) in a tidal freshwater system (Sacramento-San Joaquin
607 River Delta). *Limnology and Oceanography*, *47*(5), 1468-1476.
608 Murphy, D. D., & Hamilton, S. A. (2013). Eastward migration or marshward dispersal: Exercising
609 survey data to elicit an understanding of seasonal movement of delta smelt. San Francisco
610 Estuary and Watershed Science, 11(3).
611 Murrell, M. C., & Lores, E. M. (2004). Phytoplankton and zooplankton seasonal dynamics in a
612 subtropical estuary: importance of cyanobacteria. *Journal of Plankton Research*, *26*(3), 371-382.
613 Oksanen, J., F.G. Blanchet, R. Kindt, P. Legendre, P.R. Minchin, R. O'hara, G.L. Simpson, P.
614 Solymos, M.H.H. Stevens, and H. Wagner. 2017. Package 'vegan'. Community ecology
615 package, version 2.5-7.
616 Orsi, J. J. (1995). Food habits of several abundant zooplankton species in the Sacramento-San
617 Joaquin estuary. IEP Technical Report 41, 22 pp.
618 Peters, R. H., & Downing, J. A. (1984). Empirical analysis of zooplankton filtering and feeding rates
619 1. *Limnology and Oceanography*, *29*(4), 763-784.
620 Rautio, M., Mariash, H., & Forsström, L. (2011). Seasonal shifts between autochthonous and
621 allochthonous carbon contributions to zooplankton diets in a subarctic lake. Limnology and
622 Oceanography, 56(4), 1513-1524.
623 Rollwagen-Bollens, G., Gifford, S., & Bollens, S. M. (2011). The role of protistan microzooplankton
624 in the upper San Francisco Estuary planktonic food web: source or sink?. *Estuaries and*
625 *coasts*, *34*(5), 1026-1038.
626 Roman, M., Zhang, X., McGilliard, C., & Boicourt, W. (2005). Seasonal and annual variability in the
627 spatial patterns of plankton biomass in Chesapeake Bay. *Limnology and Oceanography*, *50*(2),
628 480-492.
629 Roy, S., Bhattacharya, S., Das, P., & Chattopadhyay, J. (2007). Interaction among non-toxic
630 phytoplankton, toxic phytoplankton and zooplankton: inferences from field
631 observations. *Journal of Biological physics*, *33*(1), 1-17.
632 Schultz, A.A., L. Grimaldo, J.L. Hassrick, A.J. Kalmbach, A.G. Smith, O. Burgess, D. Barnard, and
633 J. Brandon. 2019. Effect of Isohaline (X2) and Region on Delta Smelt Habitat, Prey and
634 Distribution During the Summer and Fall: Insights into Managed Flow Actions in a Highly
635 Modified Estuary. In Directed Outflow Project: Technical Report, ed. A.A. Schultz, 237-301.
636 Mid-Pacific Region, Sacramento, CA. U.S. : U.S. Bureau of Reclamation, Bay-Delta Office.
637 Slater, S.B., and R.D. Baxter. 2014. Diet, Prey Selection, and Body Condition of Age-0 Delta Smelt,
638 Hypomesus transpacificus, in the Upper San Francisco Estuary. San Francisco Estuary and
639 Watershed Science 12.
640 Slater, S.B., A.A. Schultz, B.G. Hammock, A. Hennessy, and C.E. Burdi. 2019. Patterns of
641 zooplankton consumption by juvenile and adult Delta Smelt (Hypomesus transpacificus). In
642 Directed Outflow Project: Technical Report, ed. A.A. Schultz, 9-54. Sacramento, CA: U.S.
643 Bureau of Reclamation, Bay-Delta Office.
644 Sobczak, W. V., Cloern, J. E., Jassby, A. D., Cole, B. E., Schraga, T. S., & Arnsberg, A. (2005).
645 Detritus fuels ecosystem metabolism but not metazoan food webs in San Francisco estuary's
646 freshwater Delta. *Estuaries*, *28*(1), 124-137.
647 Sommer, T., & Mejia, F. (2013). A place to call home: a synthesis of Delta Smelt habitat in the upper
648 San Francisco Estuary. *San Francisco Estuary and Watershed Science*, *11*(2).
649 Sommer, U., & Sommer, F. (2006). Cladocerans versus copepods: the cause of contrasting top–
650 down controls on freshwater and marine phytoplankton. *Oecologia*, *147*(2), 183-194.

Starcevich, L., G. DiDonato, T. McDonald, and J. Mitchell. 2016. A GRTS user's manual for the SDrawNPS package: a graphical user interface for generalized random tessellation stratified (GRTS) sampling and estimation. Natural Resource Report NPS/PWRO/NRR–2016/1233. National Park Service, Fort Collins, CO.

Stevens Jr, D.L., and A.R. Olsen. 2004. Spatially balanced sampling of natural resources. Journal of the American statistical Association 99: 262-278.

Stumpner, E. B., Bergamaschi, B. A., Kraus, T. E., Parker, A. E., Wilkerson, F. P., Downing, B. D., ... & Kendall, C. (2020). Spatial variability of phytoplankton in a shallow tidal freshwater system reveals complex controls on abundance and community structure. *Science of the Total Environment*, *700*, 134392.

Suzuki, K. W., Nakayama, K., & Tanaka, M. (2009). Horizontal distribution and population dynamics of the dominant mysid Hyperacanthomysis longirostris along a temperate macrotidal estuary (Chikugo River estuary, Japan). *Estuarine, Coastal and Shelf Science*, *83*(4), 516-528.

Suzuki, K. W., Kasai, A., Nakayama, K., & Tanaka, M. (2012). Year-round accumulation of particulate organic matter in the estuarine turbidity maximum: comparative observations in three macrotidal estuaries (Chikugo, Midori, and Kuma Rivers), southwestern Japan. *Journal of oceanography*, *68*(3), 453-471.

Taipale, S., Kankaala, P., Hämäläinen, H., & Jones, R. I. (2009). Seasonal shifts in the diet of lake zooplankton revealed by phospholipid fatty acid analysis. Freshwater Biology, 54(1), 90-104.

Tomas, C. R. (Ed.). (1997). Identifying marine phytoplankton. Elsevier.

Wan, Y., Qiu, C., Doering, P., Ashton, M., Sun, D., & Coley, T. (2013). Modeling residence time with a three-dimensional hydrodynamic model: Linkage with chlorophyll a in a subtropical estuary. *Ecological Modelling*, *268*, 93-102.

Wehr, J. D., Sheath, R. G., & Kociolek, J. P. (Eds.). (2015). Freshwater algae of North America: ecology and classification. Elsevier.

Whipple, A. A., Grossinger, R. M., Rankin, D., Stanford, B., & Askevold, R. (2012). Sacramento-San Joaquin Delta historical ecology investigation: exploring pattern and process. Richmond: San Francisco Estuary Institute-Aquatic Science Center.

Wilkerson, F. P., Dugdale, R. C., Hogue, V. E., & Marchi, A. (2006). Phytoplankton blooms and nitrogen productivity in San Francisco Bay. *Estuaries and Coasts*, 29(3), 401-416.

Winder, M., & Jassby, A. D. (2011). Shifts in zooplankton community structure: implications for food web processes in the upper San Francisco Estuary. *Estuaries and Coasts*, *34*(4), 675-690.

Wood, S.N. (2011) Fast stable restricted maximum likelihood and marginal likelihood estimation of semiparametric generalized linear models. Journal of the Royal Statistical Society (B) 73(1):3-36

Yoshida, T., Gurung, T., Kagami, M., & Urabe, J. (2001). Contrasting effects of a cladoceran (Daphniagaleata) and a calanoid copepod (Eodiaptomusjaponicus) on algal and microbial plankton in a Japanese lake, Lake Biwa. *Oecologia*, *129*(4), 602-610.

Young, M. J., Feyrer, F., Stumpner, P. R., Larwood, V., Patton, O., & Brown, L. R. (2021). Hydrodynamics drive pelagic communities and food web structure in a tidal environment. *International Review of Hydrobiology*, *106*(2), 69-85.

Yuan, L. L., & Pollard, A. I. (2018). Changes in the relationship between zooplankton and phytoplankton biomasses across a eutrophication gradient. Limnology and oceanography, 63(6), 2493-2507.

Tables

Table 8-1. Number of samples taken within each subregion across all four years.

Year	LCLT	LCMT	MCHT	HCMT	HCLT
2017	5	2	9	4	4
2018	2	7	7	7	4
2019	3	9	8	9	11
2020	1	9	7	12	7
Total	**11**	**27**	**31**	**32**	**26**

Table 8-2. Environmental vector and factors correlation scores across zooplankton biomass NMDS ordination space and significance of the correlation.

Variable	R Squared Value	P-Value
Specific Conductance	0.72	0.0001
Subregion^	0.54	0.0001
Chlorophyll *a*	0.53	0.0001
Nitrate	0.41	0.0001
Ammonium	0.23	0.0001
Phosphate	0.22	0.0001
Year^	0.12	0.0008
Diatom	0.11	0.0033
Green Algae	0.08	0.017
Temperature	0.07	0.034
Total Phytoplankton	0.07	0.031
Turbidity	0.05	0.069
Day of the Year	0.05	0.085
Dinoflagellates	0.05	0.080
Year Type^	0.03	0.058
Other Phytoplankton	0.02	0.44
Cyanobacteria	0.02	0.46
Cryptomonads	0.01	0.82

^ symbol indicates the factor is a categorical variable.

705 Table 8-3. Detailed summary table of generalized additive model (GAM) results for water
706 quality parameters influence on chlorophyll- *a* in the SDWSC in the fall.

707 Linear Parameters:

Variable	Estimate	Standard Error	t-value	p-value
Intercept	2.49	0.065	38.51	$<2^{-16}$

708

709 Approximate Significant of Smooth Terms

Variable	Effective Degrees of Freedom	Reference Degrees of Freedom	F-value	P-value
Nitrate	1.47	9	0.49	0.041
Ammonium	4.13^{-05}	9	0.000	0.59
Phosphate	1.44	9	0.64	0.013
Turbidity	1.34	9	0.44	0.047
Temperature	4.97^{-05}	9	0.000	0.60
Specific Conductance	4.72	9	13.25	$<2^{-16}$

710 Adjusted r^2 = 0.71, Deviance Explained = 73.3%.

Figures

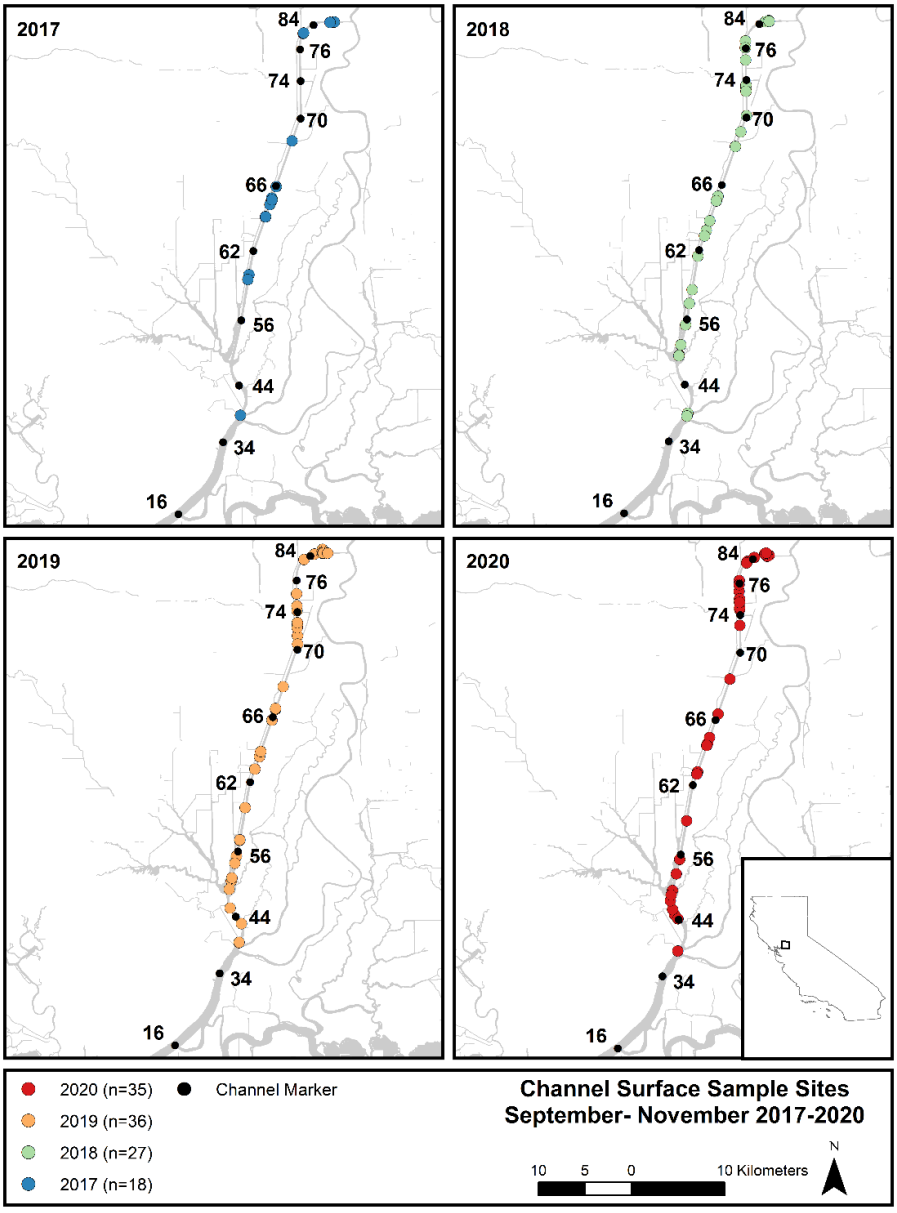

Figure 8-1. Sampling locations in the Sacramento Deep Water Ship Channel across four years (2017 – 2020) during the fall season (September – November).

Sample sizes are listed in the sample legend.

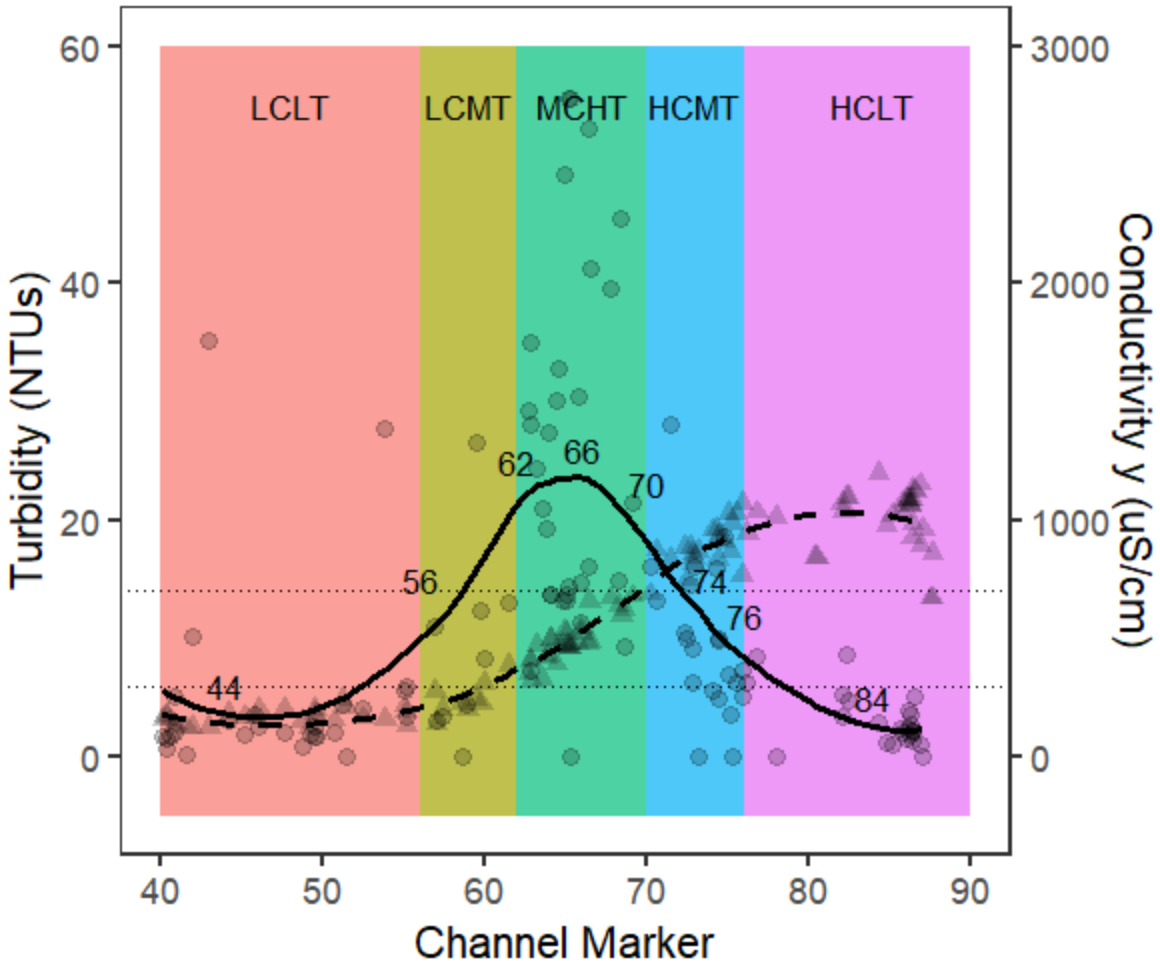

Figure 8-2. Loess fit curves for turbidity and specific conductance (conductivity) in relation to channel marker position.

Gray dots indicate turbidity values, gray triangles indicate conductivity values. Solid black line is loess fit curve for turbidity and dashed line indicates loess fit curve for conductivity. Acronyms: LCLT- Low conductivity low turbidity region, LCMT- Low conductivity moderate turbidity region, MCHT- Moderate conductivity high turbidity region, HCMT- High conductivity moderate turbidity region, and HCLT- High conductivity moderate turbidity region.

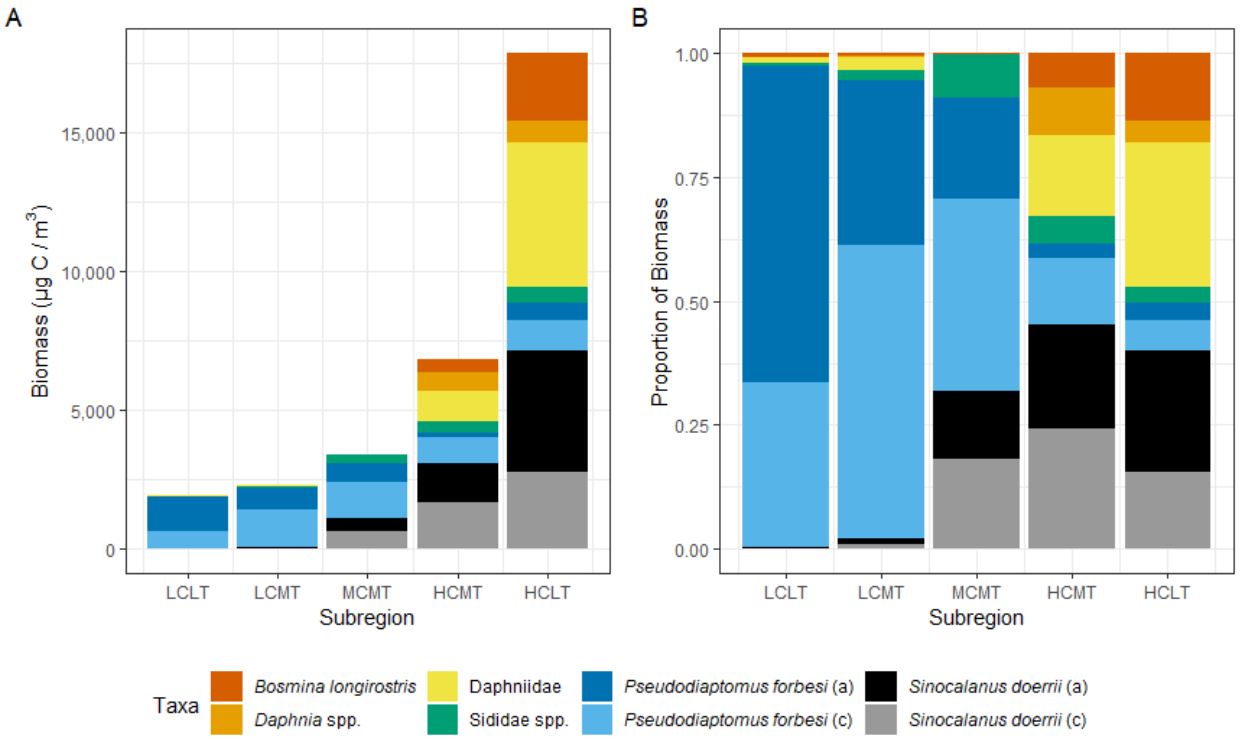

725

726 Figure 8-3. A: Mean biomass for mesozooplankton taxa for each subregion.

727 B: Proportion of mesozooplankton taxa for each subregion. (a) indicates adults and (c) indicates copepodites.

728

729

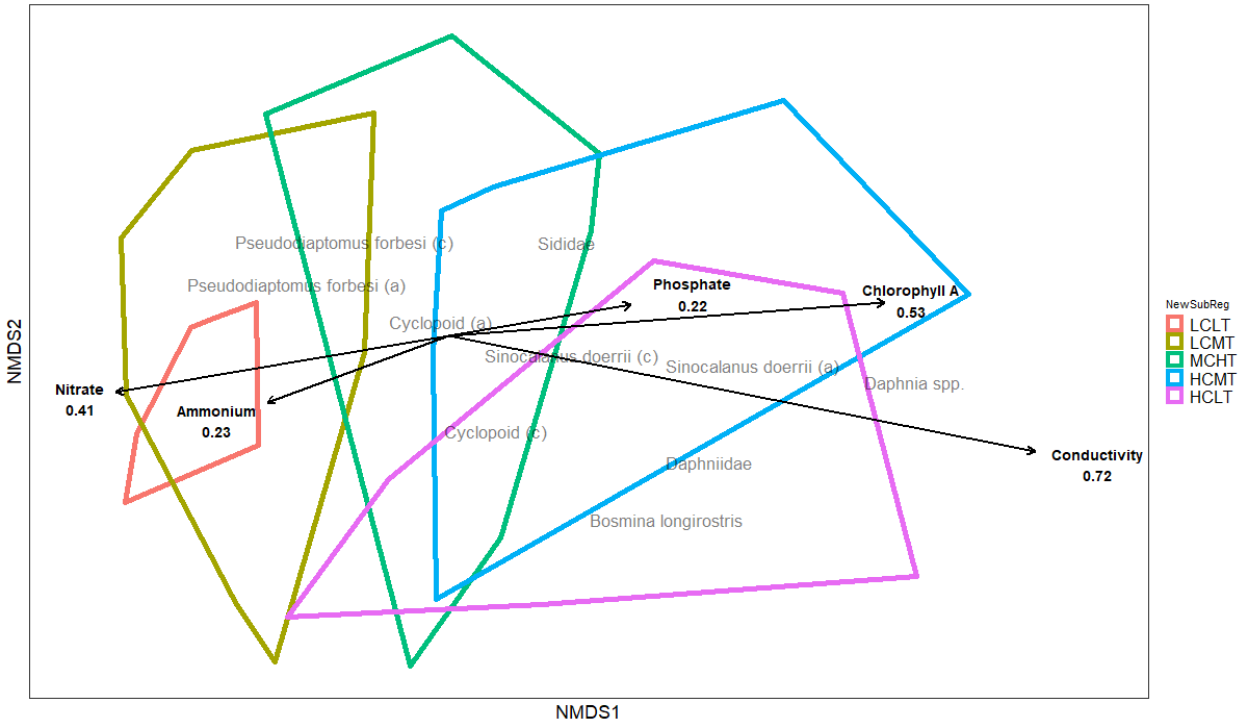

730

731 Figure 8-4. Non-Metric Multidimensional ordination of zooplankton species
732 communities across turbidity and conductivity subregions within the SDWSC.

733

734

735

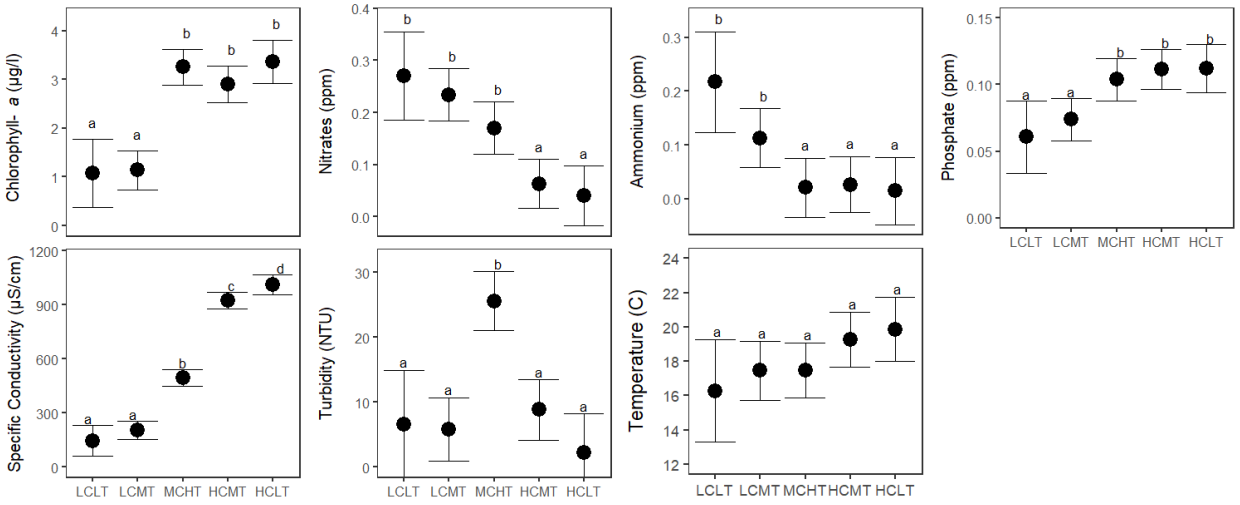

Figure 8-5. Mean water quality values and 95% confidence intervals along the SDWSC across five subregions.

Letters within each box indicate subregions with insignificant differences in mean values (pairwise comparison p-value <0.05).

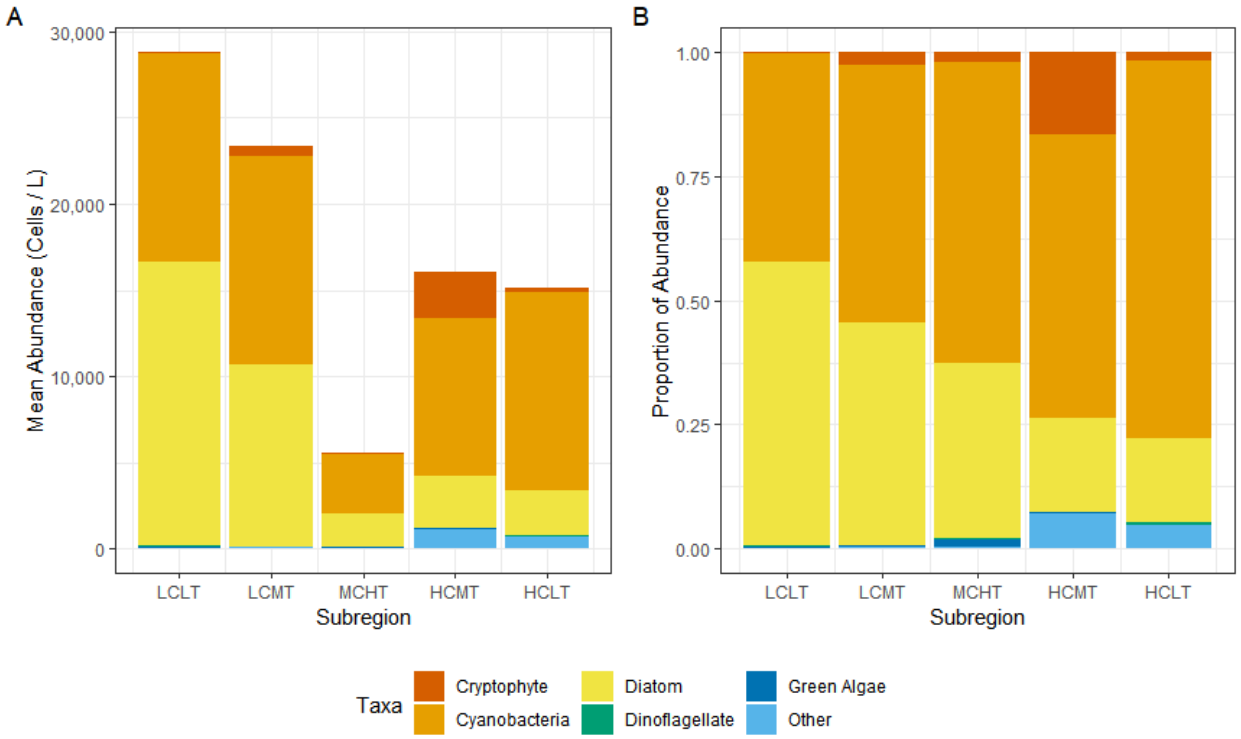

Figure 8-6. Mean cell abundance in cells per liter for each subregion for each phytoplankton taxa.

B: Proportion of phytoplankton taxa observed in each subregion. Phytoplankton data shown was only available from 2017 to 2019.

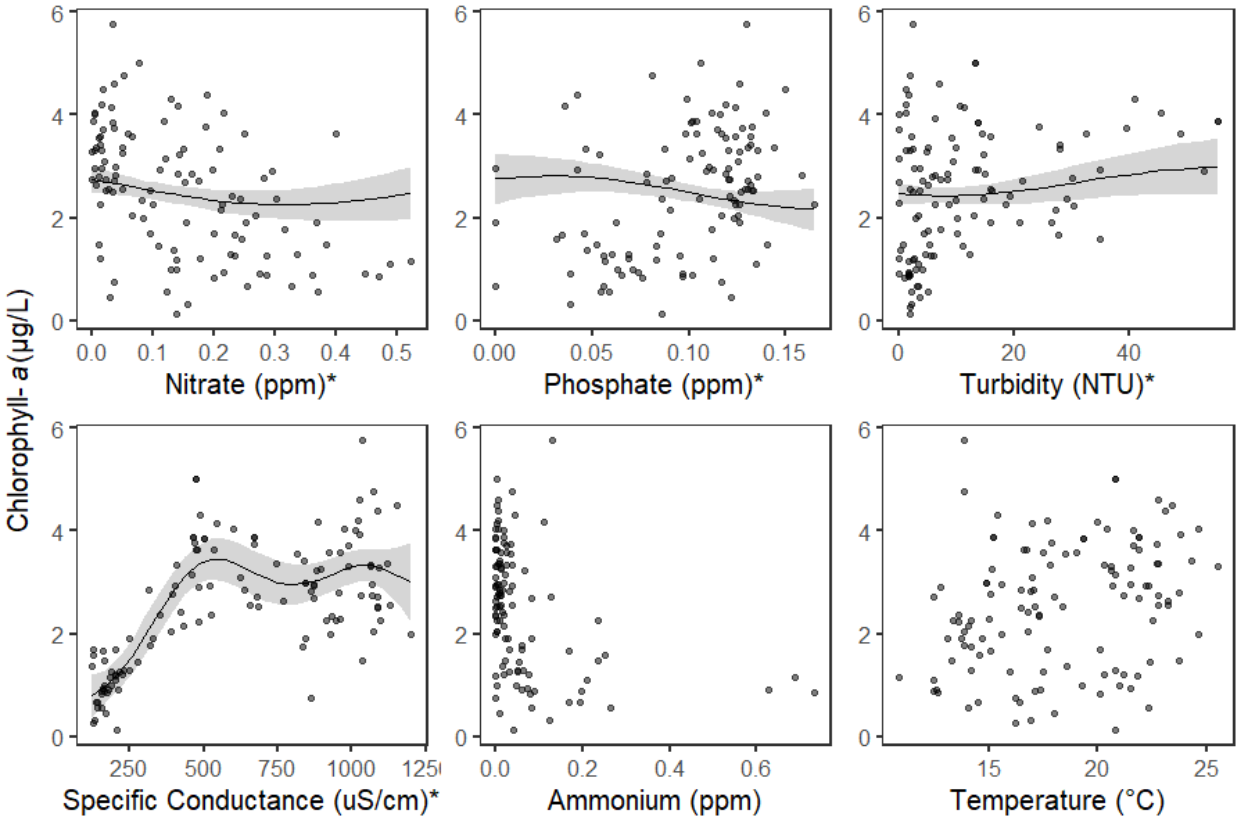

Figure 8-7. Chlorophyll-a trends in the Sacramento Deep Water Ship Channel via Generalized additive modeling.

Significance ($p < 0.05$) is indicated by *. Figures without trend lines were found to not be predictive of chlorophyll-*a* in the Sacramento Shipping channel in the fall

This page intentionally left blank.

Chapter 9: Detecting responses of Delta Smelt prey biomass to freshwater outflow management actions in a highly altered estuarine system: using power analysis to evaluate environmental monitoring sampling

Authors:

John Brandon[1*], Calvin Lee[1], April Smith[1,] Shawn Acuña[2], Andrew A. Schultz[3]

[1] ICF, 201 Mission Street, Suite 1500, San Francisco, CA 94105 USA

[2] Metropolitan Water District, 1211 L Street, #900, Sacramento, CA 95814 USA

[3]U.S. Bureau of Reclamation Bay-Delta Office -Science Division, 801 I Street, Suite 140, Sacramento, CA 95814 USA

*Corresponding author: John.Brandon@icf.com

Abstract

A suite of outflow management actions has been used to attempt to improve habitat conditions for the endangered Delta Smelt (*Hypomesus transpacificus*) in the San Francisco Estuary (estuary) and the Sacramento-San Joaquin Delta (delta). These outflow management actions (also referred to here as "actions" for short) target both abiotic and biotic factors related to Delta Smelt habitat including food availability. A statistical power analysis was conducted using environmental monitoring data and random site sampling data that have been collected to measure whether there are responses in Delta Smelt zooplankton prey to freshwater outflow management actions. The analyses used simulation to calculate the probability of detecting an increase in prey biomass during Fall X2 Action years based on a range of effect sizes given current sampling efforts in different regions of the estuary and delta. This study also evaluated the power of monitoring studies to detect a change from a smaller outflow action, the North Delta Food Subsidies (NDFS) action. Multiple scenarios were simulated, such as conducting a longer study, or increasing annual sampling effort. Overall, power to detect a difference in prey biomass during a Fall X2 Action was generally not very high unless there were large (>150%) changes in prey biomass during action years compared to non-action years. Probability of detection varied by region based on both effort and variability in prey biomass within each region. Power increased with increased annual sampling size and longer study duration, though the increase in power varied by region and simulated percent biomass increase. Simulation results also suggest the power to detect differences in total zooplankton CPUE was generally low for the NDFS action, even for relatively high effect sizes, at least for the simulation and hypothesis testing approach taken. Power to detect moderate changes in biomass remained low regardless of increasing

sample size or increasing number of action years. Future efforts aimed at detecting the effects of managed outflow actions on prey biomass in the estuary and delta should focus on long term monitoring efforts (i.e. adding more years of data). Different levels of natural variation between study regions is also important to consider in terms of sampling effort and statistical power to detect effects, since the environmental characteristics of a region may increase variability in zooplankton abundance and biomass relative to other regions. Regions with higher levels of variability would require more sampling effort to be able to detect zooplankton responses to managed outflow actions, all else being equal.

Introduction

The San Francisco Estuary (estuary) and Sacramento-San Joaquin Delta (delta) have undergone decades of anthropogenic changes (Whipple et al. 2012). To mitigate these anthropogenic effects, habitat restorations and flow actions are being implemented to benefit native species while trying to balance the needs of multiple stakeholders who utilize water resources. Data from environmental monitoring programs have been an essential part of characterizing how these actions have changed abiotic and biotic components of the estuary and delta ecosystems. Recently, more targeted sampling such as the Enhanced Delta Smelt Monitoring (EDSM) program have also been undertaken to study endangered native fishes like the Delta Smelt (*Hypomesus transpacificus*) (USFWS 2022). Related studies stemming from this effort are aimed at understanding how ecosystem-level changes are impacting population level changes of the Delta Smelt (Schultz 2019b, Schultz 2021).

The Delta Smelt is a small, mostly annual, planktivorous, euryhaline fish endemic to the delta and parts of the estuary. Delta Smelt were federally listed as threatened in 1993 and endangered in 2009 after a decline in the population that began in the 1980s and continues until today (Moyle et al. 2018, Thomson et al. 2010, USFWS 1993). Delta Smelt populations experienced a particularly abrupt decline in the early 2000s alongside several other pelagic species that was termed the pelagic organism decline (POD) (Baxter et al. 2008, Sommer et al. 2007). Multiple studies have since been undertaken to figure out the cause and what management actions could be taken to increase the Delta Smelt population.

The biological opinion issued by the United States Fish and Wildlife Service (USFWS) includes the Fall X2 Action during wet or above normal precipitation years (USFWS 2008). X2 is defined as the distance (km) from the Golden Gate Bridge to the tidally averaged 2 ppt salinity isohaline (Jassby et al. 1995). The Fall X2 Action is focused on shifting and maintaining the position of low salinity zone (LSZ; 0.5 – 6.0 ppt) in order to increase habitat critical to Delta Smelt during the maturation stage of their life cycle. By adjusting the position of X2 during the fall season, the LSZ may increase available Delta Smelt habitat in the Suisun Bay and Marsh region. Maintaining the LSZ in the Suisun region of the estuary by reservoir releases and/or export curtailment has many hypothesized benefits including higher food availability and quality for Delta Smelt (Kimmerer et al. 2018, Brown et al. 2014). Increased freshwater flows has been positively related to increases in abundance of some zooplankton taxa (Kimmerer 2002). Decreases in prey populations have been cited as one of the causes of Delta Smelt decline, thus zooplankton abundance and biomass data have become an important component of monitoring efforts and management actions (Hartman et al. 2021, Moyle et al. 2018, Hammock et al. 2015, Sommer et al. 2007).

Other smaller scale flow actions have been carried out, such as the North Delta Food Subsidies (NDFS) action, that target other regions of the delta and estuary. The NDFS action is a focused freshwater flow pulse during the summer-fall period through the Yolo Bypass floodplain system, upstream of the Delta into the northwestern section of the Delta, the Cache Slough complex and further downstream. This action is designed to enhance transport of phytoplankton and zooplankton prey into lower portions of the delta (Frantzich et al 2021). Increased phytoplankton biomass has been positively correlated with increased zooplankton growth and reproduction (Owens et al. 2019, Montgomery 2017, Cloern & Dufford 2005, Müller-Solger et al. 2002). The NDFS actions occurred in 2016, 2018 and 2019 but only in 2016 were increases in both phytoplankton and zooplankton density detected downstream of the Yolo Bypass, raising the possibility that current sampling efforts were insufficient to statistically determine if the action had an effect, if such an effect occurred (Frantzich et al 2021, Twardochleb et al 2021).

The scale of the Fall X2 and NDFS actions are different, but an increase in prey biomass for endangered Delta Smelt is included in the suite of hypothesized outcomes for both outflow actions. Different sampling regimes have been implemented to monitor the effects of these two actions. A logical question is whether an increase in prey biomass is detectable given the current sampling effort being leveraged for each action. Power analyses have been used to evaluate the ability of a study to detect a biological pattern and provide insight into how to structure future sampling efforts (George et al. 2021, Vaudor et al 2015, Nagelkerke and Van Densen 2007, Steidl et al. 1997, Thomas 1997, Peterman 1990).

Statistical power is a function of five variables. Given values for four of the variables, a power analysis can solve for the value of the fifth variable. The five factors inherent in a power analysis are: (1) sample size; (2) sampling error; (3) effect size for the model parameter of interest; (4) alpha (or the Type I error rate, i.e. the false positive rate in terms of a null hypothesis that there is no effect being rejected, when in fact there is no effect); and (5) beta (Type II error rate, i.e. the false negative rate in terms of failing to reject the null hypothesis that there is no effect, when in fact a true effect exists for a given parameter). Statistical power is defined as one minus beta when a true (non-zero) effect exists. In other words, statistical power is the percentage of times, if sampling were repeated, that a hypothesis test would be expected to correctly reject a null hypothesis of zero effect.

Consistency in the statistical approaches used for hypothesis testing between a power analysis and future analyses is desirable for inference. The regression models used in these analyses are meant to mimic the methods that have been used or are planned to be used to test for the effects of outflow management actions, such as mixed effects regression models (Schultz et al. 2019a). However, analytical solutions for calculating statistical power based on mixed-effects models can be complex. Therefore, we have approached this power analysis through the use of simulation.

Simulation provides a flexible approach to power analysis. It is less restricted by assumptions inherent in the analytical solutions for more traditional models, like those available for ANOVA (Cohen 1988). Simulation also does not rely on assumptions like balanced sampling designs, equality in sampling variability (i.e., equal standard errors in the model residuals) between strata or years, or normality in terms of model residuals. Likewise, this computational approach is amenable to count data, particularly, over-dispersed or zero-inflated count data common in fisheries science. For these reasons, simulation has become increasingly popular for applied power analyses of ecological studies based on structured data (data that are correlated or hierarchical in nature) that are collected under unbalanced sampling designs. To this end, statistical software packages have recently been published

for running power analyses using simulation in R, where the underlying hypotheses are represented by generalized linear mixed-effects models (Green and MacLeod 2016, Johnson et al. 2015).

In these analyses we examined the statistical power of existing sampling programs to detect a response in Delta Smelt prey biomass and abundance for two freshwater flow management actions: Fall X2 and NDFS. Using data from current studies we sought to answer: 1) What is the ability to detect an increase in Delta Smelt prey at varying response sizes given the Fall X2 Action (e.g., 20, 50, or 100% increase in biomass for key zooplankton species)? 2) How does the ability to detect differences in prey biomass in response to the Fall X2 management action vary across regions of the estuary and delta? 3) How would statistical power to detect a response change given additional years of sampling or increases in annual sample sizes assuming similar sampling conditions? 4) What is the ability of current sampling to detect changes in overall zooplankton abundance with smaller scale actions such as the NDFS?

Methods

For both the Fall X2 and NDFS actions, power analyses were developed to generally mimic statistical modeling approaches (e.g., mixed-effects linear regression models) that have been used in practice to assess potential changes in zooplankton biomass associated with each action. As noted above, the power analyses were based on a simulation approach. A power analysis using simulation takes three general steps: (1) Simulate multiple (e.g., 1000 or more) data sets under a given alternative hypothesis, e.g., that the effect size of interest is some value other than zero; (2) For each simulated data set, perform a statistical test, under the null hypothesis that the effect size is zero; and (3) Record the results of the hypothesis test for each iteration (Bolker 2008). The percentage of simulations for which the null hypothesis is correctly rejected is the resulting estimate of statistical power for the simulated effect size (or sample size, etc.). This process was carried out using the *SIMR* package in R which is designed to run simulations for power analyses based on generalized linear mixed-effects models (Green and MacLeod 2016). Confidence intervals for the statistical power estimates were calculated using the *binom.confint* function in *R* based on the "exact" (Pearson-Klopper) calculation. Available data and the details for the specific regression modeling approaches analyzed for each action are provided below.

Fall X2 Action

Data for the statistical modeling to evaluate the Fall X2 Action came from the California Department of Fish and Wildlife Fall Midwater Trawl Survey (FMWT) and data collected as part of the US Bureau of Reclamation Directed Outflow Project (DOP). Zooplankton data from the FMWT surveys was accessed through the *zooper* R package (Bashevkin 2020; Bashevkin et al. 2020). Collection, processing, and biomass conversion factors of zooplankton samples are described in the IEP Zooplankton Integrated Dataset Metadata Report (Kayfetz et al. 2020). Zooplankton field sampling for the DOP are detailed in Schultz et al. (2019a) and Hassrick et al. (2021). DOP zooplankton sample processing followed methods described in the Interagency Ecological Program's Environmental Monitoring Program, except 10 aliquot counts were used instead of 20 aliquot counts to account for higher sample densities resulting from the larger volume nets used for the project (Schultz et al. 2019a).

For the Fall X2 Action analysis, DOP data from 2017-2019 and FMWT data from 2011-2019 were used. Fall X2 Actions occurred during the years 2011, 2017 and 2019. Data from the months of

September to October were analyzed, corresponding to the timeframe when the Fall X2 Action is anticipated to benefit Delta Smelt habitat and prey. Zooplankton species that were considered representative of fall (Sep–Oct) Delta Smelt prey followed previous analyses of the Fall X2 management action (Schultz et al. 2019a). These species were based on a previous gut content and diet composition study, and in particular were based on gut samples collected during September 2005–2006 (Slater and Baxter 2014). The five copepod species included in the analyses were adult *Pseudodiaptomus forbesi*, *Limnoithonia* spp., *Sinocalanus doerrii*, *Acartiella sinensis*, and *Tortanus* spp. Biomass of the five copepod species were summed for each sample.

A mixed-effects regression model was used with a random effect on sampling station. This statistical approach was chosen because it is anticipated to be used in future zooplankton analysis. To simplify interpretation of the simulation results, a relatively simple log-linear regression equation was employed for the Fall X2 power analyses. The model for this analysis as expressed in the R computing language was:

$$\log(\text{BPUE}) \sim \text{Action} + \text{Turbidity} + \text{Salinity} + \text{Temperature} + (1 \mid \text{Station}) \quad (1)$$

Where: log() represents the natural logarithm; BPUE is the biomass (micrograms carbon, μg C) per unit effort as measured in net tow volume (m^3) for the five copepod species considered; Action was coded as a binary variable (a zero or one) for each year depending on whether the Fall X2 management action occurred or not that year; Turbidity was the recorded NTU for each sample; Salinity was recorded water salinity in ppt; Temperature was the recorded water surface temperature in degrees Celsius for each sample, and; Station was the unique station ID for each sample, which was modeled as a random effect on the intercepts, i.e. each sampling station had an associated average expected BPUE in the model, which was assumed to be correlated with the other stations through the random effects structure, but not necessarily equal across stations (which would be the case if a standard regression model was fit with a fixed-effects covariate on Station instead). These particular environmental covariates were included following previous investigations into potential Delta Smelt zooplankton prey species responses after the 2017 Fall X2 management action (Schultz et al. 2019a).

The null hypothesis tested for this analysis was that BPUE (a proxy for underlying biomass) of five Delta Smelt prey species was equal between Fall X2 Action and non-action years, and therefore the estimates of statistical power pertained to the likelihood of detecting a hypothetical difference in biomass for these prey species between action and non-action years.

The data for this analysis were confined to five sampling regions of interest: Suisun Bay, Suisun Marsh, the Lower Sacramento River, Cache Slough, and the Sacramento Ship Channel (Figure 9-1). Independent models were fit to the samples collected in each region, and likewise the power to detect region-specific differences in Delta Smelt zooplankton prey species was simulated individually for each region. This approach was taken, in part, because it was of interest to examine whether changes in region specific sampling effort or a reallocation of sampling effort between regions might be desirable.

The factors considered for the power analysis included: (1) effect size, which was simulated as a percentage increase in BPUE during action years (relative to non-action years) for the five selected Delta Smelt zooplankton prey species combined; (2) increases in annual sample sizes, and (3) duration of future monitoring years, i.e., the number of years into the future that monitoring may

take place. For the last two factors, effect sizes were fixed to the estimated value from the regression fit. The sample data used to inform the Fall X2 simulations are shown in Figure 9-2.

North Delta Food Subsidies Action

For the NDFS power analysis, data were obtained from the North Delta Food Subsidies-Colusa Basin Drain Study for years 2011-2019 (Twardochleb *pers. comm.*). In general, sampling for this study occurred every two weeks from the months of June to October and sampled before, during, and after managed and non-managed fall flow pulses occurred in the study area (Figure 9-3; Twardochleb et al 2021a). The NDFS action occurred during three years in this time frame: 2016, 2018 and 2019. For the purposes of these analyses, only data from these three action years were considered, because the hypothesis that was used as a basis for the simulations was whether zooplankton abundance differed after the managed flow actions relative to zooplankton abundance before the managed flow pulse. In other words, in non-action years there were also (non-managed) flow pulses, but any effects of those non-action flow pulses are not considered in these analyses.

The regression modeling approach was based generally on the analysis of the 2019 NDFS action by Twardochleb et al. (2021a). The natural logarithm of total zooplankton catch-per-unit effort (CPUE) in each sample was the response variable. Total zooplankton CPUE was calculated as the count of individuals for all zooplankton species caught. The flow period (before or after) and study regions were modeled as fixed effect covariates. Sampling stations were modeled as random effects with varying intercepts. The model for this analysis as expressed in the R computing language was:

$$\text{Log(CPUE)} \sim \text{Flow Period} + \text{Region} + (1 \mid \text{Station}) \quad (2)$$

Where: CPUE is the total catch (in numbers) for all zooplankton species; Flow Period (either "before" or "after") is relative to the annual fall flow pulse; Region represents sampling stations that are categorized as either "upstream" or "downstream", and Station represents individual sampling stations, which were treated as random effects following recent approaches to analyzing these data (e.g., Twardochleb et al. 2021a, Davis et al. 2021).

The start and end dates for the fall flow pulse followed previous analyses of the NDFS data (Jul 14–Aug 1, 2016; Aug 28–Sep 26, 2018, and Aug 26–Sep 21, 2019). The sampling sites for this analysis are located at monitoring stations beginning from near the confluence of the Sacramento and San Joaquin Rivers, moving upstream all the way to the Colusa Basin Drainage (Figure 9-3). All monitoring sites upstream from the Yolo Bypass Toe Drain (station STTD in Figure 9-2) were considered part of the NDFS "upstream" region, and all monitoring stations downstream of station STTD were considered part of the NDFS "downstream" region. This sample assignment to two survey regions followed the post-stratification approach used in the analyses of the NDFS data by Davis et al. (2021). In other words, the NDFS study regions differed somewhat from those that have been used for the DOP study. Preliminary analyses attempted to fit a model with an interaction term on Flow Period and NDFS Region (in addition to fitting these as independent covariates as per Eqn. 2), but this was found to cause issues with the simulations converging and hence a simpler form of the model with fewer parameters was used instead. This model differed from the Fall X2 model in terms of how study regions were treated; study regions were included as covariates in the NDFS regression, as opposed to fitting independent regression models to each region in the Fall X2 analysis.

The null hypothesis tested for this analysis was the NDFS action did not result in a difference in the overall abundance of zooplankton (as measured by total zooplankton CPUE) after the managed flow pulse periods, relative to that observed before managed flow pulse periods.

The factors considered for the NDFS power analysis included: (1) effect size, which was simulated as a percentage increase in total zooplankton CPUE after flow pulse events during action years (relative to CPUE before the flow pulse events during action years), (2) increases in annual sample sizes, and (3) duration of future monitoring years during which an action occurs. The full time series of NDFS sample data by region and flow pulse period (before, during and after) are shown for reference in Figure 9-4. Samples collected during the fall flow pulse were excluded from the analyses, i.e., the hypothesis that was tested only compared total zooplankton CPUE before and after the flow pulse. The subset of the sample data used to inform the NDFS simulations are shown in Figure 9-5.

Results

Fall X2 Management Action

The power to detect differences in potential effect sizes (as measured by differences in BPUE) for the five selected Delta Smelt zooplankton prey species varied substantially between study regions (Figure 9-6). Power to detect a given effect size was highest in Suisun Bay, likely due to the relatively high level of sampling effort examined across regions during 2011-2019 (Table 9-1). Power was estimated to be greater than 0.80 in Suisun Bay for simulated effect sizes corresponding to a more than 50% (1.5 times) increase in prey species biomass during action years, relative to biomass in non-action years. Statistical power of 0.80, or an 80% chance of detecting an effect (if a true effect exists), is a level of power that is commonly referenced in survey design literature, although the desired level of power may vary on a case-by-case basis (Di Stephano 2003, Steidl et al. 1997, referenced in Thomas and Juanes 1996, Cohen 1988).

Compared to other regions, the Lower Sacramento River, Cache Slough, and Sacramento Ship Channel had similar power to detect a given response size for the biomass of selected zooplankton species. The statistical power in these regions reached or exceeded 0.80 at a simulated biomass level in action years of 180–200% (1.8 to 2.0 times) than in non-action years (Figure 9-6). Of all regions, Suisun Marsh had the lowest statistical power to detect a simulated effect size. At a simulated doubling of BPUE in action years, power in the Suisun Marsh region was estimated to be less than 0.50. This result was surprising, because Suisun Marsh does not have the lowest sample sizes out of all regions.

Simulating increases in annual sample sizes for different regions gave varying results for different response sizes. With a large effect size (a 100% increase in zooplankton prey biomass), statistical power was already at or above the 0.80 benchmark for all regions except Suisun Marsh (Figure 9-7). For a moderate increase in zooplankton biomass (50%) only Suisun Bay and the Lower Sacramento reached 0.80 or above statistical power, which took increasing survey effort to around 70 samples per year during Sep–Oct. No region reached 0.80 statistical power for the smallest effect size simulated (20%).

Simulating additional survey years (given current sampling conditions) improved statistical power most dramatically for the largest (100%) response size examined (Figure 9-8) across all regions. At

this response size, the 0.80 statistical power benchmark was reached within 10 years or less for all regions except for Suisun Marsh, which reached the benchmark at around 15 years of additional sampling. A 50% response size reached 0.80 statistical power with between 10-30 years of additional sampling for all regions except Suisun Marsh, which never reached the benchmark given additional years of sampling under the level of sampling effort during 2011-2019. For a response size of 20% none of the regions reached the 0.80 statistical power benchmark.

NDFS Management Action

Power as a function of changes in total zooplankton abundance after flow pulse periods during action years was generally low, and never reached 0.80, at least when only three action years were simulated for hypothesis testing. Under the highest response size considered, when total zooplankton abundance was twice as high after the flow pulse event compared to before the flow pulse event, power was estimated to be 0.71 (Figure 9-9).

At the lowest (20% increase in abundance) response size, statistical power was generally flat even as simulated sample sizes were increased. With a 50% increase in abundance, statistical power did improve with increasing sample size but only reached under 0.4 statistical power with an annual sample size of 100. Increasing sample size showed the greatest boost in statistical power with a 100% increase in abundance (Figure 9-10).

Given the three years of NDFS action that have occurred, at current levels of sampling effort, additional years of NDFS management actions improved the power of detection for all three simulated effect sizes to varying degrees. With a 100% increase in zooplankton abundance, power was very high (> 90% at a 4th year of NDFS action) approaching statistical power of 1.0 in the simulations at 12 NDFS action years. Statistical power for detecting a moderate increase in zooplankton abundance (50%) reached 0.80 at 15 years of NDFS action. At a 20% increase in zooplankton abundance, statistical power never reached the benchmark of 0.80, only reaching a statistical power of 0.2 at 15 years (Figure 9-11).

Discussion

The results of these analyses suggest that if sampling were repeated under the scenarios examined here, it would generally be difficult to detect increases in zooplankton abundance (NDFS) or biomass (Fall X2) levels in response to managed freshwater outflow actions at low to moderate response sizes, e.g., less than a 50% increase in zooplankton (Figs. 6 and 9). However, the statistical power to detect increases in zooplankton is substantially higher when the simulated zooplankton responses are large (e.g., a 100% increase in abundance or biomass). The results also indicate that there is an interaction between the magnitude of the simulated response and level of survey effort in the resulting estimates of statistical power. For both management action analyses, statistical power generally increased much more rapidly with increases in annual sample sizes given simulated 50% increases in zooplankton abundance or biomass than it did at the 20% simulated level of increase (Figs. 7 and 10). This pattern appeared more muted for the NDFS action (Figure 9-10), where power did not appear to increase as drastically at the 50% response size compared to the Fall X2 simulations. It is also important to note though, for this example only three years of surveys during action years were included in the NDFS simulations. When the number of simulated NDFS management action years was increased, the interaction between survey effort and response size was more consistent with the results for the Fall X2 management action (Figure 9-11). This suggests that

as the number of years with management actions increases, statistical power to detect small to moderate (20 to 50%) increases in zooplankton abundance or biomass would be expected to improve as well.

The results of the Fall X2 power analyses revealed an interesting pattern across regions (Figure 9-4). In particular, the statistical power to detect increases in prey biomass in Suisun Marsh was lower than other regions, even though the sample sizes from this region were generally similar to other regions which had higher estimated power (Figure 9-6; Table 9-1). For example, in comparison to the Cache Slough region (n = 104), sample sizes in Suisun Marsh were larger (n = 144), but the statistical power to detect an increase in prey biomass was estimated to be lower in Suisun Marsh. This result appears to be explained by the differences in sampling variability between these two areas. Suisun Marsh had the highest coefficient of variation (CV = mean / standard deviation) for any area in this comparison (CV = 0.21; Table 9-3). In contrast, Cache Slough (and Suisun Bay) had the lowest coefficient of variation of any study region (CV = 0.12). Suisun Marsh and the Cache Slough region represent two different tidal marsh habitats in the estuary and delta. Suisun Marsh is brackish water habitat with a more variable salinity field that includes several small and large channels with food webs that change on different time scales (Brown et al. 2016). The Cache Slough region in contrast remains fresh year-round. This example highlights the importance of considering not just sample sizes in terms of statistical power to detect zooplankton responses, but also inter-regional differences in variability for the species being sampled. All else being equal, additional sampling effort in more naturally variable environments like Suisun Marsh would be needed relative to other study regions, where sampling variability is lower, to achieve the same level of statistical power.

Under certain assumptions, analytical solutions (i.e., closed-formed equations) for calculating statistical power exist. For example, Cohen (1988) provides analytical solutions for comparisons based on some classical experimental designs, like ANOVA. The results presented by Cohen (1988) include closed form solutions for statistical power that are tabled as functions of sample sizes and other factors, e.g. different values of statistical power for a given effect size over a range of sample sizes.

We initially explored analytical solutions for the Fall X2 Action, but decided against such for several reasons, including: (1) Sample sizes are not equal between strata; (2) Sampling variability between strata is not expected to be equal, as discussed above for Suisun Marsh (both 1 and 2 violate assumptions for analytical solutions under an ANOVA sampling design, for example); and (3) Analytical approaches for zooplankton data have recently involved considerations of moving from more standard forms of linear regression towards mixed-effects models. To the extent feasible we have attempted to mimic the statistical modeling approach that are anticipated to be used to test for statistically significant responses in Delta Smelt prey biomass and zooplankton abundance to outflow management actions (in particular, the Fall X2 Action, which has received much attention in the system).

More complicated regression models, with additional covariates may be used in practice, or be applied in future analyses of these data sets. Estimates of statistical power, using the simulation approach taken here, relies on identifying a single hypothesis to be tested for each model run (Green and MacLeod 2016). However, in applied regression analyses the same regression model may be used to test multiple hypotheses. For example, in the case of the NDFS study, a regression model with additional covariates and interactions between covariates has recently been used to test not just

whether there was a difference in total zooplankton abundance relative to the flow pulse period, but also to test whether there were significant interactions between flow pulse periods and regions (Davis et al. 2022). In the case of the NDFS power analyses, our simulations were designed to result in estimates of statistical power to detect differences in total zooplankton abundance before and after flow pulse periods during actions years, ignoring non-action years, and we did not consider the statistical power to detect interactions between a response and regions (due to a preliminary model with an interaction term failing to converge during simulations).

Different hypotheses could be formulated for a given management action that would ask different questions than the hypotheses underlying these analyses. For example, statistical power could be estimated for the NDFS management action including both non-action years and action years. One hypothesis including both action and non-action years might be whether there is a difference in zooplankton abundance after flow pulse periods during action years, relative to zooplankton abundance after flow pulse periods during non-action years. The analyses presented here do not attempt to address the statistical power for all possible variations of hypotheses that could be tested, but instead focus on a single, relatively simple hypothesis for each management action to illustrate how larger simulated effect sizes, increased sampling effort, or additional years of data collection might be expected to influence statistical power for the survey data.

A general question that was considered during the development of this simulation study was whether there was a benefit from random versus fixed sampling station locations, in terms of detecting effects of management actions. Most of the fisheries monitoring studies in the Estuary and Delta that have long-term established sampling programs, like the FMWT survey, have a fixed sampling station design, where the same locations are re-sampled over months and years (White 2022). In contrast, the more recent EDSM survey has been designed using a Generalized Random Tessellation Sampling (GRTS) approach, which is a method for randomly assigning sampling locations conditional on achieving spatially uniform survey coverage (Stevens and Olsen 2004). A detailed examination of the power of fixed vs. random sampling locations was outside the scope of this study, but it is interesting to note that the fixed sampling location FMWT samples generally have lower sampling variability than the DOP samples, at least for the time periods included in the Fall X2 analyses (Figure 9-3). For example, during Fall X2 non-action years, the CV for the DOP samples in Suisun Marsh was approximately three times that of the FMWT samples (DOP CV = 0.28 vs. FMWT CV = 0.09). Higher sampling variability leads to lower estimates of statistical power, all else being equal. Repeatedly sampling the same fixed sites could have represented the variability at those locations but may not represent the variability in zooplankton across an entire region. To the extent that fixed sampling sites underrepresent variability across a region, the lower corresponding CVs may provide a false sense of statistical confidence in terms of inference at the regional scale.

Surveys with randomly located sampling stations that are conditional on uniform spatial coverage, like those from the DOP survey design using GRTS, may be expected a *priori* to have higher sampling variability compared to surveys with fixed sampling locations. Randomly located sampling locations with uniform spatial coverage would be expected to cover a wider range of habitat conditions, and hence could be sampling from a wider range of underlying zooplankton prey biomass levels, which hypothetically should be more reflective of the true zooplankton biomass (and its variability) across a region, compared to fixed stations. Given these considerations, if the simulation approach that was used here was employed to provide comparative estimates of statistical power between surveys with fixed versus random sampling sites, the results could be confounded to some extent by the observed differences in sampling variability between each survey approach. An

alternative approach to addressing this type of survey-design question could use simulation, but in a different framework. This would involve simulating an underlying (and not necessarily uniform) spatial density of zooplankton, and then drawing samples from the simulated density based on GRTS and fixed sampling locations. This type of simulation approach has been used to compare the performance of GRTS to alternative spatially balanced sampling approaches (e.g. Robertson et al. 2018) using the *spsurvey* package (Dumelle et al. 2022) in the *R* computing language.

The results of this study suggest that some caution is warranted in terms of interpreting non-statistically significant responses of zooplankton biomass and abundance to the Fall X2 and NDFS management actions, at least under the scenarios simulated here. In other words, if no response is detected from regression model estimates used in practice, that should not necessarily be interpreted to mean there was no response, because the power to detect a response would not be expected to be high, especially if that response is not large. Effects of an action may be obscured by other factors such as predation. Spatial subsidies of *P. forbesi* from upstream in the delta have been observed but are rapidly consumed by the invasive non-native clams in Suisun Bay, *Potamocorbula amurensis* (Kayfetz and Kimmerer 2017, Kimmerer et al. 2019). Predation is high enough that without subsidies, populations of *P. forbesi* would be near zero (Kimmerer et al. 2019). The spatial subsidies may be replacing predation losses during the same time period which would obscure any effect of an action. What constitutes a biologically impactful response size in zooplankton abundance or biomass from these management actions in terms of the population dynamics of Delta Smelt is outside the scope of this study and needs to be further studied. But, if sampling were repeated at the levels examined in these analyses, and response sizes were on the order of 50% increases in zooplankton biomass or abundance, the most influential factor for the statistical power to detect such a response appears to be the duration of sampling years, and in particular for the hypothesis tested for the NDFS study, the number of action years over which sampling may occur (Figs. 8 and 11). Given that sampling can be limited by various resources that are available (personnel, time, equipment, funding), the results of these analyses suggest that focus should be put on gathering more years of data opposed to higher sample counts for a shorter term study. Additionally, in terms of allocating sampling effort these results highlight the importance of considering differences in natural variability between study regions. The power to detect zooplankton responses to managed outflow actions in study regions with zooplankton habitat that has a relatively high level of variability would need a higher level of sampling effort to achieve a similar level of power as study regions that have less variable zooplankton habitat.

References

Bashevkin, S. M. 2020. *zooper*: an R package to download and integrate zooplankton datasets from the Upper San Francisco Estuary. Accessed via: https://github.com/InteragencyEcologicalProgram/zooper

Bashevkin, S. M., Hartman, R., Thomas, M., Barros, A., Burdi, C., Hennessy, A., Tempel, T. and Kayfetz, K. 2020. Interagency Ecological Program: Zooplankton abundance in the Upper San Francisco Estuary from 1972-2018, an integration of 5 long-term monitoring programs. Environmental Data Initiative. doi:10.6073/PASTA/0C400C670830E4C8F7FD45C187EFDCB9

457 Baxter, R., Breuer, R., Brown, L., Chotkowski, M., Feyrer, F., Gingras, M., Herbold, B., Mueller-
458 Solger, A., Nobriga, M., Sommer, T. and Souza, K., 2008. Pelagic organism decline progress
459 report: 2007 synthesis of results. Interagency Ecological Program for the San Francisco
460 Estuary. Retrieved on May, 7, p.2011.
461 Bolker, B. 2008. Ecological Models and Data in R. Princeton University Press. Princeton and
462 Oxford.
463 Brown, L. R., Baxter, R., Castillo, G., Conrad, L., Culberson, S., Erickson, G., Feyrer, F., Fong, S.,
464 Gehrts, K., Grimaldo, L., Herbold, B., Kirsch, J., Mueller-Solger, A., Slater, S., Sommer, T.,
465 Souza, K., and Van Nieuwenhuyse, E. 2014. Synthesis of studies in the fall low-salinity zone
466 of the San Francisco Estuary, September–December 2011. *US Geological Survey Scientific*
467 *Investigations Report*, *5041*, 136.
468 Brown, L. R., Kimmerer, W., Conrad, J. L., Lesmeister, S., & Mueller–Solger, A. 2016. Food webs of
469 the Delta, Suisun Bay, and Suisun Marsh: an update on current understanding and
470 possibilities for management. San Francisco Estuary and Watershed Science, 14(3).
471 Cloern, J. E. and Dufford, R. 2005. Phytoplankton community ecology: principles applied in San
472 Francisco Bay. Marine Ecology Progress Series, 285, 11-28.
473 Cohen, J. 1988. Statistical Power Analysis for the Behavioral Sciences. Hillsdale, New Jersey:
474 Lawrence Erlbaum Associates.
475 Davis, B., Adams, J., Bedwell, M., Bever, A., Bosworth, D., Flynn, T., Frantzich, J., Hartman, R.,
476 Jenkins, J., Kwan, N., MacWilliams, M., Maguire, A., Perry, S., Pien, C., Rinde, J., Treleaven,
477 T., Wright, H., Twardochleb, L. 2022. North Delta Food Subsidy Synthesis: Evaluating Flow
478 Pulses from 2011-2019. Department of Water Resources, Division of Integrated Science and
479 Engineering. Draft.
480 Di Stephano, J., 2003. How much power is enough? Against the development of an arbitrary
481 convention for statistical power calculations. Functional Ecology, 17(5), pp.707-709.
482 Dumelle, M., Kincaid, T. M., Olsen, A. R. and Weber, M. H. 2022. *spsurvey*: Spatial Sampling Design
483 and Analysis. R package version 5.3.0.
484 Frantzich, J., Davis, B. E., MacWilliams, M., Bever, A., & Sommer, T. 2021. Use of a Managed Flow
485 Pulse as Food Web Support for Estuarine Habitat. *San Francisco Estuary and Watershed*
486 *Science*, *19*(3).
487 George, S.D., Stich, D.S. and Baldigo, B.P. 2021. Considerations of variability and power for long-
488 term monitoring of stream fish assemblages. *Canadian Journal of Fisheries and Aquatic*
489 *Sciences*, *78*(3), 301-311.
490 Green, P. and MacLeod, C.J. 2016. *SIMR*: an R package for power analysis of generalized linear
491 mixed models by simulation. Methods in Ecology and Evolution 7: 493–8.
492 Hammock, B. G., Hobbs, J. A., Slater, S. B., Acuña, S., & Teh, S. J. 2015. Contaminant and food
493 limitation stress in an endangered estuarine fish. Science of the Total Environment, 532,
494 316-326.
495 Hartman, R.K., Bashevkin, S.M., Barros, A., Burdi, C.E., Patel, C. and Sommer, T., 2021. Food for
496 Thought: Connecting Zooplankton Science to Management in the San Francisco
497 Estuary. *San Francisco Estuary and Watershed Science*, *19*(3).
498 Hassrick, J.L., A.G. Smith, C.Y. Lee, D.M. Cox, A.J. Kalmbach, and A. Schultz. 2021. How an
499 estuarine prey field changes with managed freshwater outflow. Pages 245-28 in ed. A.A.
500 Schultz, In Directed Outflow Project: Technical Report 2. U.S. Bureau of Reclamation, Bay-
501 Delta Office, California-Great Basin Region, Sacramento, CA. March 2021, 349 pp.
502 Hoening, J.M. and Heisey, D.M. 2001. The Abuse of Power: The Pervasive Fallacy of Power
503 Calculations for Data Analysis. American Statistical Association. 55:1-6.

Jassby, A.D., Kimmerer, W.J., Monismith, S.G., Armor, C., Cloern, J.E., Powell, T.M., Schubel, J.R. and Vendlinski, T.J., 1995. Isohaline position as a habitat indicator for estuarine populations. Ecological Applications, 5(1), pp.272-289.

Johnson, P.C.D., Barry, S.J.E, Ferguson, H.M. and Muller, P. 2015. Power analysis for generalized linear mixed models in ecology and evolution. Methods in Ecology and Evolution 6: 133–42.

Kayfetz, K., S. M. Bashevkin, M. Thomas, R. Hartman, C. E. Burdi, A. Hennessy, T. Tempel, and A. Barros. 2020. Zooplankton Integrated Dataset Metadata Report. IEP Technical Report 93. California Department of Water Resources, Sacramento, California.

Kayfetz, K., & Kimmerer, W. (2017). Abiotic and biotic controls on the copepod Pseudodiaptomus forbesi in the upper San Francisco Estuary. Marine Ecology Progress Series, 581, 85-101.

Kimmerer, W.J., Gross, E.S., Slaughter, A.M. and Durand, J.R., 2019. Spatial subsidies and mortality of an estuarine copepod revealed using a box model. Estuaries and Coasts, 42(1), pp.218-236.

Kimmerer, W., Ignoffo, T. R., Bemowski, B., Modéran, J., Holmes, A., & Bergamaschi, B. 2018. Zooplankton dynamics in the cache slough complex of the Upper San Francisco Estuary. San Francisco Estuary and Watershed Science, 16(3).

Kimmerer, W. J., Ignoffo, T. R., Kayfetz, K. R., & Slaughter, A. M. 2018. Effects of freshwater flow and phytoplankton biomass on growth, reproduction, and spatial subsidies of the estuarine copepod Pseudodiaptomus forbesi. Hydrobiologia, 807(1), 113-130.

Montgomery, J. R. 2017. Foodweb dynamics in shallow tidal sloughs of the San Francisco Estuary. University of California, Davis.

Moyle, P. B., Brown, L. R., Durand, J. R., & Hobbs, J. A. 2016. Delta smelt: life history and decline of a once-abundant species in the San Francisco Estuary. *San Francisco Estuary and Watershed Science*, *14*(2).

Müller-Solger, A. B., Jassby, A. D., & Müller-Navarra, D. C. 2002. Nutritional quality of food resources for zooplankton (Daphnia) in a tidal freshwater system (Sacramento-San Joaquin River Delta). Limnology and Oceanography, 47(5), 1468-1476.

Nagelkerke, L. A., & Van Densen, W. L. 2007. Serial correlation and inter-annual variability in relation to the statistical power of monitoring schemes to detect trends in fish populations. *Environmental Monitoring and assessment*, *125*(1), 247-256.

Owens, S., Ignoffo, T. R., Frantzich, J., Slaughter, A., & Kimmerer, W. 2019. High growth rates of a dominant calanoid copepod in the northern San Francisco Estuary. *Journal of Plankton Research*, *41*(6), 939-954.

Peterman, R. M. 1990. Statistical power analysis can improve fisheries research and management. *Canadian Journal of Fisheries and Aquatic Sciences*, *47*(1), 2-15.

RMA (Resource Management Associates). 2021. *Numerical Modeling in Support of Reclamation Delta Smelt Summer/Fall Habitat Analysis: Calanoid Copepod Analysis Addendum*.

Robertson, B., McDonald, T., Price, C. and Brown, J. 2018. Halton iterative partitioning: spatially balanced sampling via partitioning. Environ Ecol Stat. 25:305

Schultz, A. A., editor. 2019a. Directed Outflow Project: Technical Report 1. U.S. Bureau of Reclamation, Bay-Delta Office, Mid-Pacific Region, Sacramento, CA. November 2019, 318 pp.

Schultz, A.A., L. Grimaldo, J.L., Hassrick, A.J. Kalmbach, A.G. Smith, O. Burgess, D. Barnard, and J. Brandon. 2019b. Effect of Isohaline (X2) and Region on Delta Smelt Habitat, Prey and Distribution During the Summer and Fall: Insights into Managed Flow Actions in a Highly Modified Estuary. In Directed Outflow Project: Technical Report, ed. A.A. Schultz, 237-301. Mid-Pacific Region, Sacramento, CA. U.S. Bureau of Reclamation, Bay-Delta Office.

Schultz, A.A., editor. 2021. Directed Outflow Project: Technical Report 2. U.S. Bureau of Reclamation, Bay-Delta Office, California-Great Basin Region, Sacramento, CA. March 2021, 349 pp.

Slater, S.B. and Baxter, R.D. 2014. Diet, Prey Selection, and Body Condition of Age-0 Delta Smelt, *Hypomesus transpacificus*, in the Upper San Francisco Estuary. San Francisco Estuary and Watershed Science. 12(3): doi: http://dx.doi.org/10.15447/sfews.2014v12iss3art1

Sommer, T., Armor, C., Baxter, R., Breuer, R., Brown, L., Chotkowski, M., Culberson, S., Feyrer, F., Gingras, M., Herbold, B. and Kimmerer, W., 2007. The collapse of pelagic fishes in the upper San Francisco Estuary. *Fisheries*, *32*(6), pp.270-277.

Steidl, R. J., Hayes, J. P., & Schauber, E. 1997. Statistical power analysis in wildlife research. The Journal of Wildlife Management, 270-279.

Stevens, D.L. and Olsen, A.R. 2004. Spatially balanced sampling of natural resources. J Am Stat Assoc. 99:262-278.

Thomas, L., 1997. Retrospective power analysis. Conservation Biology, 11(1), pp.276-280.

Thomas, L., & Juanes, F. 1996. The importance of statistical power analysis: an example from Animal Behaviour. Animal Behaviour, 52(4), 856-859.

Thomson, J.R., Kimmerer, W.J., Brown, L.R., Newman, K.B., Nally, R.M., Bennett, W.A., Feyrer, F. and Fleishman, E., 2010. Bayesian change point analysis of abundance trends for pelagic fishes in the upper San Francisco Estuary. *Ecological Applications*, *20*(5), pp.1431-1448.

Twardochleb L., Maguire, A., Dixit, L., Bedwell, M., Orlando, J., MacWilliams, M., Bever, A. and Davis, B. 2021a. North Delta Food Subsidies Study: Monitoring Food Web Responses to the North Delta Flow Action, 2019 Report. Department of Water Resources, Division of Environmental Sciences.

Twardochleb L., Martinez, J., Bedwell, M., Frantzich, J., Sommer, T., and B. Davis. 2021b. North Delta Food Subsidies 2021-2023 Operations and Monitoring Plan. Department of Water Resources, Division of Environmental Services.

Vaudor, L., Lamouroux, N., Olivier, J. M., & Forcellini, M. 2015. How sampling influences the statistical power to detect changes in abundance: an application to river restoration. *Freshwater Biology*, *60*(6), 1192-1207.

Whipple, A.A., Grossinger, R.M., Rankin, D., Stanford, B. and Askevold, R.A., 2012. Sacramento–San Joaquin Delta historical ecology investigation: exploring pattern and process. [Richmond (CA)]: San Francisco Estuary Institute Aquatic Science Center.

USFWS (U.S. Fish and Wildlife Service). 1993. Endangered and Threatened Wildlife and Plants; Determination of Threatened Status for the Delta Smelt. U.S. Fish and Wildlife Service, editor 50 CFR Part 17.

USFWS (U.S. Fish and Wildlife Service). 2008. Formal Endangered Species Act consultation on the proposed coordinated operations of the Central Valley Project (CVP) and State Water Project (SWP). USFWS. Technical memorandum 81420-2008-F-1481-5, Sacramento, California.

United States Fish and Wildlife Service, T. Senegal, R. Mckenzie, J. Speegle, B. Perales, D. Bridgman, K. Erly, S. Staiger, A. Arrambide, and M. Gilbert. 2022. Interagency Ecological Program and US Fish and Wildlife Service: San Francisco Estuary Enhanced Delta Smelt Monitoring Program data, 2016-2021 ver 8. Environmental Data Initiative. https://doi.org/10.6073/pasta/e1a540c161b7be56b941df50fd7b44c5 (Accessed 2022-03-08).

White, James. 2022. Fall Midwater Trawl Survey End of Season Report: 2021. California Department of Fish and Wildlife. https://nrm.dfg.ca.gov/FileHandler.ashx?DocumentId=199043.

Tables

Table 9-1. Sample sizes by year and region for the Fall X2 management action power analysis.

The management action years were 2011, 2017 and 2019 (denoted in bold). Samples collected prior to 2017 are from the CDFW FMWT survey. Numbers during 2017-2019 show the combined EDSM and FMWT sample sizes.

Year	Suisun Bay	Suisun Marsh	Lower Sacramento	Cache Slough	Sacramento Ship Channel	Total
2011	**18**	**6**	**8**	**4**	**10**	**46**
2012	17	6	8	4	10	45
2013	18	6	8	4	10	46
2014	18	5	8	4	10	45
2015	16	5	8	4	10	43
2016	17	6	8	3	10	44
2017	**74**	**20**	**31**	**17**	**33**	**175**
2018	54	34	46	19	25	178
2019	**70**	**56**	**61**	**48**	**58**	**293**
Total	**302**	**144**	**186**	**107**	**176**	**915**

606 **Table 9-2. Sample sizes are shown for each action year, by region and flow period (before or**
607 **after) for the NDFS power analysis.**

Year	Flow Period	Upstream	Downstream	Total
2016	Before	8	8	16
2016	After	20	16	36
2018	Before	23	20	43
2018	After	13	14	27
2019	Before	12	8	20
2019	After	12	8	20
Total		**88**	**74**	**162**

608

609

610 Table 9-3. Summary statistics for the biomass samples (BPUE) of five Delta Smelt
611 zooplankton prey species included in the Fall X2 management action analysis.

612 Sample means (in natural log-space) and the associated coefficients of variation (standard deviation divided by mean)
613 are shown for each region during 2011–2019.

Region	Mean	CV
Suisun Bay	7.67	0.12
Suisun Marsh	7.17	0.21
Lower Sacramento	8.01	0.16
Cache Slough	8.15	0.12
Sac Ship Channel	8.47	0.19

614

615

Figures

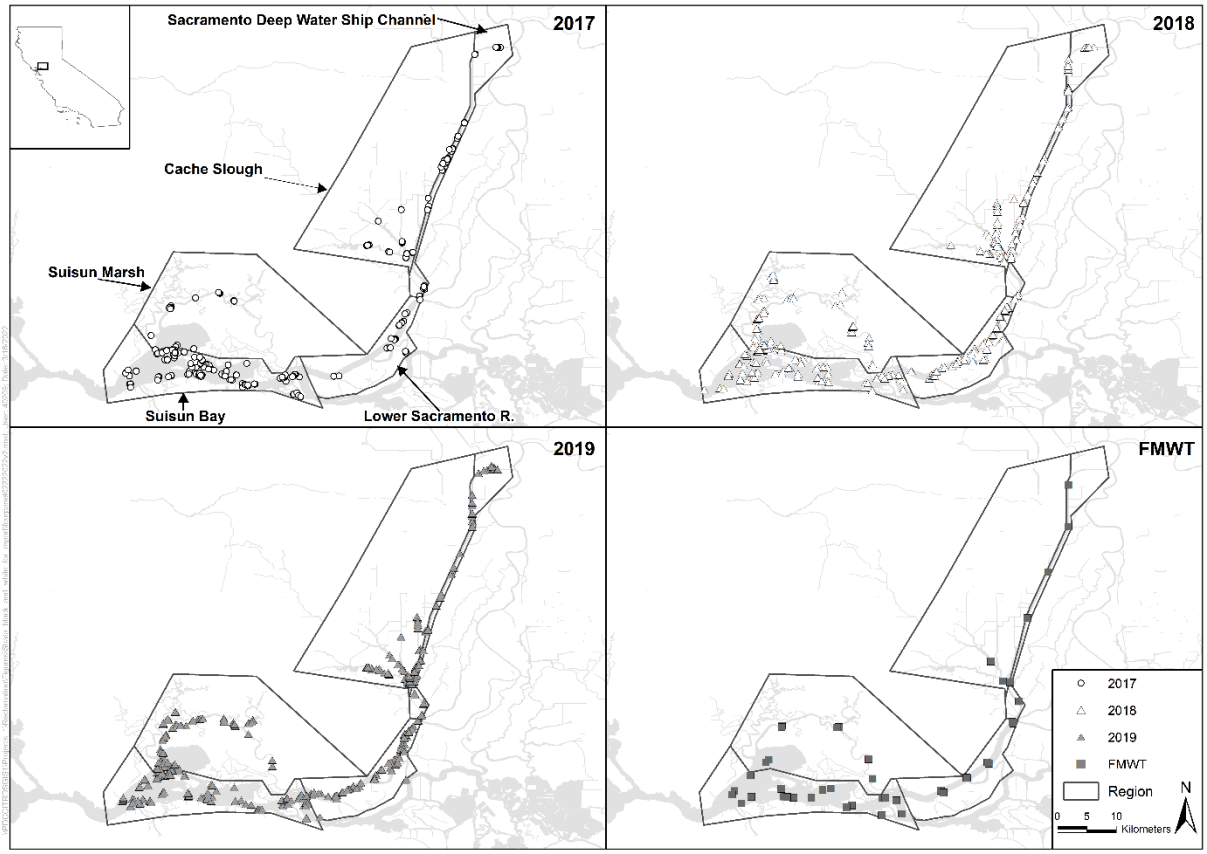

Figure 9-1. Map of the estuary and delta showing regions considered in the power analyses for the Fall X2 management action.

Fall Midwater Trawl (FMWT) stations are fixed location sampling stations represented by squares. Only FMWT stations that fell within the five regions examined in this study were used.

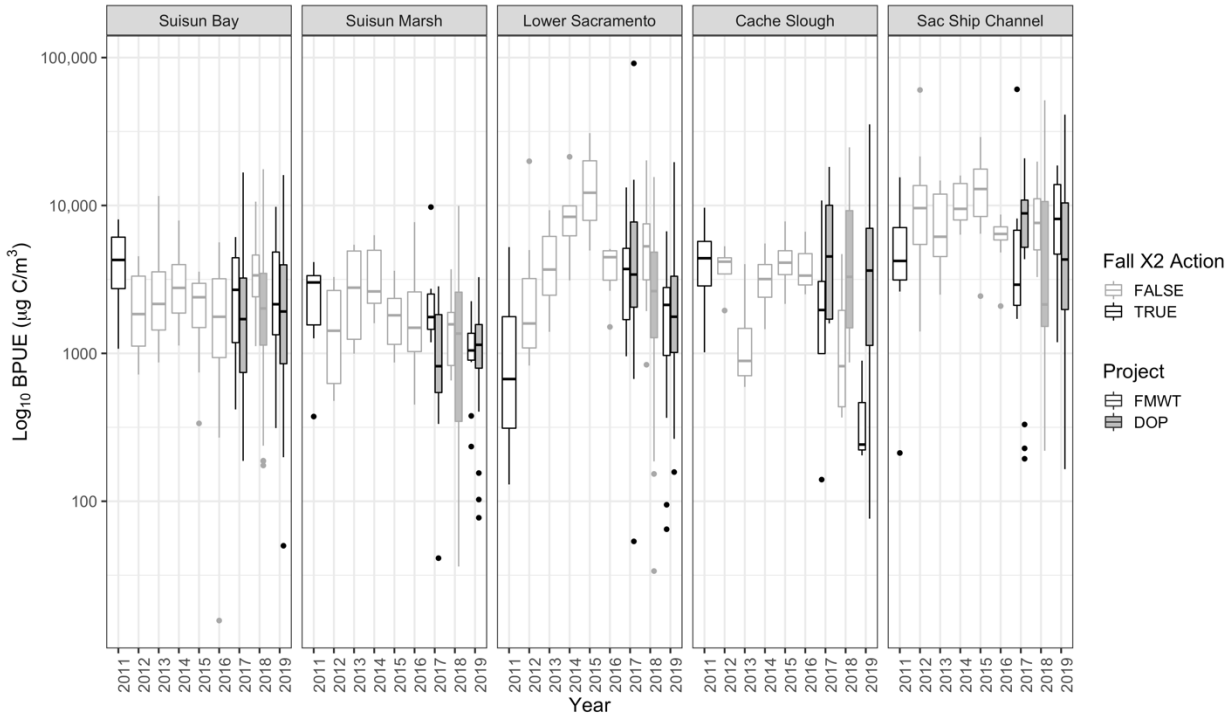

Figure 9-2. Log_{10} biomass per unit effort (BPUE; micrograms carbon per cubic meter, µg C / m^3) during Sep–Oct is shown by year and separated by region for the Fall X2 management action analyses.

Boxplots with black lines represent samples collected action years, while those with gray lines represent non-action years. Boxplots filled with gray represent samples collected under the DOP survey and those filled with white are from the FMWT. The DOP survey began in 2017, and separate boxes are plotted side-by-side during 2017–2019 for comparison between the two surveys. Median BPUE values are represented by the horizontal lines, the upper and lower edges of the boxes represent the 25th and 75th percentiles (the interquartile range), the whiskers extend 1.5 times the interquartile range, and samples with values beyond the whiskers are plotted as individual points.

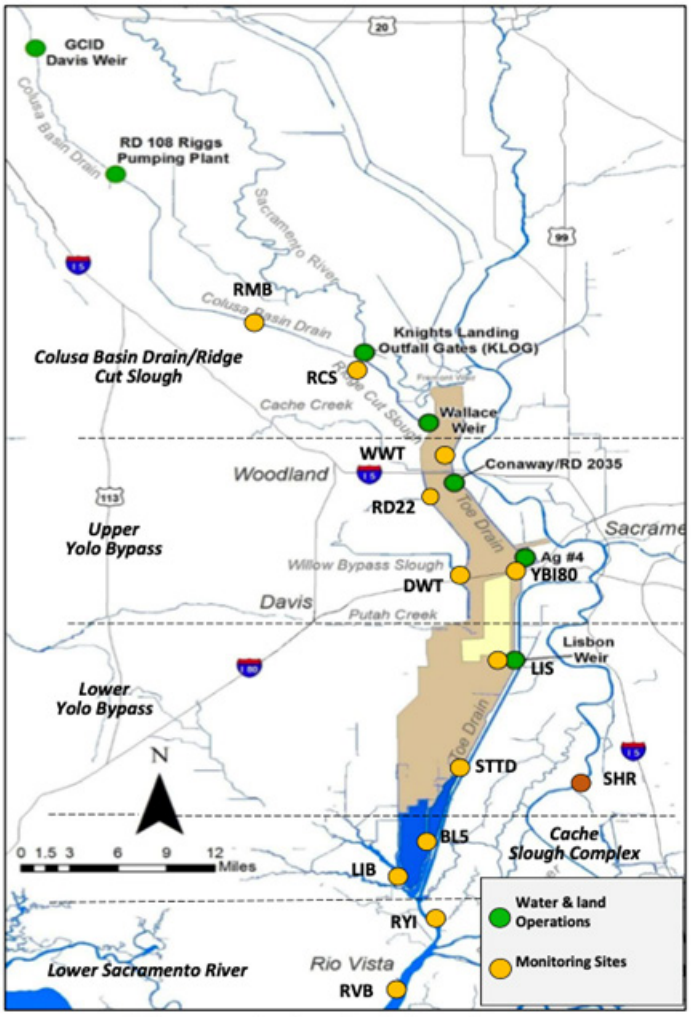

634

635 Figure 9-3. NDFS survey area showing regions (from Twardochleb et al. 2021a, p. 12).
636 Sampling sites are in yellow circles.

637 Monitoring sites downstream of site STTD were considered “downstream”, site STTD and sites upstream were
638 considered “upstream” following Davis et al. (2021).

639

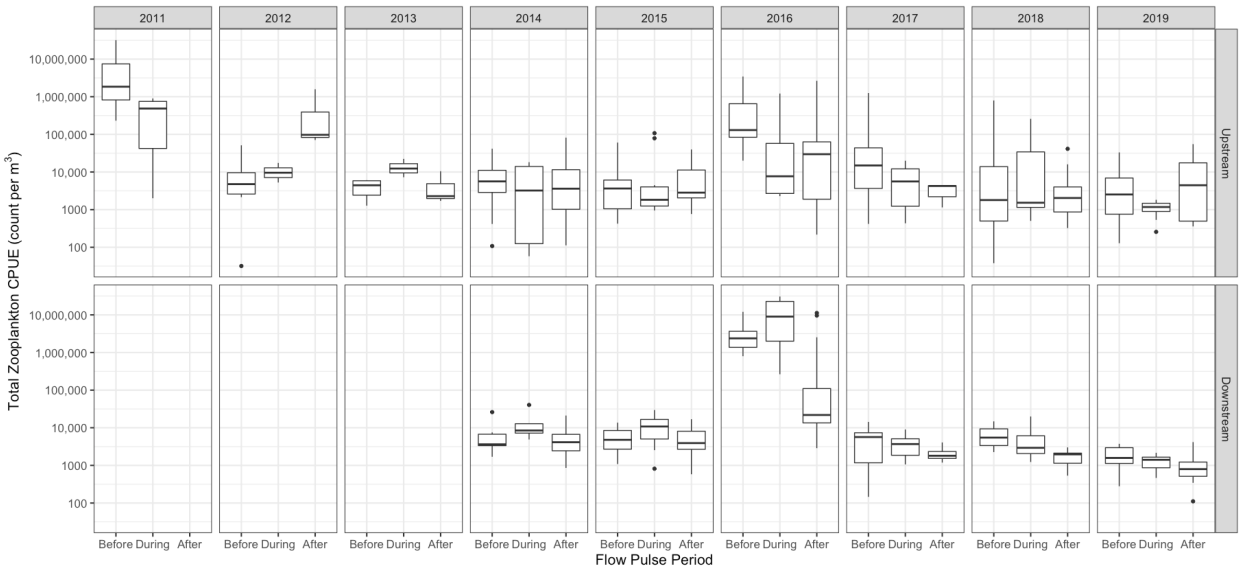

640

641 Figure 9-4. Log$_{10}$ total zooplankton CPUE by year, flow period, and region for the NDFS
642 survey data used in these analyses.

643 The entire data set is shown here for completeness, although only a subset of the data during action years was used
644 to inform the power analyses.

645

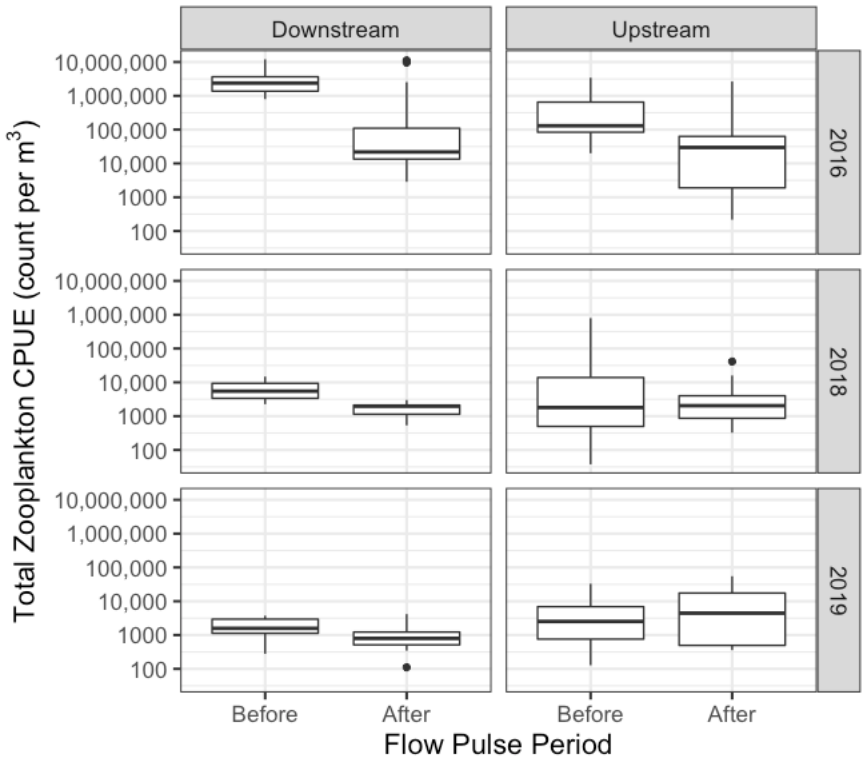

646

647 Figure 9-5. Log_{10} total zooplankton CPUE by action year, flow period, and region for the
648 NDFS survey data that were used to inform the power analyses simulations.

649

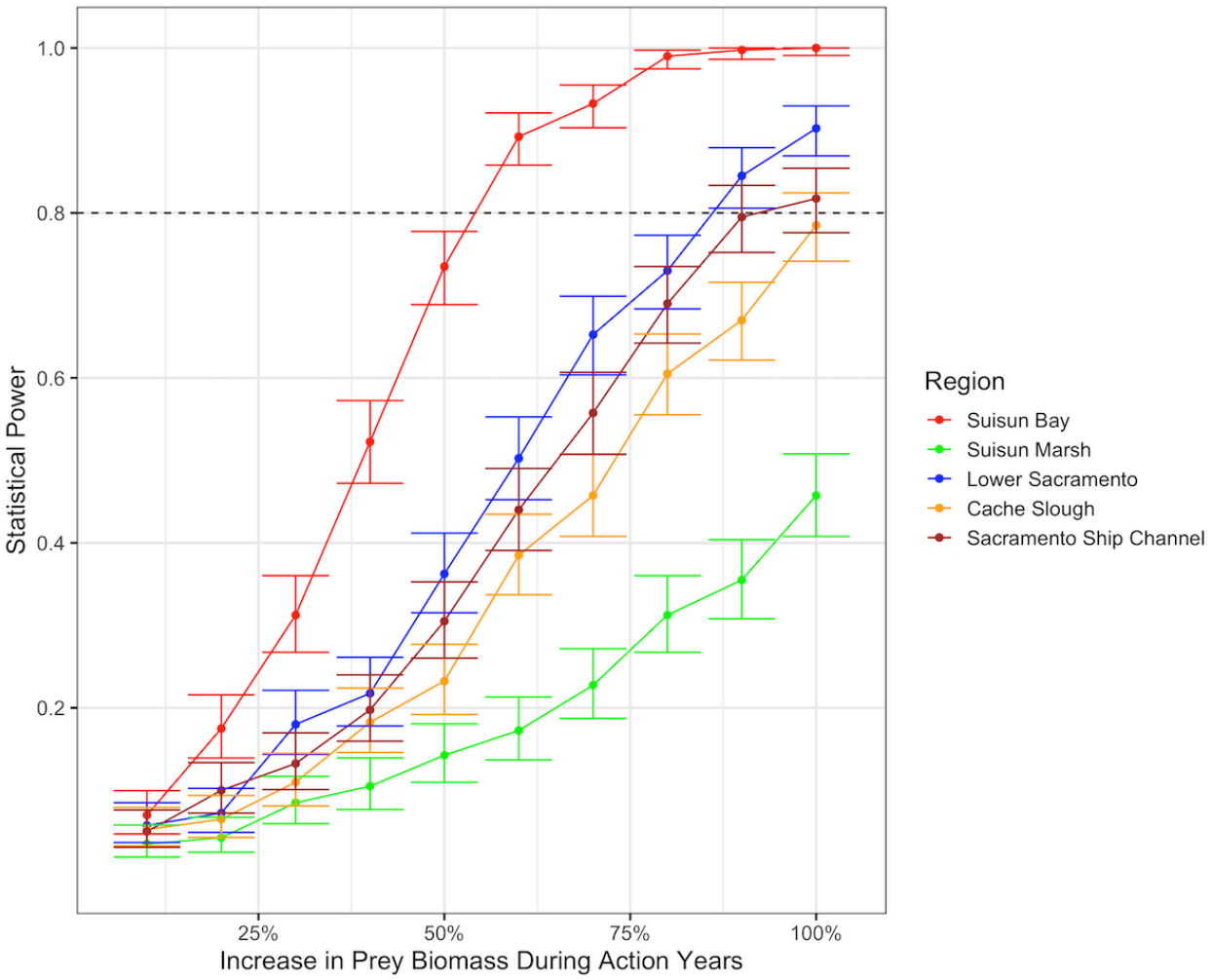

Figure 9-6. Statistical power to detect a simulated percentage increase in zooplankton biomass during action years, relative to biomass in non-action years, for the five Delta Smelt zooplankton prey species included in the Fall X2 analyses.

The percentage increase is measured relative to biomass in non-action years on the x-axis; a simulated 50% increase during action years represents 1.5 times the level of biomass in non-action years, and a 100% increase represents a doubling of biomass during action years. The dashed horizontal line represents statistical power equal to 0.80, or an 80% chance of detecting a given effect size if sampling was repeated. Sample sizes were held equal to the numbers collected in the field for each region (Table 1).

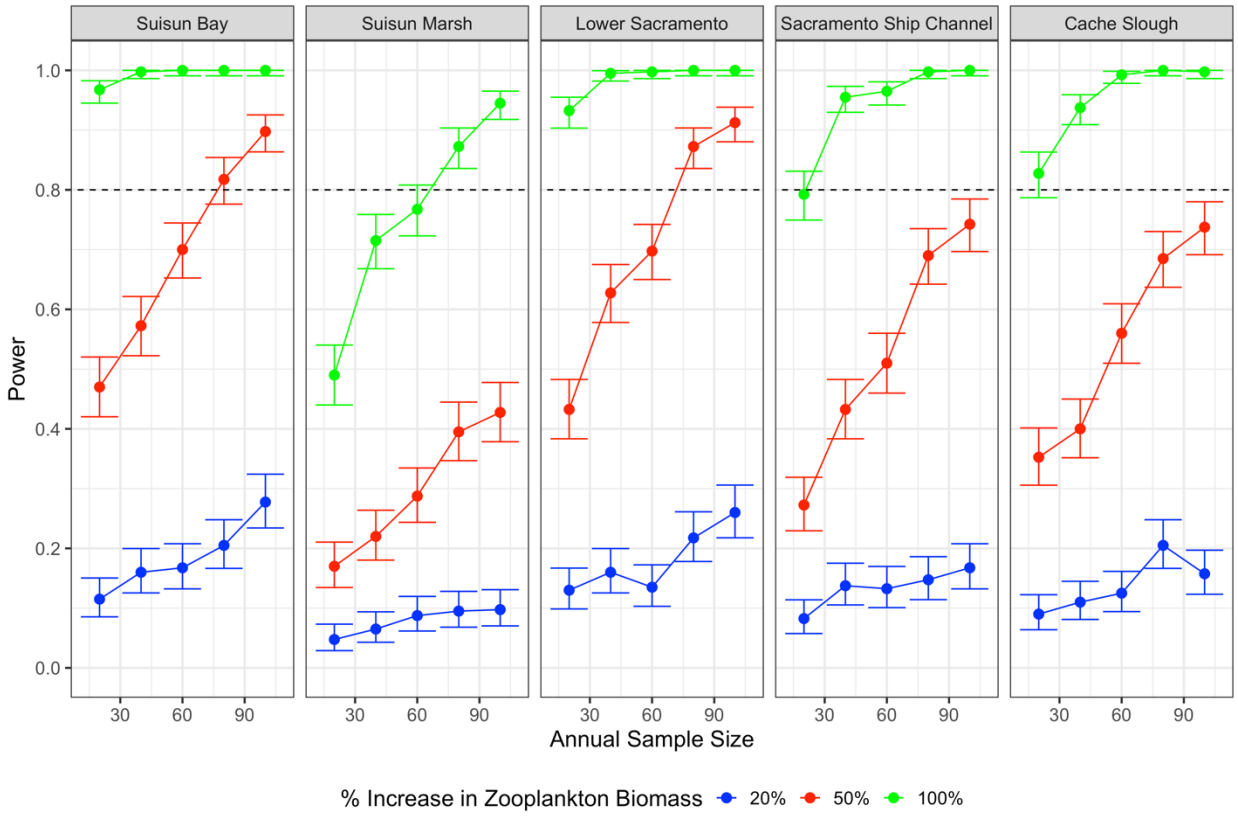

659

660 Figure 9-7. Statistical power as a function of annual sample size for the Fall X2
661 management action.

662 Each power curve is a function of a different simulated percentage increase in zooplankton prey species biomass
663 during action years, relative to that during non-action years. The percentage increase is measured as per Figure 6. The
664 dashed horizontal line represents statistical power equal to 0.80, or an 80% chance of detecting a given effect size if
665 sampling was repeated. These simulations assume that nine years of sampling occur (matching the 2011-2019
666 timeframe), with each year having the same annual sample size shown on the x-axis.

667

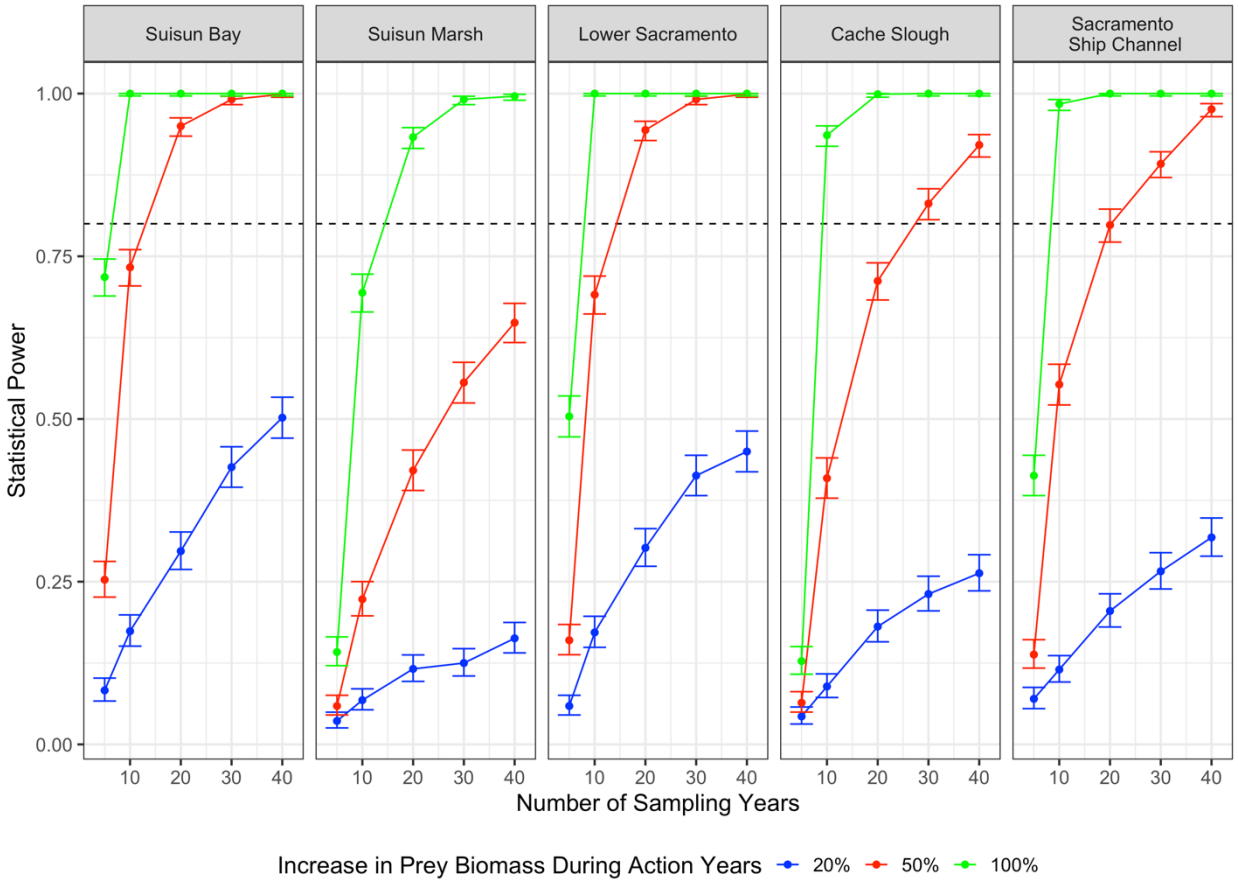

668

669 Figure 9-8. Statistical power for the Fall X2 management action analyses are shown as a
670 function of total survey years incorporated in the hypothesis test.

671 Each power curve is a function of a different simulated percentage increase in the five Delta Smelt zooplankton prey
672 species included in the Fall X2 analyses in management action years versus non-action years. The percentage increase
673 is measured as per Figure 6. The dashed horizontal line represents statistical power equal to 0.80, or an 80% chance of
674 detecting a given effect size.

675

676

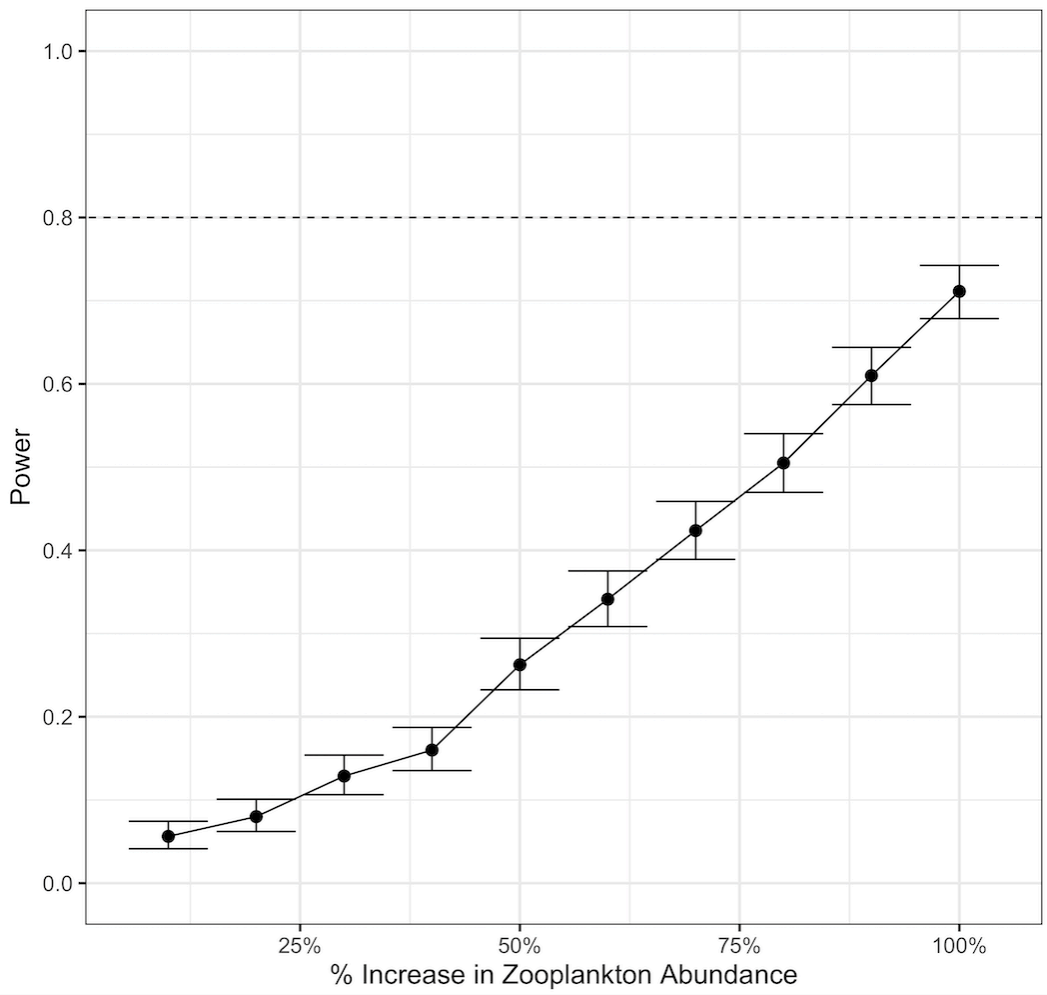

677

678 Figure 9-9. Statistical power to detect a simulated percentage increase in total
679 zooplankton CPUE after the flow pulse during NDFS action years, relative to total
680 zooplankton CPUE before the flow pulse during action years.

681 A simulated 50% increase in abundance after the flow pulse represents 1.5 times the abundance before the flow
682 pulse, and a 100% increase represents a doubling of CPUE after the flow pulse. The dashed horizontal line represents
683 statistical power equal to 0.80, or an 80% chance of detecting a given effect size if sampling was repeated for the data
684 considered in this analysis. These simulations assume that three action years are available for hypothesis testing.

685

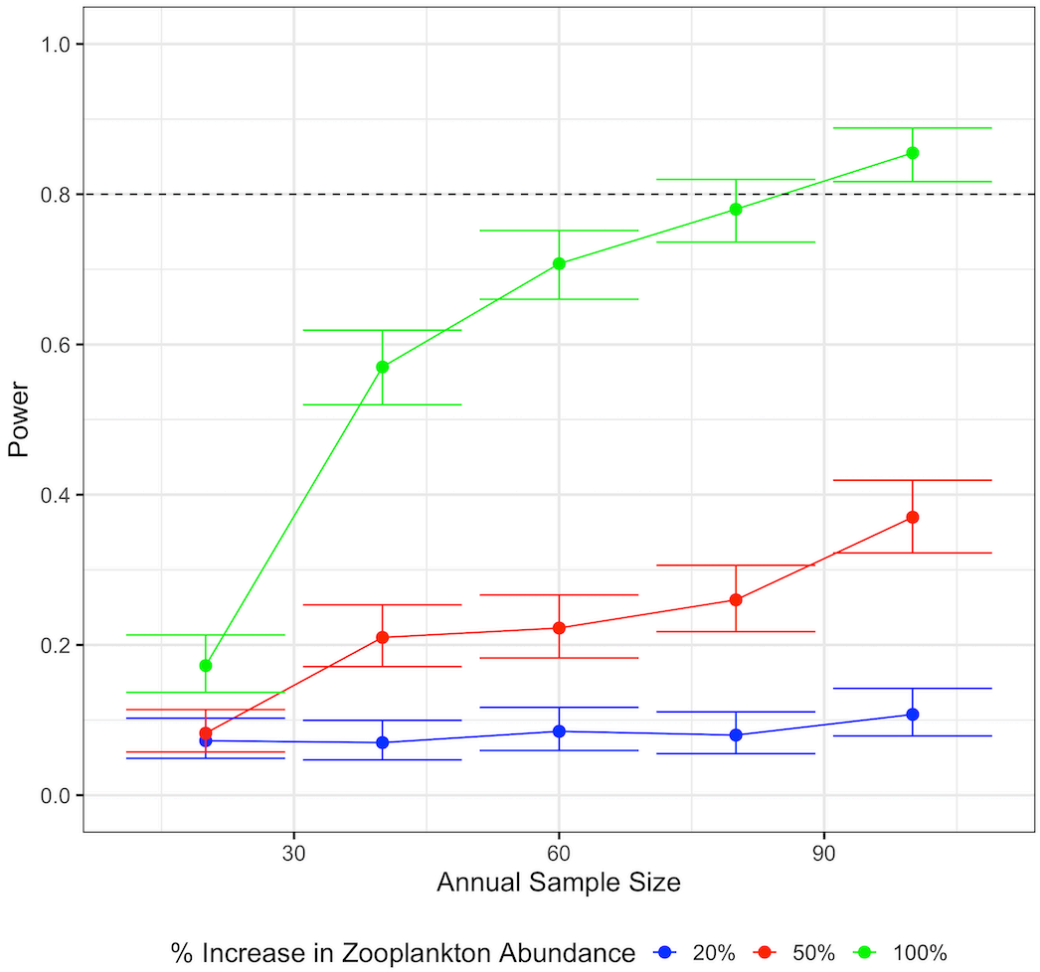

686

687 Figure 9-10. Statistical power as a function of annual sample size for the NDFS
688 management action.

689 Each power curve is a function of a different simulated percentage increase in total zooplankton CPUE after the flow
690 pulse during NDFS action years, relative to total zooplankton CPUE before the flow pulse during action years. The
691 percentage increase is measured as per Figure 6. The dashed horizontal line represents statistical power equal to 0.80,
692 or an 80% chance of detecting a given effect size if sampling was repeated. These simulations assume that three
693 action years are available, and samples are combined across years for hypothesis testing, with each year having the
694 same annual sample size shown on the x-axis.

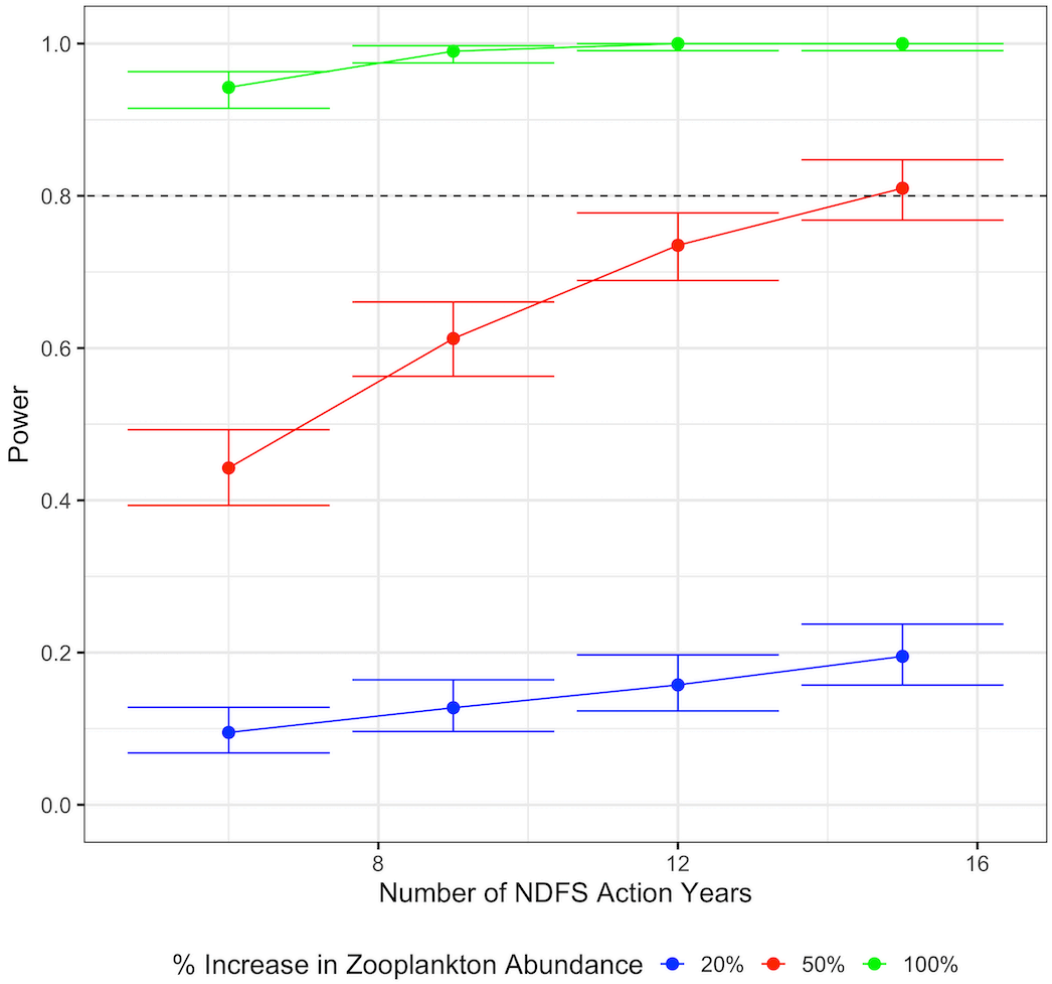

Figure 9-11. Statistical power as a function of the number of NDFS management action years.

Each power curve is a function of a different simulated percentage increase in total zooplankton CPUE after the flow pulse during NDFS action years, relative to total zooplankton CPUE before the flow pulse during NDFS action years. The percentage increase is measured as per Figure 6. The dashed horizontal line represents statistical power equal to 0.80, or an 80% chance of detecting a given effect size if sampling was repeated. These simulations assume that samples are combined across action years for hypothesis testing.